**Carbonyl Reductases and Pluripotent Hydroxysteroid Dehydrogenases of the Short-Chain Dehydrogenase/Reductase Superfamily:**

**Structural Aspects of Oligomerization in 3α-Hydroxysteroid Dehydrogenase /Carbonyl Reductase from *Comamonas testosteroni*:**

**New Approaches for efficient Protein Design**


# Dissertation

zur

Erlangung des Doktorgrades

der Naturwissenschaften

(Dr. rer. nat.)


dem

Fachbereich  Biologie

der

PHILIPPS-UNIVERSITÄT MARBURG


vorgelegt von

Frank Hoffmann

aus Siegen


Marburg/Lahn 2009

Vom Fachbereich Biologie der Philipps-Universität Marburg

als Dissertation angenommen                                    17. Juni 2009


Erstgutachter:                                        Prof. Dr. W. Buckel

Zweitgutachter:                                       Prof. Dr. E. Maser

Tag der mündlichen Prüfung:                           17. Juli 2009

Meiner Familie in Liebe gewidmet

# Part I

**Carbonyl Reductases and Pluripotent Hydroxysteroid Dehydrogenases of the Short-Chain Dehydrogenase/Reductase Superfamily**

**Page 2 ff**

# Part II

**Structural Aspects of Oligomerisation in 3α-Hydroxysteroid Dehydro-genase /Carbonyl Reductase from *Comamonas testosteroni*:**
New Approaches for efficient Protein Design

**Page 69 ff**

# Part I

# Carbonyl Reductases and Pluripotent Hydroxysteroid Dehydrogenases of the Short-Chain Dehydrogenase/Reductase Superfamily

**Frank Hoffmann**

*Institute of Toxicology and Pharmacology for Natural Scientists,*
*University Medical School Schleswig-Holstein, Campus Kiel,*
*Brunswiker Strasse 10, 24105 Kiel, Germany*

# Part I

# Table of Contents

# I   Abstract

Carbonyl reduction of aldehydes, ketones and quinones to their corresponding hydroxy derivatives plays an important role in the phase-I metabolism of many endogenous (biogenic aldehydes, steroids, prostaglandins, reactive lipid peroxidation products) and xenobiotic (pharmacologic drugs, carcinogens, toxicants) compounds. Carbonyl-reducing enzymes are grouped into two large protein superfamilies, the aldo-keto reductases (AKR) and the short-chain dehydrogenases/reductases (SDR). Whereas aldehyde reductase and aldose reductase are AKRs, several forms of carbonyl reductase belong to the SDRs. In addition, there exist a variety of pluripotent hydroxysteroid dehydrogenases (HSDs) of both superfamilies which specifically catalyze the oxidoreduction at different positions of the steroid nucleus, and which also catalyze rather non-specifically the reductive metabolism of a great number of non-steroidal carbonyl compounds. The present review summarizes recent findings on carbonyl reductases and pluripotent HSDs of the SDR protein superfamily.

# II  Introduction

## II.1      Carbonyl Reduction

Metabolic reduction is the counterpart to oxidative pathways and plays an important role in the phase-I metabolism of carbonyl group bearing substances. Carbonyl reduction means the formation of a hydroxy group from a reactive aldehyde or ketone moiety and is generally regarded as an inactivation or detoxification step since the resulting alcohol is easier to conjugate and to eliminate. Not only are these carbonyl-containing compounds widespread in the environment and enter the body as xenobiotics and environmental pollutants, but they can also be generated endogenously through normal catabolic oxidation and deamination reactions. Many endogenous compounds such as biogenic amines, steroids, prostaglandins and other hormones are metabolized through carbonyl intermediates (Felsted and Bachur, 1980; Forrest and Gonzalez, 2000). In addition, lipid peroxidation within the cell results in the production of reactive carbonyls such as acrolein, 4-hydroxynonenal, 4-oxononenal and malondialdehyde, while oxidative damage to DNA generates base propenals (Esterbauer *et al.*, 1982). Dietary sources of carbonyl-containing compounds are diverse and include aldehydes found in fruits as well as the breakdown product of ethanol, acetaldehyde  (Ellis and Hayes, 1995; Maser and Oppermann, 1997). Pharmacologic drugs represent further sources of exposure to carbonyl-containing compounds (Maser, 1995; Rosemond and Walsh, 2004) (cf. chapter 4.5).

From the pharmacologist's point of view, carbonyl reduction has been shown to be of significance in various inactivation processes of drugs bearing a carbonyl group. On the other hand, the carbinols formed may retain therapeutic potency, thus prolonging the pharmacodynamic effect of the parent drug, or, in some instances, a compound gains activity through carbonyl reduction.

From the toxicologist's point of view, carbonyl reduction plays an important role in the toxification of drugs such as daunorubicin and doxorubicin (cf. chapter 4), whereas numerous reports corroborate the concept of carbonyl-reducing enzymes being involved in detoxification processes of endogenous and xenobiotic reactive carbonyl compounds.
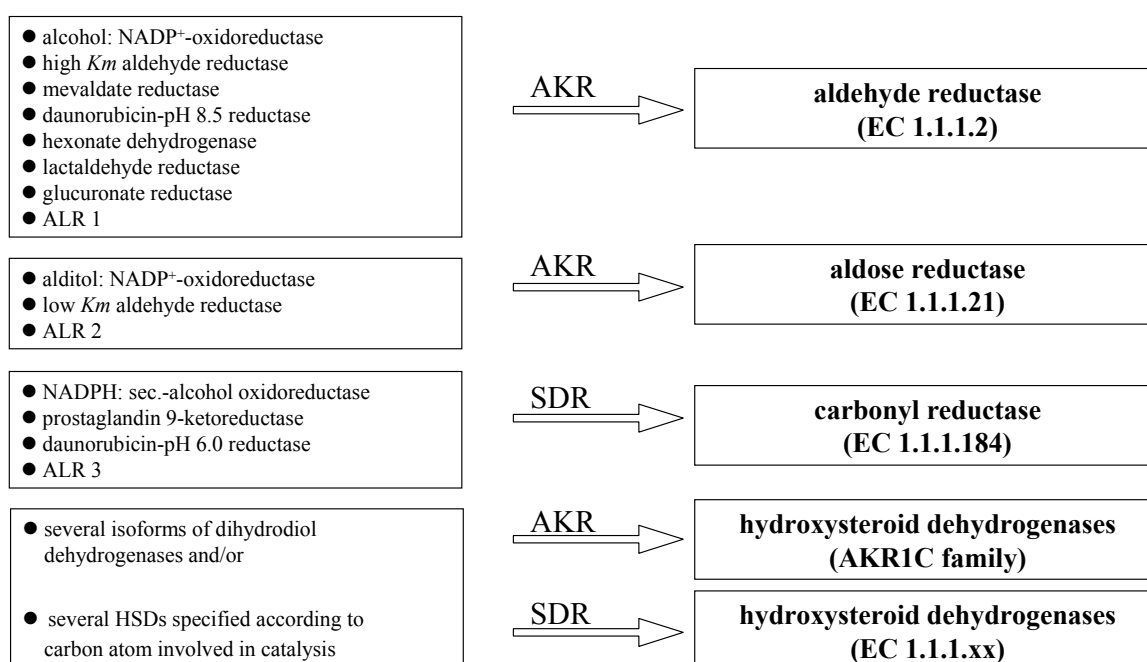
Compared with the oxidative cytochrome P450 (CYP) system, carbonyl-reducing enzymes had, for a long time, received considerably less attention. However, the advancement of carbonyl reductase molecular biology has allowed the identification and characterization of several carbonyl-reducing enzymes, including pluripotent hydroxysteroid dehydrogenases that are involved in xenobiotic carbonyl compound metabolism, in addition to catalyzing the oxidoreduction of their physiologic steroid substrates [reviewed in (Maser, 1995)].

## II.2      Enzymes Mediating Carbonyl Reduction

Enzymes catalyzing the reductive metabolism of carbonyl compounds are ubiquitous in nature, but the majority of the research work was performed in mammalian cells and tissues. Carbonyl-reducing enzymes have been reported in a variety of non-mammalian organisms, such as plants (Baker and Agard, 1994), bacteria (Zelinski *et al.*, 1994; Oppermann and Maser, 1996; Oppermann *et al.*, 1998), yeast (Peters *et al.*, 1993; Wada *et al.*, 1998), fish and insects (Oppermann *et al.*, 1998). In mammals, these enzymes have been analyzed in more detail, amongst others, in rabbit (Ahmed *et al.*, 1978; Ahmed *et al.*, 1979; Sawada *et al.*, 1979; Felsted and Bachur, 1980; Imamura *et al.*, 1993), rat (Ahmed *et al.*, 1978; Hara *et al.*, 1987), mouse (Ahmed *et al.*, 1978; Nakayama *et al.*, 1986; Iwata *et al.*, 1990a), guinea pig (Sawada *et al.*, 1979; Nakayama *et al.*, 1986), monkey (Lee and Levine, 1974a; Iwata *et al.*, 1990a), chicken (Lee and Levine, 1974b; Cagen *et al.*, 1979), pig (Tanaka *et al.*, 1992), dog (Hara *et al.*, 1986b; Iwata *et al.*, 1990a) and  bovine species (Iwata et al., 1990a).

Human carbonyl-reducing enzymes occur in many different tissues like liver (Ahmed *et al.*, 1979; Sawada and Hara, 1979; Sawada *et al.*, 1979; Felsted and Bachur, 1980; Hara *et al.*, 1986b), lung (Nakayama *et al.*, 1986; Nakanishi *et al.*, 1995), heart (Imamura *et al.*, 1999a; Imamura *et al.*, 1999b), kidney (Higuchi *et al.*, 1993; Imamura *et al.*, 1993), brain (Wermuth, 1981; Cromlish *et al.*, 1985; Iwata *et al.*, 1989; Iwata *et al.*, 1990b; Inazu *et al.*, 1992b; Wermuth *et al.*, 1995), ovary (Iwata *et al.*, 1989; Aoki *et al.*, 1997; Guan *et al.*, 1999), and adrenal (Oppermann *et al.*, 1991; Maser *et al.*, 1992) and are known to exhibit broad substrate specificities for xenobiotic aldehydes and ketones as well as for physiological carbonyl compounds such as biogenic aldehydes (Smolen and Anderson, 1976), prostaglandins (Hayashi *et al.*, 1989; Inazu and Satoh, 1994), and steroid hormones (Pietruszko and Chen, 1976; Ikeda *et al.*, 1984; Maser, 1995).

The difference in tissue and intracellular distribution suggests that several enzymes may be involved in the enzymatic reduction of carbonyl compounds and that the intracellular multiplicity of the enzymes may have some relation to their physiological function. Since the early seventies, a multitude of carbonyl-reducing enzymes has been purified and characterized in terms of substrate specificity and kinetic constants (Fig.1). While lots of data on these enzymes were accumulating, it was speculated that several of these enzymes are in fact identical to one another. On the basis of their primary structure, three of these enzymes were classified as aldehyde reductase (EC 1.1.1.2), aldose reductase (EC 1.1.1.21) (Bohren *et al.*, 1989) and carbonyl reductase (EC 1.1.1.184) (Wermuth *et al.*, 1988) (Fig. II-1) . As proposed by the scientific community working in this field, these enzyme names were adopted in the International Enzyme Nomenclature System and received their respective EC number. In addition, it turned out that there exist several isoforms of dihydrodiol dehydrogenase, which, initially, were summarized under EC 1.3.1.20. An interesting observation was that several hydroxysteroid dehydrogenases (HSDs) specifically catalyze the oxidoreduction at different positions of the steroid nucleus on the one hand, but on the other hand rather non-specifically catalyze the reductive metabolism of a great variety of non-steroidal xenobiotic carbonyl compounds. This was also true for the dihydrodiol dehydrogenases which were later shown to be HSDs (cf. chapter 1.2.2 of this review) (Ratnam *et al.*, 1999).



- alcohol: $NADP^+$-oxidoreductase
- high *Km* aldehyde reductase
- mevaldate reductase
- daunorubicin-pH 8.5 reductase
- hexonate dehydrogenase
- lactaldehyde reductase
- glucuronate reductase
- ALR 1

AKR → **aldehyde reductase (EC 1.1.1.2)**

- alditol: $NADP^+$-oxidoreductase
- low *Km* aldehyde reductase
- ALR 2

AKR → **aldose reductase (EC 1.1.1.21)**

- NADPH: sec.-alcohol oxidoreductase
- prostaglandin 9-ketoreductase
- daunorubicin-pH 6.0 reductase
- ALR 3

SDR → **carbonyl reductase (EC 1.1.1.184)**

- several isoforms of dihydrodiol dehydrogenases and/or

AKR → **hydroxysteroid dehydrogenases (AKR1C family)**

- several HSDs specified according to carbon atom involved in catalysis

SDR → **hydroxysteroid dehydrogenases (EC 1.1.1.xx)**

**Fig. II-1: Multiplicity of enzymes involved in carbonyl reduction**

Sequence comparisons and data base searches revealed that the enzymes mediating carbonyl reduction obviously belong to two large protein superfamilies. Whereas aldehyde reductase and aldose reductase belong to the aldo-keto reductases (AKR) (Jez *et al.*, 1997a), carbonyl reductase turned out to be a member of the short-chain dehydrogenases/reductases (SDR) (Jornvall *et al.*, 1995). The situation is not so clear-cut with the HSDs, since they were shown to belong to either the AKR or SDR superfamily. Until now, several of these pluripotent HSDs have been described**.** The coincident ability of these pluripotent enzymes to metabolize endogenous steroids and to reduce xenobiotic carbonyl compounds has evidently been invented twice and subsequently been conserved during evolution in these two different protein superfamilies, corresponding to the principle of convergent evolution (reviewed in (Maser, 1995)). At present, 12 different pluripotent carbonyl-reducing enzymes belonging to the AKR and SDR protein superfamilies are known in humans (Matsunaga *et al.*, 2006).

Sequence comparison, chemical modification and site-directed mutagenesis studies, combined with crystallographic analyses and bioinformatic data, led to the identification of important structural features and consensus sequences of these enzymes (see below).

## 1.1 The Aldo-Keto Reductase (AKR) Superfamily

The aldo-keto reductase (AKR) superfamily represents a growing superfamily of NADP(H)-dependent oxidoreductases, which accept many structurally different substrates of endogenous and exogenous origin. This protein superfamily includes, amongst others, aldose reductase (EC 1.1.1.21), aldehyde reductase (EC 1.1.1.2) and several HSDs (EC 1.1.1.x), some of which have previously been designated dihydrodiol dehydrogenases (EC 1.3.1.20) (Jez *et al.*, 1997b). These enzymes are monomeric $(\alpha/\beta)_8$-barrel proteins, about 320 amino acids in length, which bind their cosubstrate without a Rossmann-fold motif (Jez *et al.*, 1997b). The active site of the AKR members contains a conserved tetrad of the amino acids Tyr, His, Asp and Lys. Found in almost every living organism, the AKRs metabolize steroids, sugars, prostaglandins, polycyclic aromatic hydrocarbons, and a great variety of non-steroidal aldehydes and ketones.

The broad substrate specificity of some AKR proteins has led to some ambiguities, e.g. the indomethacin-sensitive cytosolic rat liver 3α-HSD has previously also been described as di-hydrodiol dehydrogenase, chlordecone reductase, or bile acid binding protein. To address these issues, a new nomenclature system for the AKR superfamily has been established (Jez *et al.*, 1997b). Based on amino acid sequence identities of the different AKR members, the superfamily currently comprises 14 families: AKR1 – AKR14. Mammalian AKRs are found predominantly in the AKR1 and AKR7 families, whereas members of the AKR2 – AKR5 and AKR8 – AKR14 families have been identified in plants, yeast and bacteria. The AKR6 family is formed by the β-subunit of the *Shaker*-related voltage-gated $K^+$-channel. An excellent source of more information is available on the AKR superfamily homepage (www.med.upenn.edu/akr) which has been created by TM Penning and coworkers. Many of the mammalian AKRs are potential therapeutic targets, and structure-based drug design may lead to compounds with the desired specificity and clinical efficacy.

## 1.2    Short-Chain Dehydrogenase/Reductase (SDR) Superfamily

The second superfamily to which carbonyl-reducing enzymes belong, the short-chain dehydrogenases/reductases (SDR), comprises a wide range of procaryotic and eukaryotic enzymes involved in functions as diverse as the metabolism of steroids, sugars, aromatic hydrocarbons and prostaglandins, the fixation of nitrogen and the synthesis of antibiotics (Persson *et al.*, 1991; Jornvall *et al.*, 1995). The superfamily is made up of enzymes averaging 250 – 350 amino acids in length which function independently of metal cofactors, and its members are readily distinguishable from those of the medium-chain and long-chain alcohol dehydrogenase superfamilies (Persson *et al.*, 1991; Jornvall *et al.*, 1995). Among the members of the various families and subfamilies of the SDRs, there are no structural similarities to the AKR proteins in spite of overlapping substrate specificities (Flynn and Green, 1993; Maser, 1995).

They exist as soluble or, in some cases, membrane-bound proteins, mostly homodimers or homotetramers (Ghosh *et al.*, 1994b; Ghosh *et al.*, 1995; Tanaka *et al.*, 1996a; Tanaka *et al.*, 1996b; Benach *et al.*, 1998). All SDR proteins share well-conserved primary structure elements that are restricted to certain segments in the sequence, indicating a possibly common fold, active site, reaction mechanism, and cosubstrate and substrate binding regions (Persson *et al.*, 1991; Jornvall *et al.*, 1995). Analysis of the three-dimensional structure of the SDRs

characterized so far shows that both NAD(H) and NADP(H) bind to the classical βαβ motif of the Rossmann fold which is characteristic of the coenzyme-binding domain of many other dehydrogenases (Duax et al., 2000). It depends on their predominant function as a dehydrogenase or reductase whether they use either NAD(P) or NAD(P)H as cosubstrate (cf. chapter 2.3.3 of this review).

The SDRs comprise a large and highly divergent superfamily with about 3000 known forms, including species variants (Persson *et al.*, 2003). They share a residue identity of typically 15-30% in pairwise comparison (Kallberg *et al.*, 2002a), indicating early duplicatory origins and extensive divergence (Jornvall *et al.*, 1995). Nevertheless, the folding pattern of the members whose structures have been solved so far is conserved with largely superimposable peptide backbones (Krook *et al.*, 1993b; Ghosh *et al.*, 2001).

The SDRs have initially been subdivided into two large families, the "classical" with 250-odd residues and the "extended" with 350-odd residues (Jörnvall *et al.*, 1995). Based on patterns of charged residues in the cosubstrate-binding region, these families have recently been classified in seven subfamilies of "classical" SDRs and three subfamilies of "extended" SDRs. Three further families are novel entities, denoted "intermediate", "divergent" and "complex", encompassing short-chain alcohol dehydrogenases, enoyl reductases and multifunctional enzymes, respectively (Persson *et al.*, 2003).

One of the most important physiological functions of the SDR enzymes appears to be the conversion of signalling molecules to either the active or inactive state (Krozowski, 1992).

## II.3      Hydroxysteroid Dehydrogenases as Carbonyl Reductases

Hydroxysteroid dehydrogenases (HSDs) are pyridine nucleotide-dependent oxidoreductases which mediate the interconversion of secondary alcohols and ketones. They play pivotal roles in the biosynthesis and inactivation of steroid hormones. Steroid hormones act by binding to receptor proteins in target cells, which leads to transcriptional regulation of different gene products and the desired physiological response. In target tissues, HSDs convert potent steroid hormones to their cognate inactive metabolites (and *vice versa*) and thus regulate the occupancy of steroid hormone receptors (Penning *et al.*, 1997; Duax *et al.*, 2000). The reactions

they catalyze are position- and stereospecific and usually involve the interconversion of a carbonyl and a hydroxyl group on either the steroid nucleus or side chain. In normal cell physiology, HSDs therefore function as important prereceptor regulators of signalling pathways by acting as "molecular switches" for receptor-active and receptor-inactive hormone (Monder and White, 1993; Penning *et al.*, 1996; Labrie *et al.*, 1997). Because the enzymes have much greater tissue specificity than the receptors, they have emerged as attractive targets for the design of potent and selective drugs that combat steroid-related disorders. HSDs are found in every organism investigated so far.

Interestingly, several HSDs exhibit other activities besides steroid oxidoreduction. In addition to being specific for their physiological steroid substrate, they can catalyze the carbonyl reduction of a great variety of non-steroidal aldehydes, ketones and quinones (reviewed in (Maser, 1995). Accordingly, HSDs participate in drug metabolism and play a significant role in the defence of an organism against the deleterious effects of endogenous and exogenous toxicants. Due to the fact that several enzymes of both superfamilies exhibit pluripotency for steroidal and non-steroidal carbonyl substrates (Maser, 1995), AKR and SDR seem to be the result of a convergent evolution.

Extensively characterized HSDs with carbonyl-reducing activity of the AKR superfamily are 3α-HSD (mammalian), 17β-HSD (mammalian) and 20α-HSD (mammalian and protozoan) [reviewed in (Maser, 1995; Matsunaga *et al.*, 2006)]. These HSDs are now classified within the AKR1C-subfamily. Extensively characterized HSDs with carbonyl-reducing activity of the SDR superfamily are 3α-HSD (bacterial), 3α/20β-HSD (mammalian and bacterial) and 11β-HSD (mammalian) [reviewed in (Maser, 1995; Matsunaga *et al.*, 2006)].

The sections below include recent findings on pluripotent HSDs/carbonyl reductases of the SDR protein superfamily.

# III General Features of the SDR Superfamily Enzymes

## III.1    Historical Background: Functional Characterization

Carbonyl reductases of the SDR superfamily accept some of the same substrates as do other carbonyl-reducing enzymes from the AKR superfamily  (Wermuth *et al.*, 1982). SDR carbonyl reductases do also metabolize aromatic ketones and quinones (Wermuth, 1982). In general, the metabolism of a broad spectrum of xenobiotic substrates results in their detoxification or inactivation, since the chemically more reactive carbonyl compounds (aldehyde or ketone) have been converted to less reactive and less lipophilic hydroxy intermediates that are easier to conjugate and to eliminate (Felsted and Bachur, 1980; Wermuth, 1985; Wermuth *et al.*, 1986; Atalla and Maser, 1999).

Human carbonyl reductase (CBR1) had been supposed to be involved in prostaglandin and steroid metabolism in some tissues (Lee and Levine, 1974a; Felsted and Bachur, 1980; Wermuth, 1981). Later, Wermuth (Wermuth *et al.*, 1986) and Schieber (Schieber *et al.*, 1992) showed that, due to high non-physiological Km values and low turnover numbers of the enzyme, as well as due to low tissue concentrations of the prostaglandin or steroid substrates, these compounds can at best be only poor endogenous substrates. In contrast, quinones from polycyclic aromatic hydrocarbons were much better substrates than prostaglandins or steroids (Wermuth *et al.*, 1986). The best substrates for human CBR1 comprise K region ortho-quinones of polycyclic aromatic hydrocarbons such as benzo[a]anthracene and benzo[a]pyrene (Wermuth *et al.*, 1986). Menadione and 9,10-phenanthrenequinone are excellent carbonyl reductase substrates, and menadione is often used as a model quinone substrate (Wermuth *et al.*, 1986).

Previously, it was suggested that carbonyl reductases could be divided into two groups with respect to their substrate specificity for endogenous prostaglandins and steroids (Ohara *et al.*, 1995). The first group, the carbonyl reductases of human tissues (Wermuth, 1981; Schieber *et al.*, 1992), pig kidney (Wermuth, 1981; Schieber *et al.*, 1992), and rat ovary (Iwata *et al.*, 1989) have been demonstrated or suggested to be identical to prostaglandin 9-ketoreductase or NADP$^+$-dependent 15-hydroxyprostaglandin dehydrogenase. The second group comprised hepatic carbonyl reductases of rats (Penning *et al.*, 1984), rabbits (Sawada *et al.*, 1980;

Fischer *et al.*, 1985), guinea pigs (Hara *et al.*, 1986a) and mice (Sawada *et al.*, 1988). This group did also possess 3α- or 17β-hydroxysteroid dehydrogenase and dihydrodiol dehydrogenase (DDH) (EC 1.3.1.20) activities and the individual enzymes have been thought to be identical to hydroxysteroid dehydrogenases and/or DDHs (Ohara *et al.*, 1995). As pointed out above, these enzymes are today classified as members of the AKR superfamily where they constitute the AKR1C subfamily (Hyndman *et al.*, 2003; Penning, 2005; Matsunaga *et al.*, 2006).

Lacking molecular tools, inhibitors have been used to characterize and to differentiate the multiplicity of carbonyl-reducing enzymes. As inhibitors for carbonyl reductases, flavonoids such as rutin, quercetin or quercitrin (Ahmed *et al.*, 1979; Sawada and Hara, 1979; Sawada *et al.*, 1979; Felsted and Bachur, 1980) have been used. In contrast, phenobarbital served as a diagnostic inhibitor of aldehyde reductase (Felsted and Bachur, 1980). Other inhibitors that have been identified for two carbonyl reductases from rat ovary were indomethacin, furosemide and disulfiram (Iwata *et al.*, 1989).

## III.2    SDR Superfamily Classification

The superfamily of short-chain dehydrogenases/reductases (SDR) includes members of great functional diversity, with sequence homologies of only 15-30%, but with very conserved specific sequence motifs as well as highly conserved folding patterns. The SDR superfamily was established in 1981 (Jornvall *et al.*, 1981). At that time, only two members were known to belong to this family, prokaryotic ribitol dehydrogenase and an insect alcohol dehydrogenase. Today, the SDR superfamily consists of more than 3000 members which cover a wide substrate spectrum including alcohols, sugars, steroids, prostaglandins, aromatic compounds and xenobiotics (Persson *et al.*, 2003). Their general primary structure is composed of a cofactor-binding region at the N-terminal part, a catalytic active site in the central part, a substrate-binding region, and a C-terminal extension important for oligomerization. Despite the low sequence identity, their three-dimensional structures superimpose very well, except for the C-terminal region, where the diversity between the SDR proteins is much higher (Persson *et al.*, 2003).

Initially, the SDR superfamily had been divided into 2 families, the "classical" and the "extended" SDRs. Classical SDRs consist of one-domain subunits of about 250 residues, whereas members of the "extended" SDR family consist of one-domain subunits of about 350 residues. Members of both families catalyze NAD(P)(H)-dependent oxidation/reduction reactions. Persson and coworkers (Persson *et al.*, 2003) further characterized the two families. The "extended" and "classical" families within the SDR superfamily differ, amongst others, in the glycine-rich pattern of the cofactor-binding region (Jornvall *et al.*, 1995). The three glycine residues are characteristic for NAD(P)H-binding and are spaced differently in the two families (Jornvall *et al.*, 1981; Jornvall *et al.*, 1999; Persson *et al.*, 2003). Further differences occur in the motif positioned close to strand β4, which is less conserved among "extended" SDRs than among "classical" SDRs, as well as in the residues adjacent to the active site, a fact which has been described in more detail in (Persson *et al.*, 2003).

Persson and coworkers (Persson *et al.*, 2003) used a trained hidden Markov model (Karplus *et al.*, 1998; Karplus *et al.*, 2005) which was based on a multiple sequence alignment with known SDRs as seed sequences to search the databases Swissprot (Apweiler *et al.*, 2000; Bairoch and Apweiler, 2000) and KIND (Kallberg and Persson, 1999) for further members of the SDR superfamily. They found that the SDR superfamily can be clustered into five instead of two families, namely the "intermediate", "divergent" and "complex" families, in addition to the already established "classical" and "extended" families. The overall features of these five families of the SDR superfamily are summarized in (Table III-1). The carbonyl reductases which we focus on in this article belong to the family of "classical" SDRs.

Carbonyl reductases which belong to the group of "classical" SDRs reduce aldehydes and keto groups of prostaglandins, steroids, pterins, and quinones derived from polycyclic aromatic hydrocarbons. In addition, many keto drugs as well as the aliphatic keto side chain of the anthracycline anticancer drugs daunorubicin and doxorubicin are reduced (Bachur, 1976; Ahmed *et al.*, 1978; Ahmed *et al.*, 1981; Felsted and Bachur, 1982).

| family \ feature | Divergent | Classical | Intermediate | Extended | Complex |
|---|---|---|---|---|---|
| Monomer size | | ~ 250 residues | ~ 250 residues | ~ 350 residues | |
| Cofactors | NADH | NAD(P)(H) | | NAD(P)(H) | NADP(H) |
| Catalytic reaction | | Oxidation/reduction | | | Beta-ketoacyl reduction |
| Cofactor binding | GxxxxxSxA (in bacteria) | TGxxxGhG | G/AxxGxxG/A | TGxxGhaG | |
| Coenzyme binding | N-terminal | N-terminal | N-terminal | N-terminal | N-terminal |
| Active site | YxxMxxxK | YxxxK | | | YxxxN |
| Substrate binding | C-terminal | C-terminal | C-terminal | C-terminal | C-terminal |
| Sequence identity (according to swissprot) | 28-99% | 8-99% | 27-99% | 10-99% | 20-74% |
| Examples | Enoyl reductases from bacteria and plants | Oxidoreductases (EC1.-.-.-), steroid dehydrogenases (including 11β-HSD1, 11β-HSD2, 3α-HSD/CR, 3α/20β-HSD), carbonyl reductases (including human CBR1 and CBR3) | Drosophila alcohol dehydrogenase | Isomerases (EC 5.-.-.-, galactose, epimerases) ; lyases (EC 4.-.-.- , glucose dehydratases) oxidoreductases | Parts of multifunctional enzyme complexes (fatty acid synthase) |

**Table III-1: Features of the five families within the SDR superfamily according to Persson and coworkers (Kallberg *et al.*, 2002b; Persson *et al.*, 2003).**

Each of the five SDR families contain conserved sequence patterns, where "a" signalises an aromatic residue, "h" a hydrophobic residue, and "x" any residue. Amino acid residues are given in the one-letter code. Items with no data mean that no information was available in the literature.

## III.3    Structural Features of the SDR Members

As indicated above, the criterion for SDR membership is the occurrence of typical sequence motifs which are arranged in a specific manner, called Rossmann fold (Rossmann *et al.*, 1975). These conserved residues play significant roles in the catalytically active site, the substrate binding region, the cofactor binding motif, and the C-terminal extension (Fig. III-1 and Fig. III-2).
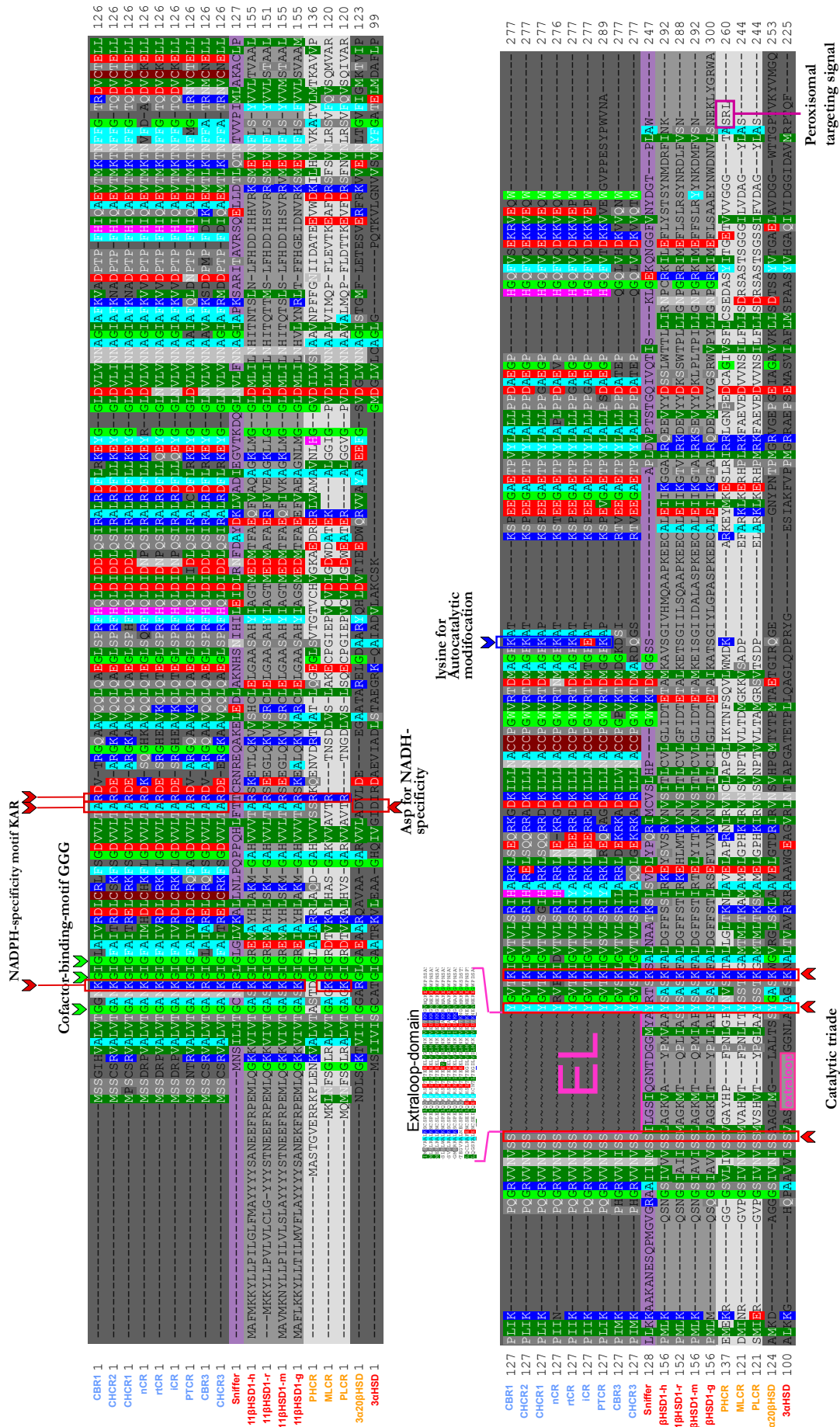
**Fig. III-1: Multiple sequence alignments of some well-known members of the SDR superfamily**
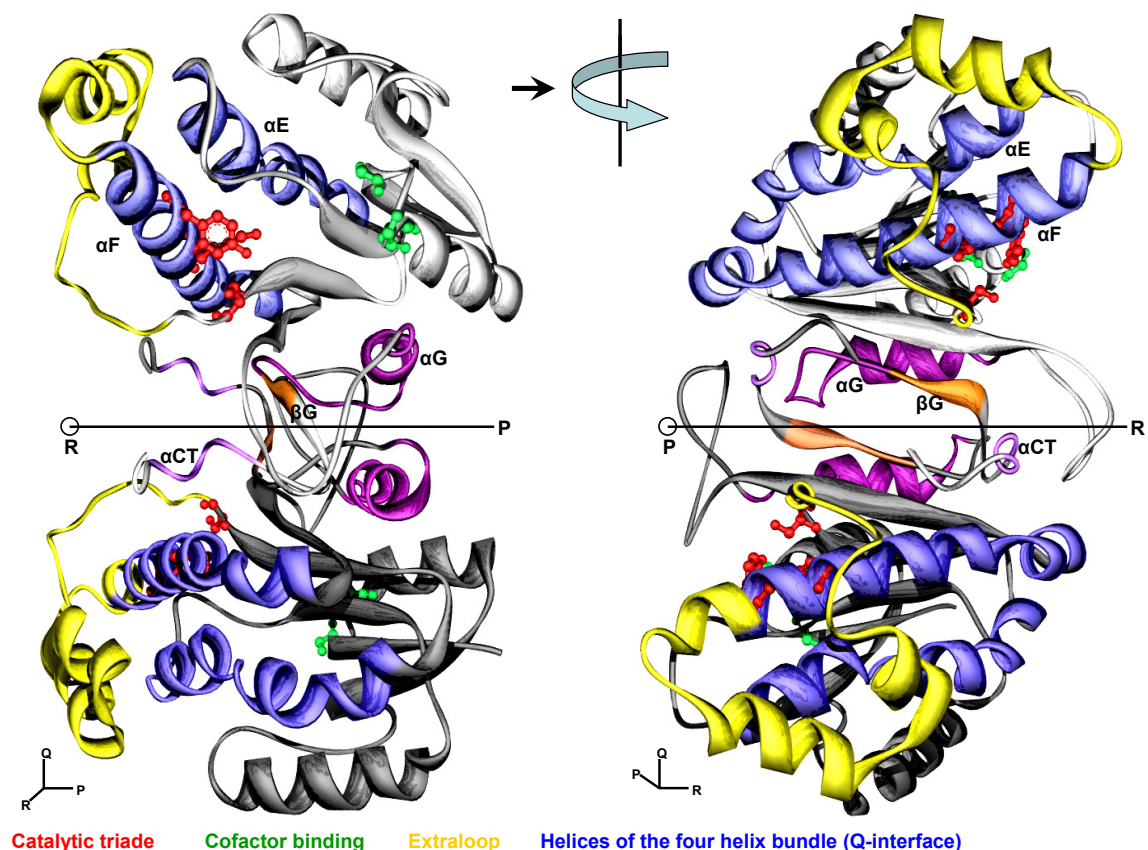
Abbreviations: CBR1, CBR3 (human carbonyl reductase 1 and 3); CHCR1, CHCR2, CHCR3 (Chinese hamster carbonyl reductases 1-3); iCR, nCR, rtCR (inducible, non-inducible and rat-testis carbonyl reductase); *Sniffer* (carbonyl reductase *Sniffer* from *Drosophila*); 11β-HSD1-h, 11β-HSD1-m, 11β-HSD1-r, 11β-HSD1-g (11β-HSDs from human, mouse, rat and guinea pig); PHCR (pig heart carbonyl reductase); MLCR (mouse lung carbonyl reductase); PLCR (pig lung carbonyl reductase); 3α/20β-HSD (*S. hydrogenans*); 3α-HSD/CR (*C. testosteroni*).

The alignment indicates the existence of an extraloop-domain upstream of the conserved Tyr-x-x-x-Lys motif within the monomeric enzymes from human, Chinese hamster and rat. This extraloop-domain can also be found in the dimeric 3α-HSD/CR from *C. testosteroni*. Monomeric enzymes are marked in blue, dimeric enzymes in red and tetrameric enzymes in yellow. Colored residues represent conservation of 50% identity. Alignment was performed using the clustalW- and bioedit-program.

The overall structure of the SDR superfamily members is built up of a sequence of alternating α-helices and β-strands. These β-strands form a four- or five-stranded parallel β-sheet with two or three α-helices residing on either side. This dinucleotide binding motif composed of βαβ units is called Rossmann fold (Rossmann *et al.*, 1975). The Rossmann fold in the SDR superfamily is very stable, tolerating, despite little sequence conservations, some mutations at every site of the folding motif without loss of function (Duax *et al.*, 2000). It is less readily understood how a protein conformation as consistent as the Rossmann fold has no structurally conserved residues. Once substrate specificity evolved, changes in the active site could lead to loss of function or change in specificity. It appears that in the SDR superfamily, function evolved early, while specificity evolved later (Duax *et al.*, 2000).

### III.3.1    Catalytic Triade and Catalytic Mechanism

Already in 1981, the importance of the Tyr-x-x-x-Lys segment as the most conserved sequence motif of the SDRs became apparent (Jornvall *et al.*, 1981). Nearly all "classical" SDR enzymes use the conserved Tyr-Lys-Ser motif as catalytic residues (Jornvall *et al.*, 1995), whereas the enzymes of the "divergent" use the sequence motif Tyr-x-x-Met-x-x-x-Lys  with the tyrosine being positioned three amino acids upstream as compared to Tyr-x-x-x-Lys. The subfamily of the "complex" SDRs have the unique motif Tyr-x-x-x-n (where n means any other amino acid) at the active site (Persson *et al.*, 2003). The amino acids which constitute the catalytic triad are critically important for enzyme function. They appear to maintain a fixed position relative to the scaffolding of the βαβ-folding and the cofactor position.

**Catalytic triade**    **Cofactor binding**    **Extraloop**    **Helices of the four helix bundle (Q-interface)**

**Fig. III-2: Folding topology of 3α-HSD/CR from *C. testosteroni*.**

The conserved structural elements involved in oligomerization are named only for the upper one of the two subunits. Note that the four helix bundle (Q-interface; blue) is blocked by the extraloop-domain (yellow). Therefore, oligomerization (dimerization) takes place only via helix αG and strand βG (P-interface; purple).

Most likely, all SDRs share a common reaction mechanism which follows a compulsory ordered pathway with the cofactor binding first (Grimm *et al.*, 2000b). After the hydroxyl or carbonyl substrate binds, the so-called substrate binding loop becomes well ordered and covers the substrate as well as the catalytic center from the aqueous environment. This substrate binding loop is highly flexible in most apo-structures of SDRs. Ghosh and coworkers (Ghosh *et al.*, 1994b) proposed a model for 3α/20β-HSD in which the conserved residues Tyr, Lys and Ser, together with solvent molecules, could catalyze the reaction in the catalytic cavity (Fig. III-3). The Tyr hydroxyl has been proposed to be the proton donor in an electrophilic attack on the substrate carbonyl in a reduction reaction (Ghosh *et al.*, 1994b). The positively charged side chain of Lys is positioned in proximity to the hydroxyl oxygen of Tyr and facilitates the proton transfer. The Ser also participates in catalysis by stabilizing the reaction intermediates or as part of a proton-relay network. After the proton is transferred from Tyr to

the 20-keto oxygen of the steroid, it can be replenished by the solvent surrounding the residues in the catalytic cavity (Ghosh *et al.*, 1994b; Duax *et al.*, 2000). The substrate is oriented by the catalytic Ser which stabilizes the transient reaction intermediate (Grimm *et al.*, 2000b). The conserved Lys-residue plays a dual role in the catalytic triad. It orients the cofactor by forming hydrogen bonds to the nicotinamide-ribose moiety and lowers the $pK_a$ of the catalytic Tyr via electrostatic interaction (Ghosh *et al.*, 1994b; Auerbach *et al.*, 1997; Benach *et al.*, 1999).
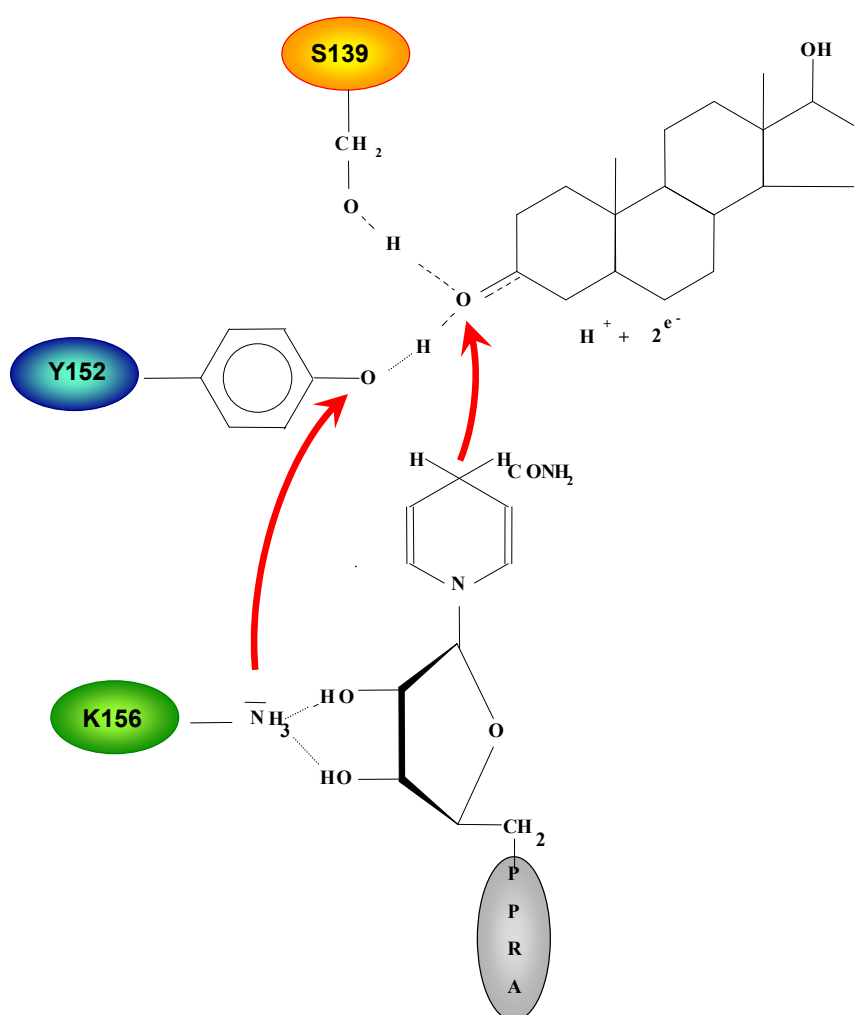


**Fig. III-3: Reaction mechanism and catalytic triade exemplified by 3α/20β-HSD from *S. hydrogenans***

### III.3.2 Substrate Binding and Substrate-Binding Loop

Most of the amino acid residues which are partially conserved within the SDR superfamily members are located in the core of the Rossmann fold and are primarily hydrophobic (Duax *et al.*, 2000). The only conserved residues in the substrate-binding cleft are those of the catalytic triad: Ser, Tyr and Lys. No conserved residues can be found in the substrate-binding site. This is indicative for the fact that, for example, the HSDs show high selectivity for their specific physiological steroid substrate. However, for the carbonyl reductases, specific endogenous substrates have not been identified until now, they rather display broad substrate specificities, ranging from steroids, prostaglandins, sugars and alcohols to xenobiotic aldehydes and ketones (Duax *et al.*, 2000).

Usually, SDR enzymes have a substrate-binding loop of more than 20 residues which covers the active site and becomes well ordered after the hydroxyl or carbonyl substrate binding. This loop region is located between β-strand F (βF) and α-helix G (αG) and is very often disordered in apo-structures (without substrate) of SDR enzymes. After substrate binding, the loop shows a well-defined, mainly α-helical, geometry. In *Sniffer* from Drosophila no α-helical secondary structure element is apparent in the substrate-binding loop (Sgraja *et al.*, 2004). Here, in the presence of $NADP^+$, only a short loop could be detected in the electron density which connects strand βF and helix αG (Sgraja *et al.*, 2004) (Fig. III-4) .

When the α-carbon backbone of known SDR structures is superimposed, the conserved residues appear at the core of the structure and in the cofactor-binding domain, but not in the substrate-binding pocket (Duax *et al.*, 2000). Contrary to the variability in the substrate-binding pocket, the association of the Rossmann fold with the cofactor binding is very consistent and the NADP(H) binding domains exhibit architectural integrity, despite having sequence variations (Duax *et al.*, 2000). The variability in the substrate-binding pocket is plausible when keeping in mind the variety of structures used as substrates by different members of the SDR superfamily (Duax *et al.*, 2000).

### III.3.3 Cofactor Binding

In the N-terminal part of the SDR proteins, a glycine-rich pattern important for cofactor binding has been identified (Jornvall *et al.*, 1995). This conserved sequence motif includes three glycine residues which are located at comparable points in their sequences and form a turn between a *β*-strand and an *α*-helix that border the cofactor-binding site (Duax *et al.*, 2000). Structural analysis has shown that the glycine residues interact with the pyrophosphate moiety of the cofactor. The individual subfamilies of the SDR superfamily differ regarding the spacing of the three glycine residues, where the Gly-x-x-x-Gly-x-Gly motif, for example, is characteristic for the subfamily of the "classic" SDRs (Jornvall *et al.*, 1981; Jornvall *et al.*, 1999). The use of either reduced or oxidised NAD(P) as cofactor depends on their predominant function as a dehydrogenase or reductase of individual members of the SDR superfamily. In addition, both NAD(H) and NADP(H) bind to the classical βαβ motif of the Rossmann fold. The specificity for NADP(H), rather than to NAD(H), is conferred by two highly conserved basic residues in the N-terminal part of the peptide chain. Tanaka et al. (Tanaka *et al.*, 1996a) identified two basic residues (Lys-17 and Arg-39) in the tetrameric mouse lung carbonyl reductase (MLCR) which promote NADPH binding by interaction with the 2'-phosphate group. These residues are believed to confer specificity for NADPH in other SDRs as well.

Human monomeric carbonyl reductase (CBR1) exhibits less than 25% overall sequence identity with tetrameric MLCR (Jornvall *et al.*, 1995). However, similar to MLCR, human CBR1 has distal basic (Lys-15 and Arg-38) and neutral (Ala-37) residues at positions corresponding to Lys-17, Arg-39 and Thr-38 in tetrameric MLCR (Tanaka *et al.*, 1996a) and is strictly NADPH-dependent (Wermuth *et al.*, 1988; Sciotti and Wermuth, 2001). Sciotti and Wermuth (Sciotti and Wermuth, 2001) showed that a positive charge at positions 15 and 38 and the absence of a negative charge at position 37 significantly contribute to NADPH specificity. SDR enzymes which are NAD-dependent lack these two basic residues. Instead, an Asp which is adjacent to the position of the distal basic residue in NADPH-dependent enzymes appears to determine NAD specificity (Sciotti *et al.*, 2000). Sequence alignments of NAD-dependent enzymes with the NADPH-dependent tetrameric and monomeric carbonyl reductases show that Ala-37 of the monomeric and Thr-38 of the tetrameric carbonyl reductase correspond to the Asp residue which plays a role in NAD specificity. Sciotti and Wermuth (Sciotti and Wermuth, 2001) substituted Asp for Ala-37 in the strictly NADPH-dependent human CBR1. Unexpectedly, the Asp residue had little effect on the NADH-dependent activity and NADPH

was still the preferred substrate of the mutant Ala37Asp. Therefore, factors other than only the absence of Asp at position 38 must be responsible for the low efficiency of monomeric human CBR1 in the presence of NADH Fig. III-1.

### III.3.4    C-terminal Extension and $3_{10}$-Helices

Many enzymes of the SDR superfamily contain a C-terminal extension consisting of several α-helices. Examples are human estrogenic 17β-HSD (Ghosh *et al.*, 1995) and the Drosophila enzymes alcohol dehydrogenase (DADH) and *Sniffer*. Benach and coworkers showed in DADH that these C-terminal helices, which are of more variable character, are main elements of dimer association and that these structural features have additional importance in closing of the active site cavity upon cofactor and substrate binding (Benach *et al.*, 1998).

$3_{10}$-helices are structural elements which are present as α-helical extensions in loops and as connectors between β-strands (Pal and Basu, 1999). In many cases they occur independently of any other neighbouring secondary structural elements and form novel super-secondary structural motifs. These motifs have possible implications for protein folding, local conformational relaxations and biological functions (Pal and Basu, 1999).

The *Sniffer* protein has both structural features which contribute together to dimer formation. At the C-terminal end of the *Sniffer* protein there is a short loop with a sharp turn directly following strand βG. This loop runs perpendicular to the central β-sheet of the Rossmann fold and touches the $3_{10}$-helix following strand βE. The C-terminal ends of the two monomers approach each other and the indole moiety of the Trp-248 interacts through its planar ring system with the side-chain of Ile-159 which is rooted at the $3_{10}$-helix of the second subunit (Sgraja *et al.*, 2004).

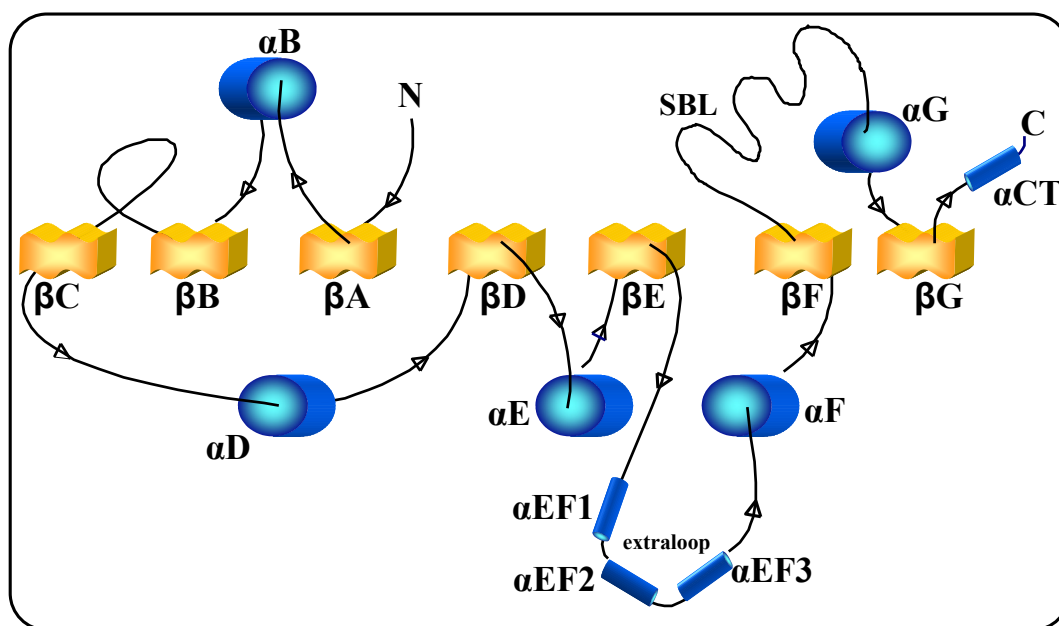### III.3.5    Oligomerization and Interfaces

The enzymes of the SDR superfamily can be divided into different groups concerning their oligomerization behaviour, their subcellular localization and the existence of structural elements with significant effects on protein folding. Most enzymes of the superfamily appear as either homodimers, e.g. *Sniffer* (Sgraja *et al.*, 2004), DADH (Benach *et al.*, 1998) and dihy-

dropteridine reductase (DHPR) (Varughese *et al.*, 1992), or homotetramers like 3α/20β-HSD (Ghosh *et al.*, 1994b) and mouse lung carbonyl reductase (Tanaka *et al.*, 1996a). Only few members occur as monomers like for example human carbonyl reductase (CBR1) (Wermuth, 1981) and pig testicular carbonyl reductase (PTCR) (Ghosh *et al.*, 2001). In spite of the low residue identities between the SDR members, the folding pattern of the individual (sub-) units is highly conserved with largely superimposable peptide backbones (Krook *et al.*, 1993b; Ghosh *et al.*, 2001) (Fig. III-4).

Two types of oligomerization, involving different structural elements, can be found. One type of monomer association is the so-called P-axis interface comprising the antiparallel associa-tion of β-strand G and α-helix G of each subunit (Ghosh *et al.*, 1994b). This type of oli-gomerization is usually found in homotetrameric SDRs and has only been observed in one dimeric SDR, namely 3α-HSD/CR from *C. testosteroni* (Grimm *et al.*, 2000a). The P-axis interface does not involve significant hydrophobic interactions (Ghosh *et al.*, 1994b) and is less critical to the structural integrity of the active site than the second type of oligomeriza-tion, the so-called Q-axis interface.

The Q-axis interface consists of α-helix E and α-helix F of each of the two subunits to form a bundle of four helices. This four helix bundle represents the most important structural motif of the Q-axis interface, especially in dimeric SDR proteins. It is predicted to be important for the integrity of the active site clefts and has been shown to be critical to function (Puranen *et al.*, 1997; Ghosh *et al.*, 2001). In addition, although more than half of the crystal structures of SDRs exhibit the same quaternary structure, only the four helix bundle as the main structural feature of the Q-axis interface that involves the largest surface area of association (Ghosh *et al.*, 1994b) is conserved among the SDRs.

**Fig. III-4: Typical Rossmann fold of SDR enzymes exemplified by 3α-HSD/CR from *C. testosteroni*.**

3α-HSD/CR contains an unordered substrate binding loop (SBL) and an extraloop-domain between strand βE and helix αF which normally are part of the four helix bundle as the main structural feature of the oligomerization Q-interface.

The dimerization interface is close to the active site and stabilizes the interior of the molecule. Tsigelny and Baker postulated that the neighbouring amino acids of the conserved tyrosine and lysine residues in the active site of SDR family members might interact with the hydrophobic outer surface of the αF helix and hence stabilize the dimer interface of the proteins (Tsigelny and Baker, 1995b). Therefore, it is suggested that monomerization of dimeric or tetrameric proteins in the SDR family most likely abolishes their enzyme activity. Hoffmann and coworkers (Hoffmann *et al.*, 2006) redesigned the region of the interfacial four helix bundle in the dimeric 3α-HSD/CR from *C. testosteroni*, which comprises an additional α-helical subdomain preventing the enzyme of dimerization along the typical Q-axis interface. Their data of a soluble and active protein will give further insights into the requirements of a protein for the architecture of the active site and the structural elements comprising the Q-axis interface.

In the dimeric human 17β-HSD, Puranen and coworkers (Puranen *et al.*, 1997) substituted amino acids of the four helix bundle within the hydrophobic Q-axis interface resulting in inactive multi-aggregates of the protein, while neither dimers nor monomers were detectable. Ghosh and coworkers were also able to show that the four helix bundle is critical for protein

function. Disruptions of the helix arrangement had negative effects on the integrity of the catalytic centres of the oligomerizing monomers in 3α/20β-HSD of *S. hydrogenans* (Ghosh *et al.*, 2001).

An example for a cytosolic and monomeric carbonyl reductase is human CBR1. The reason for the monomeric structure of this enzyme is a so-called additional extraloop-domain between the Q-interfacial strand βE and helix αF which is believed to prevent oligomerization along the Q-axis interface built up of the four helix bundle. Other monomeric carbonyl reductases include this α-helical subdomain as well, but with different length. Among the monomeric carbonyl reductases with an additional subdomain are pig testicular carbonyl reductase (PTCR) which has a sequence identity to human CBR1 of nearly 85%, as well as the cytosolic and monomeric carbonyl reductases of rat (non-inducible, nCR; inducible, iCR; testis, rtCR) and Chinese hamster (CHCR).

The group of tetrameric carbonyl reductases is not as consistent as the group of monomeric carbonyl reductases. Tetrameric carbonyl reductases can be found on the subcellular level in the mitochondria (namely carbonyl reductases from mouse and pig lung) (Nakayama *et al.*, 1986; Oritani *et al.*, 1992) and in the cytoplasm, i.e. 3α/20β-HSD from *S. hydrogenans* (Ghosh *et al.*, 1992; Ghosh *et al.*, 1994a; Ghosh *et al.*, 1994b)**.** The tetrameric carbonyl reductase from pig liver is a peroxisomal protein which contains the SRL-tripeptide (serine-arginine-leucine) as a peroxisomal targeting signal (Usami *et al.*, 2003) (cf. chapter IV ).

The Q-interfacial dimer interface of which *Sniffer* provides a typical example is also present in tetramers (3α/20β-HSD). This interface is stabilized by interactive associations of symmetry related α-helices αE and αF. It has been shown that while conservative variations in amino acids (i.e. substitution of one hydrophobic residue for another) is tolerated, non-conservative mutations can disrupt dimer formation and cause loss of function (Duax *et al.*, 2000).

A special case represents dimeric 3α-HSD/CR from *C. testosteroni*. This enzyme does not undergo oligomerization along the Q-axis interface, because the protein contains an α-helical extraloop-domain within this Q-interfacial four helix bundle. As with the monomeric carbonyl reductases containing this α-helical extraloop-domain, oligomerization along this interface region is prevented because of the disruption of the Q-axis interface. Most interestingly, 3α-HSD/CR performs dimerization along the P-axis interface (Grimm *et al.*, 2000b). However, this type of oligomerization via the P-axis interface can only be found in tetrameric SDRs such as for example in 3α/20β-HSD from S. *hydrogenans* (Ghosh *et al.*, 1994b) (see above).

# IV Pluripotent Carbonyl Reductases of the SDR Superfamily

Carbonyl-reducing enzymes can be found ubiquitously in nature and they have been shown to catalyze the NADPH-dependent reduction of a wide variety of biologically and pharmaco-logically active substrates, as well as a variety of endogenous and xenobiotic carbonyl compounds including quinones (Felsted and Bachur, 1980; Wermuth, 1985; Ohara *et al.*, 1995; Oppermann and Maser, 2000; Breyer-Pfaff *et al.*, 2004; Breyer-Pfaff and Nill, 2004; Maser, 2004; Maser *et al.*, 2005; Hoffmann *et al.*, 2006; Martin *et al.*, 2006; Maser *et al.*, 2006). As suggested for two-electron transferring quinone reductases (Lind *et al.*, 1982), carbonyl reductase might function as a cellular mechanism to control the toxicity of quinones, especially in humans (Wermuth *et al.*, 1986). In addition, reactive aldehydes derived from lipid peroxidation were found to be substrates for the enzyme (Doorn *et al.*, 2004; Hoffmann *et al.*, 2006). Interestingly, activity toward endogenous prostaglandins and steroids has been demonstrated, although the low catalytic efficiency reported raised skepticism that these compounds are physiological substrates of carbonyl reductases and that the corresponding pathways represent a physiological role for the enzymes (Chang and Tai, 1981; Wermuth, 1981; Jarabak *et al.*, 1983; Forrest and Gonzalez, 2000).  Therefore, a general detoxification role for foreign and metabolically derived carbonyl compounds seems to account for the enzymes' wide substrate specificity and its ubiquitous distribution in human tissues (Wirth and Wermuth, 1992). An evolutionary classification of the SDR superfamily members involved in carbonyl reduction is shown in Fig. IV-1.
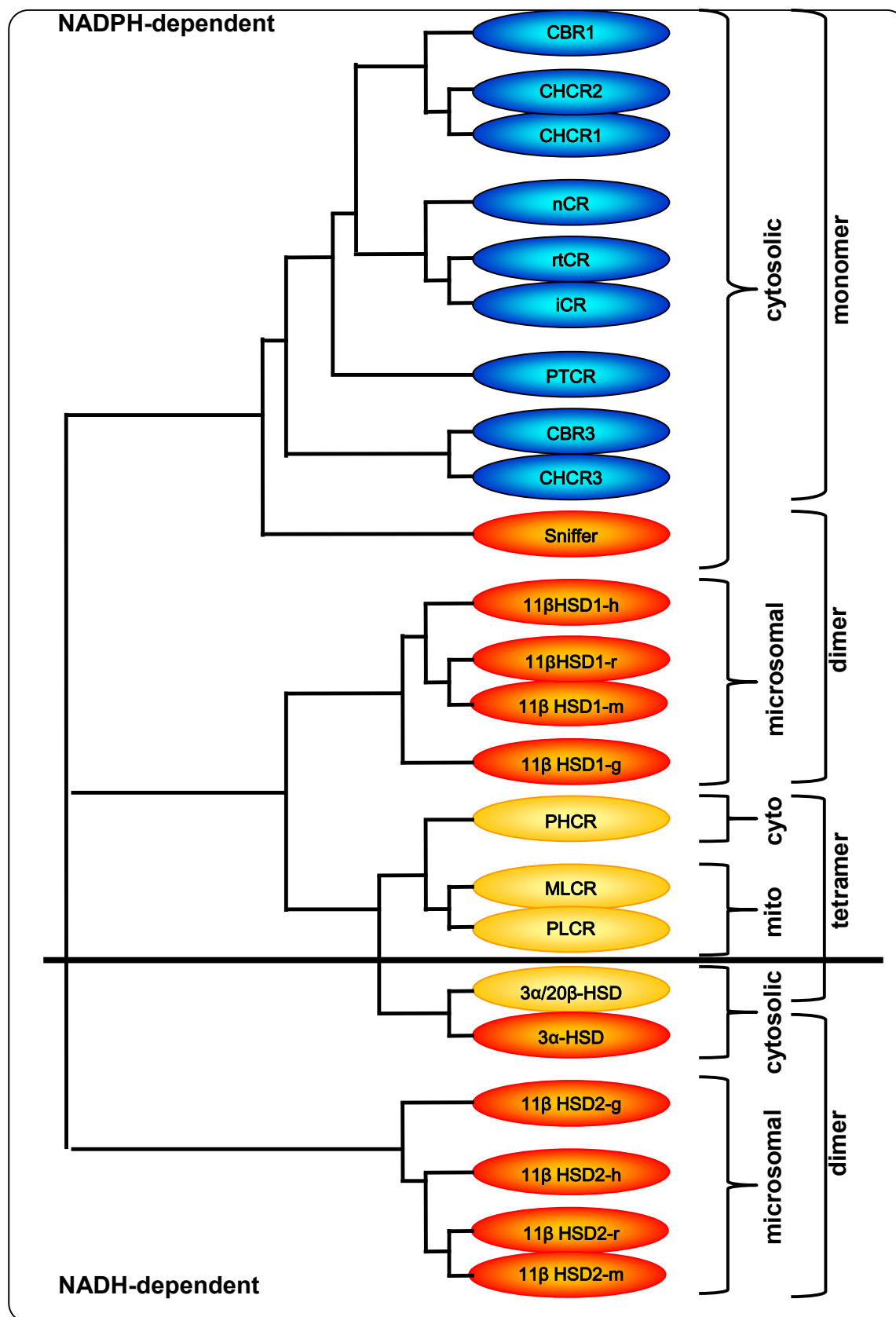
**Fig. IV-1: Evolutionary tree of carbonyl-reducing enzymes from different species**

The nomenclature is according to Fig.2.

## IV.1    Carbonyl Reductases in Non-Mammals

Carbonyl reduction in microorganisms was mainly investigated by chemists who are interested in the production of optically active alcohols (Roberts, 1997; Faber, 1998). However, the studies were generally performed with crude cell extracts and the specific enzyme involved was often unclear. Only a few papers reported serious work on the purification, identification and characterization of carbonyl reductases and aldehyde reductases from microorganisms such as *Saccharomyces cerevisiae (*Ypr1p, 2-methylbutyraldehyde reductase) (Ford and Ellis, 2001; Ford and Ellis, 2002), *Sporobolomyces salmicolor*, *Candida magnoliae* (NADPH-dependent aldehyde reductase, ARII) (Kita et al., 1999), *Geotrichum candidum* (Matsuda et al., 2000), *Rhodococcus erythropolis* (carbonyl reductase, RECR) (Zelinski et al., 1994), and *Escherichia coli* (2,5-diketo-D-gluconate reductase) (Oh *et al.*, 1999; Yum *et al.*, 1999a; Yum *et al.*, 1999b; Habrych *et al.*, 2002; Thibault *et al.*, 2004). In the future, reduction of carbonyl compounds by microorganisms might gain great importance for biotechnological uses (Ellis, 2002) or in the field of environmental sciences.

### IV.1.1    3α/20β-Hydroxysteroid Dehydrogenase of *Streptomyces hydrogenans*

*Streptomyces hydrogenans* belongs to the actinomycetes which are common in soil, plant debris, dung, house dust, and many other habitats (Waksman, 1961; Backlund *et al.*, 2005). 3α/20β-Hydroxysteroid dehydrogenase (3α/20β-HSD) from *S. hydrogenans* is an NADH-linked enzyme which is involved in the reversible oxidation of the 3α-group of androstane derivatives and the 20*β*-group of pregnane derivatives (Sweet and Samant, 1980). Interestingly, although there is no known steroid hormone function in bacteria, the *S. hydrogenans* gene encodes a hydroxysteroid dehydrogenase enzyme (Duax *et al.*, 2000).

The structure of 3α/20β-HSD was the first structure solved and determined by X-ray diffraction of an enzyme belonging to the SDR superfamily and the third structure of an enzyme for which steroids are the substrate (Ghosh *et al.*, 1991). The active form of the enzyme is a tetramer. The four identical monomers each consist of 253 amino acids with a calculated molecular mass of around 26 kDa and containing a single domain incorporating the active site and the Rossmann fold cofactor binding motif (Ghosh *et al.*, 1994b).

In a proposed catalytic mechanism of the 3α/20β-HSD enzyme, the Tyr-152 hydroxyl proton initiates the electrophilic attack on the 20-keto oxygen of the steroid (Duax *et al.*, 2000). The

positively charged side chain of Lys-156 lies in close proximity to the Tyr-152 hydroxyl oxygen and facilitates proton transfer. Ser-139 participates in catalysis by stabilizing the reaction intermediates and as part of a proton-relay network, in which a proton, once transferred from Tyr-152 to the 20-keto oxygen of the steroid, can be replenished by the solvent network surrounding these residues in the catalytic cavity (Ghosh *et al.*, 1994b; Duax *et al.*, 2000). This mechanism of catalysis does also apply to other members of the SDR superfamily.

### IV.1.2    3α-Hydroxysteroid Dehydrogenase/Carbonyl Reductase of *Comamonas testosteroni*

Procaryotic 3α-hydroxysteroid dehydrogenase/carbonyl reductase (3α-HSD/CR) has been first described in the gram-negative bacterium *Pseudomonas testosteroni* which was later renamed *Comamonas testosteroni* and reclassified as belonging to the β2-group of the Proteobacteria (Michel-Briand, 1969; Michel-Briand and Roux, 1969; Skalhegg, 1975; Aukrust *et al.*, 1976; Shikita and Talalay, 1979; Tamaoka *et al.*, 1987; Oppermann *et al.*, 1993; Suzuki *et al.*, 1993; Abalain *et al.*, 1995; Floch *et al.*, 1995). *C. testosteroni* has been first isolated from soil, mud and water, but has also been found in clinical isolates of patients suffering from purulent meningitis (Arda *et al.*, 2003)**,** endocarditis (Heredia *et al.*, 2004) and cystic fibrosis (Coenye *et al.*, 2002).

These bacteria are strictly aerobic, nonfermentative and chemoorganotrophic. They rarely attack sugars, but grow well on organic acids and amino acids (Willems et al., 1992). In addition, *C. testosteroni* is able to grow on steroids as sole carbon source (Talalay *et al.*, 1952).

3α-HSD/CR is one of the first enzymes of the steroid catabolic pathway and, therefore, plays a central role in steroid metabolism in *C. testosteroni*. The enzyme mediates the oxidoreduction at position 3 of the steroid nucleus of a great variety of $C_{19-27}$ steroids. This reaction is of importance in the initiation of the complete degradation of these relatively inert substrates and may significantly contribute to the bioremediation of hormonally active compounds in the environment. The enzyme is also involved in the degradation of fusidic acid, thereby providing resistance of *C. testosteroni* towards this steroid antibiotic produced by the fungus *Fusidium coccineum* (Oppermann *et al.*, 1996).

In addition to steroids, 3α-HSD/CR accepts as substrates a wide spectrum of non-steroid xenobiotic carbonyl compounds such as the cytochrome P450 inhibitor metyrapone, a metyrapone-based class of environmentally safe anti-insect agents, e.g. NKI 42255 (2-(1-imidazolyl)-1-(4-methoxyphenyl)-2-methyl-1-propanone) (Darvas *et al.*, 1991; Belai *et al.*, 1995; Oppermann *et al.*, 1996) (cf. chapter V.8 ; Detoxification of Insecticides), or the significantly smaller p-nitrobenzaldehyde (Oppermann and Maser, 1996; Mobus and Maser, 1998). Due to this fact, the enzyme's name was extended from 3α-hydroyxsteroid dehydrogenase (3α-HSD) to 3α-hydroyxsteroid dehydrogenase/carbonyl reductase (3α-HSD/CR).

Interestingly, the expression of 3α-HSD/CR in *C. testosteroni* is inducible by steroids (Möbus et al., 1997). Steroid-induced bacterial cells exhibit a significantly faster degradation of steroids, as well as a faster uptake and metabolism of NKI 42255 (Oppermann *et al.*, 1996). Therefore, induction by steroids results not only in an increase of resistance towards the steroid antibiotic fusidic acid, but also in an enhancement of insecticide detoxification (Oppermann *et al.*, 1996).

3α-HSD/CR uses NAD(H) as cofactor, depending on the reaction direction. Biochemical and structural analysis revealed that the enzyme appears as a homodimer with a mode of oligomerization along the P-axis interface analogous to tetramerization of 3α/20β-HSD from *S. hydrogenans* (Ghosh *et al.*, 1994b). Until then, this way of oligomerization had never been observed in a dimeric SDR enzyme, where dimerization usually takes place via the Q-axis interface (Grimm *et al.*, 2000a), e.g. in *Drosophila melanogaster* alcohol dehydrogenase (Benach *et al.*, 1998) and *Sniffer* (Sgraja *et al.*, 2004) (cf. chapter III.3.5; Oligomerization and Interfaces).

### IV.1.3    Insect Carbonyl Reductase: *Sniffer* of *Drosophila melanogaster*

The *Drosophila melanogaster* carbonyl reductase *Sniffer* is a NADPH-dependent member of the SDR superfamily. The enzyme shows similarity with human carbonyl reductases CBR1 (27,4%) and CBR3 (24,9%) (Botella *et al.*, 2004).

Interestingly, *Sniffer* knock-out mutants had a reduced lifespan, showed  motoric dysfunctions and exhibited age-related and oxidative stress-induced neurodegeneration (Botella *et al.*,

2004). All symptoms of the altered phenotype resembled those in patients with neurodegenerative dysfunction. Histological analysis of the central nervous system showed an increased vacuolization and apoptosis in the brain of mutant flies compared to wild-type flies. In contrast, overexpression of the carbonyl reductase *Sniffer* not only rescued the phenotype but even induced a prolonged survival of neurons under hyperoxia conditions in wild-type flies (Botella et al., 2004). These results suggested an important role of the carbonyl reductase *Sniffer* in the neuroprotection against oxidative stress.

Besides being structurally related to CBR1, the *Sniffer* protein exhibited carbonyl reductase activities with the CBR1 substrates 9,10-phenanthrenequinone, p-nitrobenzaldehyde, pyridine-4-carboxaldehyde and menadione (Botella *et al.*, 2004). Since human CBR1, in turn, was shown to catalyze the carbonyl reduction of 4-oxononenal (Doorn *et al.*, 2004), it is anticipated that the mechanism of neuroprotection by *Sniffer* in Drosophila is due to the detoxification of reactive aldehydes derived from lipid peroxidation after oxidative stress (Hoffmann *et al.*, 2006) (cf. chapter V.3 ; Neuroprotection by Carbonyl Reductase?).

Gel-filtration experiments and the crystal structure revealed unambiguously that *Sniffer* appears as a dimer in solution, with a molecular mass of each monomer of 28 kDa. In the *Sniffer* protein the two long helices αE and αF from two adjacent protein molecules associate to form the four helix bundle (Sgraja *et al.*, 2004) (cf. chapter III.3.5; Oligomerization and Interfaces). This mode of oligomerization is observed in most other dimeric SDRs whose structures have been solved so far (Ghosh *et al.*, 1994b; Tanaka *et al.*, 1996a; Benach *et al.*, 1998). The only exception of this rule is 3α-HSD/CR from *C. testosteroni*, where dimerization occurs via an interface region observed only in homotetrameric SDRs (Grimm *et al.*, 2000a) (cf. chapter III.3.5; Oligomerization and Interfaces).

## IV.2     Carbonyl Reductases in Mammals

### IV.2.1     Monomeric Cytosolic NADPH-Dependent Carbonyl Reductases

*IV.2.1.1 Human Carbonyl Reductase 1 (CBR1)*

Human carbonyl reductase (CBR1) is a cytosolic and monomeric member of the SDR super-family (Wermuth *et al.*, 1988; Wirth and Wermuth, 1992; Forrest and Gonzalez, 2000). The enzyme is widely distributed in human tissues, such as liver, epidermis, stomach, small intes-tine, kidney, neuronal and glial cells of the CNS, and smooth muscle fibres (Wirth and Wer-muth, 1985; Wirth and Wermuth, 1992; Forrest and Gonzalez, 2000). Small amounts of CBR1 were found e.g. in cerebellum, oral cavity, oesophagus, kidney and skeletal muscle (Wirth and Wermuth, 1992)

One of the first isolations of this enzyme was from human brain (Ris and von Wartburg, 1973). According to its broad substrate specificity, CBR1 from human brain was previously also designated as secondary alcohol-NADP$^+$ oxidoreductase (EC 1.1.1.184) (Wirth and Wermuth, 1992) and aldehyde reductase 1 (Ris and von Wartburg, 1973). In 1981, Wermuth suggested the name carbonyl reductase (CBR1) to better describe the reduction of a wide va-riety of carbonyl substrates (Wermuth, 1981; Wermuth *et al.*, 1986). The substrate specificity of human CBR1 suggested initially that the enzyme is an aldo-keto reductase. However, structural investigations revealed no significant homologies to the aldo-keto reductases but, in contrast, indicated the relationship to the short-chain dehydrogenase (SDR) superfamily (Bohren *et al.*, 1989).

*Substrate diversity*

Wermuth and coworkers found that the enzyme reduces a number of biologically and phar-macologically active carbonyl compounds. During catalysis the *pro* 4S hydrogen atom of the nicotinamide ring of NADPH is transferred to the substrate. Human CBR1 exhibits relatively poor reductive activity towards aliphatic and alicyclic ketones, with the exception of daun-orubicin and the glutathione adduct of prostaglandin A$_1$ (Wermuth, 1981).

The best substrates are quinones, *e.g.* menadione, ubiquinone-1, phenanthrenequinone and tocopherolquinone followed by ketoaldehydes (e.g. phenylglyoxal), aromatic aldehydes con-taining an electron-withdrawing substituent, e.g. 4-nitrobenzaldehyde or methylglyoxal, and the biogenic aldehydes, indol-3-acetaldehyde and 4-hydroxyphenylacetaldehyde (Wermuth, 1981). Quinones, some of which are substrates of human CBR1, play important roles as oxi-dation-reduction catalysts in biological processes. For example, ubiquinones (coenzyme Q)

are constitutive parts of the respiratory chain, and tocopherolquinone (vitamin E) is thought to protect lipids of biological membranes against lipid peroxidation (Wermuth, 1981).

Due to its capability of daunorubicinol formation, CBR1 has also been named daunorubicin-pH 6.0 reductase, ALR3 (Flynn and Green, 1993) and xenobiotic ketone reductase with pH 6.0 activity (Ahmed et al., 1978).

Wermuth found that CBR1 metabolized prostaglandin $E_1$ and prostaglandin $E_2$, whereas prostaglandin $A_1$ was not reduced at all (Wermuth, 1981). While human CBR1 was shown to accomplish the reduction of the 9-keto group of prostaglandin $E_2$ to form prostaglandin $F_{2\alpha}$, the enzyme was later shown to be identical to prostaglandin-9-reductase (Schieber et al., 1992; Schieber and Ghisla, 1992). However, the metabolic potency of $PGE_1$ and $PGE_2$ carbonyl reduction was only 2% of that observed with menadione. Moreover, the relative velocity for this reaction was 60-fold lower than for 9,10-phenantrenequinone reduction (Wermuth, 1981). This casts doubt on a role of CBR1 in prostaglandin metabolism. In addition to 9-keto reduction, CBR1 was shown to catalyze the NADP-dependent oxidation of the hydroxy group at position 15 of prostaglandins. Therefore, CBR1 has also been named NADP-linked 15-hydroxy-prostaglandin dehydrogenase. It should be noted that oxo-reduction at position 9 and hydroxy-dehydrogenation at position 15 are inactivation steps of prostaglandins (cf. chapter V.1 ; Roles in Steroid and Prostaglandin Metabolism). The fact that the glutathione adduct of prostaglandin $A_1$ is a substrate of CBR1, but free $PGA_1$ is not (Wermuth, 1981), might be explained by the finding that CBR1 has a glutathione binding site in close proximity to the catalytic centre [reviewed in (Doorn et al., 2004)].

*Human CBR1 orthologues in other species*

Human CBR1 orthologues with sequence identities of more than 80% to CBR1 have been identified in several other species such as pig, rabbit, hamster, rat and mouse. The enzyme from pig testes (PTCR) was the first CBR1 orthologue whose three-dimensional structure has been solved (Ghosh et al., 1993). PTCR does also exhibit 20β-HSD activity towards $C_{21}$-steroids (Tanaka et al., 1992). Whereas in most species the enzyme is distributed in many tissues, it does not occur in rat liver. Rather, three CBR1 orthologues have been identified in rat reproductive tissues of both sexes and have been named rat testis (rtCR), gonadotropin-

inducible (iCR) and noninducible (nCR) carbonyl reductase (cf. chapter IV.2.1.5; Rat Carbonyl Reductases (iCR, nCR, rtCR)).

*Molecular forms and autocatalytic modification of CBR1*

Purification of human brain CBR1 yields three forms which differ in their pI-value, but which exhibit very similar enzymatic properties (Wermuth, 1981; Inazu *et al.*, 1992b). The three enzyme forms show isoelectric points of 6.95, 7.85 and 8.5, but no apparent differences in the amino acid composition (Wermuth, 1981; Nakayama *et al.*, 1985; Inazu *et al.*, 1992b). They differ from each other only by small structural modifications (see below). Three forms of CBR1 are also detected on purification from human liver cytosol by gel filtration, ion exchange, hydroxy apatite and affinity chromatography (Atalla *et al.*, 2000).

Finally, it was shown that the three isoforms, which show the same catalytic activity towards menadione (Bohren *et al.*, 1987; Wermuth *et al.*, 1993), result from covalent modifications of a lysine residue (Krook *et al.*, 1993a; Wermuth *et al.*, 1993; Sciotti *et al.*, 2000). Forrest and coworkers first reported the occurrence of this modified lysine residue at position 239 of CBR1, although at that time the nature of the modification was not clarified (Forrest et al., 1990). This modification is performed by an autocatalytic process involving the formation of a Schiff base between the ε-amino group of lysine and 2-oxocarboxylic acids, e.g. pyruvate and 2-oxoglutarate (Krook *et al.*, 1993c; Wermuth *et al.*, 1993). A covalent adduct is formed by reduction of the double bond. This autocatalytic modification has never been observed in other SDRs, nor in another oxidoreductase and is unique to human CBR1 (Sciotti *et al.*, 2000). A similar modification cannot be found in pig or rabbit carbonyl reductases (see below).

This process is in line with structural data from computer modeling and crystallization data, which located the modified lysine residue outside of the active site cleft (Krook *et al.*, 1993b; Tanaka *et al.*, 2005). Sciotti and coworkers suggested a specific structure which is required for this modification reaction (Sciotti *et al.*, 2000). In human, rat and mouse carbonyl reductase the region near lysine 239 is highly conserved. For example, rabbit carbonyl reductase, instead of a lysine, has an asparagine at this position which cannot react with 2-oxocarboxylates. Mouse carbonyl reductase has not been examined for autocatalytic modification by 2-oxocarboxylates. The mouse sequence shows absolute conservation of residues

near lysine 239. This fact suggests that the mouse enzyme can undergo autocatalytic modification as well (Sciotti *et al.*, 2000).

The reaction of lysine 239 in carbonyl reductase with 2-oxocarboxylates seems to be physiological, because the three autocatalytically modified forms of human CBR1 are found in untreated brain cytosol (Wirth and Wermuth, 1992). The degree of modification of lysine depends on the metabolic state of the cells, because transformed *E. coli* cells which are incubated in media with glucose show an increased yield of pyruvate-modified CBR1 (Bohren et al., 1994).

*Inhibitors*

Enzyme activity can be inhibited by flavonoids, e.g. quercetin and rutin, indomethacin, furosemide, ethacrynic acid, flufenamic acid and dicoumarol (Wermuth, 1981; Atalla *et al.*, 2000; Usami *et al.*, 2003). 4-Hydroxy-mercuribenzoate and iodoacetate inactivate the enzyme. Neither NADPH nor substrate protect the enzyme from the loss of activity (Wermuth, 1981).

### IV.2.1.2  9-Keto-Prostaglandin Reductase and 15-Hydroxy-Prostaglandin Dehydrogenase

Studies on the physiological role of carbonyl reductases indicated an involvement in endogenous prostaglandin metabolism. This field was greatly activated when it turned out that some prostaglandin dehydrogenases were shown to be SDR enzymes. Two different cytosolic types of human prostaglandin dehydrogenase have then been characterized in more detail, a monomeric NADP(H)-linked enzyme and a dimeric NAD(H)-linked enzyme. Both belong to the SDR superfamily, have similar conformations regarding their modelled three-dimensional structure, but they are highly divergent regarding their primary structure, exhibiting identical residues at only the 20% level (Krook *et al.*, 1993b).

The NADP-dependent enzyme turned out to be identical to carbonyl reductase (EC 1.1.1.184) which does obviously also act as 9-keto reductase and 15-hydroxy dehydrogenase in prostaglandin metabolism (cf. chapter IV.2.1.1; Human Carbonyl Reductase 1 (CBR1)). The NAD-dependent 15-hydroxy-prostaglandin dehydrogenase is a key enzyme involved in the biological inactivation of many prostaglandins (Ensor and Tai, 1991). The enzyme is known

to be ubiquitously expressed in several organs in mammals and seems to be downregulated in cancer tissues (Backlund *et al.*, 2005). Until today, there is no evidence that NAD-dependent 15-hydroxy-prostaglandin dehydrogenase participates in xenobiotic carbonyl reduction.

### IV.2.1.3 Human Carbonyl Reductase 3 (CBR3) and 4 (CBR4)

In their search for genes contributing to Down syndrome, Watanabe and coworkers (Watanabe *et al.*, 1998) identified a novel carbonyl reductase gene which they named *CBR3*. The *CBR3* gene is located 62 kb downstream from the original *CBR1* gene on human chromosome 21q22.2. Comparison of the genomic structure of *CBR1* and *CBR3* indicated differences in the introns and surrounding regions but high conservation of the three exons. Coding sequence comparisons revealed 77.0 and 84.0% identity on the nucleotide and predicted amino acid level, respectively, with human CBR1 and, based thereon, CBR3 classified as a monomeric NADPH-dependent oxidoreductase.

However, until recently there have been no reports on the catalytic properties of CBR3. Lakhman and coworkers (Lakhman *et al.*, 2005) were the first to characterize the catalytic properties of recombinant CBR3 with the prototypical quinone substrate menadione (Wermuth *et al.*, 1988). While studying the functional significance of a natural allelic variant of human *CBR3*, these authors observed a V244M polymorphism that appears common among different ethnic groups and encodes for CBR3 protein isoforms with distinctive catalytic properties. In detail, blacks showed a higher frequency of the M244 allele than did whites. In addition, DNA panels from 10 ethnic groups presented a wide range of *CBR3* V244M genotype distribution. Comparative three-dimensional analyses based on the structure of the homologous porcine carbonyl reductase suggested that the V244M substitution is positioned in a region critical for interactions with the NADP(H) cofactor. These findings support the notion that *CBR3* genetic polymorphisms may impact general CBR1-mediated biotransformations (Lakhman *et al.*, 2005). Further research remains to be conducted to elucidate the physiological significance of CBR3, as compared to CBR1 and to genetic polymorphisms.
Sequencing of the human genome revealed the existence of a third human isoform of carbonyl reductase (gene name: *CBR4*, Swiss Prot accession number: Q8N4T8), based on conserved domain profiles. The corresponding protein is named carbonic reductase 4 (CBR4). While the sequences of CBR1 and CBR3 are 72% identical, CBR4 shows only low similarity to CBR1

and CBR3 (23% and 22% identity, respectively). Until now, no data characterizing the enzyme regarding function and tissue distribution are available (Strausberg *et al.*, 2002; Ota *et al.*, 2004).

### IV.2.1.4 Chinese Hamster Carbonyl Reductases (CHCR 1-3)

Terada and coworkers (Terada *et al.*, 2001) isolated three different cDNAs encoding carbonyl reductase in Chinese hamster (CHCR). Comparison of the amino acid composition revealed that CHCR1 is highly identical to CHCR2 (>96%) and to other mammalian carbonyl reductases (>81%). CHCR3 has a high identity to human CBR3 (>86%) and a relatively lower identity to the other CHCRs (<76%). Structure prediction of the typical αβαβ-Rossmann fold motif of the CHCRs indicated the presence of a typical dinucleotide cofactor- binding motif which is similar to other SDR enzymes.

CHCR1 and CHCR2 show potent reductase activities towards 4-benzoylpyridine, 4-nitrobenzaldehyde and pyridine-4-carboxaldehyde. For CHCR2, metyrapone and steroids like 5β-androstane-3,17-dione, 5α-androstane-3,17-dione and 5α-androstane-17β-ol-3-one are better substrates (Terada *et al.*, 2001). CHCR3 has relatively lower activity towards 4-nitrobenzaldehyde and pyridine-4-carboxaldehyde than CHCR1 and CHCR2.

Terada and coworkers examined the function of the three CHCRs in prostaglandin metabolism (Terada *et al.*, 2003). They found that prostaglandins, e.g. $PGE_2$, failed to act as a substrate for CHCR3, whereas CHCR1 and CHCR2 showed reductase activity towards $PGB_2$ and $PGE_2$. CHCR1 and CHCR2 exhibited dehydrogenase activity towards $PGA_2$, $PGB_2$, $PGD_2$, $PGE_2$ and $PGF_{2\alpha}$. These findings suggest that both enzymes can catalyze the oxidoreduction of both the 9- and 15-hydroxy groups of these prostaglandins (Terada *et al.*, 2003). The broad substrate specificity of CHCR1 suggests that this enzyme is involved in the oxidoreduction of the 11-hydroxy group of prostaglandins, in addition to 9- and 15-hydroxy groups (Terada *et al.*, 2003). Additionally, CHCRs show reductase activity towards a variety of androstane and pregnane steroids, as well as towards benzoylpyridine, daunorubicin and isatin (Terada *et al.*, 2003).

### IV.2.1.5  Rat Carbonyl Reductases (iCR, nCR, rtCR)

Aoki and coworkers (Aoki *et al.*, 1997) isolated two closely related genes encoding an inducible and a noninducible carbonyl reductase in rat ovary. The inducible carbonyl reductase (iCR) is strongly inducible by pregnant mare serum gonadotropin (PMSG), whereas the noninducible carbonyl reductase (nCR) is constitutively expressed. Both carbonyl reductases are also expressed in rat testis and share a sequence identity of 86% with 277 (iCR) and 276 (nCR) amino acids. The iCR and nCR show sequence homologies of 86% and 80% to human CBR1, respectively (Aoki *et al.*, 1997).

It is interesting to note that, while human CBR1 is ubiquitously expressed in many tissues, rat iCR and nCR are only expressed in gonadal and adrenal tissues. There is no carbonyl reductase expressed in rat liver (Wermuth *et al.*, 1995).

A third carbonyl-reductase-like enzyme is exclusively expressed in rat male and female reproductive tissues and adrenal glands (rat testis carbonyl reductase, rtCR). Its expression in the ovary is modulated by gonadotropins and estrogens (Inazu *et al.*, 1992a; Inazu and Satoh, 1994). The amino acid sequence of this enzyme is highly homologous to iCR (98%) and nCR (86%) from rat reproductive tissues, but with the substitution of some amino acids (5 substitutions to iCR, 37 to nCR) (Aoki *et al.*, 1997)**.**

Recombinant rtCR most efficiently catalyzed the reduction of quinones, e.g. menadione, followed by xenobiotic aromatic aldehydes and ketones. Endogenous steroids like dihydrotestosterone and 5α-androstane-3,17-dione were also accepted as substrates, indicating that rtCR could be involved in steroid hormone metabolism (Wermuth *et al.*, 1995).

rtCR shows the same length and a 86% positional identity with human CBR1 (Wermuth *et al.*, 1995). Similar to human CBR1, rtCR can catalyze its own autocatalytic modification by pyruvate and 2-oxoglutarate (cf. chapter IV.2.1.1; Human Carbonyl Reductase 1 (CBR1)). Wermuth and coworkers concluded that rtCR and human CBR1 represent species-specific forms of the same enzyme (Wermuth *et al.*, 1995).

### IV.2.1.6 Pig Testicular Carbonyl Reductase (PTCR)

Porcine testicular carbonyl reductase (PTCR) resembles human and rat carbonyl reductases in that it belongs to the SDR superfamily and catalyzes the NADPH-dependent metabolism of steroids and prostaglandins, as well as that of xenobiotic aldehydes and ketones (Tanaka *et al.*, 1995; Nakajin *et al.*, 1997). Because of its ability to reduce the 20-carbonyl group of $C_{21}$-steroids, e.g. the conversion of 17α-hydroxyprogesterone to 17α/20β-dihydroxy-4-pregnen-3-one, the enzyme is also known as 20β-hydroxysteroid-dehydrogenase (Tanaka *et al.*, 1992). The purified enzyme shows vigorous 3α- and 3β-HSD activities with 5α-androstan-17β-ol-3-one (5α-dihydrotestosterone) as substrate. Therefore, the enzyme has sometimes been named PTCR/3α/β (Ohno *et al.*, 1991). Additional names for the enzyme are prostaglandin-$E_2$-9-reductase and prostaglandin 9-ketoreductase, as well as 15-hydroxyprostaglandin dehydrogenase ($NADP^+$), because the enzyme catalyzes the NADPH-dependent reduction of prostaglandins (Ahmed *et al.*, 1978; Wermuth *et al.*, 1982; Ohara *et al.*, 1995; Forrest and Gonzalez, 2000).

PTCR shows a sequence identity to human CBR1 of about 85% (Tanaka *et al.*, 1992) and is with a score of 80% also highly identical to rtCR (rat testis carbonyl reductase). However, PTCR lacks the 13 additional amino acid residues at the C-terminus of human and rat carbonyl reductases (Tanaka *et al.*, 1995). In contrast to bacterial 3α/20β-HSD, human 17β-HSD type 1 (Ghosh *et al.*, 1995) and 11β-HSD type 1 (Maser *et al.*, 2002; Maser *et al.*, 2003), as well as Drosophila alcohol dehydrogenase (Benach *et al.*, 1998), which occur as oligomers (dimers, tetramers), the carbonyl reductases from pig (PTCR), rat (iCR, nCR, rtCR) and human (CBR1) are monomeric. This monomeric structure is the result of a 41-residue insertion at a strategic location in front of the conserved Tyr-x-x-x-Lys motif. This insertion describes an all-helix subdomain that packs against interfacial helices, thus eliminating the four helix bundle interface conserved in the SDR superfamily and thereby preventing oligomerization (Ghosh et al., 2001) (cf. chapter III.3.5; Oligomerization and Interfaces). PTCR was the first known monomeric structure within the SDR superfamily.

Among the SDRs known so far, the carbonyl reductase *Sniffer* in Drosophila (cf. chapter 3.1.3) shows the greatest similarity to PTCR with regard to crystal structure, apart from the 41 amino acid residue insertion following strand βE (Ghosh *et al.*, 2001; Sgraja *et al.*, 2004).

### IV.2.1.7 Tetrameric Peroxisomal Carbonyl Reductase

In addition to monomeric carbonyl reductases of human (Wermuth *et al.*, 1988), pig (Tanaka *et al.*, 1992), rat (Tajima *et al.*, 1999) and rabbit (Gonzalez *et al.*, 1995), there do also exist tetrameric forms of carbonyl reductase. These are distributed as soluble forms either in mitochondria, as it is known for carbonyl reductases in the lungs of mouse, guinea pig and pig (cf. chapter IV.2.1.8; Tetrameric Mitochondrial Carbonyl Reductases), or in peroxisomes. These homotetrameric forms exhibit sequence identities to human CBR1 and its animal orthologues of only around 20%. To distinguish these tetrameric forms from monomeric CBR1 (and orthologues) as well as from human CBR3, they have occasionally been termed CBR2 (Matsunaga *et al.*, 2006).

Usami and coworkers (Usami *et al.*, 2003) identified and described a tetrameric carbonyl reductase from the peroxisomes of pig heart (PHCR), but the enzyme is ubiquitously expressed in pig tissues, including the liver. The monomers of the homotetramer have a molecular mass of 27 kDa, and the protein shows the typical conserved residues of the SDR superfamily regarding cofactor binding and the catalytically active site (Jornvall *et al.*, 1995). The C-terminus bears a SRL (Ser-Arg-Leu) tripeptide sequence, which is a variant of the type 1 peroxisomal SKL (Ser-Lys-Leu) targeting signal (Usami *et al.*, 2003).

PHCR is not able to reduce aliphatic aldehydes and ketones, sugars, 3/20-ketosteroids, prostaglandins and sepiapterine (Usami *et al.*, 2003), however, the recombinant enzyme shows high reductase activity towards pyridine-4-aldehyde, 3- and 4-benzoylpyridines, menadione, 4-hexanoylpyridine, alkyl phenyl ketones, α-dicarbonyl compounds and all-trans retinal (Usami *et al.*, 2003). The enzyme can be inhibited by kaempferol, quercetin, genistein and myristic acid (Usami *et al.*, 2003).

### IV.2.1.8 Tetrameric Mitochondrial Carbonyl Reductases

Tetrameric NADPH-dependent carbonyl reductases have been found in mitochondria of mouse (Nakayama *et al.*, 1986; Matsuura *et al.*, 1994), guinea pig and pig lung (Oritani *et al.*, 1992). The pig lung enzyme consists of four subunits with molecular masses of 24 kDa each (Oritani et al., 1992).  The subunits of the guinea pig enzyme have a molecular mass of 32 kDa (Nakayama *et al.*, 1986).

*In vitro* translation experiments from the mRNA coding for the guinea pig lung enzyme lead to the suggestion that the translated protein is transported into the organelle without being processed (Nakayama et al., 1988). According to Hartl et al. (1989) the amino terminal sequence of pig lung fulfils the requirements for the presequences of most mitochondrial matrix proteins (Pfanner *et al.*, 1988; Tropschug *et al.*, 1988; Hartl *et al.*, 1989; Neupert *et al.*, 1990; Pfanner *et al.*, 1990a; Pfanner *et al.*, 1990b).

Tetrameric mitochondrial pulmonary carbonyl reductase exhibits low substrate specificity and affinity for aromatic and aliphatic carbonyl compounds. It catalyses the reduction of various aliphatic and aromatic carbonyl compounds and the oxidation of secondary alcohols and aliphatic aldehydes in several animal lungs (Nakayama *et al.*, 1982; Nakayama *et al.*, 1986; Matsuura *et al.*, 1988; Matsuura *et al.*, 1989; Hara *et al.*, 1991; Oritani *et al.*, 1992). Because of its substrate specificity and localization in pulmonary epithelial cells, Hara and coworkers (Nakanishi *et al.*, 1995) suggested that tetrameric lung carbonyl reductase functions in the pulmonary metabolism of endogenous carbonyl compounds derived from lipid peroxidation, as well as in the metabolism of 3-ketosteroids and fatty aldehydes, in addition to the detoxification of xenobiotics (Nakanishi *et al.*, 1995). MLCR exhibits high cofactor preference for NADP(H) but does also accept NADH at much higher concentrations (Nakanishi *et al.*, 1995). Interestingly, MLCR is inhibited by the alcohol dehydrogenase inhibitor pyrazole (Nakanishi *et al.*, 1995)**,** which is in contrast to cytosolic monomeric carbonyl reductases. Nakanishi and coworkers (Nakanishi *et al.*, 1995) also postulated that, even in lung cells, the expression of carbonyl reductase is regulated by environmental and hormonal factors, of which fatty acids are the most interesting because of their enhancement of the enzyme activity (Hara *et al.*, 1992).

As indicated above, tetrameric carbonyl reductase has also been found in the mitochondrial fraction of lung cell homogenates of mouse (MLCR) (Matsuura *et al.*, 1990). From the various lung cell populations, bronchiolar and alveolar epithelial cells show high levels of MLCR expression (Matsuura *et al.*, 1990; Oritani *et al.*, 1992), whereas much lower levels were found in other tissues, like for example in adipocytes (Nakanishi *et al.*, 1995). According to immunocytochemical studies, the enzyme is located in the mitochondrial matrix of mouse lung epithelial cells (Matsuura *et al.*, 1994).

In 1995 Tanaka and coworkers (Tanaka *et al.*, 1995; Tanaka *et al.*, 1996a) solved the ternary three-dimensional structure of MLCR with NADPH and 2-propanol, and showed that the protein comprises four identical 29 kDa protein subunits (Tanaka *et al.*, 1996a). Each monomer consists of 244 amino acid residues and shows 85% identity to pig tetrameric carbonyl reductase (PHCR) but only 17% identity to human carbonyl reductase (CBR1). Like other SDR superfamily members, tetrameric mitochondrial carbonyl reductases contain the typical cofactor and active site consensus sequences (Nakanishi *et al.*, 1993; Nakanishi *et al.*, 1995).

### IV.2.1.9 Dimeric Microsomal Carbonyl Reductase: 11β-HSD Type 1

11β-Hydroxysteroid-dehydrogenase (11β-HSD); EC 1.1.1.146) is a microsomal enzyme responsible for the interconversion of the active glucocorticoids cortisol (in man) and corticosterone (in rodents) to their hormonally inactive 11-keto metabolites, cortisone and 11-dehydrocorticosterone, respectively (Monder and Shackleton, 1984). Thus far, two isoformic types of the enzyme, 11β-HSD1 and 11β-HSD2, have been cloned and structurally and functionally characterized. Both belong to the SDR protein superfamily. Although displaying dehydrogenase and reductase activities *in vitro*, the dominant *in vivo* function of the type-1 enzyme is obviously glucocorticoid 11-oxoreduction, thus generating active cortisol from inactive cortisone precursors. In glucocorticoid target tissues, notably the liver, 11β-HSD1 is suggested to regulate exposure of active glucocorticoids to the classical glucocorticoid (type II) receptor (Fig. IV-2).
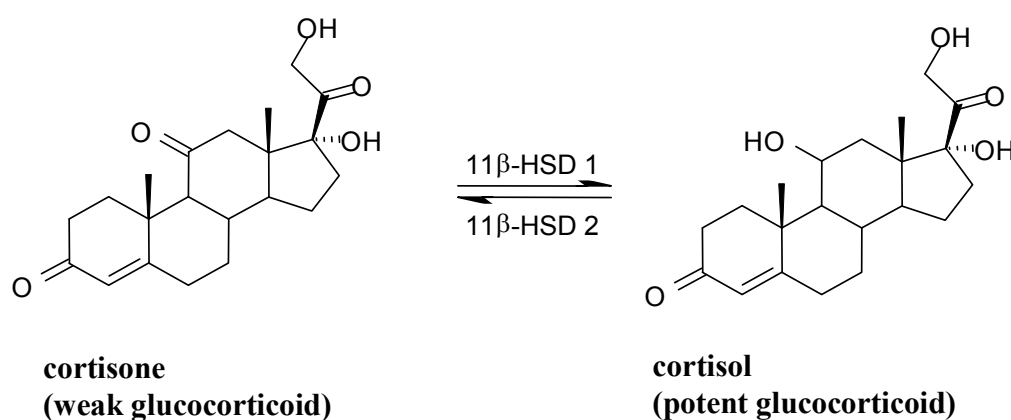


**cortisone**
**(weak glucocorticoid)**

**cortisol**
**(potent glucocorticoid)**

**Fig. IV-2:** *In vivo* **reaction of 11β-HSD 1 and 11β-HSD 2**

11β-HSD 1 distributes ubiquitously with major sites of expression in liver and adipose tissues. It acts as an oxo-reductase and generates receptor-active cortisol from inactive cortisone. By catalyzing inactivation of cortisol to cortisone, 11β-HSD 2 protects the mineralocorticoid receptor in aldosterone target tissues.

11β-HSD2 seems to work exclusively as dehydrogenase, by inactivating 11-hydroxyglucocorticoids and thereby ensuring mineralocorticoid specificity of aldosterone to the mineralocorticoid (type I) receptor [reviewed in (Seckl, 1997))]. 11β-HSD2 is a high- affinity NAD-dependent enzyme with an apparent $Km$ for 11-hydroxyglucocorticoids in the low nanomolar range (Stewart et al., 1994). It is found principally in mineralocorticoid target tissues such as the kidney and colon, where it protects the mineralocorticoid receptor from cortisol excess. Mutations in the gene encoding 11β-HSD2 are responsible for a heritable form of hypertension, apparent mineralocorticoid excess (Stewart et al., 1996), in which cortisol acts as a potent mineralocorticoid. There is general consensus that the type 2 form of 11β-HSD acts as a hormone-inactivating enzyme, since in vitro and in vivo data suggest it to function exclusively as an 11β-dehydrogenase of physiological glucocorticoids (Seckl, 1997). However, with the synthetic glucocorticoids 11-dehydro-dexamethasone and 9α-fluorocortisone reductase activities of 11β-HSD2 could be detected (Li et al., 1997; Quinkler et al., 1997).

Unfortunately, all attempts failed to purify 11β-HSD type 2 in a functional state, such that it is not yet possible to ascribe non-steroidal carbonyl-reducing activity to this enzyme. Accordingly, the discussion below focusses primarily on the hepatic isoform 11β-HSD1.

Whereas the biological functions of 11β-HSD2 are fairly well determined, at least in aldosterone target tissues, the role of 11β-HSD1 is less well understood. 11β-HSD1 has been referred to as a low affinity glucocorticoid oxidoreductase, exhibiting Km values in the μM range. Both dehydrogenase and reductase activities could be demonstrated in homogenates or with purified mouse liver enzyme in the presence of NADP+ and NADPH, respectively (Maser and Bannenberg, 1994a; Maser and Bannenberg, 1994b), whilst under physiological conditions this enzyme has been considered to function predominantly as reductase (Seckl, 1997). Furthermore, mice homozygous for a targeted disruption of the 11β-HSD1 gene are unable to regenerate corticosterone from inert dehydrocorticosterone (Kotelevtsev et al., 1997). The preferential reaction direction of the type 1 form seems to be dependent on cellular context, translational modifications, subcellular environment, substrate and cosubstrate. The discrepancy to in vitro observations may result from cell disruption and tissue homogenisation, and

indicates the importance of local 11β-HSD1 environment and stabilization of the three-dimensional enzyme architecture.

A variety of diseases, including insulin resistance/type2 diabetes, dyslipidemia, and obesity, have been discussed in relation to 11β-HSD1. Recently, 11β-HSD1 knock-out mice were found to resist high-fat diet-induced obesity and showed an improved lipid and lipoprotein profile as well as hepatic insulin sensitivity (Masuzaki *et al.*, 2001). In contrast, the phenotype of transgenic mice overexpressing 11β-HSD1 selectively in adipose tissue resulted in marked insulin resistance and hyperlipidemia (Masuzaki et al., 2001). Hence, the ongoing research on the potency and pharmaceutical properties of 11β-HSD1 inhibitors will be critical for the successful discovery of effective human therapeutic agents to treat the metabolic syndrome (Alberts et al., 2002).

As described above, most of the short-chain dehydrogenase/reductase (SDR) enzymes are active as either homodimers or –tetramers (Krook *et al.*, 1993b; Jornvall *et al.*, 1995; Tsigelny and Baker, 1995b; Tsigelny and Baker, 1995a; Penning, 1997; Grimm *et al.*, 2000b). By gel permeation chromatography, it was shown that 11β-HSD1 occurs as dimeric enzyme in human liver (Maser *et al.*, 2002). The kinetic data of 11β-HSD1 published so far demonstrated an enzyme with a micromolar affinity for glucocorticoids (GCs) (Agarwal *et al.*, 1990; Moore *et al.*, 1993; Maser and Bannenberg, 1994b; Maser and Bannenberg, 1994a; Quinkler *et al.*, 1997; Adams *et al.*, 2000). This hardly seemed compatible with a role of 11β-HSD1 to regulate access of GCs to the GR since both endogenous 'free' GC levels as well as the dissociation constants of the GR for GCs range in low nanomolar concentrations. This enigma was solved by functional studies and detailed kinetic analyses with purified 11β-HSD1 from human liver (Maser *et al.*, 2002). When Michaelis-Menten kinetics were considered with the purified enzyme, the Km values for GC oxidoreduction ranged in low micromolar concentrations. However, oligomeric enzymes often display kinetics other than that described by the Michaelis-Menten equation. When applying sigmoidal dose-response kinetic as a significantly better model to fit data, cooperative kinetics of 11β-HSD1 with cortisone and dehydrocorticosterone (glucoorticoid 11-oxo-reducing activity) were observed (Maser *et al.*, 2002).

Enzyme cooperativity is an important feature, especially of enzymes acting as regulators in physiological processes. 11β-HSD 1 has been shown to dynamically adapt to low as well as to

high substrate concentrations, thereby providing the fine-tuning required as a consequence of great variations in circadian plasma glucocorticoid levels (Maser *et al.*, 2002).

The distribution of 11β-HSD1 among tissues has been extensively studied, and its expression shown in glucocorticoid target tissues, such as liver, lung, gonad, cerebellum, and pituitary. Interestingly, evidence is emerging to suggest a fundamental role for 11β-HSD1 in the reductive metabolism of non-steroidal carbonyl compounds in mammals, in addition to its implication in glucocorticoid activation (Maser and Bannenberg, 1994a; Maser and Bannenberg, 1994b; Maser *et al.*, 1994; Maser, 1995; Maser and Oppermann, 1995; Oppermann *et al.*, 1995; Maser *et al.*, 1996; Rekka *et al.*, 1996; Maser, 1997; Maser and Oppermann, 1997; Maser, 1998).

With the enzyme purified to homogeneity it was demonstrated that 11β-HSD1 is capable of acting as carbonyl reductase in the detoxification of aldehydes, ketones and quinones, like for example metyrapone, p-nitroacetophenone, p-nitrobenzaldehyde, menadione, oracin, and the tobacco-specific nitrosamine NNK [reviewed in (Hoffmann *et al.*, 2006))]. Inhibition experiments revealed strong sensitivity of xenobiotic carbonyl reduction to glucocorticoids and other endogenous steroids. The competitive nature of this inhibition suggests that both, steroids (glucocorticoids) and xenobiotic carbonyl substances bind to the same catalytically active site of 11β-HSD1. It is concluded that 11β-HSD1 plays an important role in phase-I biotransformation of pharmacologically relevant carbonyl substances as well as protecting organisms against toxic aldehydes, ketones and quinones by converting them to less lipophilic and more soluble and conjugatable metabolites. Thus, 11β-HSD1 contributes to an expanding list of pluripotent hydroxysteroid dehydrogenases which are involved in reductive xenobiotic carbonyl metabolism as well as being specific towards their physiological steroid substrate.

In case of oracin, 11β-HSD1 enzyme cooperativity may become important with respect to the plasma concentrations that could be achieved with oracin, and to enhance the chemotherapeutic efficacy of this novel anti-cancer drug (Wsol *et al.*, 2004) (cf. chapter 4.6). Due to its cooperativity for carbonyl reduction, 11β-HSD1 is also able to metabolize even nanomolar concentrations of the tobacco-specific nitrosamine 4-methylnitrosamino-1-(3-pyridyl)-1-butanone (NNK), a fact which is important in view of the relatively low levels of this carcinogen ob-

served in smokers (Maser *et al.*, 2003) (cf. chapter V.7 ; Protection against Tobacco Smoke-Derived Lung Cancer).

11β-HSD1 is potently (in nanomolar concentrations) inhibited by glycyrrhetinic acid, the main constituent of licorice (Maser *et al.*, 2003). Hence, licorice exposure may affect NNK detoxification by inhibition of 11β-HSD1 (Maser, 2004).

As a membrane-bound protein it has an extended N-terminal part relative to other SDR proteins. This hydrophobic segment is likely to anchor in or span the membrane and it contains a possible cleavage signal-peptide sequence which is very similar in all 11β-HSD structures (Krozowski, 1992).

# V  Biological Functions of Carbonyl-Reducing Enzymes

The physiological role of several HSDs in steroid metabolism is known so far, however, some exhibit pluripotency for steroid and non-steroid substrates (cf. chapter IV; Pluripotent Carbonyl Reductases of the SDR Superfamily) (Maser, 1995), thereby contributing to important detoxification reactions. The physiological role of the carbonyl reductases is still not clear. In some cases, their tissue distribution suggests  physiological  roles in the endogenous metabolism of prostaglandins (Lee and Levine, 1974a), steroids, or tetrahydrobiopterin synthesis (Park *et al.*, 1991). On the other hand, with regard to their wide substrate spectrum a general role in the detoxification of xenobiotic and endogenous reactive non-steroid carbonyl compounds has been suggested (Wermuth *et al.*, 1986). Moreover, it is believed that their most important biological role is the protection from damage by accumulation of toxic carbonyl compounds, such as for example quinones (Wermuth *et al.*, 1986), aflatoxin $B_1$ (Ellis and Hayes, 1995), aldophosphamide, tripeptidyl aldehydes, chordecone  [reviewed in (Maser, 1995)], and the tobacco-specific nitrosamine NNK [reviewed in (Maser, 1997; Maser, 2004)]. As will be outlined in the following chapter, it is difficult to ascribe an exclusive role for endogenous or exogenous substrates to carbonyl reductases, but several examples will emphasize their contribution as general means in detoxification processes.

## V.1      Roles in Steroid and Prostaglandin Metabolism

The role of 3α/20β-HSD of *S. hydrogenans* (cf. chapter **IV.1.1;** 3α/20β-Hydroxysteroid Dehydrogenase of *Streptomyces hydrogenans*), 3α-HSD/CR from *C. testosteroni* (cf. chapter IV.1.2; 3α-Hydroxysteroid Dehydrogenase/Carbonyl Reductase of *Comamonas testosteroni*) and 11β-HSD1 (cf. chapter IV.2.1.9; Dimeric Microsomal Carbonyl Reductase: 11β-HSD Type 1) of mammalian species in the metabolism of steroids is well established and has been discussed in chapter 3 of this review. Interestingly, some of the carbonyl reductases also metabolize steroids. After CBR1 has been described as important enzyme in the detoxification of carbonyl compounds (Wermuth, 1985), Satoh and coworkers (Iwata *et al.*, 1989; Iwata *et al.*, 1990b) suggested a new role for carbonyl reductases in steroid metabolism because of the ability to metabolize 3-ketosteroids and because of the exclusive expression in rat reproductive tissues and adrenals. Since then, the activity of carbonyl reductases has been found to be

regulated by estrogens and gonadotropins and was suggested to be important for the ovulation process (Inazu and Satoh, 1994; Inazu and Fujii, 1997; Espey *et al.*, 2000; Fujii *et al.*, 2005). In line with these findings is the fact that certain 5α-reduced steroids, e.g. dihydrotestosterone, are among the best substrates of carbonyl reductase from rat ovary, whereas 5β-reduced steroids are not reduced (Wermuth, 1995). The ability of carbonyl reductases to interconvert prostaglandin $F_{2\alpha}$ and prostaglandin $E_2$ suggests a further regulatory role of this enzyme in prostaglandin function (Iwata *et al.*, 1989; Espey *et al.*, 2000) (cf. chapter V ; Biological Functions of Carbonyl-Reducing Enzymes).


## V.2      Tetrahydrobiopterin Synthesis

Tetrahydrobiopterin ($BH_4$) is required as a cofactor for aromatic amino acid hydroxylases which synthesize precursors of catecholamine and indoleamine neurotransmitters in the brain. $BH_4$ is also a cofactor of nitric oxide synthase which generates nitric oxide as a messenger molecule. The biosynthesis of $BH_4$ includes two carbonyl reduction steps: First, an intermediate, 6-pyruvoyltetrahydropterin ($PPH_4$) is reduced to 6-(1'-oxo-2'-hydroxypropyl)-tetrahydropterin (1'-$OXPH_4$) or 6-(1'-hydroxy-2'oxopropyl)-tetrahydropterin (2'-$OXPH_4$). Second, these intermediates are converted to $BH_4$ (Fig. V-1).
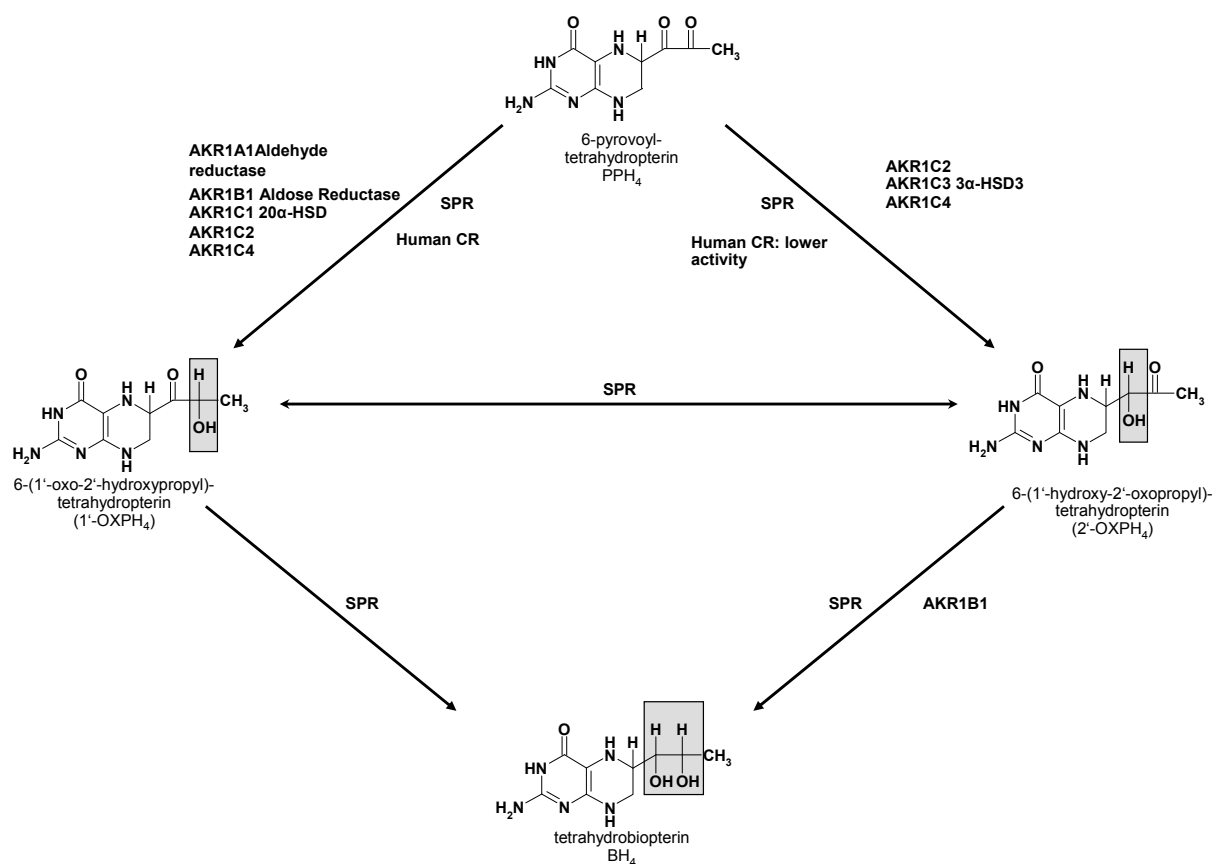
**Fig. V-1: Biosynthetic pathways from 6-pyruvoyltetrahydropterin (PPH4) to tetrahydrobiopterin (BH4)** (for details see text)

The enzyme sepiapterin reductase (SPR) is the main catalyst in $BH_4$ formation in that it catalyzes the carbonyl reduction of both keto groups of $PPH_4$ to the corresponding diol form $BH_4$ (Park *et al.*, 1991; Iino *et al.*, 2003). According to its primary structure, SPR belongs to the SDR superfamily (Jornvall *et al.*, 1995). Interestingly, patients with SPR deficiency show normal urinary excretion of pterins and no hyperphenylalaninemia, which suggests an alternative pathway of $BH_4$ formation from $PPH_4$.

Park and coworkers (Park *et al.*, 1991) reported that human CBR1 is able to reduce $PPH_4$ to $1'$-$OXPH_4$ and $2'$-$OXPH_4$, the latter being further converted to $BH_4$ by AKR1B1 (aldose reductase). They suggested an alternative pathway of $PPH_4$ carbonyl reduction to form $BH_4$. More detailed analysis revealed that, compared to its $1'$-$OXPH_4$-forming activity, human carbonyl reductase has a quite low activity to form $2'$-$OXPH_4$ (Iino *et al.*, 2003). From the AKR superfamily, AKR1A1 (human aldehyde reductase), AKR1B1 and AKR1C1 (human 20$\alpha$-HSD) form only $1'$-$OXPH_4$, whereas AKR1C2 (human 3$\alpha$-HSD type 3) and AKR1C4 (hu-

man 3α-HSD type 1) can form both, 1'-$OXPH_4$ and 2'-$OXPH_4$ as the major and minor products (Iino et al., 2003). AKR1C3 (3α-HSD type 2) only produces 2'-$OXPH_4$ from $PPH_4$ (Iino *et al.*, 2003). In the further reaction pathway, AKR1B1 reduces specifically the 2'-keto group from 2'-$OXPH_4$ to form $BH_4$. This reaction is not catalyzed by AKR1A1, AKR1C1, AKR1C2, AKR1C4 and human CBR1 (Iino *et al.*, 2003). On the other hand, AKR1B1 is not able to form $BH_4$ from 1'-$OXPH_4$.

Interestingly, two carbonyl reductases (CRI and CRII) have been discovered in the fat body of the silkworm *bombyx mori* which differ from SPR and human CBR1, because CRI shows specificity for the reduction of the 2'-keto group of $PPH_4$ and 2'-$OXPH_4$, and CRII specifically reduces the 1'-keto group of $PPH_4$ and 1'-$OXPH_4$ (Iino *et al.*, 2000; Iino *et al.*, 2003). Enzymes similar to silkworm CRI and CRII do also exist in chicken (Iino *et al.*, 2003). Accordingly, in humans, CBR1 together with some AKR enzymes show a kind of "housekeeping" nature and play a role in case of normal pathway deficiency.

## V.3   Neuroprotection by Carbonyl Reductase?

Oxidative stress in brain is the major cause of neurodegenerative disorders including Alzheimer`s, Parkinson`s, Huntington`s and Creutzfeld-Jakob disease (Sayre *et al.*, 2001; Dawson and Dawson, 2003). Apparently, all these diseases share a common pathogenesis which is based on an intracellular imbalance between the formation of free radicals and antioxidative defence mechanisms. The central nervous system appears to be particularly vulnerable to oxidative stress because of its high rate of oxygen utilization, high content of unsaturated lipids and because, in contrast to other organs, its anti-oxidative capacity is comparatively weak.

Despite the increasing number of reports finding a causal relation between oxidative stress and neurodegeneration, little is known about the genetic elements that confer protection against the deleterious effects of oxidation in neurons. An important element that acted as a neuroprotective agent in the cellular defence mechanism against oxidative stress was recently found by Botella et al. (Botella *et al.*, 2004). They demonstrated that oxidative stress is a direct cause of neurodegeneration in the *Drosophila* central nervous system and they identified a new gene, *sniffer*, in *Drosophila melanogaster* which prevents age-dependent and oxidative stress-induced neurodegeneration. According to bioinformatic studies on the primary struc-

ture, it turned out that *Sniffer* is a carbonyl reductase (CBR1) (Wermuth *et al.*, 1988). However, the precise mechanism of neuroprotection by *Sniffer* in *Drosophila* remained obscure (Botella *et al.*, 2004).

Reactive oxygen species (ROS) seem to play a significant role in neuronal cell death in that they generate reactive aldehydes by membrane lipid peroxidation. Examples of such toxic compounds are 4-oxonon-2-enal (ONE), 4-hydroxynon-2-enal (HNE) and acrolein, which contain an α,β-unsaturated aldehyde capable of reacting with cysteine, histidine, and lysine in proteins via Michael addition to the C=C bond (Nadkarni and Sayre, 1995). Primary amines may alternatively react with the carbonyl group to form Schiff bases (Nadkarni and Sayre, 1995). Importantly, a large number of neurodegenerative disease states is associated with increased accumulation of protein adducts derived from reactive aldehydes produced by lipid peroxidation (Shapiro, 1998) (Fig. V-2).
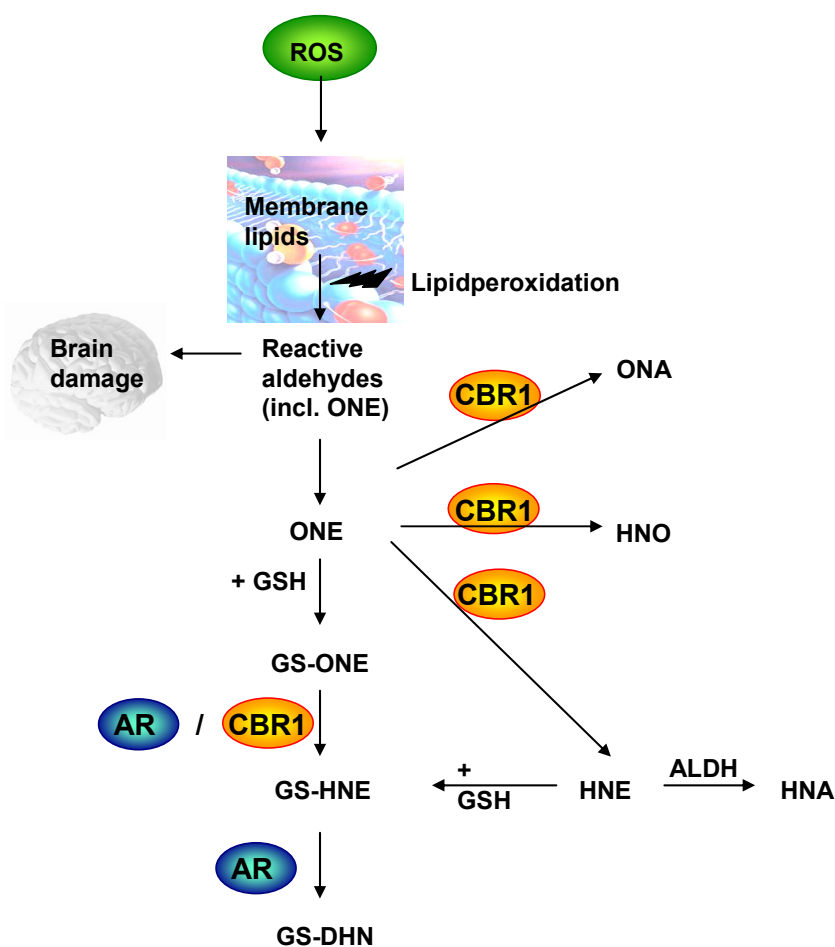


**Fig. V-2: Scheme on the metabolic inactivation of the lipid peroxidation product 4-oxonon-2-enal .**

Abbreviations:
DHN = 4-dihydroxynonene;
HNA = 4-hydroxynonan-acid;
HNE = 4-hydroxynon-2-enal;
HNO = 1-hydroxynon-2-en-4-one;
ONA = 4-oxononanal;
ONE = 4-oxonon-2-enal;
GSH = reduced glutathione,
AR = aldose reductase (AKR1B1);
ALDH = aldehyde dehydrogenase;
CBR1 = human carbonyl reductase.

In general, routes of detoxification of these carbonylic lipids include spontaneous and enzyme-catalyzed glutathione (GSH) conjugation and either oxidation by aldehyde dehydrogenase or carbonyl reduction catalyzed by AKR or SDR enzymes, the carbonyl reductase *Sniffer* belonging to the latter (cf. chapter IV.1.3, Insect Carbonyl Reductase: *Sniffer* of *Drosophila melanogaster*). Intriguingly, human CBR1 was recently demonstrated to have activity toward a product of lipid peroxidation in that it catalyzed the reduction of 4-oxonon-2-enal (ONE) (Doorn *et al.*, 2004). ONE was previously found to be a major product of lipid peroxidation and is a particularly potent genotoxin (Dawson and Dawson, 2003), which reacts with DNA bases to form substituted etheno-adducts. In addition, ONE is highly reactive toward the protein nucleophiles cysteine, histidine, lysine, and arginine, and also toward thiols, which suggests that it may also play a role in lipid peroxidation-mediated cross-linking of proteins (Lin *et al.*, 2005). Importantly, ONE has recently been found to be both more neurotoxic and more protein-reactive than 4-hydroxynon-2-enal (HNE) (Lin *et al.*, 2005).

NADPH-dependent ONE ketone reduction resulted in the production of HNE, and ONE aldehyde reduction yielded 1-hydroxynon-2-en-4-one (HNO) (Doorn *et al.*, 2004). Furthermore, CBR1 was shown for the first time to catalyze hydride transfer to the C=C double bond of ONE, resulting in 4-oxononanal (ONA). Interestingly, the glutathione adduct of ONE (GS-ONE) was also found to be a substrate for CBR1, resulting in the production of GS-HNE.

The *sniffer* gene is expressed within the entire cortex of the fly brain, where all neuronal cell bodies are localized. *Sniffer* is, so far, the only known functional carbonyl reductase in *Drosophila melanogaster* which emphasizes the importance of this enzyme as a neuroprotective agent (Botella *et al.*, 2004). This is supported by the fact that CBR1 has been first isolated and cloned from human brain (Wermuth, 1981), suggesting that human brain may be an important site of CBR1 distribution. Hence, several lines of evidence suggest that carbonyl reductases represent a significant pathway for the detoxification of reactive aldehydes derived from lipid peroxidation and that carbonyl reductases in humans are essential for neuronal cell survival and to confer protection against oxidative stress-induced brain degeneration (Hoffmann *et al.*, 2006).

# V.4     Quinone Detoxification

Quinones are ubiquitous in nature and constitute an important class of naturally occurring compounds that are found in plants, fungi, bacteria, and mammals and that function primarily as components of the electron transport chains involved in cellular respiration and photosynthesis (O'Brien, 1991). Human exposure to quinones can occur via drug therapy, via the diet or via airborne pollutants. In addition, mammals themselves synthesize quinones, primarily by oxidative metabolism of aromatic precursors, including endogenous compounds such as catecholamines and estrogens as well as xenobiotics. Endogenous polymeric quinones are for example the melanins that are oxidative condensates of dopa, dopamine, and cysteine, and which comprise the pigments of hair and skin (Monks *et al.*, 1992). In view of the inevitable human exposure to quinones and their inherent reactivity, a substantial amount of research has focused on the chemistry and biochemical toxicology of these compounds.

Quinones may be toxic to cells by a number of mechanisms including redox cycling, arylation, intercalation, induction of DNA strand breaks, interference with mitochondrial respiration, and the generation of site-specific free radicals. Much research has emphasized the role of oxidative stress and redox cycling in this toxicity (O'Brien, 1991; Monks *et al.*, 1992). Quinones may undergo enzymatic one-electron reduction by microsomal NADPH-cytochrome P450 reductase, microsomal NADH-cytochrome $b_5$ reductase, and mitochondrial NADH-ubiquinone oxidoreductase, resulting in the formation of semiquinones. Semiquinones may be toxic per se or react with molecular oxygen, thus forming superoxide anion radical and regenerating the parent quinone, which is then available for re-reduction and hence undergoes a futile redox cycling. The net result of this redox cycling is an oxidative stress resulting from disproportionate consumption of cellular reducing equivalents and the generation of active oxygen species (O'Brien, 1991; Monks *et al.*, 1992).

Alternatively, two-electron reduction of quinones has generally been considered to be a detoxification pathway since the resulting hydroquinone may be conjugated with glucuronic acid or sulfate and excreted  into the bile (Wermuth *et al.*, 1986; Lind *et al.*, 1990; Maser, 1993). Two-electron reduction of quinones is catalyzed by cytosolic NAD(P)H: quinone oxidoreductase (NQO; EC 1.6.99.2; a flavoprotein previously known as DT-diaphorase), cytosolic carbonyl reductase, and microsomal 11β-HSD1 (Maser, 1993). Two NQO-enzymes are

known, the NAD(P)H: quinone acceptor oxidoreductase (NQO1, DT-diaphorase) and dihy-
dronicotinamide riboside: quinone oxidoreductase (NQO2). NQO2 exhibits a high sequence
identity to DT-diaphorase and is considered to be an isozyme of DT-diaphorase (Adams *et al.*,
2000).

In some cases, such as with bioreactive alkylating agents, reduction by NQO leads to activa-
tion of the compound (Ross *et al.*, 1993). It has also been proposed, for example, that reduc-
tion of 1,4-naphthoquinones and their glutathionyl conjugates by NQO may lead to redox
cycling dependent on the rate of reduction to the hydroquinone followed by its autooxidation
back to the parent quinone (Brunmark *et al.*, 1988; Buffinton *et al.*, 1989). The detoxification
of quinones is conventionally understood in terms of their conjugation with glucuronate or
sulfate. The two-electron reduction of the quinone is a chemical requirement in the course of
its conjugation to a glucuronide, hence preventing further redox transitions..

NQOs are obligate two-electron reductases which can utilize either NADH or NADPH as an
electron donor (Lind et al., 1990). Importantly, two carbonyl-reducing enzymes of the SDR
superfamily have also been described to catalyze the two-electron reduction of quinones, cy-
tosolic carbonyl reductase and microsomal 11β-HSD1, thereby forming conjugatable hydro-
quinone metabolites (Fig. IV-3).
Wermuth and coworkers reported that CBR1, but not NQO, provides the enzymatic basis of
quinone detoxification in man (Wermuth *et al.*, 1986).
For example, quinones such as ubiquinone-1, menadione, and phenanthrenequinone are the
best substrates for human brain carbonyl reductase (Wermuth, 1981).
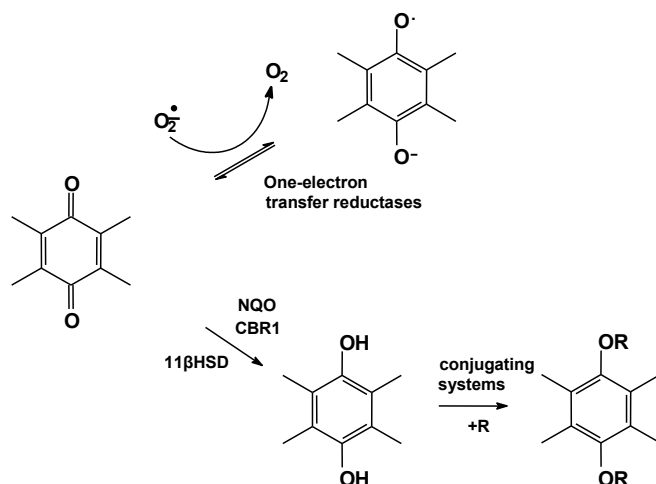


**Fig. V-3: Role of 11β-HSD1 and CBR1 in quinone detoxification.**

(NQO = NAD(P)H: Quinone-oxidoreductase; R = UDP-glucuronic acid or other conjugant)

However, whereas NQOs and carbonyl

reductase are soluble proteins, thereby acting as quinone "scavengers" in cytosol, membrane-bound 11β-HSD1 may play an exceptionally important role as protective device against endogenous membrane damage. Due to its subcellular localization in the endoplasmic reticulum, 11β-HSD1, by catalyzing hydroquinone formation (Yokota *et al.*, 1992), prevents semiquinone-induced oxygen radical generation and subsequent lipid peroxidation of membranes.

The exact molecular mechanisms involved in quinone or hydroquinone cytotoxicity are still largely unknown. Their use as antitumor drugs and antibiotics, together with their widespread occurrence in nature, makes it imperative to understand their metabolic activation/inactivation and the resulting effects on cellular function. Whether a particular quinone is cytotoxic will depend on the biochemical makeup of the target cell. All cells have enzymes for the reductive metabolism of quinones, but the capacity of reductases carrying out a one-electron reduction versus those carrying out a two-electron reduction would be expected to cause large variations in the activation or de-activation of quinones. The biological significance of carbonyl reductase and 11β-HSD1 in these systems requires further investigation.

## V.5      Carbonyl Reduction in Drug Metabolism and Pharmacology

In general, carbonyl reduction plays a significant role in the phase-I metabolism of carbonyl-containing drugs (Bachur, 1976; Ahmed *et al.*, 1979; Felsted and Bachur, 1980; Imamura *et al.*, 1993; Rosemond and Walsh, 2004) by converting them to less lipophilic alcohol metabolites. These reduced alcohol metabolites can then be excreted as well as rapidly converted to glucuronyl or sulfate conjugates by phase-II metabolizing enzymes, which facilitate their elimination. A summary of pharmacologically relevant drugs that undergo carbonyl reduction is given in Table V-1.

As is known from other phase-I reactions like oxidation by the cytochrome P450 system, carbonyl reduction is of significance in a variety of drug inactivation processes such as for example for warfarin, haloperidol, or the anti-tumor drugs oracin (Wsol et al., 2003; Wsol et al., 2004), daunorubicin (Ax et al., 2000) and doxorubicin (Maser, 1995). For the latter it is assumed that the alcohol metabolite doxorubicinol is responsible for the cardiotoxicity observed upon doxorubicin chemotherapy (Olson *et al.*, 2003). On the other hand, the respective carbinols formed may retain their therapeutic potency (e.g. metyrapol from metyrapone), thus prolonging the pharmacodynamic effect of the parent drug or, in some instances, a compound

gains activity through carbonyl reduction, as is the case for pentoxifylline, chloral hydrate, and the prodrug precursors of the β-adrenergic blockers propranolol and alprenolol. An important example of drug activation by carbonyl reduction is dolasetron. This drug is administered in its keto form and undergoes carbonyl reduction by CBR1 and several AKR enzymes (Breyer-Pfaff and Nill, 2004). The resulting alcohol reduced dolasetron has a 40-fold higher serotonin antagonist activity compared to the parent compound (Boeijinga et al., 1992). Fenofibrate undergoes hydrolytic cleavage to fenofibric acid followed by ketone reduction, and reduced fenofibric acid contributes to the lipid-lowering activity of this drug (Caldwell, 1989).

| **Drugs:** | acetohexamide, actinomycin D, adriamycin, befunolol, chloral hydrate, daunorubicin, dolasetron, ethacrynic acid, fenofibrate, haloperidol, hydromorphone, isatin, ketoconazole, ketoprofen, levobunolol, lisofylline, loxoprofen, metyrapone, mitomycin C, moperone, naftazone, naloxone, naltrexone, oxisuran, pentoxifylline, tienilic acid, timiperone, trifluperidol, warfarin, wortmannin |
|---|---|
| **Toxicants/ Carcinogens:** | acetophenone, [acetaldehyde] (after ethanol oxidation), [aflatoxin B1], alachlor, aldehydes (various, e.g. from fruits), [aldophosphamide], benzaldehyde, benzoylpyridine, chlordecone, 3-deoxyglucosone, methylglyoxal, quinones (ubiquinone, naphthoquinone, phenanthrenequinone, benzanthracenequinone etc.), NNK (tobacco-specific nitrosamine), zearalenone. |
| **Endogenous:** | biogenic aldehydes, endogenous quinones (e.g. metabolites from catecholamines), prostaglandines, products of lipid peroxidation (acrolein, 4-hydroxynonenal, malondialdehyde etc.), steroids. |

**Table V-1: Multiplicity of carbonyl substrates**

The opioid antagonists naloxone and naltrexone are stereoselectively metabolized by carbonyl reduction at the C-6 oxogroup to 6β-naloxol (Yamano et al., 1999) and 6β-naltrexol (Dayton and Inturrisi, 1976), respectively. Of the carbonyl-reducing enzymes isolated from human liver cytosol, AKR1C4 proved to be the most efficient in naltrexone reduction followed by AKR1C2, whereas CBR1 was devoid of activity (Breyer-Pfaff and Nill, 2004). A high-affinity stereoselective carbonyl reduction of ketotifen and of 10-oxonortriptyline has recently been reported (Breyer-Pfaff and Nill, 1999; Breyer-Pfaff and Nill, 2000).

## V.6    Role in Chemotherapy Resistance

In anti-tumor chemotherapy, the occurrence of drug resistance is a major obstacle and originates principally from pharmacodynamic or pharmacokinetic mechanisms. Anthracyclines like daunorubicin (DRC) and doxorubicin (DOXO) are the most valuable cytostatic agents in chemotherapy, but their usefulness is limited by intrinsic or acquired resistance towards these drugs. Anthracycline resistance is not merely the result of alterations in drug uptake and retention (McGrath and Center, 1987; Gessner *et al.*, 1990; Ramachandran *et al.*, 1993; Toffoli *et al.*, 1994), but also mediated by enzymatic anthracycline detoxification that is upregulated upon exposure to these drugs (Soldan *et al.*, 1996a; Soldan *et al.*, 1996b). Interestingly, 13-hydroxy metabolites of anthracyclines, such as doxorubicinol and daunorubicinol, are significantly less potent than the parent drug in terms of inhibiting tumor cell growth *in vitro* (Beran *et al.*, 1979; Ozols *et al.*, 1980; Yesair *et al.*, 1980; Dessypris *et al.*, 1986; Schott and Robert, 1989; Ohara *et al.*, 1995; Olson *et al.*, 2003), suggesting that carbonyl reduction is an important biochemical mechanism in the detoxification of carbonyl group-bearing anthracyclines. Therefore, elevated levels of anthracycline carbonyl-reducing enzymes constitute a mechanism in the development of resistance towards DRC and DOXO (Soldan *et al.*, 1996a; Soldan *et al.*, 1996b).

Three enzymes capable of catalyzing DRC carbonyl reduction have been identified in human liver: AKR1A1 (aldehyde reductase) and AKR1C2 (dihydrodiol dehydrogenase 2) from the AKR superfamily and carbonyl reductase (CBR1) from the SDR superfamily (Ohara *et al.*, 1995) (Fig. V-4).

In a study by Ax and coworkers (Ax *et al.*, 2000), a resistant descendant of the human stomach carcinoma cell line EPG85-257 was selected in the presence of increasing concentrations of DRC. The resulting cells were used to evaluate an induced carbonyl reduction as a new determinant in DRC resistance. $IC_{50}$ values of DRC increased almost 8-fold in the resistant descendants compared to the parental cell line. Resistant cells possessed 6-fold higher levels of carbonyl-reducing activity, leading to the less toxic 13-hydroxy metabolite daunorubicinol. The 6-fold higher daunorubicinol formation roughly parallels the 8-fold increase of DRC $IC_{50}$ values during cell selection, and therefore was suspected to account for DRC resistance in these cells. The determination of specific carbonyl-reducing enzymes known to be involved in

DRC detoxification, revealed that mainly the mRNA expression of CBR1 increased in the resistant descendant, in addition to some minor increase in AKR1B1 and AKR1C2 levels. Hence, DRC resistance in human stomach carcinoma cells may mainly result from an induction of CBR1.



**DAUNORUBICIN**                                  **DAUNORUBICINOL**
                                                  **Metabolite less active**
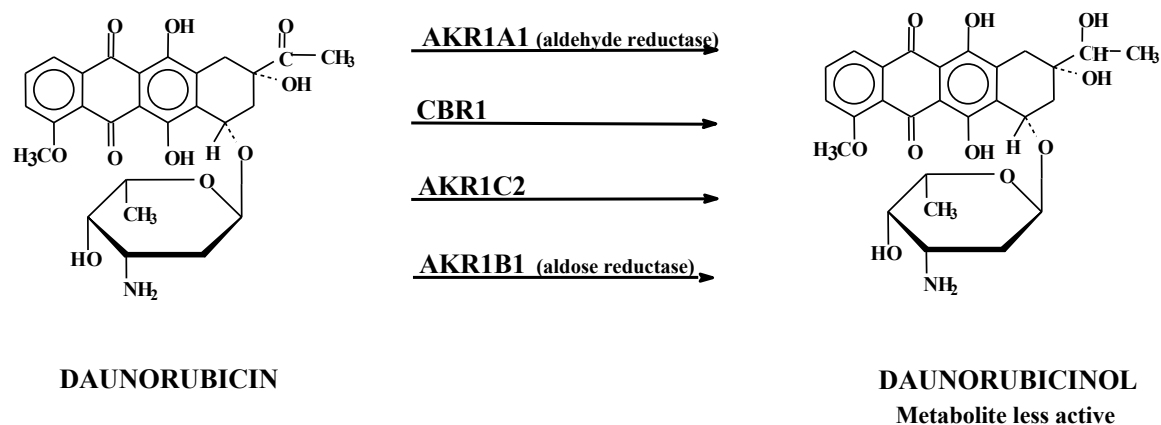
**Fig. V-4: Scheme of daunorubicin carbonyl reduction**
(for details see text)

Oracin, is a new anti-cancer drug which is presently in phase II clinical trials. The main advantages of this novel chemotherapeutic are the possibility of peroral administration, the absence of cardiotoxicity (Gersl *et al.*, 1996) (which e.g. is the main dose-restricting factor in clinical chemotherapy of DOXO), the negative results in the Ames test on mutagenicity, very low hepatotoxicity, and its favorable pharmacokinetics. From its chemical structure, a DNA intercalation mode of action can be inferred, similar to that of anti-tumor antibiotics from the anthracycline group. In addition, several other mechanisms affecting tumor cell growth have been proven. They involve the inhibition of topoisomerase II (Miko *et al.*, 2002), the stimulation of aerobic consumption of glucose and, to a lesser extent, the formation of lactate in tumor cells, as well as induction of apoptosis (Melka, 1993).

Metabolic studies have revealed carbonyl reduction of oracin to dihydrooracin (DHO) as the main metabolic pathway in common laboratory animals (Szotakova *et al.*, 1996; Wsol *et al.*, 1996; Wsol *et al.*, 1998) as well as in human liver (Wsol *et al.*, 2000). Reduction of the pro-chiral carbonyl group at the 11-position of oracin leads to the formation of chiral DHO, which was found both in microsomal and cytosolic fractions of all species studied (Wsol *et al.*, 1999).

The enzyme responsible for oracin carbonyl reduction in human liver microsomes was identified as 11β-HSD1  (cf. chapter IV.2.1.9, Dimeric Microsomal Carbonyl Reductase: 11β-HSD Type 1) (Szotakova *et al.*, 1996; Wsol *et al.*, 1996; Wsol *et al.*, 1998; Wsol *et al.*, 2003; Wsol *et al.*, 2004). In human liver cytosol, CBR1 and three members of the aldo-keto reductase (AKR) superfamily were found to mediate oracin carbonyl reduction, namely AKR1C1, 1C2 and 1C4. Interestingly, AKR1C2 and AKR1C4 are absolutely stereospecific and produce (+)-DHO exclusively, whereas AKR1C1 produces also minor amounts of (−)-DHO. On the other hand, the efficiency of AKR1C1 in oracin reduction is higher by at least one order of magnitude than those of the other two enzymes.

The clinical consequences of these findings remain to be established. It is noteworthy that several flavonoids serve as potent inhibitors of carbonyl-reducing enzymes (Wermuth, 1985; Inazu *et al.*, 1992b). Co-administration of flavonoids during anthracycline chemotherapy may, therefore, represent an attractive means to bypass classical drug resistance via inhibition of DRC and DOXO detoxification by carbonyl reduction.

As stated above, prevention of carbonyl reduction may represent a potential approach to enhancing the safety and efficiency of cytostatics in clinical chemotherapy (Propper and Maser, 1997). This could be achieved either by inhibiting the enzymes responsible for drug inactivation or by chemically modifying the chemotherapeutic molecule, such that it looses its affinity for the inactivating enzymes. This latter approach was used in case of the novel chemotherapeutic benfluron (B), where a dimethoxy substitution of the parent compound resulted in the development of 3,9-dimethoxybenfluron (D) (Miko *et al.*, 1991). Benfluron (B) is a potential benzo[*c*]fluorene antineoplastic agent with high activity against a broad spectrum of experimental tumors *in vitro* and *in vivo* (Miko *et al.*, 1991). The introduction of the two methoxy groups lead to a protection of the carbonyl group, such that 3,9-dimethoxybenfluron gained a 9-fold resistance against carbonyl reduction compared to benfluron (Skalova *et al.*, 2002). Carbonyl reduction of D in comparison to that of B was 4 times less extensive in human liver microsomes and and 6 − 10 times less extensive in cytosol. Moreover, about 10 − 20 times higher amounts of dihydro-B than dihydro-D were produced in primary cultures of human hepatocytes. Two human enzymes of the SDR superfamily, 11βHSD1 and CBR1, were shown to reduce B and D. With 11βHSD1, about 10 times higher rates of carbonyl reduction were observed for B than for D

The results clearly demonstrate that dimethoxy substitution protects the carbonyl group of the benzo[*c*]fluorene moiety against the deactivation by microsomal and cytosolic reductases. Therefore, chemical modification seems to be a promising way of preventing the metabolic inactivation of anti-cancer drugs and may be advantageous in the development of potent chemotherapeutics, as are information on the participating enzymes and their specific inhibitors.

## V.7     Protection against Tobacco Smoke-Derived Lung Cancer

Among the more than 40 different carcinogens present in tobacco and tobacco smoke, 4-methylnitrosamino-1-(3-pyridyl)-1-butanone (NNK = nicotine-derived nitrosamine ketone) is the most potent and abundant (Hecht, 1998). NNK is generated by nitrosation of nicotine during tobacco curing and smoking (Hecht, 1998). It induces lung tumors in all laboratory animal species tested (Hoffmann *et al.*, 1985; Hecht, 1994) and has also been shown to induce nasal cavity, pancreatic, and liver tumors in rats (Hoffmann *et al.*, 1985; Hecht, 1994). From studies on the occurrence, carcinogenicity and metabolic activation of tobacco-specific nitrosamines, NNK is believed to play a role in human tobacco-related cancers (Hoffmann *et al.*, 1985; Hecht, 1994). NNK requires metabolic activation in order to exert its carcinogenic effect and there are competing pathways for NNK activation and detoxification (Fig. V-5. The major pathways of NNK metabolic activation proceed by α-hydroxylation at the carbons adjacent to the *N*-nitroso group. This leads to a series of unstable intermediates that alkylate DNA and hemoglobin. The DNA alkylation products are critical in carcinogenesis by NNK (Hecht, 1996).

However, the competing pathway for NNK activation is NNK detoxification, which proceeds via carbonyl reduction of NNK to NNAL, followed by glucuronidation of NNAL (Fig. V-5). Although N-oxidation has been considered as a NNK inactivation reaction, this pathway plays only a minor role in man *in vitro* and *in vivo* (Hecht, 1994; Carmella *et al.*, 1997). It has therefore been postulated that the susceptibility of a tissue to tumor formation may vary depending on the extent of the competing pathways α-hydroxylation versus carbonyl reduction (Maser *et al.*, 1996; Maser, 1997; Maser, 1998; Atalla *et al.*, 2000; Maser, 2004).

Carbonyl reduction to NNAL is a very efficient pathway of NNK in animal and human tissues (Maser, 1997; Maser, 1998). In laboratory animals, the main metabolites in blood and urine after i.v. administration of NNK resulted from carbonyl reduction (followed by glucuronidation or N-oxidation), indicating that carbonyl reduction to NNAL greatly exceeds metabolism by NNK α-hydroxylation (Adams *et al.*, 1985a; Adams *et al.*, 1985b; Hecht *et al.*, 1993). The predominance of carbonyl reduction has been confirmed by a characterization and quantification of NNK metabolites in the urine of smokers and smokeless tobacco users. The results clearly demonstrate that detoxification of NNK *in vivo* occurs mainly by carbonyl reduction and glucuronidation (Fig. V-5) (Maser, 1997; Maser, 1998).

*In vitro* studies revealed that NNAL was the major metabolite in hepatocytes and liver microsomal preparations indicating that the liver plays the predominant role in metabolism of NNK. In rodent lung tissue, carbonyl reduction was in the same range as α-hydroxylation and N-oxidation, whereas in rat nasal mucosa no NNAL was detectable (Maser, 1997; Maser, 1998). The absence of NNAL formation in the nasal mucosa might explain why nasal mucosa is particularly susceptible to NNK-induced carcinogenesis.

In numerous studies, cytochrome P450 isozymes mediating NNK activation via α-hydroxylation have been investigated. However, although constituting the major pathway of NNK metabolism in several tissues, the enzymes that catalyze the carbonyl reduction of NNK to NNAL have awaited their characterization since 1980 (Hecht, 1996).

We could finally isolate and characterize five different enzymes catalyzing NNK carbonyl reduction in man (Fig. V-5). These are microsomal 11β-hydroxysteroid dehydrogenase type 1 (11β-HSD1) (EC 1.1.1.146) (Maser *et al.*, 1996; Maser, 1998) and cytosolic carbonyl reductase (CBR1) (EC 1.1.1.184) (Atalla *et al.*, 2000), both enzymes belonging to the SDR superfamily. In addition, three members of the AKR superfamily have been shown to mediate NNK carbonyl reduction, namely AKR1C1, AKR1C2 and AKR1C4 (EC 1.3.1.20) (Atalla *et al.*, 2000), previously designated as dihydrodiol dehydrogenases DDH1, DDH2 and DDH4, respectively.

Because NNK is metabolized to both the (*S*)- and (*R*)-enantiomers of NNAL, two diastereomeric glucuronides of NNAL are formed (Hecht, 1998). This is important, since

stereochemical aspects of NNAL and NNAL-glucuronide formation could play an important role in the metabolic detoxification of NNAL as well as its carcinogenic activity (Hecht, 1998; Upadhyaya *et al.*, 1999). Enantiomer analysis of NNAL produced from NNK in human liver and lung cytosol gave results in accordance with a predominant role of CBR1 and the AKR1C enzymes in these compartments (Breyer-Pfaff *et al.*, 2004) .
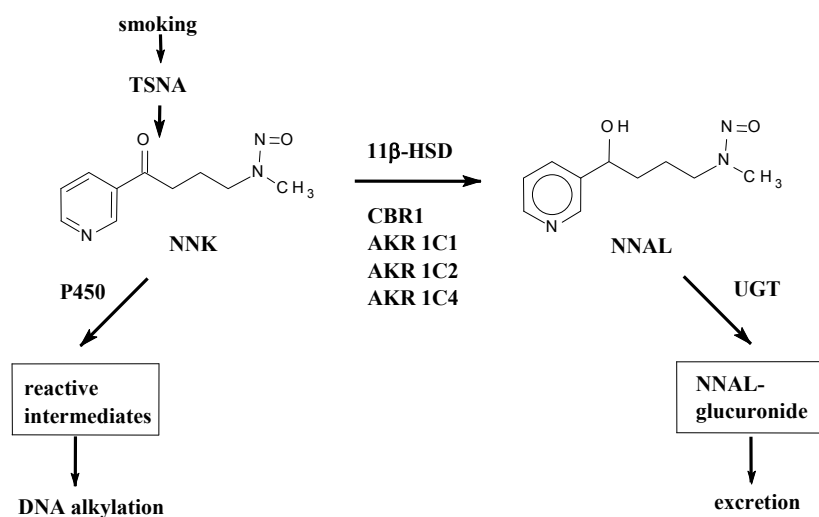


**Fig. V-5: The metabolic activation and inactivation of 4-(methylnitrosamino)-1-(3-pyridyl)-1-butanone (NNK).**

Abbreviations:
TSNA, tobacco-specific nitrosamines;
P450, cytochrome P450;
NNAL, 4-(methylnitrosamino)-1-(3-pyridyl)-1-butanol;
UGT, UDP-glucuronosyl-transferase;
11β-HSD 1, 11β-hydroxy-steroid dehydrogenase type 1;
CBR1, human carbonyl reductase;
AKR, aldo-keto reductase.

Any impact on NNK carbonyl reduction could have consequences with regard to NNK-induced cancerogenesis. For example, differences in tissue expression of NNK reductases may be causally related to the organospecificity of NNK-induced cancerogenesis. Moreover, genetic polymorphisms, age-dependent differential expression (Maser *et al.*, 1994) and/or modulation by several xenobiotics of NNK reductase activity may impair the activation-detoxification balance in favour of activation, rendering the lung vulnerable to the carcinogenic effect. It is, therefore, important to study the tissue distribution of NNK-activating and -inactivating enzymes in order to understand the biochemical mechanisms of NNK carcinogenesis.

Several studies on the profile of NNK metabolites in smokers' urine have revealed high inter-individual variations with respect to NNAL, NNAL-glucuronide and NNAL-N-oxide quantities (Carmella *et al.*, 1995; Meger *et al.*, 1996). It is these variations that are of greatest interest, since they may not only be linked to lung cancer susceptibility but also to a genetic polymorphism in terms of NNK reductase expression. Only 16 % of habitual smokers develop lung cancer, suggesting that individual susceptibility and environmental factors (e.g. air pollution) contribute to the risk of developing this disease. Interestingly, a number of studies have

demonstrated a familial component to lung cancer risk. Evidence supporting familiality suggests that the etiology of lung cancer includes shared genes, shared environments, or both. Association studies performed on polymorphic genes coding for phase-I and phase-II enzymes that play a role in the activation of carcinogens in tobacco smoke, i.e. CYP1A1, CYP2D6, CYP2E1, and GSTM1, have often yielded conflicting results (Schwartz *et al.*, 1996). Therefore, it would be of greatest interest to perform studies on family history of lung cancer and putative aberrations or polymorphisms in NNK-metabolizing enzymes in these individuals. For example, experiments on the expression of 11β-HSD1 in human lung demonstrated that the level of this NNK carbonyl-reducing enzyme varied by a factor of 20 in only ten patients investigated (Soldan *et al.*, 1999).

A variety of factors may influence the detoxification capacity of the NNK reductases, thereby contributing to the interindividual variabilities observed in the response to smoking. As an example, the fact that chronic alcohol consumption greatly enhances the carcinogenic response to smoking and tobacco-derived nitrosamines (Ahrendt *et al.*, 2000) may be causally related to an inhibitory action of ethanol treatment of rats on 11β-HSD1 activity (Valentino *et al.*, 1995); in addition, ethanol exerted weak inhibitory effects on human AKR1C1, 1C2 and 1C4 *in vitro* (Atalla *et al.*, 2000).

11β-HSD1 and the three AKR enzymes are potently (in nanomolar to low micromolar concentrations) inhibited by glycyrrhetinic acid (GA), the main constituent of licorice (Monder *et al.*, 1989; Reidenberg, 2000; Maser *et al.*, 2003; Ota *et al.*, 2004). Consequently, by shifting the NNK/NNAL equilibrium towards NNK activation, GA as a tobacco additive or as a confectionery may potentiate the carcinogenic response towards cigarette smoking. Moreover, GA is known to act as an inducer of cytochromes P450 (Paolini *et al.*, 1999). The resulting increase in NNK activation would be synergistic to NNK reductase inhibition, thereby further aggravating the toxicological consequences of smoking.

## V.8    Detoxification of Insecticides

Agricultural and domestic use of neuroactive zoocides is still widespread, and new types of anti-insect agents are continually sought in order to avoid the possible side effects in vertebrates. In this respect, much effort has been spent to exploit the invertebrate or insect-specific hormonal system (Belai *et al.*, 1995). The poly-hydroxylated ecdysteroids serve as moulting hormones in arthropods and are unique to nonvertebrates. The cytochrome P450-dependent monooxygenase system is important for the biosynthesis of insect ecdysteroids in which ecdysone 20-monooxygenase plays a central role in ecdysone activation to 20-hydroxyecdysone. The development of anti-ecdysteroid agents that inhibit or inactivate cytochrome P450 and thus prevent the formation of active moulting hormones offers promising opportunities to selectively disrupt insect reproduction and development. Based on the findings that metyrapone is a potent cytochrome P450 inhibitor, several metyrapone analogues have been synthesized and found to be toxic to insects by impairing ecdysteroid activation *in vivo* (Belai *et al.*, 1995).

Since metyrapone itself is mainly reduced at its ketone moiety to the hydroxy metabolite metyrapol, the same metabolic fate was anticipated in case of the insecticidic metyrapone analogues (Rekka *et al.*, 1996). Indeed, these azole analogues of metyrapone are extensively metabolized via carbonyl reduction by 11β-HSD1 in microsomes and CBR1 in the cytosol of human liver (Rekka *et al.*, 1996). Interestingly, cytotoxicity assays reveal that the resulting hydroxy metabolites are far less toxic to mammalian cells than the parent compounds, indicating that carbonyl reduction represents an important detoxification step of the biologically active insecticides in mammals (Rekka *et al.*, 1996). By mediating their detoxification in non-target organisms, such as humans and other mammals, 11β-HSD1 and CBR1 provide the basis for a selectivity between insects and humans and a safer application of these biologically active insecticides.

The reduced alcohol metabolite formation of the metyrapone azole analogues by 11β-HSD1 and CBR1 can be strongly influenced by substituents of the phenyl ring (Rekka *et al.*, 1996). Therefore, by using as substrates a diverse spectrum of these molecules, with different substituents, it should be possible to derive from the kinetic data a hypothetical optimal substrate configuration.

# VI Physiological Implications

Pluripotent hydroxysteroid dehydrogenases (HSDs) are of special interest because of their selectivity for oxidoreduction at specific carbon atoms at the steroid nucleus, combined with their rather unspecific metabolic affinity for non-steroidal carbonyl compounds [reviewed in (Maser, 1995)]. This substrate pluripotency is important for many aspects of both cell physiology and toxicology. Substrate interactions may lead to either malfunctions of steroid hormones or to an impaired detoxification of harmful aldehydes, quinones and ketones.

The existence of enzymes that have arisen independently to have a common activity has been repeatedly observed before in different enzyme groups. In many cases, such analogous enzymes seem to evolve by recruitment of enzymes acting on different but related substrates, i.e. by minor structural change of a protein that leads to a novel specificity or even a new class of reactions. It remains to be elucidated whether the selective pressure to resist the deleterious effects of toxic aldehydes, ketones and quinones, coupled with independent adaptation to endocrine requirements makes the recruitment of these pluripotent HSDs particularly advantageous.

With their pluripotent substrate specificities, the HSDs of this study add to an expanding list of those enzymes that, on the one hand, are capable of catalyzing the carbonyl reduction of non-steroidal endo- and xenobiotics, and that on the other hand exhibit great specificity for their physiological substrates [reviewed in (Maser, 1995)]. As the HSD/carbonyl reductase project continues to progress, it is anticipated that new members of these groups of enzymes, which play important roles in not only the metabolism of xenobiotics but also the biotransformation of a variety of endogenous steroids, are bound to emerge.

# VII  Perspectives

Apparently, the role of HSDs and other carbonyl-reducing enzymes in biotransformation has been underestimated. There is increasing evidence for the crucial involvement of these enzymes in the detoxification of carcinogens and the development of tumor resistance towards cytostatics. The further determination of structure-function relationships and expression analyses of the particular enzymes are therefore prerequisites for the understanding of interactions and implications with the endogenous hormone metabolism and the development and risk assessment of drugs and biocides.

Knowledge on the pluripotent activity of these enzymes for a specific toxic and/or cancerogenic substrate would improve risk estimates from exposures in the home and workplace. Thus, as the pieces to the puzzle of carbonyl-reducing enzymes are put together, further possibilities are revealed that may have application in basic sciences and medicine. Future studies, including heterologous expression in appropriate systems, will be aimed to definitively establish their role in detoxification processes.

# VIII Zusammenfassung

Die Carbonylreduktion von Aldehyden, Ketonen sowie Quinonen zu ihren entsprechenden Hydroxylderivaten spielt eine wichtige Rolle im Phase-I- Metabolismus vieler endogener (biogene Aldehyde, Steroide, Prostaglandine, Produkte der oxidativen Degradation von Lipiden) sowie xenobiotischer Verbindungen (pharmakologische Verbindungen, Karzinogene, Toxine).

Carbonylreduktasen lassen sich in zwei große Protein-Superfamilien untergliedern, die Aldo-Keto-Reduktasen (AKR) und die kurzkettigen Dehydrogenasen/Reduktasen (SDR). Während Aldehydreduktasen und Aldosereduktasen zu den AKR gehören, zählen verschiedene Formen der Carbonylreduktasen zu den SDRs. Zusätzlich existiert eine Gruppe von pluripotenten Hydroxysteroid-Dehydrogenasen (HSDs) beider Superfamilien, die spezifisch die Oxidoreduktion an verschiedenen Positionen des Steroid-Nukleus katalysieren. Weiterhin katalysiert die Gruppe der HSDs unspezifisch den reduktiven Metabolismus einer großen Zahl an nicht steroidalen Carbonylverbindungen. Der vorliegende Übersichtsartikel fasst die letzten Erkenntnisse über Carbonylreduktasen und pluripotente HSDs der SDR Protein-Superfamilie zusammen.

# Part II

## Structural aspects of Oligomerisation in 3α-Hydroxysteroid Dehydrogenase /Carbonyl Reductase from *Comamonas testosteroni*: New Approaches for Efficient Protein Design

**Frank Hoffmann**

*Institute of Toxicology and Pharmacology for Natural Scientists,*

*University Medical School Schleswig-Holstein, Campus Kiel,*

*Brunswiker Strasse 10, 24105 Kiel, Germany*

## Published in:

# Part II

# Table of Contents

# I   Introduction

## I.1      3α-HSD/CR of C. testosteroni as a Model System

One of the most important model systems of bacterial steroid degradation is the Gram-negative bacterium *Comamonas testosteroni*, which belongs to the beta-group of the proteo-bacteria, and which is known to be able to grow on testosterone as sole carbon source. These strictly aerobic, nonfermentative, chemoorganotrophic bacteria rarely attack sugars, but grow well on organic acids and amino acids (Willems et al., 1992). As a member of this family *C. testosteroni* is able to use steroids as sole carbon source and may be an attractive means for the removal of these stable compounds from the environment.

Since the pioneering work of Talalay and co-workers it is well known that 3α-hydroxysteroid dehydrogenase/carbonyl reductase (3α-HSD/CR) from *C. testosteroni* is one of the first enzymes of the steroid catabolic pathway and, therefore, plays a central role in steroid metabolism (Marcus and Talalay, 1956). In a comparison of the protein patterns separated by two-dimensional gel electrophoresis of testosterone-induced *C. testosteroni* cells versus control extracts, a strong increase of 3α-HSD/CR expression was found (Möbus et al., 1997). As one physiological function 3α-HSD/CR catalyzes the interconversion of hydroxy and oxo groups at position 3 of the steroid ring structure. Moreover, this enzyme is capable of catalyzing the carbonyl reduction of nonsteroidal xenobiotic carbonyl compounds (Oppermann et al., 1996). It has been demonstrated that this substrate pluripotency not only enhances the metabolic capacity of insecticide degradation, but also increases the resistance of *C. testosteroni* to the steroid antibiotic fusidic acid (Oppermann et al., 1998).

3α-HSD/CR from *C. testosteroni* is a member of the short-chain dehydrogenase/reductase (SDR) superfamily. The primary structure of 3α-HSD/CR shows two sequence motifs which are typical for the enzymes of the SDR family. First, the amino-terminal cofactor binding motif $Gly^8$-x-x-x-$Gly^{12}$-x-$Gly^{14}$ and second, the $Tyr^{155}$-x-x-x-$Lys^{159}$ motif which is structurally located in the active site and forms together with the conserved $Ser^{114}$ a catalytic triad. Probably all enzymes of the SDR family share a common reaction mechanism which follows a compulsory ordered pathway with the cofactor binding first. After binding of the hydroxyl or carbonyl substrate a so-called substrate binding loop, which is highly flexible in most apo-SDR enzymes, becomes well ordered and shields the substrate as well as the catalytic center from aqueous environment. Together with a hydride ion a proton is transferred via the Tyr-

residue of the catalytic triad. In parallel the catalytic Ser orients the substrate and stabilizes the transient reaction intermediate.

Alternatively to this pathway it has been proposed that the deprotonated Ser may act as a catalytic base with the Tyr playing a subsidiary role during catalysis (Winberg et al., 1999). The Lys in the catalytic triad plays a dual role both in the proper orientation of the cofactor by forming hydrogen bonds to the nicotinamide-ribose moiety and to lower the p$K_a$ of the catalytic Tyr via electrostatic interaction (Ghosh *et al.*, 1994b; Auerbach *et al.*, 1997; Benach *et al.*, 1999).

Most of the SDR enzymes are either homodimers or homotetramers (Jörnvall et al., 1995). The members of this family share an amino acid identity only in the 15% to 30% range. Despite this fact they reveal a striking similarity in their tertiary structure. Their overall structure is based upon a typical dinucleotide binding motif composed of βαβ units called Rossmann fold. This motif builds up a parallel β-sheet sandwiched between two arrays of parallel α-helices (Rossmann et al., 1975) (Fig. I-1). In 3α-HSD/CR there is an insertion of 28 amino acids within the Rossmann fold motif between strand βE and helix αF forming a predominantly α-helical subdomain (Grimm *et al.*, 2000b).
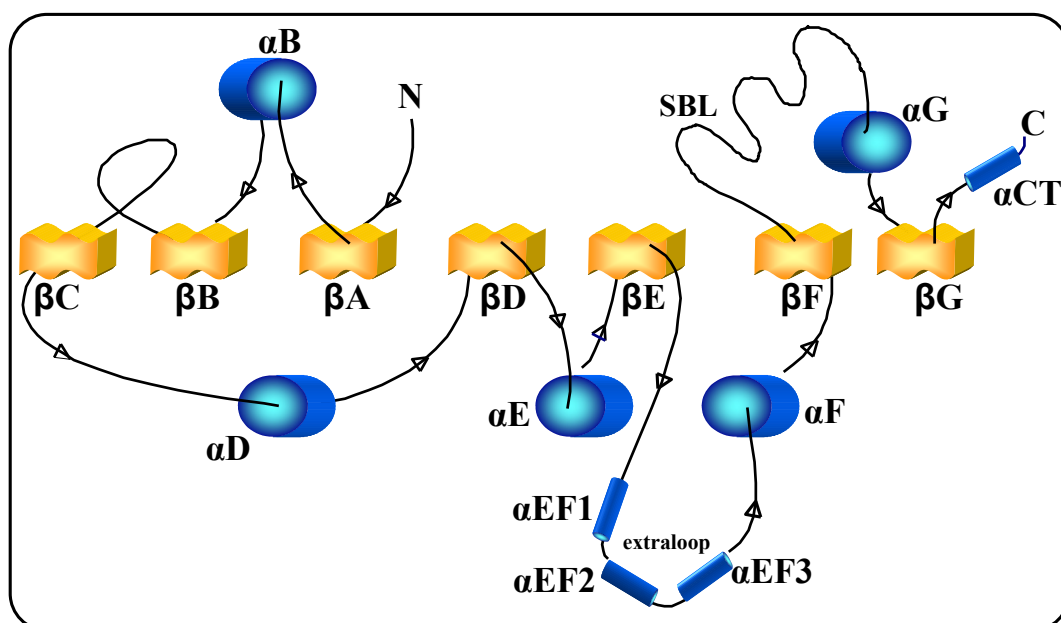


**Fig. I-1: Typical Rossmann fold of SDR enzymes exemplified by 3α-HSD/CR from *C. testosteroni.***

3α-HSD/CR contains an unordered substrate binding loop (SBL) and an extraloop-domain between strand βE and helix αF which normally are part of the four helix bundle as the main structural feature of the oligomerization Q-interface.

All structures of homotetrameric SDRs determined so far show two main subunit interfaces arranged about two non-crystallographic 2-fold axes which are perpendicular to each other and referred to as P and Q  (Ghosh *et al.*, 1994b; Tanaka *et al.*, 1996a; Grimm *et al.*, 2000b). The Q-axis interface is formed of a four helix bundle composed of helices αE and αF of two interacting subunits, e.g. in 3α/20β-HSD of *S. hydrogenans*. In all homodimeric SDRs, which structures have been determined so far, dimerization occurs along an interface corresponding to the Q-axis interface of tetrameric SDRs, e.g. alcohol dehydrogenase (ADH) of *Drosophila lebadonensis* (Benach et al., 1998). The dimer interface of alcohol dehydrogenase corresponds to the Q-axis interface of 3α/20β-HSD. Because of the 28 amino acids insertion ("extraloop") into the classical Rossmann fold motif between strand αE and αF this mode of dimerization is sterically impossible in 3α-HSD/CR (Grimm *et al.*, 2000b) Fig. V-5; p 63)

As a consequence, in 3α-HSD/CR dimerization takes place via a P-axis interface which corresponds to the P-axis interface of 3α/20β-HSD. The dimerization about a P-axis interface has been discussed as a possible mode of oligomerization in SDRs (Krook *et al.*, 1993b), but has never been observed in a crystal structure so far.

To investigate the role of the extraloop in the oligomerization behaviour of 3α-HSD/CR a mutation-approach was performed to replace the extraloop by the much shorter corresponding 3α/20β-HSD loop. This was pursued both *in silico* (by homology modeling) and *in vitro* (by applying PCR-techniques). The resulting truncated 3α-HSD/CR (3α-HSD/CR-tr) was theoretically analysed by molecular dynamics simulations and experimentally characterized by enzymatic methods.

## I.2      Correct Protein Folding as the Key for an Active and Functional Protein

Based on the crystal structure it was the aim of this study to investigate the structure-function relationship of 3α-HSD/CR from *C. testosteroni*. In both, the computer-based and the molecular biological approach a question of great importance was whether the mutant including 8 new aa instead of 36 original ones can adopt a correct native folding and how the architecture of the un-mutated regions is influenced by the redesign. Therefore a short introduction into protein structure and protein folding is given.

The structure of a protein is described on four different levels. First by the primary structure (amino acid sequence) and the secondary structure, wherein the polypeptide backbone assembles into local regions of alpha-helices and beta-sheets as the most common motifs (Wilmot and Thornton, 1988) and into coils and turn. The tertiary structure refers to the entire 3-dimensional structure of the protein. The quaternary structure describes interactions between separate polypeptide chains. These separate polypeptide chains are called domains and exist in some large protein complexes.

The biological function of a protein is dependent on the protein folding into the correct, or "native", state. Proteins are linear polymers of amino acids that fold into complex conformations dictated by the physical and chemical properties of the amino acid chain. Therefore the amino-acid composition (primary structure) of a protein can be seen as a predisposition to fold into its correct native conformation (Anfinsen, 1973). Most of the proteins do so spontaneously during or immediately after their synthesis. Other proteins require the assistance of enzymes, which, for example, catalyze the formation and exchange of disulfide bonds. Enzymes like chaperones bind to the partly folded polypeptide chain and prevent it from making illicit associations with other folded or partly folded proteins. In addition, a chaperone can promote the folding of a polypeptide chain it holds.

The folding process is mainly guided by Van der Waals forces. Water-soluble proteins bear polar and charged amino-acids on their surface whereas the hydrophobic parts of the protein are oriented inwards. This type of residue packing is assumed to be of entropic origin and to be almost perfect (Klapper, 1971; Szweda *et al.*, 1993).

There are various different parameters in the solution where protein folding occurs that influence the folding behaviour of the protein. Among these factors are the nature of the primary solvent such as water or lipids, salt concentration, temperature and the presence of chaperons. A given amino-acid sequence forms roughly the same intermediates to the correct final folding. First, secondary structural elements such as alpha helices and beta strands are built up until tertiary and quaternary structures are assembled. Tertiary structures involve covalent bonding in the form of disulfide bridges between two cysteine residues.

Protein folding is usually a spontaneous process, and often when a protein unfolds because of heat or chemical denaturation, it will be capable of refolding into the correct conformation, as soon as it is removed from the environment of the denaturant. That means that folding and unfolding under these circumstances are reversible.

A protein which is fully denatured lacks secondary and tertiary structure. This folding status can be described as "random coiled" and can be caused under some non-native conditions a protein will not fold at all. Among these are temperatures above or under the normal living conditions of the cell, high concentrations of solutions and extreme pH values.

*Molten globules as intermediates in the folding pathway*

As the first event during the folding pathway the unfolded and unordered polypeptide chain collapses and acquires most of its correct secondary structure elements like α-helices and β-strands. This state, called "molten globular state" has a looser tertiary structure than the native state. The proper packing interactions in the interior of the protein have not been formed. In this state the interior side chains may be highly mobile. They resemble more a liquid than the solid-like interior of the folded native state. The molten globular state can not be seen as a structural entity but as an ensemble of related structural elements which are rapidly interconverting. The interconversion of these states requires only a few milliseconds. After the polypeptide has reached this state the compaction to go from the molten globular state to the final native fold occurs spontaneously.

After the molten globule persistent native-like structural elements, possibly in the form of subdomains, begin to develop in a second step which can last up to 1 second. Compared to the molten globule the ensemble of conformations is much reduced but can not be referred to be a single native form. This form is reached in a final stage of folding. In this stage the formation of native interactions, hydrophobic packaging in the interior and the fixation of surface loops occur.

 Protein folding is a time-dependent process which can span from minutes or hours for the slowest proteins to time scales of milliseconds for proteins with several hundred amino acids. The fastest proteins need only a few microseconds for correct folding. Fig. I-2 shows a schematic overview of the folding process.

*The kinetics of protein folding and protein stability*

According to the thermodynamic hypothesis, a native protein structure corresponds to the global minimum of free energy in the protein-solvent system. In 1968 Levinthal showed that protein folding cannot be simulated or screened via a systematical search of all possible conformation. This would take "longer than the lifetime of a universe" (Levinthal, 1968). As is generally known proteins fold much faster. Hence, Levinthal proposed that a random conformational search does not occur in folding, and that the protein therefore must fold following a

pre-determined pathway. The protein folding process has been investigated in detail by Monte Carlo (MC) simulations (Sali, 1995a; Sali, 1995b; Dinner *et al.*, 1996). A three-stage process was postulated for protein folding: after a rapid collapse from a random-coil state to a random semi-compact globule a slow and rate-determining search through the semi-compact states takes place to find one of about several thousand similar transition states. From this state the protein-chain rapidly folds to the native state.

Although three dimensional protein structures solved on the basis of crystallographic data give the impression, a protein in its native state is not static. The structural elements, α-helices and β-strands, as well as entire domains continually undergo small movements in space. These movements can be either small fluctuations of individual atoms or collective motions of groups of atoms. The conformational changes are essential for functional activities of many proteins, e.g. for ligand binding.

The energy difference between the native state of a biologically active protein to the denatured inactive state is about 5-15 kcal/mol. This is not much more than the energy contribution of a single hydrogen bond (2-5 kcal/mol).

Two major factors contribute to the energy difference between folded and denatured state: enthalpy and entropy. Enthalpy derives from the energy of all noncovalent interactions within the polypeptide chain. Among these are "van der Waals" interactions, hydrogen bonds and ionic bonds. In the native and the denatured state the covalent bonds within and between the amino acid residues of the polypeptide are the same with the exception of disulfide bonds between cysteine residues. The noncovalent interactions differ very much between the two folding states. In the native folded state the interactions are maximized to produce a compact globular molecule with a tightly packed hydrophobic core. In the denatured unfolded state the side chains are more loosely packed. Therefore their energy contribution, the enthalpy, is much larger. The difference in enthalpy between the native and the denatured state can reach several hundred kcal/mol.

The second factor which contributes to the energy difference between the two states is entropy. This factor describes that energy is required to create order. Native folded proteins are highly ordered in one main conformation whereas unfolded denatured proteins are highly disordered with many different conformations. Like in the case of enthalpy, the difference in entropy between native and denatured state is several hundred kcal/mol, but in the opposite direction to enthalpy. Therefore the energy difference of 5-15 kcal/mol is the difference between the major factors enthalpy and entropy and is called the free energy of the system.
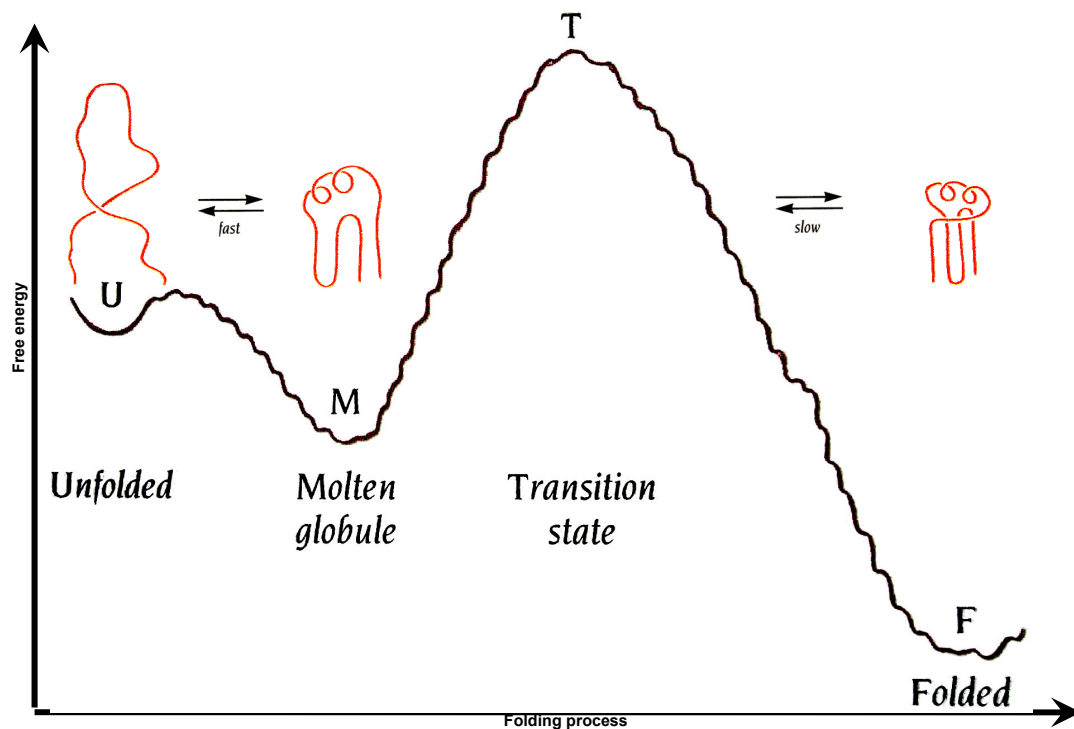


**Fig. I-2**

The polypeptide chain is flexible in the unfolded and denatured state. The molten globular state is the intermediate state with a reduced number of conformations. In comparison to the folded native state the molten globular state is less compact and the proper packing interactions in the interior of the protein have not been formed, but it has most of the secondary structure of the native state. (Rossmann *et al.*, 1975)

## I.3    Homology Modeling and Molecular Dynamics Simulations as Computational Tools

*Homology Modeling*

Today homology modeling is the most reliable technique for prediction of protein structures and requires one or more protein structures as template proteins with preferably high sequence identity. At the beginning of a modeling procedure one or more template proteins with high sequence homology to the protein which structure has to be modelled have to be identified. Then the template and the target sequences have to be aligned and the three-dimensional structure of the target sequence has to be generated on the basis of the coordinates of the aligned residues of the template proteins. For loop regions and unaligned sequence segments models are generated. Several refinement steps are performed to resolve structural implausibilities.

Several methods for molecular modeling exist which differ in the way the coordinates for the target sequence are calculated from the template structures. The method used for the modeling of the structure of the 3α-HSD/CR-Mutant in this thesis is the method of *modeling by satisfaction of spatial restrains*, implemented in the program modeller 6. This approach uses either distance geometry (Havel and Snow, 1991; Srinivasan *et al.*, 1993) or optimisation techniques (Sali and Blundell, 1993) to satisfy spatial restrains which occur at the alignment of the target sequence to the homologous template protein.  The original modeling method is based on rigid-body assembly. In this approach the model is constructed from several core regions, loops and side chains, which are taken from related structures (Browne *et al.*, 1969; Sali and Blundell, 1993; Thibault *et al.*, 2004) and involves the fitting of rigid bodies onto a framework defined as the average of the Cα atoms in the conserved folding regions. Another group of methods can be classified as modeling by segment matching. In this approach the coordinates of the not-conserved atoms are calculated on the basis of approximate positions of conserved atoms from the template protein structures (Jones and Thirup, 1986; Claessens *et al.*, 1989; Levitt, 1992; Duplomb *et al.*, 2004).

The accuracy of a comparative model corresponds to the percentage sequence identity of the two proteins and therefore correlates with the relationship between their structural and sequence similarity (Sanchez and Sali, 1998; Koehl and Levitt, 1999; Marti-Renom *et al.*, 2000). Baker and Sali showed in 2001 that models which have a sequence identity of at least

50% with their templates tend to not exceed 1 Å rms (*root mean square*) deviation with respect to main chain atoms. Comparative models with a sequence identity of 30 to 50% show about 90% of the main-chain modelled with 1,5 Å rms error. Bates and coworkers showed that the regions predicted best are often regions with biological significance, because their structure is conserved by evolution (Bates *et al.*, 2001).

*Molecular Dynamics (MD) Simulations*

Molecular Dynamics simulations provide a computational tool to simulate the motions of a molecular system. During MD-simulations the configuration space, the entirety of configurations accessible to the system, is sampled and a trajectory is generated. A prerequisite for MD-simulations is an interaction potential from which interatomic forces can be calculated. The method is based on the physical principle that at ambient temperatures biological macromolecules are never at rest and that their hierarchy of motions ranges from small fluctuations of hundredths of an Ångstrom to domain movements in the magnitude of tens of Ångstroms (Karplus and Petsko, 1990). Flexibility of a protein domain is of essential importance for protein function as it enables binding of ligands, enzyme catalysis and conformational changes in general.

Newton's equation of motion is the basis for classical MD simulations

$$\mathbf{F = m_i \ a_i}$$

In this equation the acceleration a of a particle or atom i of mass m is directly proportional to the acting force F. The acceleration a is the first derivative of the velocity with respect to time and the second derivative of the atomic positions with respect to time. Therefore expressions for the coordinates and the velocities of the particles as a function of time can be derived.

If the interatomic forces as well as a set of starting coordinates $r_i(t_0)$ and velocities $v_i(t_0)$ are known the positions $r_i(t_1)$ and the velocities $v_i(t_1)$ of the atoms for a following time $t_1 = t_0 + \Delta t$ can be evaluated. The values for positions and velocities at $t_1$ serve then to calculate positions and velocities at subsequent times $t_2$ and so forth.

The value needed is the forces between the particles. First, a suitable interaction potential has to be assigned which describes the energy of the system as a function of the atomic coordinates. In the first derivative of the potential with respect to the atom position the forces can be

derived. The potential consists of a set of empirically parameterized terms for bond lengths, bond angles and torsion angles, as well as terms for the non-bonded van der Waals interactions and Coulomb interactions. This set of parameters is defined in a molecular mechanics force field. In addition to these chemical parameters some further aspects important for practical MD simulations of biomolecules have to be defined. Among these are the definition of appropriate boundary conditions for the system minimizing the edge effects in simulations of liquids, solution or solids, the handling of the solvent, regulation of temperature and pressure and the treatment of long-range electrostatic forces (Gunsteren and Berendsen, 1990). A MD simulation results primarily in a trajectory of the simulated system which consists of a series of conformations as a function of time. The accuracy of a MD simulation heavily depends on the potential energy function and a sufficient sampling time for which the configurations of the system are generated.

In this study MD simulations are performed together with homology modeling to prove the plausibility of the approach to redesign a complete loop region in 3α-HSD/CR by substitution of the extraloop domain by a shortened homologous loop of 3α/20β-HSD on the basis of two crystallographically determined structures.

## I.4        Motivation -  A Combined *in silico* and Molecular Biology Strategy

The main subject of this study was the question, which role the additional extraloop domain plays in 3α-HSD/CR from *C. testosteroni* and if this structural feature has a fundamental role for protein stability and/or functionality. To investigate this question a mutated 3α-HSD/CR-protein (3α-HSD/CR-tr) had to be established which lacks the extraloop domain. As described in chapter I.2  the primary structure of a protein bears the information for secondary structure and correct protein folding. Solely to delete the amino acids of the alpha-helical subdomain which constitutes the extraloop-domain would lead to incorrect protein folding with consequences not only for the relative positions of the neighbouring amino acids.

As mentioned above (chapter I.1 ) the Q-axis interface as the typical interface region for dimeric SDR-proteins is built up of the four helix bundle consisting of helices αE and αF. In 3α-HSD/CR the extraloop-domain is located within this interface region which is thought to be the reason for dimerization along the P-axis interface of normally tetrameric SDR-proteins.

Mutational changes by deletion of the extraloop-domain within the Q-axis-interface would unavoidably have consequences for the oligomerization behaviour (Fig. III-2, p19.)

Another substantional criterion not only to delete the extraloop-domain is the fact, that in the SDR superfamily the amino acids of the catalytic triad are adjacent to the structural elements of the four helix bundle. Fundamental changes in the structural integrity of this region would have effects also on the catalytic efficiency of the protein.

Based on these concerns, an approach was performed in which at the end 36 amino acids of the alpha-helical extraloop-domain were substituted by an 8-residue loop of the homologous region of 3α/20β-HSD of *S. hydrogenans*. This selection showed the best quantitative scores to retain protein stability, correct folding and thereby an untouched architecture of the catalytic triad. This approach ensured that the effects which arised after mutation could be attributed to the lack of the extraloop-domain and not to the destruction of the entire protein architecture.

The complexity of the desired mutation was much higher than for single point mutations, especially because of expected changes in the solubility of the overexpressed protein. Hence, this mutation was first modelled and simulated to estimate the structural consequences for the whole protein and to minimize endevours due to intricacies in protein production..

## I.5      Aim of this Study

The aim of this study was to investigate whether the lack of this predominantly α-helical subdomain leads to the formation of a homotetramer or even a novel oligomerization mode. In this study re-design of this interface was performed on the basis of site-directed mutagenesis and according to other SDR structures by an approach combining "in silico" and "wet chemistry". Simulations of sterical and structural effects after different mutations, by applying a combination of homology modeling and molecular dynamic simulations, provided an effective tool for extensive mutagenesis studies. First activity tests after successful protein expression could constitute an evidence for an active and correctly folded protein.

# II  Materials

## II.1  Chemicals

| | |
|---|---|
| 1,1,1-Trichlorethan | Merck, Darmstadt |
| Acrylamid | Serva/Heidelberg |
| Agarose | Gibco-BRL/Eggenstein |
| Ampicillin | Appligene/Heidelberg |
| APS | Merck/Darmstadt |
| ABTS   2.2'-Azino diethyl-benzothiazoline sulfonic acid | Boehringer Mannheim |
| ATP | Boehringer/Mannheim |
| Bacto-Agar | Difco, Detroit (USA) |
| Bacto-Trypton | Difco, Detroit (USA) |
| Borsäure | Fluka, Neu-Ulm |
| Bromphenolblau | Merck/Darmstadt |
| BSA | Sigma, Deisenhofen |
| Calciumchlorid | Merck, Darmstadt |
| DAB (3,3'-Diaminobenzidintetrahydrochlorid) | Sigma/Deisenhofen |
| Dichlordimethylsilan | Sigma, Deisenhofen |
| Diethylether | Roth, Karlsruhe |
| Di-Natriumhydrogensulfat | Merck, Darmstadt |
| dNTPs | Boehringer/Mannheim |
| DTT (1,4-Dithio-L-threitol) | Fluka, Neu-Ulm |
| EDTA (Ethylendiaminotetraessigsäure) | Roth, Karlsruhe |
| Essigsäure | Fluka, Neu-Ulm |
| Ethanol | Roth, Karlsruhe |
| Ethidiumbromid | Sigma/Deisenhofen |
| Formaldehyd | Merck, Darmstadt |
| Glutaraldehyd | Sigma/Deisenhofen |
| Glycerin | Roth, Karlsruhe |
| Glycin | Roth, Karlsruhe |
| Harnstoff | Roth, Karlsruhe |

| | |
|---|---|
| Hefeextrakt | Difco, Detroit (USA) |
| Heparin | Sigma/Deisenhofen |
| Isopropanol | Roth, Karlsruhe |
| Kaliumacetat | Merck, Darmstadt |
| Kaliumchlorid | Roth, Karlsruhe |
| Magnesiumchlorid | Merck, Darmstadt |
| Magnesiumsulfat | Roth, Karlsruhe |
| Mercapthoethanol | Merck, Darmstadt |
| MOPS (Morpholinopropansulfonsäure) | Roth, Karlsruhe |
| N, N`-Methylenbisacrylamid | Serva/Heidelberg |
| Natriumacetat | Roth, Karlsruhe |
| Natriumchlorid | Roth, Karlsruhe |
| Natriumdihydrogensulfat | Merck, Darmstadt |
| Natriumdodecylsulfat (SDS) | Roth, Karlsruhe |
| Natriumhydrogenphosphat | Merck, Darmstadt |
| Natriumhydroxid | Fluka, Neu-Ulm |
| Octylphenolethylenglykolether (Triton X-100) | Serva/Heidelberg |
| Protein A Sepharose CL-4B | Pharmacia Biotech, Freiburg |
| PEG 4000 | Fluka, Neu-Ulm |
| Proteinmarker | BioRad/München |
| Salzsäure | Roth/Karlsruhe |
| TEMED | Sigma/Deisenhofen |
| Tris-(hydroxymethyl)- aminoethan | Roth/Karlsruhe |
| Tween 20 (Polyoxyethylensorbitanmonolaurat) | Sigma/Deisenhofen |
| X-Gal | Roth/Karlsruhe |
| X-Phosphat (5-Bromo-4-chloro-3-indoylphosphat) | Boehringer/Mannheim |

## II.2      Technical Equipment

| | |
|---|---|
| HPLC-System | Merck Hitachi L-6220 Intelligent Pump, |
| | Merck Hitachi AS-2000 A Autosampler |
| | Merck Hitachi L-4000 A UV Detector |
| Äkta-Explorer | Amersham Biosciences |
| Autoradiograpgiekassette | Goos, Heidelberg |
| Durchflußphotometer 2210 | LKB-Bramm |
| Elektrophoresekammern Agarose | Universität Marburg |
| Elektrophoresekammern SDS-PAGE, Protean 3 | BioRad  Münschen |
| Entwicklermaschine | Agfa-Gevaert; Gevamatic 110 |
| Superloop | Amersham Biosciences |
| Powerpack | BioRad, München |
| Glaswolle | Merck, Darmstadt |
| Kryobad | KH-3, Biometra |
| Kühlzentrifuge | Megafuge R 1.0, Heraeus |
| | Biofuge frigo, Heraeus |
| Magnetrührer | Variomag Mono, H+P Labortechnik |
| Nylonmembran Hybond-C | Amersham, Braunschweig |
| PCR-Cycler | Personal Cycler, Biometra |
| Photometer | Ultrospec 3000, Pharmacia |
| | GenQuant, Amersham, Sweden |
| Probenschüttler | IKA MTS 4, Janke und Kunkel |
| Reaktionsgefäßschüttler | Reax 2000, Heidolph |
| Röntgenfilme X-OMAT | Kodak |
| Ultrasonic Sonifier | Brandeln |
| Schüttler | WT-12, Biometra |
| Speed-Vac | Speed Vac; Uniequipe, |
| Thermoblock | Biometra, Göttingen |
| Thermoblock | Driblock DB.2A, Techne |
| Tischzentrifuge | Biofuge 13 pico, Heraeus |
| UV-Transilluminator | TI 1, Biometra |
| Vakuumzentrifuge | Uniequipe, |
| Vortex-Gerät | Vortex Genie 2, MAGV, Rabenau, Londorf |

Wasserschüttelbad                                      GFL 10013

Whatman-G50                                            Whatman, New Jersey (USA)


## II.3      Enzymes and Kits

| | |
|---|---|
| Alkalische Phosphatase, Shrimp | Roche, |
| BioRad-Reagenz | BioRAD, Richmond (USA) |
| PfuTurbo$^R$-Polymerase | Stratagene, Heidelberg |
| Pfu-Polymerase | Stratagene, Heidelberg |
| *Dpn*I | Stratagene |
| Deoxynucleotide Mix | Stratagene |
| Quick Change Site-Directed Mutagenesis Kit | Stratagene |
| Rapid DNA Ligation & Transformation Kit | MBI-Fermentas |
| Quick Ligation Kit | New England Biolabs |
| Restriktionsendonukleasen | New England Biolabs, Schwalbach |
| DNAseI | Stratagene |
| RNAse A | Boehringer, Mannheim |
| T4-DNA-Ligase | Boehringer, Mannheim |
| Topo TA Cloning Kit | Invitrogen |
| Taq DNA Polymerase | Promega |
| Taq-Polymerase | Promega, Heidelberg; |
| | Boehringer Mannheim |
| Vent-Polymerase | New England Biolabs |


## II.4      Chromatography Columns

| | |
|---|---|
| HisTrap$^{TM}$ HP Columns 5ml, pre-charged | Amersham Biosciences |
| HisTrap$^{TM}$ HP Columns 1ml, pre-charged | Amersham Biosciences |
| HiTrap$^{TM}$ Chelating Column 5ml | Amersham Biosciences |

## II.5        Bacterial Strains and Cultivation

### II.5.1        E.coli Strains

**K-12 DH 5α  (Life Technologies, Eggenstein)**
*dlacU 169, F⁻, end A1, hsd R17, sup E44, thi-1, rec A1, gyr A96, rel A1, f 80 dlac Z, dM15, Lamda⁻*

**XL10-Gold Ultracompetent Cells (Stratagene)**
Tet$^R$Δ(mcrA)183 Δ(mcrCB-hsdSMR-mrr)173 endA1 supE44 thi-1 recA1 gyrA96 relA1 lac The [F' proAB lacl$^q$Z ΔM Tn10 (Tet$^R$)Amy Cam$^R$]

**E.coli XL1 MRF' (Stratagene)**
Δ(*mcrA*)*183* Δ(*mcrCB-hsdSMR-mrr*)*173 endA1 supE44 thi-1 recA1 gyrA96 relA1 lac* [F′ *proAB lacl$^q$ZΔM15* Tn*10* (Tet$^r$)]

**BL21 (Stratagene)**
*E. coli* B F⁻ *dcm ompT hsdS*(r$_B$⁻ m$_B$⁻) *gal*

**BL21(DE3) (Stratagene)**
*E. coli* B F⁻ *dcm ompT hsdS*(r$_B$⁻ m$_B$⁻) *gal* λ(DE3)

**BL21(DE3)pLysS (Stratagene)**
*E. coli* B F⁻ *dcm ompT hsdS*(r$_B$⁻ m$_B$⁻) *gal* λ(DE3) [pLysS Cam$^r$]

**BL21-Gold strain (Stratagene)**
*E. coli* B F⁻ *ompT hsdS*(r$_B$⁻ m$_B$⁻) *dcm$^+$* Tetr *gal endA* The

**BL21-Gold(DE3)pLysS strain (Stratagene)**
*E. coli* B F⁻ *ompT hsdS*(r$_B$⁻ m$_B$⁻) *dcm$^+$* Tetr *gal* λ(DE3) *endA* Hte [pLysS Camr]

**Origami $^{TM}$ B(DE3) (Novagen)**
*E. coli* F⁻ *ompT hsdS$_B$* (r$_B$⁻m$_B$⁻) *gal dcm lacY1gor522::*TN*10*(Tc$^R$) *trxB*::kan (DE3)

### II.5.2        E.coli -Cultivation

For bacteria cultivation LB- media (Luria-Bertani-medium) was used: bactotrypton, 5g yeast extract, 5g NaCl per litre media.

For Agar-plates 1,5% Bacto-Agar was added.

For screening for ampicillin resistance ampicillin was added to a final concentration of 100μg/ml in the media.

Bacteria cultivation was performed in a horizontal shaker with temperature incubation.

## II.6      Antibodies

For Western-blot analysis the following antibodies were used

| antibody | supplier |
|---|---|
| Anti-CBR1 | AG Prof. Maser, Kiel |
| Anti-3α-HSD/CR rabbit-made | AG Prof. Maser, Kiel |
| Anti HIS-IgG, mouse -made | Amersham Biosciences, Freiburg |
| Anti rabbit IgG, goat-made, peroxidase conjugate | Sigma, Deisenhofen |
| Anti rabbit IgG, pig-made, peroxidase conjugate | DAKO GmbH, |
| Anti mouse IgG, peroxidase conjugate, sheep-made | Amersham Biosciences, Freiburg |

## II.7      Protein and DNA-Standards

**Precision Plus Protein Standard Dual Color**                     **Bio-Rad**

**MagicMark[TM] Western Protein Standard**          **Invitrogen**

**GeneRuler 50bp DNA Ladder**                          **MBI Fermentas**

**GeneRuler 100bp DNA Ladder**                        **MBI Fermentas**

**GeneRuler 1 kb DNA Ladder**                          **MBI Fermentas**

**GeneRuler DNA Ladder Mix**                           **MBI Fermentas**

## II.8        Synthetic Oligonucleotides and Plasmids

### II.8.1        Oligonucleotides

| oligonucleotide | sequence                          5' …. 3' |
|---|---|
| 3HSD-Gen1-for | ATG TCC ATC ATC GTG ATA AGC GGC TGC GCC ACC |
| 3hsd-Gen1-rev | GGA AGC CAC GGA CGA GAT GAC GAC GGC TGC GGG C |
| 3HSD-Gen2-for | GCC TAT GCG GGC AGC AAG AAT GCT TTG ACG GTG GC |
| 3HSD-Gen2-rev | TCA GGA CTG TGT CGG GCG CAT CAC CGC |
| 3HSD-Gen1-for-Nde | GGG AAT TCC ATA TGT CCA TCA TCG TGA TAA GCG GCT GCG CCA CC |
| 3HSD-Gen2-rev-Bam | GGA TCC GAG GTG AGA ACT GTG TCG GGC GCA TCA CCG C |
| 3HSDH-U1 | GCA GCG GCC TGG TGC CGG GCG GCA GC |
| 3HSDH-U2 | CAG CTT CCT TTC GGG CTT TGT TAG CAG CC |
| 3HSDH-M1 | CAG TGC CAA TCC CAT TAA GGA AGC CAC GGA CGA GAT GAC |
| 3HSDH-M2 | ATG GGA TTG GCA CTG ACA AGT GCC TAT GCG GGC AGC AAG AAT GC |
| 3HSD1 | CGT CAT CTC GTC CGT GGC TTC CTT AAT GGG ATT GGC ACT GAC AAG TGC CTA TGC GGG CAG CAA GAA TGC |
| 3HSD2 | GCA TTC TTG CTG CCC GCA TAG GCA CTT GTC AGT GCC AAT CCC ATT AAG GAA GCC ACG GAC GAG ATG ACG |
| CCGCATAGG | CCG CAT AGG CAC TTG TCA GTG CCA ATC CCA TTA AGG AAG CCA CG |
| T7-promoter | TAA TAC GAC TCA CTA TAG GG |
| T7-terminator | GCT AGT TAT TGC TCA GCG G |
| Mu22 | CAT TCT TGC TGC CCG CAT AGG C |
| 3hsd-Gen-rev-BamHI | CGC GGA TCC GAG GTC AGA ACT GTG TCG GGC GCA TCA CCG C |

## II.8.2    Plasmids

pUC18  (Norrander *et al.*, 1983)    MBI Fermentas

EcoO109I 2674    PfoI  46    BstAPI  179
AatII  2617                   NdeI  183
SspI  2501                    EheI  235
PdmI  2294
Bcgl  2215            2486        146      lacz  MCS
ScaI  2177                        236
                                 469
bla (Ap^R)           pUC18/19
                     2686 bp          BsaXI  659
                                      SapI  683

                     852             AflIII, PscI  806
GsuI  1784
Cfr10I  1779          1626
Eco31I  1766          1466
Eam1105I  1694       rep (pMB1)
                                 BseYI  1110
CaiI  1217

```
                                     PstI      HincII    Cfr9I         Acc65I    Ecl136II
                                     Sdal      SalI      Eco88I        KpnI      Eco24I    EcoRI
M13/pUC sequencing primer (-20), 17-mer  399  HindIII  Pael  Bvel  XmnI  Xbal  BamHI  SmaI  SacI  XapI  455
5' G TAA AAC GAC GGC CAG TGC cAA GCT TGC ATG CCT GCA GGT CGA CTC TAG AGG ATC CCC GGG TAC CGA GCT CGA ATT CgT AAT CAT GGT CAT AGC TGT TTC CTG 3'
3' C ATT TTG CTG CCG GTC ACG gTT CGA ACG TAC GGA CGT CCA GCT GAG ATC TCC TAG GGG CCC ATG GCT CGA GCT TAA Gca TTA GTA CCA GTA TCG ACA AAG GAC 5'
LacZ  ←   Val Val Ala Leu Ala  Leu Ser Ala His Arg Cys Thr Ser Glu Leu Pro Asp Gly Pro Val Ser Ser Ser Asn Thr Ile Met Thr Met
                                                                                                 M13/pUC reverse sequencing primer (-26), 17-mer
```

Bpu1102 I(267)
EcoR I(5706)          BamH I(319)
Aat II(5635)   Cla I(24)       Xho I(324)
Ssp I(5517)    Hind III(29)    Nde I(331)
                               Nco I(389)
Sca I(5193)                    Xba I(428)
Pvu I(5083)                    Bgl II(494)
Pst I(4958)                    SgrA I(536)
                               Sph I(691)
Bsa I(4774)      Ap (4643-5500)  EcoN I(751)
Ahd I(4713)
                pET-15b           Mlu I(1216)
                (5708bp)          Bcl I(1230)
                                  lacI (866-1945)
AlwN I(4236)                       BstE II(1397)
                                   Apa I(1427)
                ori (3882)         BssH II(1627)
BspLU11 I(3820)                    Hpa I(1722)
Sap I(3704)
Bst1107 I(3591)                    PshA I(2061)
Acc I(3590)
BsaA I(3572)                       Eag I(2284)
Tth111 I(3565)                     Nru I(2319)
                                   BspM I(2399)
                Bpu10 I(2926)      Bsm I(2704)
                        Msc I(2791)

pET15b                        Novagen

```
                T7 promoter primer #69348-3
Bgl II              T7 promoter              lac operator          Xba I                    rbs
AGATCTCGATCCCGCGAAATTAATACGACTCACTATAGGGGAATTGTGAGCGGATAACAATTCCCCTCTAGAAATAATTTTGTTTAACTTTAAGAAGGAGA

    Nco I            His•Tag                                       Nde I   Xho I  BamH I
TATACCATGGGCAGCAGCCATCATCATCATCATCACAGCAGCGGCCTGGTGCCGCGCGGCAGCCATATGCTCGAGGATCCGGCTGCTAACAAAGCCCGA
        MetGlySerSerHisHisHisHisHisHisSerSerGlyLeuValProArgGlySerHisMetLeuGluAspProAlaAlaAsnLysAlaArg

            Bpu1102 I                          thrombin          T7 terminator
AAGGAAGCTGAGTTGGCTGCTGCCACCGCTGAGCAATAACTAGCATAACCCCTTGGGGCCTCTAAACGGGTCTTGAGGGGTTTTTTG
LysGluAlaGluLeuAlaAlaAlaThrAlaGluGlnEnd

                T7 terminator primer #69337-3
```

## II.9      Buffer, Media and Solutions

### II.9.1      Media for E.coli Cultivation

LB-media

1% Bactotrypton
0.5% Hefeextrakt
85.5 mM NaCl
100 μg/ml Ampicillin (for E.coli-cultivation)

LB-Agar

1% Bactotrypton
0.5% Hefeextrakt
85.5 mM NaCl
1.5% Bacto-Agar

LB-Amp-X-Gal-plates;

1% Bactotrypton
0.5% Hefeextrakt
85.5 mM NaCl
100 μg/ml Ampicillin
40 mg/l X-Gal in 2 ml Dimethylformamid
1,5 % Agar-Agar (w/v)

### II.9.2      Buffer and Solutions for Gel Electrophoresis

Loading buffer:

0.5% Xylencyanol FF
0.5% Bromphenolblau
40% Glycerin in TAE oder TBE

TAE-buffer (20 x)

0,8 M Tris-Acetat (pH 8,3)
10 mM EDTA (pH (8,0)

Loading buffer for DNA- gel elektrophoresis

1 mg/ml Bromphenolblau (0.5%)
2 mg/ml Xylencyanol-FF
2 mg/ml Orange-G
40 % Glycerin (w/v)
1 mM EDTA (pH 8,0)

Ethidiumbromid-stock solution

10 mg/ml Ethidiumbromid in 1 x TE

### II.9.3      Solutions for DNA-Preparation from Agarose Gels

Amersham pharmacia biotech
acetat- und chaotrophaltig,
10 mM Tris-HCL pH 8.0
1 mM EDTA
80% EtOH

TE-buffer (10x)

10 mM Tris/HCL (pH 8.0)
1 mM EDTA

## II.9.4    Solutions for Preparation of Competent Cells

| SOB | | |
|---|---|---|
| | | 2 % Bacto-Trypton (w/v) |
| | | 0,5 % yeast extract (w/v) |
| | | 10 mM NaCl |
| | | 2,5 mM KCl |
| | | 10 mM $MgCl_2$ |
| | | 10 mM $MgSO_4$ |

| RF1 | | |
|---|---|---|
| | 0,302g RbCl | 10 mM RbCl |
| | 2,023g MnCl | 50 mM MnCl |
| | 0,559g KCl | 30 mM KCl |
| | 0,367g CaCl | 10 mM CaCl |
| | 35ml  85% Glycerine δ = 1.23 g/ml | 15% Glycerin |
| | ad  250 ml with sterile $H_2O$ | |

All components were solved in 50 ml A.dest. pH was adjusted to 5.8 with NaOH and the solution was sterile filtered. After addition of sterile glycerine the solution was filled up with sterile water to a final volume of 250 ml.

| RF 2 | |
|---|---|
| | 10 mM MOPS (pH 6,8) |
| | 10 mM RbCl |
| | 75 mM $CaCl_2$ |
| | 15 % Glycerin (w/v) |

Components of solution RF2 were solved in 50 ml of sterile $H_2O$ and sterile filtered. After addition of 14 ml of  85% sterile glycerine (density δ = 1,23 g/ml) the solution was filled up with 36 ml of sterile $H_2O$ to a final volume of 100 ml.

## II.9.5    Solutions for PCR

| dNTP-Mix | |
|---|---|
| | 2 mM dATP |
| | 2 mM dTTP |
| | 2 mM dCTP |
| | 2 mM dGTP |

| PCR-buffer (10 x) | |
|---|---|
| | 500 mM KCl |
| | 500 mM Tris |
| | 25 mM $MgCl_2$ |
| | 0,1 % Gelatine (w/v) |

| PBS | |
|---|---|
| | 130 mM NaCl |
| | 7 mM $Na_2HPO_4$ |
| | 3mM $NaH_2PO_4$ |

| PBT | |
|---|---|
| | 0.1% Tween 20 in PBS |

## II.9.6      Solutions for Preparation of Plasmid DNA

*Analytical scale*

| | |
|---|---|
| P1 (Resuspensation buffer) | 50 mM Tris/HCL (pH8.0) |
| | 10 mM EDTA |
| | 400µg RNAse A |
| P2 (Lysis buffer) | 200 mM NaOH |
| P3 (Neutralization buffer) | 2.55 M potassium acetate (pH 4.8) |

*Preparative scale*

| | | |
|---|---|---|
| P1-buffer | (Resuspensation buffer) | 50 mM Tris |
| | | 10 mM EDTA (pH 8,0) |
| | | RNAse A (100 µg/ml) |
| P2-buffer | (Lysis buffer) | 200 mM NaOH |
| | | 1 % SDS (w/v) |
| P3-buffer | (Neutralization buffer) | 3,2 M potassium acetate (pH 5,5) |
| Buffer QBT | (Equilibration buffer) | 750 mM NaCl |
| | | 50 mM MOPS, pH 7.0 |
| | | 15% isopropanol (v/v) |
| | | 0,15 % TritonX-100 (v/v) (pH 5,0) |
| Buffer QC (Wash buffer) | | 1.0 M NaCl |
| | | 50 mM MOPS, pH 7.0 |
| | | 15% isopropanol (v/v) |
| Buffer QF (Elution buffer) | | 1,25 M NaCl |
| | | 50 mM Tris-HCl (Ph 8,5) |
| | | 15% isopropanol (v/v) |

## II.9.7      Solutions for SDS-PAGE

| | Auftrennungsbereich 20 – 70 kDa | eingesetzt: |
|---|---|---|
| Stacking gel  5% | 30 % Acrylamid | 1.7 ml |
| | 2 % Methylenbisacrylamid | 0.6 ml |
| | 1 M Tris/HCL, pH 6.8 | 1.25 ml |
| | 10 % SDS | 100 µl |
| | A.dest. | 5.7 ml |
| | 10 % APS | 50 µl |
| | TEMED | 5 µl |

| Resolving gel: | 30 % Acrylamid | 6.25 ml |
| | 2 % Methylenbisacrylamid | 1.55 ml |
| | 1 M Tris/HCL pH 8.7 | 5.6 ml |
| | 10 % SDS | 150 µl |
| | A.dest. | 1 ml |
| | 10 % APS | 50 µl |
| | TEMED | 10 µl |

TBE-Puffer                                        siehe 1.1.8

SDS running buffer                        0.25 M Tris
                                                        1.9M Glycin, pH 6.8
                                                        1 % SDS

1 x SDS-gel-loading buffer          50 mM Tris/HCL, pH 6.8
                                                        100 mM DTT
                                                        2 % SDS
                                                        0.1% Bromphenolblau
                                                        10 % Glycerin

Coomassie-Blue-staining solution          40 % Methanol
                                                        10 % Essigsäure
                                                        1 % Coomassie Brillant Blue

Solution for de-staining                40 % Methanol
                                                        10 % Essigsäure

## II.9.8      Solutions For Renaturation of Inclusion Bodies

Lysis buffer                                        100 mM Tris-HCl, pH 7.0
                                                        5 mM EDTA
                                                        5 mM DTT (770 mg/l)
                                                        5 mM Benzamidine (780 mg/l)

Wash buffer                                        100 mM Tris-HCl, pH 7.0
                                                        5 mM EDTA
                                                        5 mM DTT (770 mg/l)
                                                        2 M Urea
                                                        2% Triton X-100 (20g/l)

Solubilization buffer                        6 M GdmCl
                                                        100 mM DTT
                                                        0,1 M Tris-HCl, pH 8,0

See "Methods" for details

## II.9.9      Solutions for Western Blot Analysis

| | |
|---|---|
| 2 x SDS-Loading buffer | 100 mM Tris/HCL pH 7.9 |
| | 200 mM DTT |
| | 4% SDS (w/v) |
| | 0.2 % Bromphenolblau (w/v) |
| | 20% Glycerin (w/v) |
| | |
| Western-transfer buffer | 25 mM Tris/HCL ,pH 8.3 |
| (Towbin *et al.*, 1979) | 192 mM Glycin |
| | 20 % (v/v) Methanol |
| | |
| Regenaration buffer | 2% SDS |
| | 62.5 mM Tris/HCL pH 6.7 |
| | 0.7% Mercaptoethanol |

## II.9.10      Solutions for Affinity Chromatography

| | |
|---|---|
| Resuspensation buffer | Tris-HCl 20mM |
| | 10% Glycerin |
| | pH 7.4 |
| | |
| Buffer A | 20 mM Kaliumdihydrogenphosphat |
| | 10 mM Imidazol |
| | 100 mM NaCl |
| | pH 7.4 |
| | |
| Buffer B | 20 mM Kaliumdihydrogenphosphat |
| | 500 mM Imidazol |
| | 100 mM NaCl |
| | pH 7.4 |
| | |
| Stripping buffer | buffer A |
| | 0,05 M  EDTA |
| | ad 100ml |
| | |
| Loading buffer | 0,1M Nickel-II-Sulfat-Hexahydrat |
| | ad 100ml |

# III Methods

## III.1      Generation of 3α-HSD/CR-Mutants by Overlap-Extension PCR-Technique

The amplification of specific DNA fragments is facilitated by polymerase chain reaction. The synthetically manufactured oligonucleotides serve as specific primers to amplify the DNA of interest. The thermo stable polymerase plays a major role in the synthesis of complementary DNA from the template. By the cyclic denaturation and renaturation the DNA region of interest amplifies exponentially.

3α-HSD/CR was cloned into the pK15 vector which served as template. The TGA stop codon sequence was modified to yield the reverse primer containing a *Bam*HI site.

To introduce the mutation, a primer pMU10 was designed containing the sequence to be inserted with flanking regions. In a second PCR the purified product was used as a primer together with a reverse primer containing the *Bam*HI restriction site. As a template for the second PCR the pK15 vector was used. A 25cycles PCR reaction was run against plasmid DNA of pK15 containing the 3α-HSD/CR gene under the conditions listed below. The resulting PCR product was digested with *Nde*I and *Bam*HI restriction enzymes to give a 690bp fragment. After PCR the fragments were purified by gel-electrophoresis and phenol-chloroform extraction. The resulting fragment was inserted into the TOPO-vector according to the supplier's manual. After restriction analysis the subclone was cloned into the pET15b vector. The insert was sequenced (Eurogentec) to confirm the correct in-frame DNA sequence and the absence of any mutations.

The reaction was done in a total volume of 20 μl by adding the following reaction components. After all components were added the reaction tubes were vortexed, centrifuged and placed in the PCR cycler.

| Template-DNA | 10 ng |
|---|---|
| Primer A (25 pmol/μl) | 5 μl |
| Primer B (25 pmol/μl) | 5 μl |
| dNTP (je 2.5 mM) | 5 μl |
| MgCl$_2$ (only with Taq-Polymerase) | 3 μl |
| 10 x PCR-buffer | 5 μl |
| Proof-Reading-Polymerase | 1 μl (= 2,5 U) |
| Taq-Polymerase | 0,2 μl (= 1U) |
| A.dest. | ad 50 μl |

The following PCR-program was used:

| Step | | Cycles | Temperature | Time |
|---|---|---|---|---|
| **1: denaturation** | | 1 | **95$^0$C** | **2 min** |
| **2: denaturation** | | | **95$^0$C** | **30 sec** |
| **3: annealing** | | | **45 $^0$C** | **30 sec** |
| **4: polymerization** | | 25x | **72$^0$C** | **1 min je kb, 1:40 min je kb bei proof-reading-Polymerase** |
| **5: polymerization** | | 1 | **72$^0$C** | **2:30 min** |
| **6: storage** | | 1 | **4$^0$C** | **∞** |


## III.2    Cloning of DNA in Plasmid DNA

### III.2.1    Production of Chemically Competent Bacteria (*Escherichia coli*)

250 ml of SOB medium was inoculated with 2.5 ml of fresh *E. coli*-culture (1:100) and incubated at 37°C with continuous shaking till it reached up to a OD600 of 0.5-0.6. After 15 minutes of incubation on ice the cells were centrifuged at (4000 rpm, 4° C, 10 min), and the pellet was resuspended in 80 ml cold RF1-buffer and placed again on ice for 15 minutes. The cells were centrifuged to pellet (4000 rpm, 4° C, 10 min) and resuspended in 20 ml RF2- buffer and incubated on ice for 15 minutes. The cell suspension was finally aliquoted into 200 μl each and quick frozen in liquid nitrogen. The cells were used immediately for transformation if needed and the remaining aliquots were frozen at -80°C for future use.

**III.2.2      Production of Chemically Competent Bacteria (*Escherichia coli*) with CaCl₂**

250 ml LB-Media were seeded with a o.N. culture in a 1:100 ratio. After amplification the number of cells was around $1 \times 10^8$ cells/ml ($\approx 0.5 - 0.6$ OD). After 15 min of incubation on ice the cells were harvested at 2000 x g for 10 min at $4^0$C  (2000 xg = 3400 rpm with  Megafuge R1). The precipitated cells were gently resuspended in 20 ml CaCL₂ and incubated on ice for 30 min. After centrifugation for 10 min at $4^0$C the precipitated bacteria were resuspended in 2 ml CaCL₂ and incubated on ice for additional 30 min. For transformation 100μl of chemical competent cells were used.

**III.2.3      Digestion of DNA with the Help of Restriction Endonucleases**

The following formula is generally used to determine the units of restriction enzyme required to cleave the DNA with a particular concentration.

**required units**  =         pmol DNA  x  number of restriction sites of the enzyme in the DNA

0.03 x number of restriction sites of the enzyme in λ-DNA

Restriction endonuclease digestion was performed using the enzymes and buffer from New England Biolabs according to the given instruction in the manual. Reactions were generally performed in the total volume of 20 μl. For some enzymes (EcoRI) which show the star activity BSA was added in a final concentration of 10% to prevent star activity. Double digestions were done with suitable buffers which are compatible with both the chosen enzymes. All digestions were done at 37°C for 2 hours.

**III.2.4      Dephosphorylation of the 5` Ends to Prevent Religation of the Vector**

To prevent the linearized vector from religation in the future ligation reactions, the 5`end of the DNA was dephosphorylated. Thus, the ester-reaction between the 5'-phosphate-ends and the free 3'-hydroxyl group is not longer possible. The DNA to be dephosphorylated was subjected to alkaline phosphates treatment subsequent to restriction reaction, where 0.5 Units of alkaline phosphatase was used in 1/10 V of the reaction buffer in a 40μl reaction volume and incubated at 37°C for 15 min. Inactivation of the enzyme was performed by incubation at $65^0$C for 10 minutes.

### III.2.5    Ligation of DNA Fragments

(Revie *et al.*, 1988)

The main principle of the ligation reaction with T4-DNA-ligase is the covalent linkage of 3'-OH-ends and 5'-phosphate ends under hydrolysis of ATP. To calculate the required concentrationsof vector-DNA and insert-DNA the following formula was used.

$$DNAsize(kb) \times \frac{2}{3} = \mu g \ / \ pmol$$

The ligation of DNA fragments requires the presence of compatible ends. 100-150 ng of vector DNA were used together with a three to fivefold molar excess of insert depending upon the insert size with 1/10 V of ligation buffer and 1 unit of T4-DNA ligase in a final reaction volume of 15-20 µl. The ligation mixture was incubated at 16°C overnight and completely applied to the ligation reaction.

### III.2.6    Transformation of Chemically Competent Bacteria

(Sambrook *et al.*, 1989)

To amplify the DNA kloned into vector-DNA the plasmids were transformed into competent cells.

200 µl competent cells were thawed on ice for 10-15 minutes, 1-10 µl plasmid DNA solution or ligation mixture was added and incubated on ice for 30 minutes. During Inkubation plasmid-DAN attaches to the outer membrane of the cells. The cells were heat shocked in 42°C waterbath for 60-90 seconds and immediately placed on ice for 5 min. During heatshock the plasmid-DNA is picked up into the the bacteria. In the mean time LB medium was warmed to room temperature. 450 µl of LB medium was added to the ice cold competent cell mixture and incubated at 37°C for 1 hour and light shaking to gain antibiotic resistance. Plate the cell mixture on LB selection plate (ampicillin 100 mg/ml, Kanamycin 50 mg/ml, IPTG, X-Gal) depending on the type of antibiotic resistant gene used.  Dry the plates and incubate in 37°C overnight.

## III.3      Amplification of Plasmid- DNA

### III.3.1     Mini Preparation of Plasmid DNA from *E. coli* (Alkaline Lysis Method)

(Birnboim and Doly, 1979)

Mini-preparation serves as a quick method for plasmid-preparation subsequent to cloning but results in only small amounts of DNA.

3 ml of LB medium containing 2,4µl of ampicillin (100mg/ml) was inoculated with a single colony of bacteria and incubated at 37°C with continuous shaking for 10-12h at 210rpm hours. To pellet down the cells the culture was centrifuged at 13000 rpm for 1 minute and the supernatant was discarded. 100µl of buffer P1 was added to resuspend the cells. After addition of 100µl of buffer P2 and gentle shaking for several times the mixture was incubated at RT for 5 minutes. In this step the cell membranes of the bacteria were lysed. To neutralize the mixture and to precipitate chromosomal DNA and proteins 100µl of buffer P3 were added and the mixture was mixed gently giving curd like appearance. After centrifugation at room temperature for 10-15 minutes at 13000 rpm the curd separates from the supernatant. The supernatant containing plasmid-DNA was transferred to another eppendorf tube. 0.5V of isopropanol was added to the supernatant and the mixture was vortexed and centrifuged at 13000 rpm for 30 minutes at 4°C. The supernatant was vortexed together with 500µl of 70% ethanol and centrifuged for 15 minutes at 13000rpm to dissolve salts. The pellet was dried and dissolved the DNA in 10-30 µl of ddH$_2$O or TE-buffer depending on the concentration required.

### III.3.2     Midi Preparation of Plasmid DNA

*(Qiagen, according to the manufacturers' instruction given in the manual)*

Midi-preparation provides the production of exceptionally pure DNA in larger quantities by using anion-exchange chromatography columns. This method uses the different behaviour of chromosomal- and plasmid-DNA at the change of basic pH to acid pH. The separated single-strands of the plasmid-DNA are able to fit together faster than the complete separated strands of the bacterial DNA.

To prepare the large amount of plasmid DNA which is pure and free of all the materials such as SDS and salts Midi preparation was done. 50ml LB media were inoculated with 50µl ampicillin and 20µl of a mini-overnight-culture and incubated overnight on a shaker at 180rpm. The incubated 50 ml bacterial culture was transferred into 50 ml Falcon tubes and centrifuged at 4000 rpm for 10 minutes. The pellet was resuspended in 4 ml of P1-buffer and the cells are

finally lysed by addition of 4ml P2-buffer with a gentel mix. This mixture was incubated for 15 minutes and 4ml of P3- Buffer is added for neutralization. The mixture was centrifuged at 6000 rpm at room temperature for 20 minutes. The curd separates from the supernatant containing plasmid DNA. Slowly the supernatant was transferred to the pre- equilibrated anion exchange column with QBT-Buffer. The solution was let to pass through the column by gravity flow. The column-matrix binds the plasmid-DNA. When all the solution was passed, the column was washed twice with QC-buffer, 10 ml each. the solution was let to pass through the column completely. Finally the plasmid DNA was eluted by adding 5 ml QF-buffer. The eluted DNA was mixed with 0.7 V isopropanol. Centrifuge at 4°C , 6000 rpm for 15 minutes. The supernatant was decanted, washed with 70% ethanol and centrifuged again as stated above. The supernatant was decanted and the DNA pellet is vacuum dried. The DNA was dissolved in required amount of $ddH_2O$ for the future use.

## III.4      Detection of DNA

### III.4.1      Agarose Gel Electrophoresis

(Sambrook *et al.*, 1989)

Agarose gel electrophoresis is used to separate DNA-fragments of more than 50 bp size because of their different behaviour during electrophoresis regarding their fragment size. Longer fragments move more slowly in the gel than smaller fragments.

For proper separation based on the size of the DNA to be analyzed the agarose concentration of 0.8 – 2% (w/v) in 1x TAE buffer was used to which ethidiumbromide was added. Agarose was boiled in 1x TAE-buffer and Ethidiumbomide was added to a final concentration of 10μg/ml. Ethidiumbormide incorporates into the DNA and enables detection of the loaded DNA.  The horizontal gels of the size 6 cm x 9 cm or 8 cm x 12 cm were used. The DNA samples to be loaded onto the gel were mixed with 1/10 V of loading buffer. As running buffer 1xTAE-buffer was used. Loading buffer contains xylencyanol FF and bromphenolblue which moves in the electric field towards the anode and flags the front of the samples. The gel was run at 50- 100 V. Subsequently the gel was documented with UV light in a UV-transilluminator and the picture was printed out. To estimate the size of the DNA fragments λ-DANN digested with *Eco*RI/*Hind*III restriction endonucleases was used.

### III.4.2    Isolation of DNA from Agarose Gels

The desired fragment was cut with a sharp scalpel under the mild UV light from the agarose gel and transferred to a dialysis tube (12mm). 600 µl TAE-buffer were added to the tube which was placed into the electrophoresis chamber. During electrophoresis for 10 min the DNA-fragment was extracted from the gel. To avoid binding of DNA to the dialysis membrane polarity was chnaged according to the following scheme:

| time | 10 min | 30 sec | 30 sec | 10 sec | 10 sec | 5 sec | 5 sec |
|---|---|---|---|---|---|---|---|
| Polarity + - | ↓ | ↑ | ↓ | ↑ | ↓ | ↑ | ↓ |

After Gel-extraction DNA solved in TAE-buffer was purified according to 5.1.

### III.4.3    Estimation of DNA-Concentrations

#### III.4.3.1 Estimation of DNA Concentrations using Spectrophotometer

Nucleic acids can be quantified due to their maximum absorption at the wavelength of $\lambda = 260$ nm using spectrophotometer. From the absorption (optical density = OD) the nucleic acid concentration can be computed in µg/ml using a quartz cuvette with the thickness of 1 cm considering the following parameters.

| Double stranded DNA in µg/ml | $OD_{260}$ x 50 x dilution factor |
|---|---|
| RNA in µg/ml | $OD_{260}$ x 37 x dilution factor |
| Single stranded DNA in µg/ml | $OD_{260}$ x 33 x dilution factor |

For spectrophotometric estimation of DNA-concentrations DNA-dilutions from 1:10 to 1:1000 were performed in quartz cuvettes with a thickness of 1cm and a volume from 10µl to 100µl. For blank value determination water or buffer was used in dependency of the DNA-dilution.

*III.4.3.2 Estimation of DNA Concentration using Agarose Gels*

If the expected DNA-concentration was very low 1µl and 0,1µl of the DNA-solution were loaded on a 1% agarose gel together with 10µl of DNA-standard. The concentration of the preparated DNA could be estimated by comparison of the fluorescent DNA-bands with the bands of the DNA-standard.

# III.5     Purification of DNA

### III.5.1     Phenol-Chlorophorm-Extraction of DNA

Phenol-chlorophorm extraction is the method of choice to eliminate proteins from DNA-solutions.Phenol can build up hydrogen bonds very easily and forms hydrophobic interactions with amino acid side-chains. Therefore phenol can dissoziate protein-DNA-conplexes into their free components. Proteins are denatured during the procedure and accumulate in the organic phenol-phase.

To purify DNA, e.g. after gel-extraction, the solution was filled up with $H_2O$ to a final volume of 200 µl. To the aqueous phase 200 µl phenol are added, vortexed and incubated at RT for 5 minutes. After centrifugation for 30 sec at 13.000 rpm the aqueous phase was discared and 200 µl of chlorophorm were added. Vortexing and centrifugation was repeated and the organic phase was discared. After a second chlorophorm-step 650 µl of 100% EtOH were added, vortexed and centrifugated at 13.000 rpm for 10 min. The supernatand was discared and the sedimented nuclein acids were washed with 600 µl of 70% EtOH. The pellet was resuspended in 10 µl $H_2O$.

### III.5.2     Precipitation of DNA from Aqueous Solutions with Alcohols

Alcohol precipitation is the method of choice to concentrate, desalt and recover nucleic acids. Precipitation is achieved by the use of high concentrations of salt and the addition of either isopropanol ort ethanol. Isopropanol precipitation of DNA is typically carried out using 0.6 – 0.7 volumes of alcohol, while ethanol precipitation requires 2-3 volumes of alchol. Therefore isopropanol is preferrd for precipitating DNA from large volumes since less alcohol is required.

### III.5.2.1 Ethanol Precipitation

(Crouse and Amorese, 1987; Ausubel et al., 1993)

Ethamol precipitation provides an effective tool to concentrate DNA and to remove proteins, salts and free nucleotides from the solution. By increasing of monovalent kations the Dielektrizitätskonstante is increased as well. Thus, the rejection of the negatively charged phosphodiesther-backbone is reduced which enables the DNA-precipitation by removal of solvent by ethanol addition.

To precipitate the DNA solved in bufer 1/20 VT 5M natriumchloride and 2.5 VT 100% ethanol were added and vortexed. Thereby, nucleid acids sample out as sodium salts and were harvested by centrifugation at 13.000 rpm at $4^0$C for 30 minutes. After washing with 70% and centrifugation at 13.000 rpm at $4^0$C for 10 minutes with EtOH the DNA was dried and resolved in 10 µl A.dest or TE-buffer.


### III.5.2.2 Isopropanol Precipitation

Isopropanol precipitation requires 0.6 – 0.7 VT of alcohol and can be performed at RT. This minimizes co-precipitation of salt and minimized the risk that co-precipitated salt will interfere with downstream applications.

Ideally salt concentration should be at 2.0 – 2.5 M final concentration. 0.7 VT room-temperature isopropanol was added to the DNA solution and vortexed. The sample was centrifuged immediately at 13.000 rpm at $4^0$C for 30 minutes. The supernatant was decanted carefully. The DNA pellet was washed by adding a suitable volume of 70% EtOH which removes co-precipitated salt and replaces isopropanol with the more volatile EtOH making the DNA easier to resolve. The sample was centrifuged again at 13.000 rpm at $4^0$C for 15 minutes, the supernatant was decanted and the pellet was air dried. DNA was resolved in a suitable volume of $H_2O$ or TE-buffer


## III.6     Sequencing

DNA sequencing was performed by MWG Biotech, (Ebersberg, Germany). For sequencing the universal T7 primers, already available by MWG, have been used.

## III.7      Overexpression of 3α-HSD/CR

The 3α-HSD/CR gene (Möbus and Maser, 1998) as well as the mutated gene was cloned into the *Nde*I/*Bam*HI restriction sites of the pET15b vector (Novagen) which additionally codes for an N-terminal His-tag sequence with an integrated thrombin-cleavage site. The corresponding primers for PCR were constructed as follows: The ATG start codon sequence was modified to yield the forward primer containing a *Nde*I site (Fig. IV-15, p143).

Transformation of *E. coli* BL21 was performed by heat shock according to the supplier's instruction. Overnight cultures harbouring the recombinant pET15b vector were diluted 1:50 into fresh LB medium containing the appropriate antibiotics (final concentration 50μg/ml ampicillin). Cells were grown to an optical density of 0.6 at 600 nm as 2l-cultures at room temperature, and then recombinant 3α-HSD/CR overexpression was induced by addition of IPTG to a final concentration of 0.1 mM. After 8 h of induction at room temperature, cells were harvested and lysed by freezing, lysozyme digestion and ultrasonication (3 x 10 s), and the debris removed by spinning at 16.000 x g for 1 h. This procedure was repeated at least for three times to ensure all cells are broken.

## III.8      Detection of Overexpressed Proteins

### III.8.1      SDS-Polyacrylamide Gel Electrophoresis (SDS-PAGE)

(Laemmli, 1970; Sambrook *et al.*, 1989)

In order to control the purity of the enzyme preparations or to perform Western blot analysis, polyacrylamide gel electrophoresis under denaturing conditions was performed to separate proteins according to their molecular weights. According to their different amino acid (aa) composition proteins carry different electric charges. SDS incorporates in constant rates into the proteins masking their individual charge from their aa-composition. After SDS-treatment the proteins differ only in their molecular mass and move in the constant electric field towards the anode.

*Preparation of the gel:*

The electrophoresis was employed using the BioRad electrophoresis apparatus Mini Protean II cell (BioRad, München, Germany). The gels (80 mm × 65 mm × 0,75 mm) composition is indicated in "materials". Cleaning of the glass plates was performed using 70% ethanol. As-

sembling of the electrophoreses apparatus was carried out according to the manufacturers instructions. For the vertical gel electrophoresis first the resolving gel was prepared. Polymerization of the solution is started by APS and TEMED which therefore should be added immediate before the solution is filled between the glass plates. After polymerization the stacking gel was prepared and filled in. In a final step the comb is placed in the glass plates.

To obtain a resolving of proteins between 20 and 70 kDa a 10% acrylamide/bisacrylamide gel was prepared (see materials).

*Electrophoresis*

Before electrophoresis the protein samples were diluted 1:2 with protein loading buffer and denatured for 5 min at 95$^{\circ}$C. Subsequently, 3-20 µl of the samples were loaded to the gel. The electrophoresis chamber was completely filled with Tris/glycine-electrophoresis buffer. The electrophoresis was started with a voltage of 80 V until the bromphenol blue marker reached the top of the separating gel then performed at 150 V until the tracking dye reached the bottom of the separating gel. As molecular weights standards in SDS-PAGE different Molecular Weight Astandards have been used (see materials).

After electrophoresis, the proteins were visualized by staining the gel at room temperature for several hours in a solution of Coomassie Brillant blue R 250. Destaining was carried out at room temperature in a mixture of water/isopropanol/acetic acid (81:12:7).

### III.8.2    Determination of Protein Concentrations

Protein concentrations were determined with the BioRad Protein Microassay (BioRad Laboratories, München, Germany) (Bradford, 1976), a dye-binding assay based on the differential colour change of a dye in response to various concentrations of protein (Bradford, 1976). The principle of this method is based on the observation that the absorbance maximum for an acidic solution of Coomassie Brillant Blue G-250 shifts from 465 nm to 595 nm when binding to protein occurs. Each time the assay was performed, a standard curve was prepared using bovine serum albumin as protein standard (0-10 mg ml-1); $A_{595}$ was corrected for the blank. 0.8 ml of appropriately diluted samples or bovine serum albumin were mixed with 0.2 ml dye protein reagent and the absorbance of the solution at 595 nm was measured at room temperature with a spectrophotometer (Kontron) after 10 minutes.

### III.8.3 Protein Immunodetection by Western blot Analysis

(Towbin *et al.*, 1979; Ogata *et al.*, 1983; Kyhse-Andersen, 1984)

After electrophoresis, the protein samples were transferred from an unstained SDS-polyacrylamide gel to polyvinylidene fluoride membrane (ProBlott PVDF-Membran, Applied Biosystems, Weiterstadt, Germany) using a Semy-dry transfer system (Trans-Blot SD, Bio-Rad Laboratories, München, Germany). The transfer was performed using 3 tiers of whatman-paper saturated with cathode-buffer, the protein gel, a Hybond-C membrane saturated with anode-buffer and additional 6 tiers of whatman paper saturated with anode-buffer. Protein transfer could be monitored using a prestaned protein standard. The Tris/glycine buffer system was used as transfer buffer, as indicated in "Materials".

The electroblotting was performed applying a constant current of 0.8 mA/cm$^2$ for 2 h. Following the electrotransfer of proteins, the membrane was blocked for at least 30 min with 5% (w/v) dried milk in PBST with gentle shaking at room temperature. After washing the membrane for 3 times with PBST the membrane was then incubated at 4$^0$C over night with 1:10.000 dilutions of a rabbit anti-3α-HSD/CR antibody in 2.5 % (w/v) dried milk in PBST. After washing 3 × 10 min with PBST, in order to remove the unbound primary antibody, the membrane was incubated for 2 h in 2.5 % (w/v) dried milk in PBST with 1:20000 dilutions of alkaline phosphatase-conjugated anti- (rabbit IgG) antibody, (Amersham Biosciences, Freiburg, Germany). Excess of conjugates was removed by washing the membrane 3 × 10 min with PBST. Immunodetection was performed with the protocol for the ECF detection kit provided by Amersham Biosciences using the Kodak X-OMAT films to detect the light emitted during the reaction of the substrate ECF with the alkaline phosphatase-linked to the secondary antibody.

To detect the His-tag conjugated to the 3α-HSD/CR-protein anti-His-antibody, mouse made, (Amersham Biosciences) was used in 1:5000 dilution. The second antibody, anti mouse IgG, peroxidase conjugate, sheep-made was used in 1:50.000 dilution.

*Detection of chemiluminescence with x-ray radiographs*
After incubation with ECL-reagent the membrane was put into a transparency film and inserted together with the x-ray-film into the autoradiography cassette. Different exposure times were tested to yield the best contrast and less background.

### III.8.4    Enzyme Linked ImmunoSorbent Assay (ELISA)

The Enzyme-Linked Immunosorbent Assay (ELISA) is a useful and powerful method to detect proteins as antigens in the range of ng/ml to pg/ml in solutions by an antibody. Based on the principle of antibody-antibody interaction, this test allows for easy visualization of results and can be completed without the additional concern of radioactive materials use. The test is performed in a 8 cm x 12 cm plastic plate which contains an 8 x 12 matrix of 96 wells, each of which are about 1 cm high and 0.7 cm in diameter.

As the main principle a first antibody is specific for the protein to be detected and the second antibody which is specific for the first antibody bears a linked enzyme. The linked enzyme causes a chromogenic or fluorogenic substrate to produce a signal.

As a standard 200, 100, 50, 25, 12.5, 6.25 ng of purified 3α-HSD/CR protein was applied in coating buffer into the wells. 200µl of 12 different samples were tested according to the scheme in Fig. III-1. Each sample was diluted 1:100 in wash-buffer. The coating buffer fixes the antigen to the surface of the wells. After 30 min incubation at $37^0$C all wells are washed with 250 µl of wash buffer. 200µl of anti-3α-HSD/CR-antibody, diluted 1:1000 in wash buffer, are added to the samples. After washing for 3 times with wash buffer excess of unbound antibodies are removed and only the antibody-antigen complexes remains attached to the well. A second antibody (DAKO, anti rabbit, pig made) was added in 1:1000 dilution (in wash buffer) which will bind to any antigen-antibody complexes. The second antibody is coupled to the substrate-modifying enzyme HRP. After 30 min incubation at $37^0$C and washing for 4 times with 250µl of wash buffer the substrate (100µl ABTS, Böhringer) was added to the wells which are converted by the enzyme to elicit a chromogenic signal. After final incubation for 30 min at $37^0$C the chromogen was measured at 404 nm. The reference was measured at 490 nm. The enzyme (HRP) linked to the second antibody acts as an amplifier: even if only few enzyme-linked antibodies remain bound, the enzyme molecules will produce many signal molecules.

| A | 1 | 2 | 3 | 4 | 5 | 6 | 7 | 8 | 9 | 10 | 11 | 12 |
|---|---|---|---|---|---|---|---|---|---|----|----|----|
| B | Standard 200ng 200µl | Standard 25ng 200µl | Probe 1 200µl | Probe 2 200µl | Probe 3 200µl | Probe 4 200µl | Probe 5 200µl | Probe 6 200µl | Probe 7 200µl | Probe 8 200µl | Probe 9 200ml | Probe 10 200µl |
| C | Standard 200ng 200µl | Standard 25ng 200µl | Control | Control | Control | Control | Control | Control | Probe 11 | Probe 11 | Probe 11 | Probe 11 |
| D | Standard 100ng | Standard 12.5ng | Probe 1 | Probe 2 | Probe 3 | Probe 4 | Probe 5 | Probe 6 | Probe 7 | Probe 8 | Probe 9 | Probe 10 |
| E | Standard 100ng | Standard 12.5ng | Probe 1 | Probe 2 | Probe 3 | Probe 4 | Probe 5 | Probe 6 | Probe 7 | Probe 8 | Probe 9 | Probe 10 |
| F | Standard 50ng | Standard 6.25ng | Control | Control | Control | Control | Control | Control | Probe 12 | Probe 12 | Probe 12 | Probe 12 |
| G | Standard 50ng | Standard 6.25ng | Probe 1 | Probe 2 | Probe 3 | Probe 4 | Probe 5 | Probe 6 | Probe 7 | Probe 8 | Probe 9 | Probe 10 |
| H | | | | | | | | | | | | |

**Fig. III-1: ELISA for detection of 3α-HSD/CR during overexpression.**

## III.9   Affinity Chromatography

Affinity chromatography allows to separate proteins on the basis of a reversible interaction between the protein and a ligand coupled to a chromatography matrix which is specific for the protein to be purified. The technique combines high resolution and selectivity, easy handling and high capacity for the protein of interest.

The protein which should be purified has a N-terminal $(His)_6$ tag which allows purification according to the IMAC principle (Immobilized Metal Affinity Chromatography). Doubly charged cations such as $Ni^{2+}$ are immobilized by a chelating ligand to the chromatography matrix. These cations dispose interactions with the His-side chains.

For Affinity chromatography an Äkta-Explorer (Amersham Biosciences) was used. His-Trap$^{TM}$ HP columns are used to purify the recombinant His-tagged protein.

Recombinant protein was applied in resuspension buffer after cell-lysis into a superloop (50 ml) which was mounted to the Äkta-Explorer.

The following program including application of the protein to the column, several wash steps and elution was run. Pure protein was eluted by a linear gradient of imidazole (0 to 0.5 M) in 20 mM phosphate buffer, pH 7.5 and 0.1 M NaCl. Fractions containing purified 3α-HSD/CR were stored at $-80^{\circ}C$ or immediately further tested.

### III.9.1    Scouting

To find ideal purification conditions scouting was performed. Scouting is reasonable in the first experimental phase to select purification conditions for each stage of the purification and to test them.

In scouting unit operation candidates are selected and tests are performed that screen for their performance at small scale. From these studies a purification scheme can be proposed. To reduce work load scouting was only performed for purification conditions which are known to work in general for the given purification system.

## III.10    Pulse-Renaturation of Inclusion Bodies

### III.10.1    Resuspensation and Breaking of the Cells

After protein expression the pellet of 1l of bacteria culture was resuspended in 4ml lysis-buffer/g of cell-pellet. Lysozyme was added to a final concentration of 200μg/ml and the solution was incubated for 20 minutes at room temperature. After Incubation sonification for several cycles (5 sec on, 5 sec off) was performed to break the cells. During centrifugation at 22.000 g for 1h cells which are not broken and inclusion bodies were harvested.

To wash the cell-pellet the material was resuspended in 10ml/g material in wash buffer and centrifuged at 22.000 g for 30 minutes. This procedure was repeated till the supernatant showed no clouding. To reduce viscosity of the supernatant the solution was treated with DNAseI for 1h at $37^0$C at a final concentration of 20mg/l DNAseI-enzyme. At this stage all cells are broken and soluble protein can be found in the supernatant after centrifugation. The pellet contains only inclusion bodies and material of the broken cells.

### III.10.2    Inclusion Body Solubilisation

The pellet containing the inclusion bodies were incubated for 2h at $20^0$C in solubilisation buffer. DTT was added to reduce disulfide bridges. During incubation the protein concentration should be at 5mg/ml. To remove the reductant the solution was dialyzed against 6 M GdmCl, pH 4.5 without DTT.

The following conditions were tested to refold the 3α-HSD/CR protein to the native state from the denatured state (Table III-1).

| | additives | | | | | | | | | |
|---|---|---|---|---|---|---|---|---|---|---|
| | EDTA | DTT | Tris-HCl, pH 7.5 | L-Arginin-Chloride | GdmCl | Sorbitol | Ammoni-umsulfate | NAD | Pyro-phosphate | Tris |
| 1 | 5 mM EDTA | 2mM DTT | 1 M Tris-HCl, pH 7.5 | L-Arginin-Chlo-ride, 0.5 M | GdmCl 0.5 M | 20% Sorbitol | | | | |
| 2 | 5 mM EDTA | 2mM DTT | 1 M Tris-HCl, pH 7.5 | L-Arginin-Chlo-ride, 1 M | GdmCl 0.5 M | 20% Sorbitol | | | | |
| 3 | 5 mM EDTA | 2mM DTT | 1 M Tris-HCl, pH 7.5 | L-Arginin-Chlo-ride, 1 M | GdmCl 0.5 M | 20% Sorbitol | Ammo-niumsul-fate 0.5 M | | | |
| 4 | 5 mM EDTA | 2mM DTT | 1 M Tris-HCl, pH 7.5 | L-Arginin-Chlo-ride, 1 M | GdmCl 0.5 M | 20% Sorbitol | Pyro-phos-phate 150 mM | NAD 5 mM | | |
| 5 | 5 mM EDTA | 2mM DTT | | L-Arginin-Chlo-ride, 0.5 M | | | | | | |
| 6 | 5 mM EDTA | 2mM DTT | | L-Arginin-Chlo-ride, 1 M | | | | | | |
| 7 | 5 mM EDTA | 2mM DTT | | | GdmCl 0.5 M | | | | | |
| 8 | 5 mM EDTA | 2mM DTT | | | | 20% Sorbitol | | | | |
| 9 | 5 mM EDTA | 2mM DTT | | | | | Ammo-niumsul-fate 0.5 M | | | |
| 10 | 5 mM EDTA | 2mM DTT | | | | | | NAD 5 mM | | |
| 11 | 5 mM EDTA | 2mM DTT | | | | | | | Pyro-phos-phate 150 mM | |
| 12 | 5 mM EDTA | 2mM DTT | | | | | | | | 1M Tris |
| 13 | 5 mM EDTA | | | | | | | | | |
| 14 | 5 mM EDTA | | 1M Tris-HCl, pH 7,5 | | | | | | | |
| 15 | 5 mM EDTA | | | | GdmCl 0.5 M | | | | | |
| 16 | 5 mM EDTA | | | | | 0.06 mg/ml Lauryl-Malto-side | | | | |
| 17 | 5 mM EDTA | | | | | | 20% Glycerol | | | |

**Table III-1: Refolding screen of denatured protein.**

All approaches were performed with a protein concentration of 1mg/ml, at $4^0$C and over night. Refolding of the protein was performed by a dialysis-approach in which 5 ml of the denatured protein (in 6 M GdmCl, pH 4.5) was dialysed against 200 ml of the refolding solution at $4^0$C over night. After the dialysis the final concentration of guanidine hydrochloride is

reduced approximately 40-fold. After refolding the renaturation-solutions were dialyzed against 50mM M Tris-HCl, pH 8,0 and centrifuged at 25.000 rpm, $4^0$C for 30 minutes. Removal of arginine will precipitate improperly folded protein.

### III.10.3    PEG-Concentration Strategy

To concentrate the protein-solutions in the most gentle way PEG 4000 was used. The protein solutions in the dialysis-tubes (~25ml) were embedded each in ca 400 ml volume of PEG 4000 which dehumidifies the dialysis tubes. After 12 h at $4^0$C the dialysis tubes were opened and the protein solutions stored at $4^0$C for further testing.
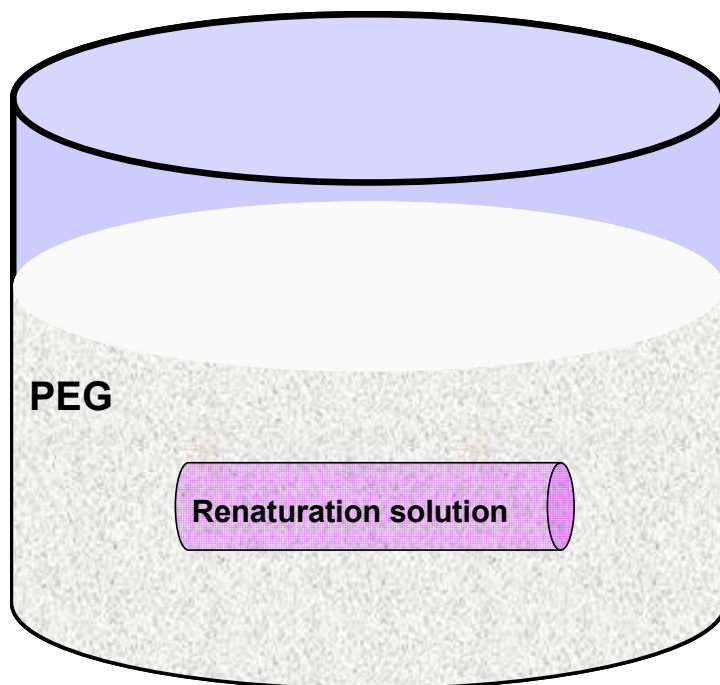


**Fig. III-2: PEG-concentration of renaturation solution**

## III.11    Assay of pNBA Carbonyl Reduction

To test biological activity of 3α-HSD/CR mutant a Metyrapone- and pNBA-assay was performed. The following components were incubated for 1h at $37^0$C and the reaction was stopped by placing the reaction mixture on ice.

| p-nitrobenazaldehyde | | metyrapone | |
|---|---|---|---|
| 10μl | Phosphate-buffer, 50 mM | 20μl | Phosphate-buffer, 50 mM |
| 20μl | NADPH-regenerating system<br>2 mg NADP<br>6 mg Glucose-6-Phosphate<br>100μl Phosphate-buffer, 50 mM<br>100μl MgCl$_2$, 100 mM<br>5μl Glucose-6-Phosphate-Dehydrogenase | 20μl | NADPH-regenerating system<br>2 mg NADP<br>6 mg Glucose-6-Phosphate<br>100μl Phosphate-buffer, 50 mM<br>100μl MgCl$_2$, 100 mM<br>5μl Glucose-6-Phosphate-Dehydrogenase |
| 10 μl | p-nitrobenzaldehyde, 5 mM, in 50% EtOH | 10 μl | metyrapone, 5 mM |
| 60 μl | protein | 50 μl | protein |

After incubation a small amount of NaCl, 20μl ammonia (diluted 1:1) and 200 μl of acetic acid ethyl ester were added, vortexed for 10 seconds and centrifuged for 1 minute to sediment organic material. The phase at the top was collected. The phase at the bottom of the eppendorf tube was vortexed and centrifuged with 100μl acetic acid ethyl ester for 2 times. All phases at the top of the tube were collected and evaporated for 20 minutes. The material was resuspended in 100 μl of 0.1% ammonium acetate pH 7.2 and 30% acetonitrile.

### III.11.1    Detection by HPLC

Detection and determination of carbonyl reduction was performed using a reverse-phase HPLC system consisting of a C$_{18}$-column (Merck) and an isocratic mobile phase of 0.1% ammonium acetate pH 7.2, 30% acetonitrile. The HPLC system consists of a Merck Hitachi L-6220 Intelligent Pump, Merck Hitachi AS-2000 A Autosampler, Merck Hitachi L-4000 A UV Detector and a 4.6 mm £ 25 cm LiChrosphere 100 RP18 column (Merck, Germany). Detection of substrates was at 254 nm (metyrapone, *p*-nitrobenzaldehyde). Elution was performed with an eluent of 30% acetonitrile in 0.1% ammonium acetate buffer, pH 7.4. The

identity of metyrapol and p-nitrobenzalcohol was determined by injecting authentic standards of both substances onto the HPLC system.

## III.12    Homology Modeling and MD-Simulations

A three-dimensional model of the 3α-HSD/CR-tr monomer was generated with MODELLER 6 (Sali and Blundell, 1993), version 6a, using standard settings. A two-step procedure was followed in order to generate the 3α-HSD/CR-tr model: in a first instance, the substrate binding loop, which is not resolved in the crystal structure of 3α-HSD/CR (PDB 1fjh), was modelled into the structure of the 3α-HSD/CR wildtype; the structure of ADH (PDB 1a4u) was used as template for this purpose. Ten protein models were generated from which the model with the lowest MODELLER target function value was selected. In a second step, the tetramerization-preventing "extraloop" (residues 118-153) was removed from the 3α-HSD/CR structure and replaced by an 8-residue loop of 3α/20β-HSD; PDB structure 2hsd was used as template for modeling the 3α-HSD/CR-tr structure with this inserted 3α/20β-HSD loop. To analyze the stability and plausibility of this model, molecular dynamics (MD) simulations were performed. For comparative purposes, the structure of the 3α-HSD/CR wildtype with the modelled substrate binding loop was also subjected to MD simulations. The simulations were carried out with AMBER 6 (Case et al., 1999), using the Cornell et al. force field (Cornell et al., 1995) (parm99). The protein was simulated in aqueous solution using a box of TIP3P water molecules (Jorgensen *et al.*, 1983) and periodic boundary conditions. Long-range electrostatics were considered through the Particle Mesh Ewald (PME) method (Darden et al., 1993). After minimization, heat-up to 300 K and initial equilibration, a trajectory of 1 ns length was sampled under NPT conditions and saved at regular intervals of 0.5 ps. The temperature was kept constant by coupling to a heat bath through the Berendsen algorithm (Berendsen *et al.*, 1984), pressure was adjusted by isotropic position scaling using a Berendsen-like algorithm. Covalent bonds to hydrogen atoms were constrained by the SHAKE algorithm (Ryckaert *et al.*, 1977), allowing a time step of 2 fs to be used.

## III.13    Abbreviations

| | |
|---|---|
| Fig. | Figure |
| ABTS | 2.2'-Azino diethyl-benzothiazoline sulfonic acid |
| ADH | Aldehyde Dehydrogenase |
| PEG | Poly ethylene glycol |
| APS | Ammoniumpersulfat |
| ATP | Adenosintriphosphat |
| bp | Base pair |
| cDNA | „complementary DNA" |
| Ci | Curie |
| DAB | 3,3'-Diaminobenzidintetrahydrochlorid |
| dATP | Desocyadenintriphosphat |
| dCTP | Desoxycytosintriphosphat |
| dGTP | Desoxyguanintriphosphat |
| DMSO | Dimethylsulfoxit |
| dNTP | Desoxynukleotidtriphosphat |
| DTT | 1,4-Dithio-L-threitol |
| dTTP | Desoxythymidintriphosphat |
| FITC | Fluorescein-5-isothiocyanat |
| IgG | Immunbglobulin G |
| IPTG | Isopropyl-$\beta$-galaktosid |
| kDA | Kilodalton |
| MOPS | Morpholinopropansulfonsäure |
| $M_r$ | Relative mass |
| mRNA | messenger-RNA |
| NBT | 4-Nitroblautetrazolimchlorid |
| nt | Ribonukleotide |
| OD | Optical density |
| ORF | offener Leserahmen (open reading frame) |
| PCR | Polymerase-Chain-Reaction |
| RNAse | Ribonuklease |
| rpm | „radiation per minute" |
| RT | Room temperature |
| SDS | Natriumluarylsulfat |
| TAE | Tris-Acetat-EDTA |
| TBE | Tris-Borat-EDTA |
| TCE | „translational control element" |
| TE | Tris-EDTA |
| TEMED | N,N,N', N'-Tetramethylethylendiamin |
| Tris | Tris-(hydroxymethyl)-aminomethan |
| TritonX-100 | Octylphenolpolyethylenglycolether |
| Tween 20 | Polyoxyethylensorbitanmonolaurat |
| U | Unit |
| IMAC | Immobilized Metal Affinity Chromatography |
| UV | Ultraviolett light |
| v/v | volume per volume |

| MD | Molecular Dynamic |
|---|---|
| PDB | Protein Data Bank |
| VT | Volume part |
| w/v | *weight per volume* |
| PME | Particle Mesh Ewald |
| X-Gal | 5-Brom-4-Chlor-3-indoyl-β-D-galaktosid |

# IV Results and Discussion

## IV.1 Structural Characterization Identifies the Extraloop-Domain as a Putative Sterical Inhibitor of Common Dimerization

### IV.1.1 The Dimerization Pattern of 3α-HSD/CR Represents a Novelty within the SDR-Superfamily

The majority of the SDR enzymes appear as either homodimers or homotetramers (Jornvall *et al.*, 1995). Despite the fact that they share an amino acid identity of only in the 15 to 30% range they reveal a striking similarity in their tertiary structure. This tertiary structure is based upon the typical dinucleotide binding motif composed of βαβ units for members of the SDR superfamily which is called Rossmann fold. This motif builds up a parallel β-sheet sandwiched between two arrays of parallel α-helices (Rossmann et al., 1975) (Fig. I-1; Introduction) Typical examples for different types of oligomerization follow consolidated ways of arrangement of the monomer-subunits. Fig. IV-1 shows typical examples for the arrangement of identical monomers within the SDR enzymes.

Tetrameric SDR enzymes show an arrangement of the four identical monomers via two distinct oligomerization interfaces, Q and P. An example for this way of oligomerization is the bacterial 3α/20β-HSD from *Streptomyces hydrogenans*. Enzymes which exist of two identical monomers in general feature a dimerization via the Q-axis interface. This is the predominant way of oligomerization within dimeric SDR enzymes. An example for this it is alcohol dehydrogenase of *Drosophila lebadonensis*.

However, 3α-HSD/CR of *C.testosteroni* as dimeric enzyme, features an unusual type of oligomerization, via the P-axis interface, which otherwise can only be found in tetrameric SDR enzymes.

Detailed structural analysis of different members of the SDR-superfamily elucidates the mechanism and requirements of the different types of oligomerization within the SDR enzymes.
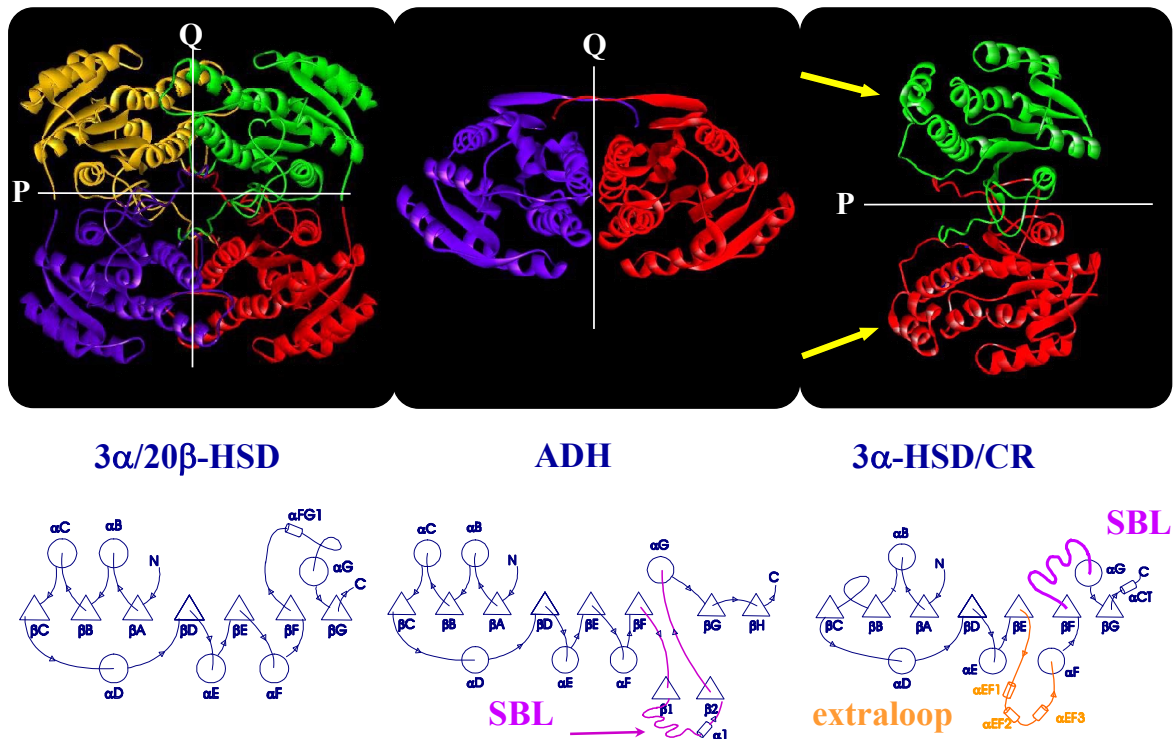
**Fig. IV-1: Overview of oligomerization behaviour of SDR enzymes**

All SDR enzymes follow the typical Rossmann fold motif consisting of a central β-sheet between two arrays of α-helices. 3α-HSD/CR shows a novel type of dimerization along the P-axis-interface and contains an α-helical subdomain („extraloop") which is marked by arrows.

## IV.1.2    Three Dimensional Comparison of Different Oligomerization Behaviours Reveals Distinct Structural Elements

### IV.1.2.1    Structural Alignment of Three SDR Proteins

Within the SDR superfamily distinct oligomerization behaviours can be found. These types of oligomerization are based on typical structural equipment which enables the proteins exhibiting these structural elements to accumulate in distinct ways. Alignment analyses based on structural information derived from the PDB-Protein Data Bank (http://www.rcsb.org) were performed to compare the structural configuration of typical representatives of the different oligomerization classes (Fig. IV-2). Structural features like helices and sheets are graphically added on the structural basis for human carbonyl reductase 1 (CBR1), as well as the nomenclature of these.
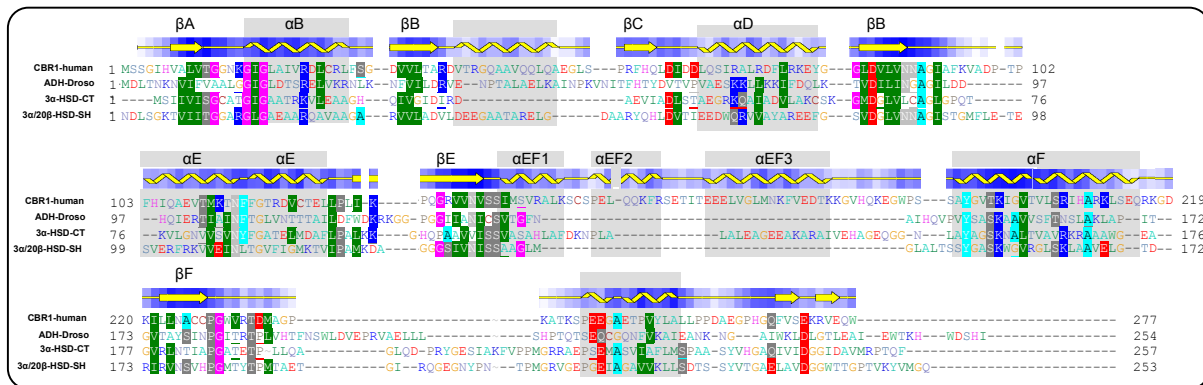
**Fig. IV-2: Structural alignment of 4 members of the SDR superfamily**

Structural information are based on Protein Data Bank. Alignment was done with the program CE-MC (Guda *et al.*, 2001; Guda *et al.*, 2004; Guda *et al.*, 2006)

Human carbonyl reductase 1 (CBR1) whose structure has been solved only a few years ago (Tanaka *et al.*, 2005) exhibits a monomeric structure. Structural comparison to other members of this family reveals the existence of an additional alpha-helical subdomain between the Q-interfacial strand βE and helix αF comparable to that of 3α-HSD/CR from *C.testosteroni*. This structural feature is believed in homology to 3α-HSD/CR to prevent oligomerization along the Q-axis interface built up of the four helix bundle. This α-helical subdomain can be found in other monomeric carbonyl reductases as well, but with different length. Among the monomeric carbonyl reductases with an additional subdomain are pig testicular carbonyl reductase (PTCR) which has a sequence identity to human CBR1 of nearly 85%, as well as the cytosolic and monomeric carbonyl reductases of rat (non-inducible, nCR; inducible, iCR; testis, rtCR) and Chinese hamster (CHCR).

Alcohol dehydrogenase (ADH) from *Drosophila lebadonensis* can be seen as a typical protein for dimerization of two identical monomers across the Q-axis and features α-helix E and α-helix F as the main structural features of each of the two subunits to form a bundle of four helices. This four helix bundle represents the most important structural motif of the Q-axis interface, especially in dimeric SDR proteins and is therefore the most widespread type of dimerization within dimeric proteins of the SDR superfamily.

As a typical example for a tetrameric SDR-protein with four identical monomers oligomerizing along the P- and Q-axis 3α20β-HSD from *Streptomyces hydrogenans* was included in the alignment. Fig. IV-2 demonstrates that 3α20β-HSD lacks the alpha-helical extraloop subdo-

main and exhibits only a 6-amino acid sequence as link between strand βE and helix αF (see also Fig. IV-3). Based on the fact that 3α20β-HSD from *Streptomyces hydrogenans* appears as homotetramer which apparently bears structural features for both oligomerization interfaces P and Q this protein was included in the modeling and simulation approaches to elucidate the peculiar oligomerization behaviour of 3α-HSD/CR from *C.testosteroni*.

3α-HSD/CR from *C.testosteroni* consists of two identical monomers showing the typical SDR architecture of the Rossmann fold (Grimm *et al.*, 2000b). Nevertheless the topology of this dimeric protein differs in some details from that of other proteins within the SDR protein superfamily which are believed to have significant consequences on the overall folding topology.

The canonical structural motif is as expected a βαβ-dinucleotide binding motif (Rossmann fold) which consists of a central six-stranded parallel β-sheet sandwiched between two arrays of α-helices (Rossmann *et al.*, 1975; Grimm *et al.*, 2000b). Likewise the folding pattern is, according to other SDR proteins, extended at its COOH terminus by at least one additional α-helic (αG) and a seventh partallel β-strand (βG) (Fig. IV-3; Fig. IV-4). Contrary to the typical folding pattern in 3α-HSD/CR the Rossmann fold motif is truncated. It lacks helix αC and shows an only rudimentary left strand βC. These structural modifications can also be found in dihydropterin reductase (Varughese *et al.*, 1992) and GDP-fucose synthetase (Somers *et al.*, 1998), also members of SDR superfamily. Additionally 3α-HSD/CR contains an insertion of 28 amino acids within the Rossmann fold motif between strand βE and helix αF (Fig. IV-2; Fig. IV-3) which forms a predominantly α-helical subdomain.

This 28 amino acids insertion ("extraloop") is believed to prevent the typical dimerization via the Q-axis interface involving helices αE and αF by making it sterically impossible (Grimm *et al.*, 2000b) (Fig. IV-4; Fig. IV-5). As well as in the monomeric carbonyl reductases containing this α-helical extraloop-domain, oligomerization along this interface region is prevented because of the disruption of the Q-axis interface. Consequently in 3α-HSD/CR dimerization takes place via a P-axis interface which corresponds to the P-axis interface of 3α/20β-HSD. The dimerization about a P-axis interface has been discussed as a possible mode of oligomerization in SDRs (Krook *et al.*, 1993b) but has never been observed in a crystal structure so far. However, this type of oligomerization via the P-axis interface can only be found in tetrameric SDRs such as for example in 3α/20β-HSD from S. *hydrogenans* (Ghosh *et al.*, 1994b).
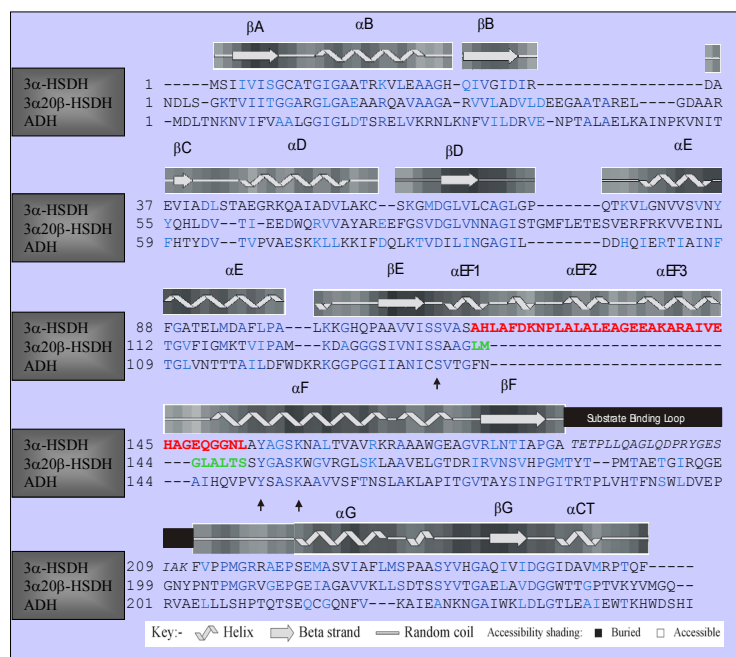
**Fig. IV-3: Structural alignment of the SDR enzymes 3α-HSD/CR, 3α/20β-HSD and ADH.**

All SDRs known so far lack the additional „extraloop"-domain (red). The homologous region of 3α/20β-HSD is given in green.

## IV.1.2.2    Distinct Sructural Elements of SDR Enzymes have varying Influence of the Folding Topology

### Catalytic Triade and Catalytic Mechanism

Jörnvall and coworkers described already in 1981, the importance of the Tyr-x-x-x-Lys segment as the most conserved sequence motif of the SDRs (Jornvall *et al.*, 1981) which is nearly used by all "classical" SDR enzymes as an conserved catalytic residues Tyr-Lys-Ser (Jornvall *et al.*, 1995) Slightly different composition of the catalytic residues can be found within the "divergent" and the "complex" class within the SDR superfamily (see Part I). The amino acids which constitute the catalytic triad are critically important for enzyme function (for catalytic mechanism refer to Part I). They appear to maintain a fixed position relative to the scaffolding of the βαβ-folding and the cofactor position.

### Substrate Binding and Substrate-Binding Loop

In the core of the Rossmann fold most of the primarily hydrophobic amino acid residues which are partially conserved within the SDR superfamily members are located (Duax *et al.*, 2000). Within the substrate-binding cleft the only conserved residues are those of the catalytic triad: Ser, Tyr and Lys. No conserved residues can be found in the substrate-binding site. This is indicative for the fact that, for example, the HSDs show high selectivity for their specific physiological steroid substrate.

Usually, SDR enzymes have a substrate-binding loop of more than 20 residues which covers the active site and becomes well ordered after the hydroxyl or carbonyl substrate binding. This loop region is located between β-strand F (βF) and α-helix G (αG) and is very often disordered in apo-structures (without substrate) of SDR enzymes. After substrate binding, the loop shows a well-defined, mainly α-helical, geometry. However, in *Sniffer* from Drosophila no α-helical secondary structure element is apparent in the substrate-binding loop (Sgraja *et al.*, 2004). Here, in the presence of $NADP^+$, only a short loop could be detected in the electron density which connects strand βF and helix αG (Sgraja *et al.*, 2004).

When the α-carbon backbone of known SDR structures is superimposed, the conserved residues appear at the core of the structure and in the cofactor-binding domain, but not in the substrate-binding pocket (Duax *et al.*, 2000). Contrary to the variability in the substrate-binding pocket, the association of the Rossmann fold with the cofactor binding is very consistent and the NADP(H) binding domains shows architectural integrity, despite having sequence variations (Duax *et al.*, 2000). The variability in the substrate-binding pocket is plausible when keeping in mind the variety of structures used as substrates by different members of the SDR superfamily (Duax *et al.*, 2000).

### *Cofactor Binding*

In the N-terminal part of the SDR proteins, a glycine-rich pattern important for cofactor binding has been identified (Jornvall *et al.*, 1995). This conserved sequence motif includes three glycine residues which are located at comparable points in their sequences and form a turn between a *β*-strand and an *α*-helix that border the cofactor-binding site (Duax *et al.*, 2000). Structural analysis has shown that the glycine residues interact with the pyrophosphate moiety of the cofactor. The individual subfamilies of the SDR superfamily differ regarding the spacing of the three glycine residues, where the Gly-x-x-x-Gly-x-Gly motif, for example, is characteristic for the subfamily of the "classic" SDRs (Jornvall *et al.*, 1981; Jornvall *et al.*, 1999). The use of either reduced or oxidised NAD(P) as cofactor depends on their predominant function as a dehydrogenase or reductase of individual members of the SDR superfamily. In addition, both NAD(H) and NADP(H) bind to the classical βαβ motif of the Rossmann fold. The specificity for NADP(H), rather than to NAD(H), is conferred by two highly conserved basic residues in the N-terminal part of the peptide chain. Tanaka et al. (Tanaka *et al.*, 1996a) identified two basic residues (Lys-17 and Arg-39) in the tetrameric mouse lung carbonyl reductase

(MLCR) which promote NADPH binding by interaction with the 2'-phosphate group. These residues are believed to confer specificity for NADPH in other SDRs as well.

Human monomeric carbonyl reductase (CBR1) shows less than 25% overall sequence identity with tetrameric MLCR (Jornvall *et al.*, 1995). However, similar to MLCR, human CBR1 has distal basic (Lys-15 and Arg-38) and neutral (Ala-37) residues at positions corresponding to Lys-17, Arg-39 and Thr-38 in tetrameric MLCR (Tanaka *et al.*, 1996a) and is strictly NADPH-dependent (Wermuth *et al.*, 1988; Sciotti and Wermuth, 2001). Sciotti and Wermuth (Sciotti and Wermuth, 2001) showed that a positive charge at positions 15 and 38 and the absence of a negative charge at position 37 significantly contribute to NADPH specificity. SDR enzymes which are NAD-dependent lack these two basic residues. Instead, an Asp which is adjacent to the position of the distal basic residue in NADPH-dependent enzymes appears to determine NAD specificity (Sciotti *et al.*, 2000). Sequence alignments of NAD-dependent enzymes with the NADPH-dependent tetrameric and monomeric carbonyl reductases show that Ala-37 of the monomeric and Thr-38 of the tetrameric carbonyl reductase corresponds to the Asp residue which plays a role in NAD specificity. Sciotti and Wermuth (Sciotti and Wermuth, 2001) substituted Asp for Ala-37 in the strictly NADPH-dependent human CBR1. Unexpectedly, the Asp residue had little effect on the NADH-dependent activity and NADPH was still the preferred substrate of the mutant Ala37Asp. Therefore, factors other than only the absence of Asp at position 38 must be responsible for the low efficiency of monomeric human CBR1 in the presence of NADH (cf Part I, Fig. III-2 chapter III.3.3, Cofactor Binding, p19).

3α-HSD/CR shows the typical amino-terminal cofactor binding motif $Gly^8$-x-x-x-$Gly^{12}$-x-$Gly^{14}$. As cofactor 3α-HSD/CR and depends on NAD(H) and hardly accepts NADP(H) which supports the catabolic nature of 3a-HSDH (Grimm *et al.*, 2000b).

This is supported by structural analyses. In the binary complex $NAD^+$ is bound at the carboxyl-terminal ends of the β-strands and is well superimposable with the cofactors present in other binary or ternary complexes of SDRs. Therefore both ribose rings are present as 29 endo-conformers, the nicotinamide ring is bound in a *syn* and the adenine base in an *anti*-torsion  angle to the respective ribose moiety (Grimm *et al.*, 2000b).

In 3α-HSD/CR Asp-32 is like in other SDRs, highly conserved among enzymes preferring NAD(H) . The side chain carboxylate of Asp-32 forms hydrogen bonds to both the 2´ and the 3' OH group of the adenosine ribose.

For correct cofactor binding Lys-159, a residue of the catalytic triade, plays also a crucial role and provides proper orientation of the cofactor by forming hydrogen bonds to the nicotinamide moiety. Additionaly Lys-159 lowers the pKa of the catalytic Tyr via electrostatic interaction (Ghosh *et al.*, 1994b; Auerbach *et al.*, 1997; Benach *et al.*, 1999).

This implicates that not only the correct structural localization of residues involved in cofactor but also the correct structural arrangement of other residues which partly assist e.g. the amino acids responsible for cofactor binding, is essential for cofactor binding as an important criterion for correct enzyme function.

### *C-terminal Extension and $3_{10}$-Helices*

Many enzymes of the SDR superfamily contain a C-terminal extension consisting of several α-helices. Examples are human estrogenic 17β-HSD (Ghosh *et al.*, 1995) and the Drosophila enzymes alcohol dehydrogenase (DADH) and *Sniffer*. Benach and coworkers showed in DADH that these C-terminal helices, which are of more variable character, are main elements of dimer association and that these structural features have additional importance in closing of the active site cavity upon cofactor and substrate binding (Benach *et al.*, 1998).

$3_{10}$-helices are structural elements which are present as α-helical extensions in loops and as connectors between β-strands (Pal and Basu, 1999). In many cases they occur independently of any other neighbouring secondary structural elements and form novel super-secondary structural motifs. These motifs have possible implications for protein folding, local conformational relaxations and biological functions (Pal and Basu, 1999).

The *Sniffer* protein has both structural features which contribute together to dimer formation. At the C-terminal end of the *Sniffer* protein there is a short loop with a sharp turn directly following strand βG. This loop runs perpendicular to the central β-sheet of the Rossmann fold and touches the $3_{10}$-helix following strand βE. The C-terminal ends of the two monomers approach each other and the indole moiety of the Trp-248 interacts through its planar ring system with the side-chain of Ile-159 which is rooted at the $3_{10}$-helix of the second subunit (Sgraja *et al.*, 2004).
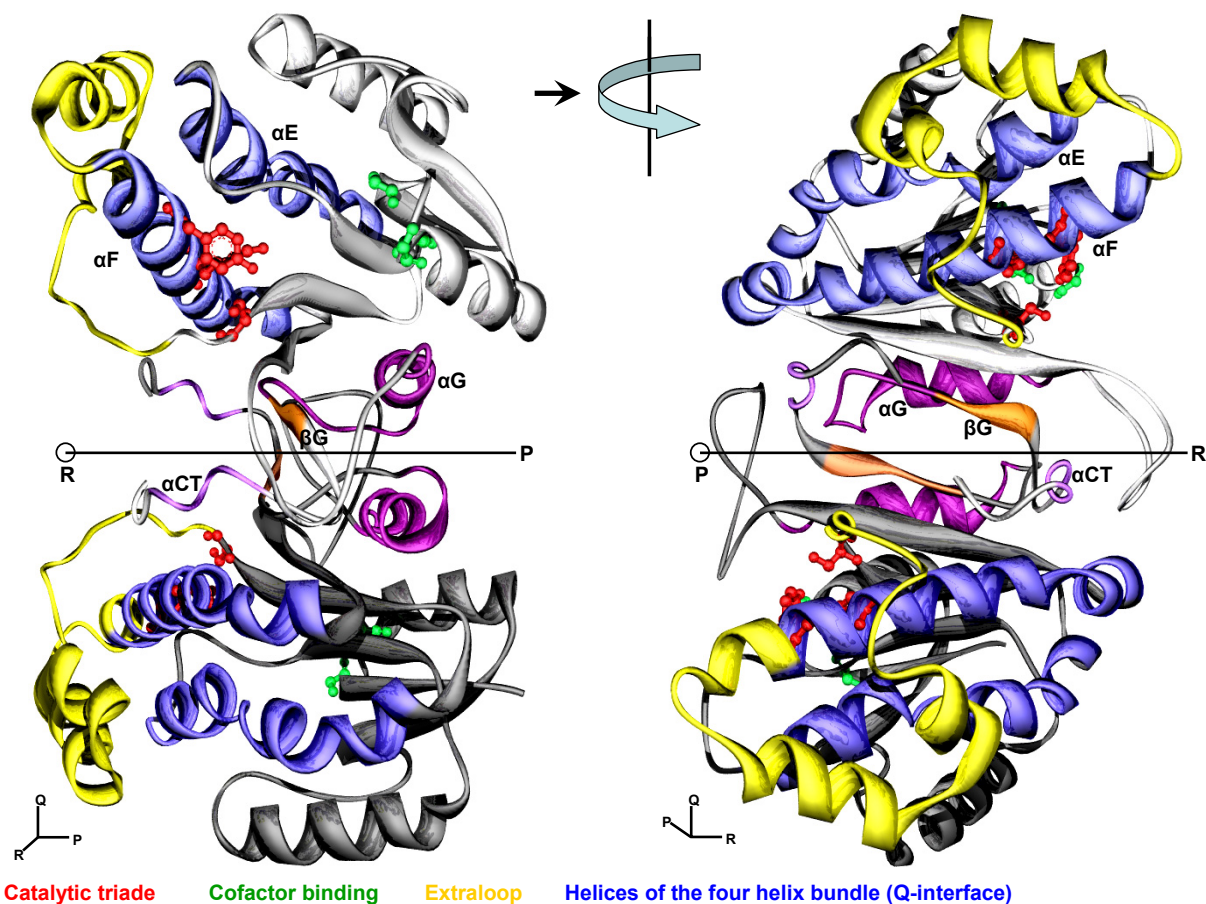
**Catalytic triade**      **Cofactor binding**      **Extraloop**      **Helices of the four helix bundle (Q-interface)**

**Fig. IV-4: Structural elements involved in folding topology as in 3α-HSD/CR from *C. testosteroni***

## *Oligomerization and Interfaces*

The enzymes of the SDR superfamily can be divided into different groups concerning their oligomerization behaviour, their subcellular localization and the existence of structural elements with significant effects on protein folding. Most enzymes of the superfamily appear as either homodimers, e.g. *Sniffer* (Sgraja *et al.*, 2004), DADH (Benach *et al.*, 1998) and dihydropteridine reductase (DHPR) (Varughese *et al.*, 1992), or homotetramers like 3α/20β-HSD (Ghosh *et al.*, 1994b) and mouse lung carbonyl reductase (Tanaka *et al.*, 1996a). Only few members occur as monomers like for example human carbonyl reductase (CBR1) (Wermuth, 1981) and pig testicular carbonyl reductase (PTCR) (Ghosh *et al.*, 2001). In spite of the low residue identities between the SDR members, the folding pattern of the individual (sub-) units is highly conserved with largely superimposable peptide backbones (Krook *et al.*, 1993b; Ghosh *et al.*, 2001) (Part I, Fig. III-1 p.18, Fig. IV-1 p.28).

Two types of oligomerization, involving different structural elements, can be found. They use two main subunit interfaces arranged about two non-crystallographic 2-fold axes which are perpendicular to each other and referred to as P and Q  (Ghosh *et al.*, 1994b; Tanaka *et al.*, 1996a; Grimm *et al.*, 2000b) (Fig. IV-1; Fig. IV-4).

One type of monomer association is the so-called P-axis interface comprising the antiparallel association of β-strand G and α-helix G of each subunit (Ghosh *et al.*, 1994b). This type of oligomerization is usually found in homotetrameric SDRs and has only been observed in one dimeric SDR, namely 3α-HSD/CR from *C. testosteroni* (Grimm *et al.*, 2000a). The P-axis interface does not involve significant hydrophobic interactions (Ghosh *et al.*, 1994b) and is less critical to the structural integrity of the active site than the second type of oligomeriza-tion, the so-called Q-axis interface.

All structures of homotetrameric SDRs determined so far show the wo main subunit inter-faces referred to as P and Q  (Ghosh *et al.*, 1994b; Tanaka *et al.*, 1996a; Grimm *et al.*, 2000b). The Q-axis interface consists of α-helix E and α-helix F of each of the two subunits to form a bundle of four helices. This four helix bundle represents the most important structural motif of the Q-axis interface, especially in dimeric SDR proteins. It is predicted to be important for the integrity of the active site clefts  and has been shown to be critical to function (Puranen *et al.*, 1997; Ghosh *et al.*, 2001). In addition, although more than half of the crystal structures of SDRs exhibit the same quaternary structure, only the four helix bundle as the main structural feature of the Q-axis interface that involves the largest surface area of association (Ghosh *et al.*, 1994b) is conserved among the SDRs.

The dimerization interface is close to the active site and stabilizes the interior of the molecule. Tsigelny and Baker postulated that the neighbouring amino acids of the conserved tyrosine and lysine residues in the active site of SDR family members might interact with the hydro-phobic outer surface of the αF helix and hence stabilize the dimer interface of the proteins (Tsigelny and Baker, 1995b). Therefore, it is suggested that monomerization of dimeric or tetrameric proteins in the SDR family most likely abolishes their enzyme activity. Hoffmann and coworkers (Hoffmann *et al.*, 2006) redesigned the region of the interfacial four helix bun-dle in the dimeric 3α-HSD/CR from *C. testosteroni*, which comprises an additional α-helical subdomain preventing the enzyme of dimerization along the typical Q-axis interface. Their data of a soluble and active protein will give further insights into the requirements of a protein for the architecture of the active site and the structural elements comprising the Q-axis inter-face.

In the dimeric human 17β-HSD, Puranen and coworkers (Puranen *et al.*, 1997) substituted amino acids of the four helix bundle within the hydrophobic Q-axis interface resulting in inactive multi-aggregates of the protein, while neither dimers nor monomers were detectable. Ghosh and coworkers were also able to show that the four helix bundle is critical for protein function. Disruptions of the helix arrangement had negative effects on the integrity of the catalytic centres of the oligomerizing monomers in 3α/20β-HSD of *S. hydrogenans* (Ghosh *et al.*, 2001).

An example for a cytosolic and monomeric carbonyl reductase is human CBR1. The reason for the monomeric structure of this enzyme is a so-called additional extraloop-domain between the Q-interfacial strand βE and helix αF which is believed to prevent oligomerization along the Q-axis interface built up of the four helix bundle. Other monomeric carbonyl reductases include this α-helical subdomain as well, but with different length. Among the monomeric carbonyl reductases with an additional subdomain are pig testicular carbonyl reductase (PTCR) which has a sequence identity to human CBR1 of nearly 85%, as well as the cytosolic and monomeric carbonyl reductases of rat (non-inducible, nCR; inducible, iCR; testis, rtCR) and Chinese hamster (CHCR).

The group of tetrameric carbonyl reductases is not as consistent as the group of monomeric carbonyl reductases. Tetrameric carbonyl reductases can be found on the subcellular level in the mitochondria (namely carbonyl reductases from mouse and pig lung) (Nakayama *et al.*, 1986; Oritani *et al.*, 1992) and in the cytoplasm, i.e. 3α/20β-HSD from *S. hydrogenans* (Ghosh *et al.*, 1992; Ghosh *et al.*, 1994a; Ghosh *et al.*, 1994b)**.** The tetrameric carbonyl reductase from pig liver is a peroxisomal protein which contains the SRL-tripeptide (serine-arginine-leucine) as a peroxisomal targeting signal (Usami *et al.*, 2003) (cf. chapter IV.2.1.7; Tetrameric Peroxisomal Carbonyl Reductases, Part I, p41).

The Q-interfacial dimer interface of which *Sniffer* provides a typical example is also present in tetramers (3α/20β-HSD). This interface is stabilized by interactive associations of symmetry related α-helices αE and αF. It has been shown that while conservative variations in amino acids (i.e. substitution of one hydrophobic residue for another) is tolerated, non-conservative mutations can disrupt dimer formation and cause loss of function (Duax *et al.*, 2000).

A special case represents dimeric 3α-HSD/CR from *C. testosteroni*. This enzyme does not undergo oligomerization along the Q-axis interface, because the protein contains an α-helical extraloop-domain within this Q-interfacial four helix bundle. As with the monomeric carbonyl reductases containing this α-helical extraloop-domain, oligomerization along this interface region is prevented because of the disruption of the Q-axis interface. Most interestingly, 3α-HSD/CR performs dimerization along the P-axis interface (Grimm *et al.*, 2000b). However, this type of oligomerization via the P-axis interface can only be found in tetrameric SDRs such as for example in 3α/20β-HSD from S. *hydrogenans* (Ghosh *et al.*, 1994b) (see above).

### IV.1.3    The Extraloop-Domain of 3α-HSD/CR could be Responsible for the Abnormal Oligomerization Pattern in spite of a Complete Set of Typical Structural Motifs

3α-HSD/CR from C.testosteroni features all structural elements which are typical for oligomerization along the Q-axis interface. Among these are  α-helix E and α-helix F of each subunit forming the so called four helix bundle and the localization of these four helix bundle close to the active side of the protein stabilizing the interior of the molecule. Oligomerization along the Q-acis interface is described in detail in part I, section II "General features of SDR superfamily enzymes".
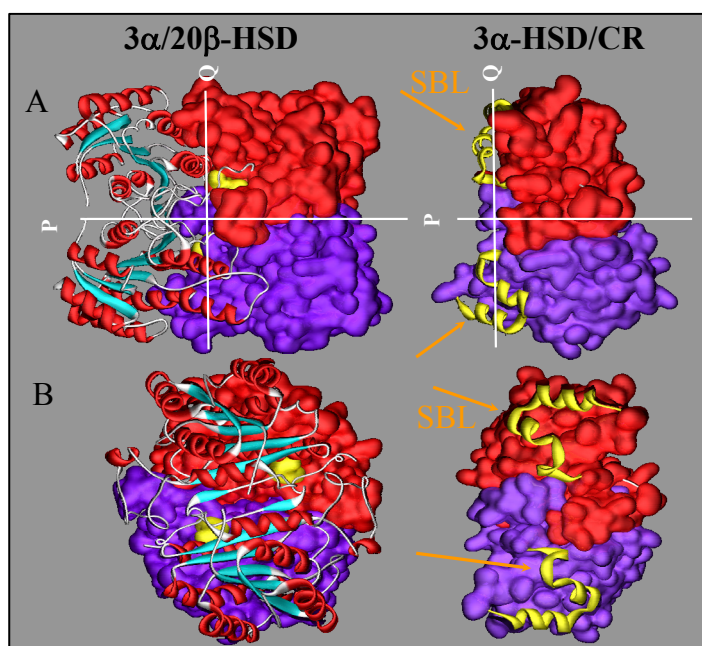


**Fig. IV-5: „extraloop"-domain in 3α-HSD/CR blocks the formation of a tetramer**

Left: The additional α-helical subdomain (yellow) prevents 3α-HSD/CR from dimerization along the Q-axis interface.

In addition to the structural setting for Q-axis oligomerization 3α-HSD/CR is equipped with a couple of structural elements typical for P-axis oligomerization, e.g. the antiparallel association *of β-strand G and α-helix G of each subunit and the carboxyterminal helix αCT.*

In 3α-HSD/CR there is an insertion of 28 amino acids within the Rossmann fold motif between strand βE and helix αF forming a predominantly α-helical subdomain (Grimm *et al.*, 2000b). Additionally the enzyme lacks helix αC and has only a rudimentary strand βC. Because of the 28 amino acids insertion ("extraloop") into the classical Rossmann fold motif between strand αE and αF this mode of dimerization is sterically impossible in 3α-HSD/CR (Grimm *et al.*, 2000b) (Fig. IV-5). As a consequence, in 3α-HSD/CR dimerization takes place via a P-axis interface which corresponds to the P-axis interface of 3α/20β-HSD. The *P*-axis interface is mainly formed by the parallel packing of two αG helices and by side chain-to-main chain interactions between the βG strands of two neighbouring subunits. In addition, the carboxyl-terminal helix αCT of each subunit is packing against the αF helix of the other subunit. The dimerization about a P-axis interface has been discussed as a possible mode of oligomerization in SDRs (Krook *et al.*, 1993b) but has never been observed in a crystal structure so far.

## IV.2     Combination of *in silico* Based Approach and Molecular Biology Methodology

To investigate the role and importance of the additional α-helical subdomain on the type of oligomerization and its impact on the stability and therefore activity of the protein a combined *in silico* and molecular biological approach has been performed. In this approach the question has to be followed if the deletion of this alpha-helical subdomain leads to the formation of a homotetramer or even a novel oligomerization mode and if the mutant deleted by this extraloop still active. In this combined approach first the structure to be manipulated has to be determined, then as *in silico*-steps the new amino acid sequence has to be modelled on the basis of the 3α20βHSD-pdb-structure, MD-simulations have to be performed and the calculated conformations have to be interpreted. The *in silico* steps are aimed not to destroy the entire architecture of the protein by solely deleting the extraloop domain but rather to redesign the folding topology as if the protein would originally not have this additional α-helical subdomain.

## IV.3    An *In Silico* – Approach Provides Insight into the Possible Sterical Perturbations after Redesign of the Extraloop-Domain

## IV.4    Molecular Modeling of the SBL and the Redesigned Loop-Region
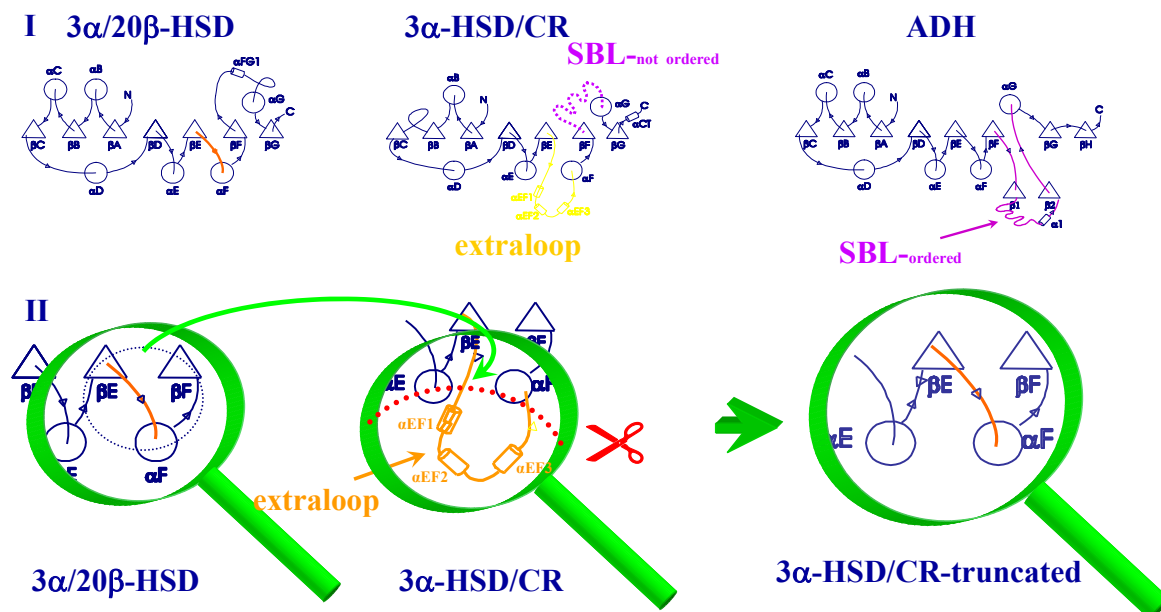


**Fig. IV-6: Overview of mutagenesis approach**

**I:** Comparison of different members of the SDR Superfamily with respect to their folding pattern and structural features regarding the alpha-helical extraloop subdomain.
**II:** Approach of redesigning the extraloop domain of 3α-HSD/CR with the corresponding structural feature of 3α/20β-HSD.

To investigate the role of the extraloop in the oligomerization behaviour of 3α-HSD/CR a mutation-approach was performed to replace the extraloop by the much shorter corresponding 3α/20β-HSD loop. This was pursued both *in silico* (by homology modeling) and *in vitro* (by applying PCR-techniques). The resulting truncated 3α-HSD/CR (3α-HSD/CR-tr) was theoretically analysed by molecular dynamics simulations and experimentally characterized by enzymatic methods (IV.5 , p142).

Detailed analysis of a previous 3α-HSD/CR-tr model generated from the templates (PDB 1fjh, 1a4u, and 2hsd) in a one-step procedure (Hoffmann et al., 2003) revealed some unsatisfactory deviations from the primary template, i.e. the wildtype 3α-HSD/CR (1fjh). Therefore, homology modeling was repeated by following the two-step procedure described above, which al-

lowed for a more controlled insertion of the new loops. The top-ranked model obtained from this refined approach and its behaviour in the subsequent MD simulation is analyzed herein.

### IV.4.1 Modeling of the Crystallographic Unordered Substrate Binding Loop yields an One-Chain-Protein as a Basis for Further Simulation Approaches

As a first step molecular modeling of the structurally unordered substrate binding loop (SBL) of 3α-HSD/CR was performed on the basis of the structurally ordered SBL of alcohol dehydrogenase of Drosophila lebadonensis (1a4u). Fig. IV-7A shows the structural alignment of alcohol dehydrogenase (ADH) as template protein and 3α-HSD/CR. Fig. IV-7B shows the TOP-file which defines the different parameters and values of this modeling step. In this approach the sequence of the unordered SBL of 3α-HSD/CR was structurally aligned to the amino acids of the structurally well ordered SBL of ADH to obtain a one-chain protein subunit as unconditional requirement for the further modeling and simulation steps. Modeling of the SBL maintains the position of the residual amino acids not to implement unnecessary deviations for the residues already structurally well ordered. Ten protein models were generated from which the model with the lowest MODELLER target function value was selected.

This modeling step results in an one-chain protein with the original crystallographic coordinates for all residues except for the ones of the substrate binding loop. Preliminary coordinates for these residues were obtained from the modeling by means of the SBL of ADH.

A

```
>P1;1a4u
structureX:1a4u:1:A:254:A:alcohole dehydrogenase:::
-MDLTNKNVIFVAALGGIGLDTSRELVKRNLKNFVILDRVE-NPTALAELKAIN
PKVNITFHTYDV--TVPVAESKKLLKKIFDQLKTVDILINGAGIL--------D
DHQIERTIAINFTGLVNTTTAILDFWDKRKGGPGGIIANICSVTGFNAIHQVPV
YSASKAAVVSFTNSLAKLAPITGVTAYSINPGITRTPLVHTFNSWLDVEPRVA-
ELLLSHPTQTSEQCGQNFV---KAIEANKNGAIWKLDLGTLEAIEWTKHWDSHI*


>P1;3hsd+T+SBL
unknown:3hsd+T+SBL: : : : : : : :
-----MSIIVISGCATGIGAATRKVLEAAGH-QIVGIDIR-------------
----DAEVIADLSTAEGRKQAIADVLAKC--SKGMDGLVLCAGLGP-------Q
TKVLGNVVSVNYFGATELMDAFLPA---LKKGHQPAAVVISSVASLMGLALTSA
YAGSKNALTVAVRKRAAAWGEAGVRLNTIAPGATETPLLQAGLQDPRYGESIAK
FVPPMGRRAEPSEMASVIAFLMSPAASYVHGAQIVIDGGIDAVMRPTQF-----*
```

B

```
INCLUDE
SET OUTPUT_CONTROL = 1 1 1 1
SET ALNFILE              = '../alis/3hsd+T+SBL.pir'
SET KNOWNS               = '1a4u'
SET MD_LEVEL             = 'refine2'
SET SEQUENCE             = '3hsd+T+SBL'
SET ATOM_FILES_DIRECTORY = '../pdbs'
SET OUTPUT_DIRECTORY     = './'
SET PDB_EXT              = '.pdb'
SET ALIGNMENT_FORMAT     = 'PIR'
SET STARTING_MODEL       = 1
SET ENDING_MODEL         = 3
SET DEVIATION            = 4.000000
SET FINAL_MALIGN3D       = 1
CALL ROUTINE             = 'model'
```

**Fig. IV-7: Structural alignment for modelling of SBL**

**A:** Structural alignment of amino acid sequence of 3α-HSD/CR including the amino acids of the substrate binding loop (SBL) to the three dimensional structure of alcohol dehydrogenase from Drosophila lebadonensis (1a4u).

**B:** TOP-file for modeling of the amino acid sequence of 3α-HSD/CR-substrate binding loop to the known structure of the SBL of alcohol dehydrogenase to obtain a one-chain protein for subsequent modeling steps.

### IV.4.2    Modeling of the Homologous T-loop Region of 3α/20β-HSD of *S.hydrogenans* into 3α-HSD/CR Generates the Truncated 3α-HSD/CR Protein

In a second modeling step, the "extraloop" (residues 118-153), which is assumed to prevent tetramerization or dimerization along the alternative Q-axis interface, was removed from the 3α-HSD/CR structure and replaced by an 8-residue loop of 3α/20β-HSD; PDB structure 2hsd was used as template for modeling the 3α-HSD/CR-tr structure with this inserted 3α/20β-HSD loop.

Fig. IV-9 shows the structural alignment of the truncated 3α-HSD/CR protein sequence with that of 3α20β-HSD which serves as a basis for the modeling step perfomed with the program MODELLER 6. The program MODELLER generates 3 different models of the truncated 3α-HSD/CR which were put into the MD-analysis. Fig. IV-8 shows an overlay of these 3 different models generated by MODELLER 6. Expectedly some deviations between the 3 models can be observed for the regioni of the inserted shortened extraloop-domain from 3α20β-HSD. The orientation of the catalytic residues is nearly the same.
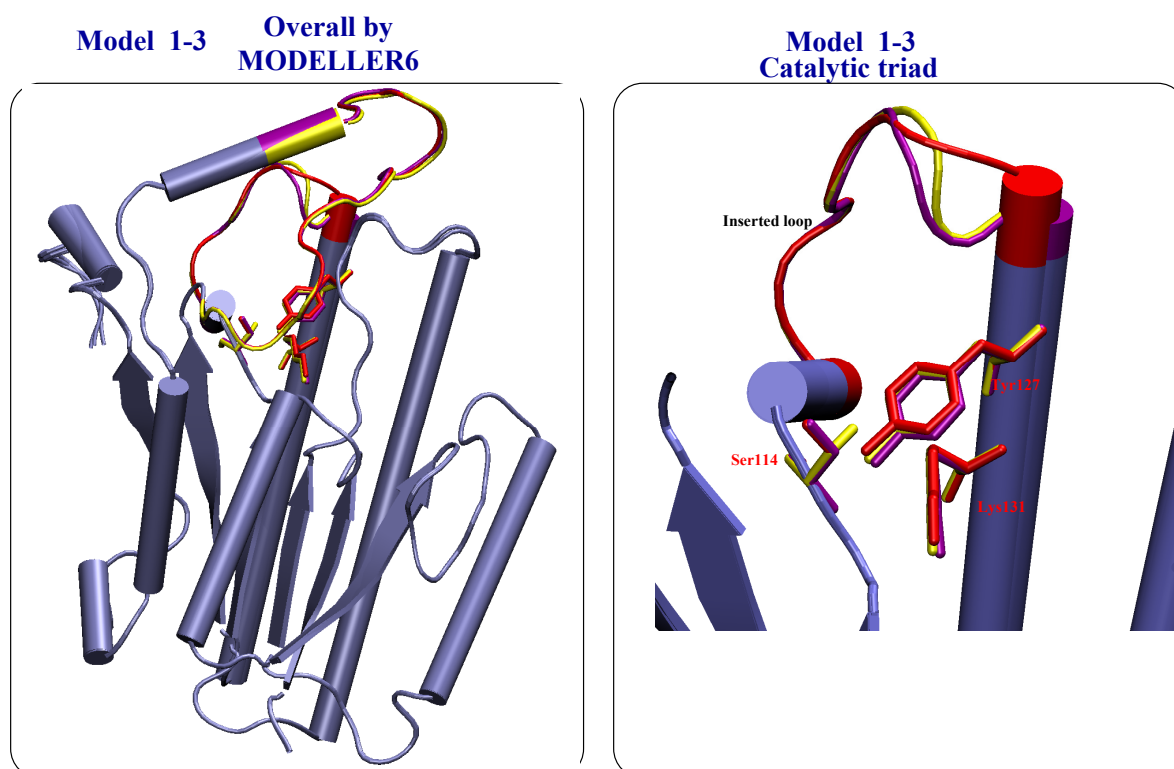


**Fig. IV-8: Overlay of the 3 models of 3α-HSD/CR-tr**

This overlay of the 3 models is generated by the modeller 6 program. Some differences can be clearly identified in the region of the inserted short loop. The position of the catalytic residues is very simlar in al 3 models.

```
>P1;2hsd
structureX:2hsd: 2 :A: 255 :D:3 alpha, 20 beta-hydroxysteroid
dehydrogenase(holo form:(streptomyces hydrogenans): 2.64:18.80
NDLSGKTVIITGGARGLGAEAARQAVAAGARVVLADVLDEEGAATARELGDAARYQHLDV
TIEEDWQRVVA--YAREEFGSVDGLVNNAGISTGMFLETESVERFRKVVEINLTGVFIGM
KTVIPAMKDAGGGSIVNISSAAGLMGLALTSSYGASKWGVRGLSKLAAVELGTDRIRVNS
VHPGMTYTPMTAETGIRQGEGNYPNTPMGRVGEPGEIAGAVVKLLSDTSSYVTGAELAVD
GGWTTGPTVKYVMGQ*

>P1;3hsd_mut
unknown:3hsd_mut: : : : : : : 0.00: 0.00
MSI----IVISGCATGIGAATRKVLEAAGHQIVGIDIRDAEVIA-------------DL
STAEGRKQAIADVLAKCSKG-MDGLVLCAGLGP-------QTKVLGNVVSVNYFGATELM
DAFLPALKKGHQPAAVVISSVASLMGLALTSAYAGSKNALTVAVRKRAAAWGEAGVRLNT
IAPGATETPFV-----------P--PMGRRAEPSEMASVIAFLMSPAASYVHGAQIVID
GGIDA---VMRPTQF*
```

```
INCLUDE
SET OUTPUT_CONTROL = 1 1 1 1
SET ALNFILE              = '../alis/3hsd+T+SBL.pir'
SET KNOWNS               = '2hsd'
SET MD_LEVEL             = 'refine2'
SET SEQUENCE             = '3hsd+T+SBL'
SET ATOM_FILES_DIRECTORY = '../pdbs'
SET OUTPUT_DIRECTORY     = './'
SET PDB_EXT              = '.pdb'
SET ALIGNMENT_FORMAT     = 'PIR'
SET STARTING_MODEL       = 1
SET ENDING_MODEL         = 3
SET DEVIATION            = 4.000000
SET FINAL_MALIGN3D       = 1
CALL ROUTINE             = 'model'
```

**Fig. IV-9: Structural alignment for modelling of extraloop-region**

Structural alignment (A) and TOP-file (B) for modeling of shortened amino acid sequence between βE and αF of 3α20β-HSD into the truncated pdb-structure of 3α-HSD/CR.

### IV.4.3 Molecular Dynamic Simulation of Three Mutant Models in Comparison to the Wildtype Gives an Outlook on Their Structural Stability

Molecular dynamics (MD) is a special form of computer simulation in which all atoms and molecules are allowed to interact for a defined period of time under known laws of physics and preassigned parameters. As a result of this simulation a view of the motion of the atoms is given. Molecular systems generally consist of a vast number of particles and are affected by a multitude of physical and chemical parameters. Therefore it is impossible to find the properties of such complex systems analytically. Numerical methods are used to circumvent this problem. Because of the fact that the most important chemico and physico parameters which have an impact on the system of molecules and atoms to be examined are defined in the simulation by algorithms MD simulations represent an interface between laboratory experiments and theory, and can be understood as a "virtual experiment".

The objective of a MD simulation is to calculate the temporally process of a molecular system in a predefined force field based on a starting configuration by means of Newton's equation of motion. During the simulation the acceleration on all atoms of the system is calculated which results in a new position of the atoms at a consecutive point of time. The length of thos timeframe has to be chosen correctly to record even motions with the highest frequencies. A trajectory is a series of consecutive configurations of the molecule.

The proteins in this approach were simulated in aqueous solution using a box of explicit water molecules and periodic boundary conditions. Fig. IV-10 shows a model of such periodic boundary conditions in which a box of water containing the molecule is adjacent to the next box of water. After minimization, heat-up to 300 K and initial equilibration, a trajectory of 1 ns length was sampled and saved at regular intervals of 0.5 ps.



**Fig. IV-10: Periodic boundary conditions.**

### IV.4.4 Comparative Simulation of the Wildtype Protein as Basis for Validation of Observed Structural Deviations.

To assess the observed root-mean-square deviation (rmsd), the differences between values predicted by MD-simulation, for the Cα-atoms of the protein backbone as well as for the all-atom rmsd comparative molecular dynamic simulations of the wildtype protein were performed. To use comparable proteins for this approach the sequence of the structurally unordered substrate binding loop (SBL) of 3α-HSD/CR was modelled accordingly to the approach for the truncated protein on the basis of the crystallographic well ordered SBL of alscohol dehydrogenase (1a4u). All three models of 3α-HSD/CR wildtype derived from the last modeling step were put into the simulation (Fig. IV-11). The model with the best score was further analyzed and discussed in comparison to the truncated 3α-HSD/CR-tr. Detailed analysis of the MD-simulation of the wildtype protein is discussed in the following chapter.
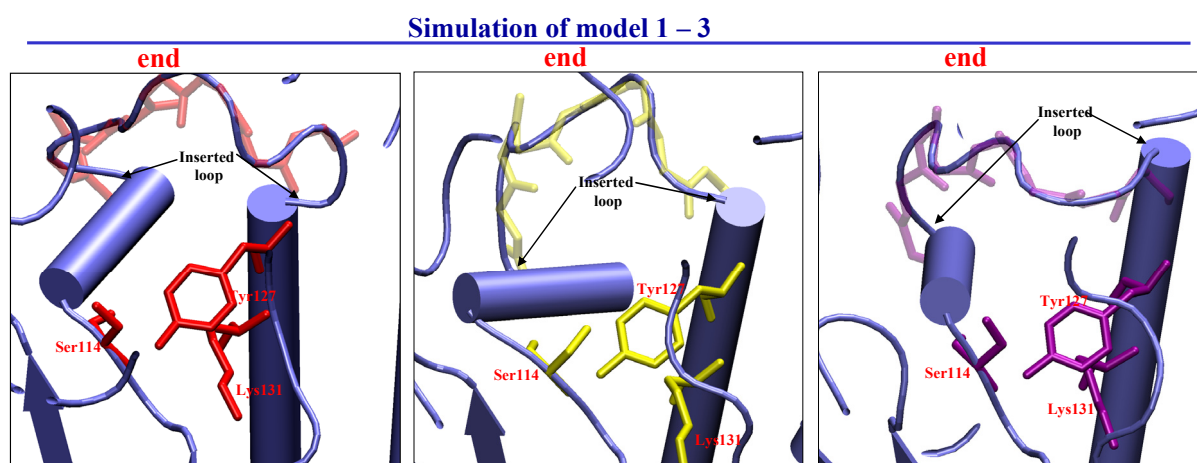


**Fig. IV-11: End-conformation of the three models of 3α-HSD/CR wildtype after MD simulation**

### IV.4.5 Comparative Analysis of the Simulated Structure of 3α-HSD/CR-tr and the Wildtype Protein Reveals Distinct Hot Spots of Flexibility.

Overall, the model with the highest score displays significantly higher stability during the simulation. After an increase during the first 400 ps, the root-mean-square deviation (rmsd) of the $C^{\alpha}$ atoms from the starting structure oscillates around 2 Å, indicating that the overall fold is well maintained. Analyzing the all-atom rmsd on a per-residue basis shows that apart from some rather exposed side chains the largest deviations and motions occur in the C-terminal area (residues 218-229) and in the substrate binding loop. Especially the latter is not unexpected given the experimentally known flexibility of this loop. Somewhat smaller deviations

and less pronounced mobility compared to the substrate binding loop are observed for the inserted 3α/20β-HSD loop. Most importantly, the distance between the terminal residues of this loop (Leu 118 and Ser 125) remains close to the starting value of 13.8 Å and shows a simulation average of 14.3 +/- 0.6 Å. As a consequence, no significant changes are also observed with respect to the orientation of the three catalytic residues (Ser 114, Tyr 127, Lys 131). In fact, their mutual $C^{\alpha}$ distance in the starting model is perfectly maintained throughout the simulation (Fig. IV-12; Fig. IV-14). Moreover, only very small fluctuations are observed for the entire catalytic triad, which is in line with the generally proposed structural stability of such areas in enzyme binding sites (Luque and Freire, 2000).
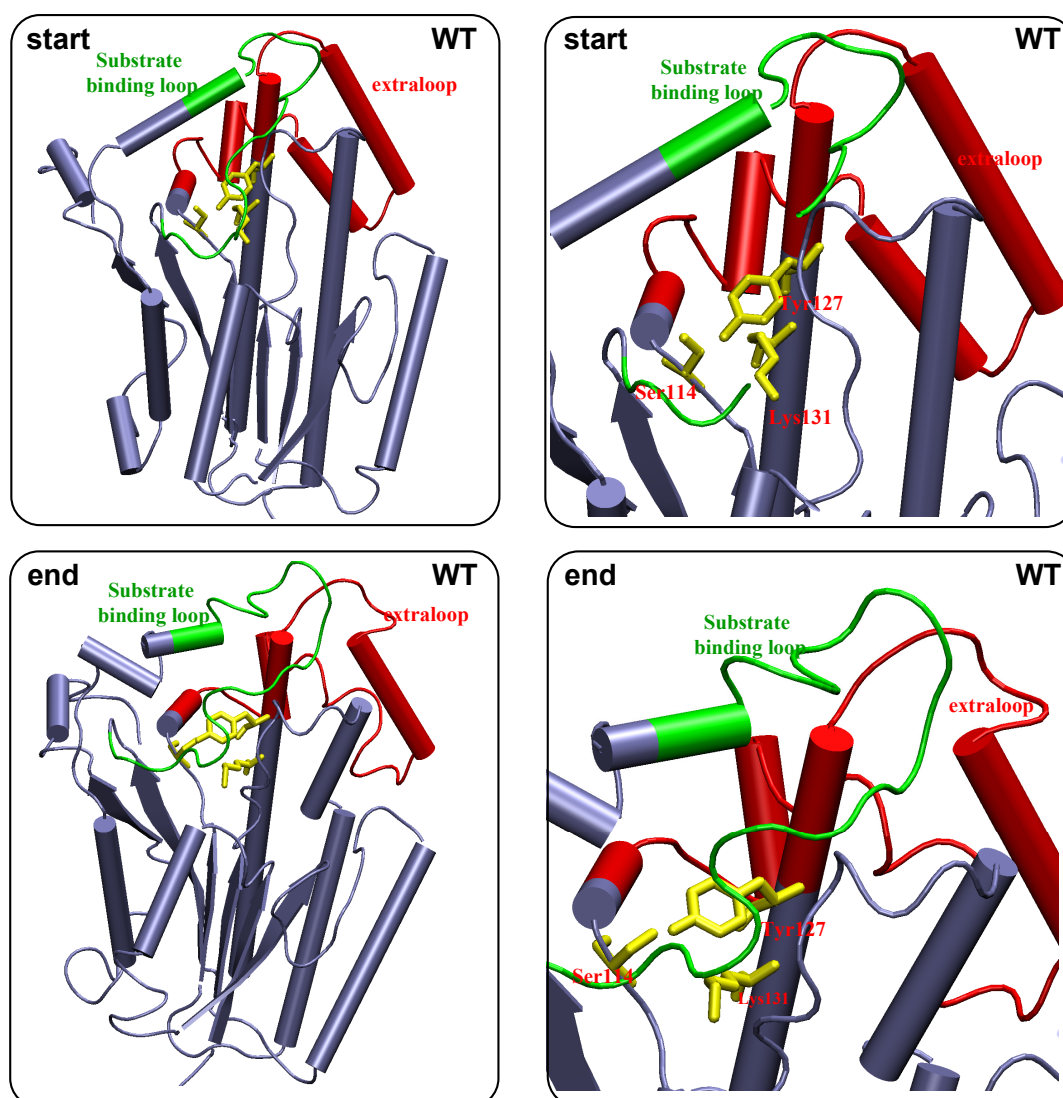


**Fig. IV-12: Comparative simulation of 3α-HSD/CR-wildtype protein**

Although the $C^\alpha$ rmsd and the all-atom rmsd averaged over the trajectory are 0.1 Å smaller than in the 3α-HSD/CR-tr simulation, the standard deviations of the rmsd averages (and thus the structural fluctuations) are increased by more than a factor of two (0.12 Å for the $C^\alpha$ atoms in the mutant, 0.30 Å in the wildtype). This increased flexibility leads also to distortions in the active-site, where the catalytic residues occasionally adopt alternative conformations and show on average larger mutual distances than in the starting structure (Fig. IV-12; Fig. IV-14). Also the average distance between the terminal residues of the extraloop (Ala 118 and Leu 153) is slightly widened. In total, 55 $C^\alpha$ atoms in the wildtype MD show standard deviations of the rmsd value larger than 0.65 Å. Among these, there is the entire substrate binding loop (which is unresolved in the crystal structure due to its high mobility) and all ten $C^\alpha$ atoms with B-factors above 30.00 $Å^2$ in 1fjh. The other residues found to be very flexible in the MD show lower B-factors, but are mainly part of the long C-terminal section involved in the dimer interface of the 3α-HSD/CR homodimer in crystal structure 1fjh (Fig. IV-13).

Analysis of the all-atom rmsd on a per-residue basis reveals distinct hot spots of flexibility. Since the structure was simulated as a monomer (in analogy to the mutant), it is reasonable to suggest that the lack of the dimer interface is the main reason for their increased flexibility. Interestingly, this higher degree of mobility could also be detrimental for catalytic activity, considering the alterations observed at the active site during the MD simulation. In contrast, the mutant monomer shows less pronounced flexibility (only 19 $C^\alpha$ atoms show standard deviations of the rmsd value larger than 0.65 Å). Apparently, in the absence of the stabilizing dimer contact the short 3α/20β-HSD loop of the mutant confers higher stability to the protein than the much longer extraloop of the wildtype.

Based on these analyses, the model appears reasonable and suggests that the 3α-HSD/CR-tr construct should also be catalytically active. Interestingly, the comparative simulation of the 3α-HSD/CR wildtype with the modelled substrate binding loop reveals a higher overall flexibility for the wildtype than for the mutant.
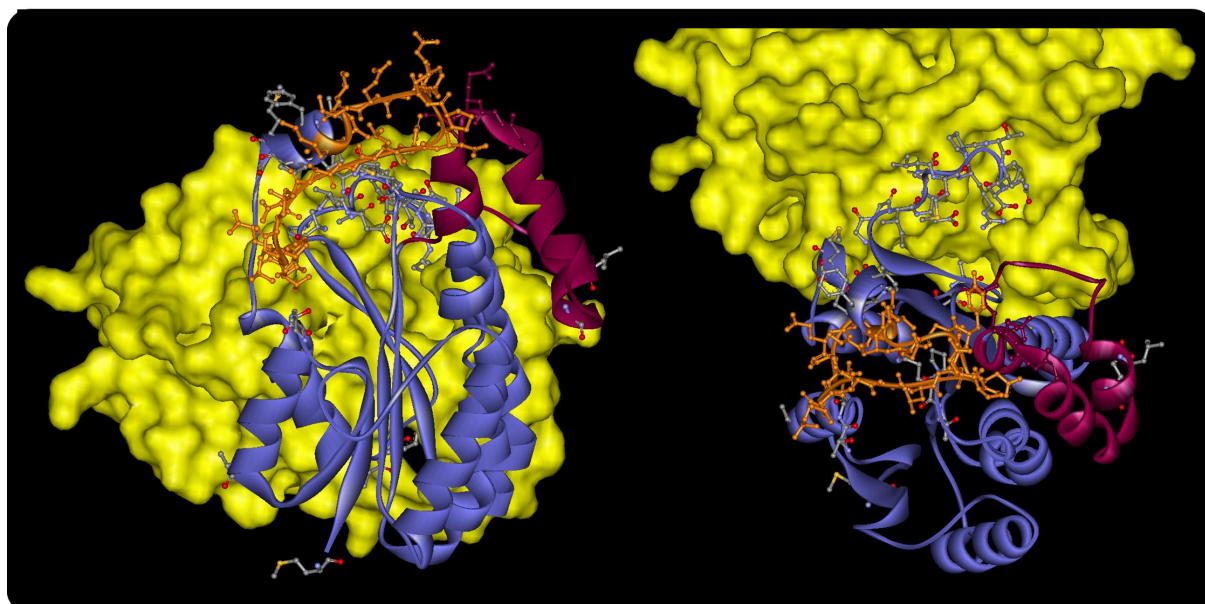
**Fig. IV-13: Positions of the most flexible residues in the simulated WT-structure with the modelled SBL-loop.**

The simulated monomer is shown in blue ribbons with the SBL (188 - 208) in orange and the extraloop (118 – 153) in purple. Residues showing $C^\alpha$-atom-rmsd standard deviations larger than 0.65Å are highlighted in ball-and-stick representation. To illustrate the relative position of the dimer interface, the simulated WT-monomer was superimposed with monomer A of crystal structure 1fjh; in the resulting superposition, monomer B of the 3α-HSD/CR homodimer is shown as yellow surface.
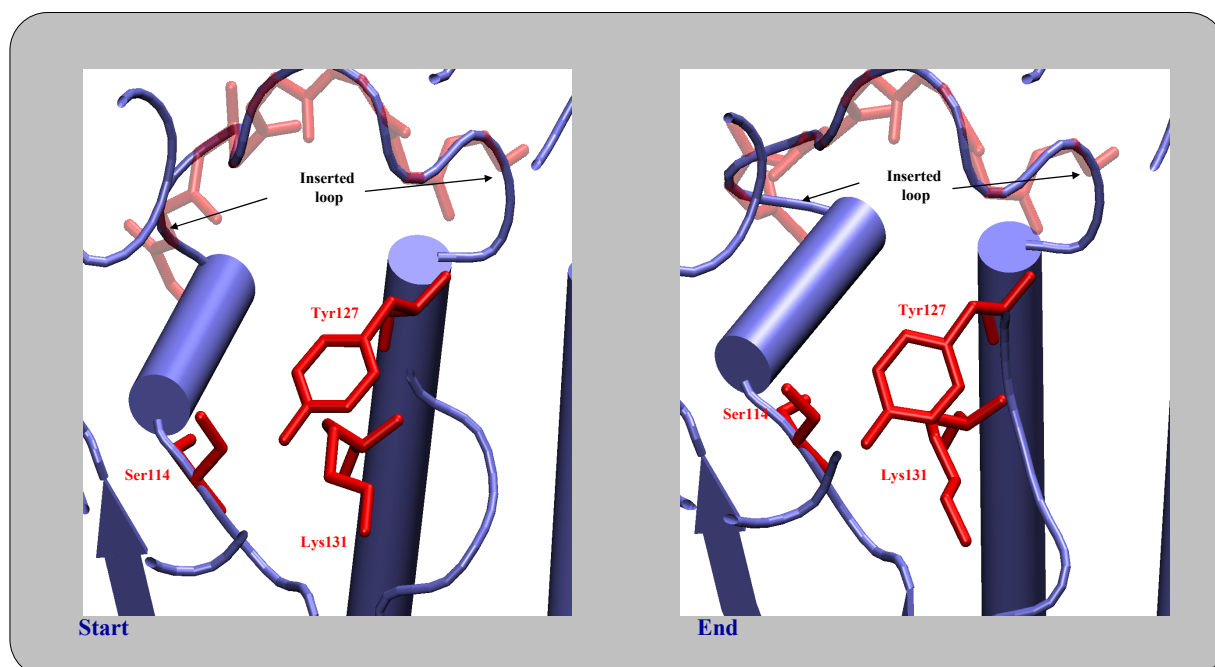


**Fig. IV-14: Start and end conformation of the inserted loop and the catalytic residues in 3α-HSD/CR-tr, model 1**

The distance between the terminal residues of this loop (Leu 118 and Ser 125) remains close to the starting value of 13.8Å and shows a simulation average of 14.3 Å. No significant changes are also observed with respect to the orientation of the three catalytic residues (Ser 114, Tyr 127, Lys 131).

## IV.5    Molecular Biology Approach to Delete the Extraloop Domain Yields a Biological Active Protein.

### IV.5.1    Overlap Extension PCR-Strategy to Delete Extraloop Domain

The cloning of 3α-HSD/CR was performed previously (Möbus and Maser, 1998). Based on this sequence primers were designed to perform overlap extension PCR. In this overlap extension PCR the sequence for the additional α-helical subdomain was replaced by the sequence for the homologous short region of 3α/20β-HSD (Fig. IV-15). The first PCR with primers *Nde*I-for and PMu10 resulted in a fragment containing the first part of the 3α-HSD/CR gene and the inserted sequence for the 3α/20β-HSD-loop. This fragment was used as a primer together with primer *Bam*HI-rev in a second PCR with vector pK15 as template resulting in a 690 bp fragment (3α-HSD/CR-tr) containing the inserted sequence of the 3α/20β-HSD-loop. Sequencing of the 3α-HSD/CR-tr-gene cloned into the pET15b-vector confirmed the correct in-frame DNA sequence and the absence of any mutations.
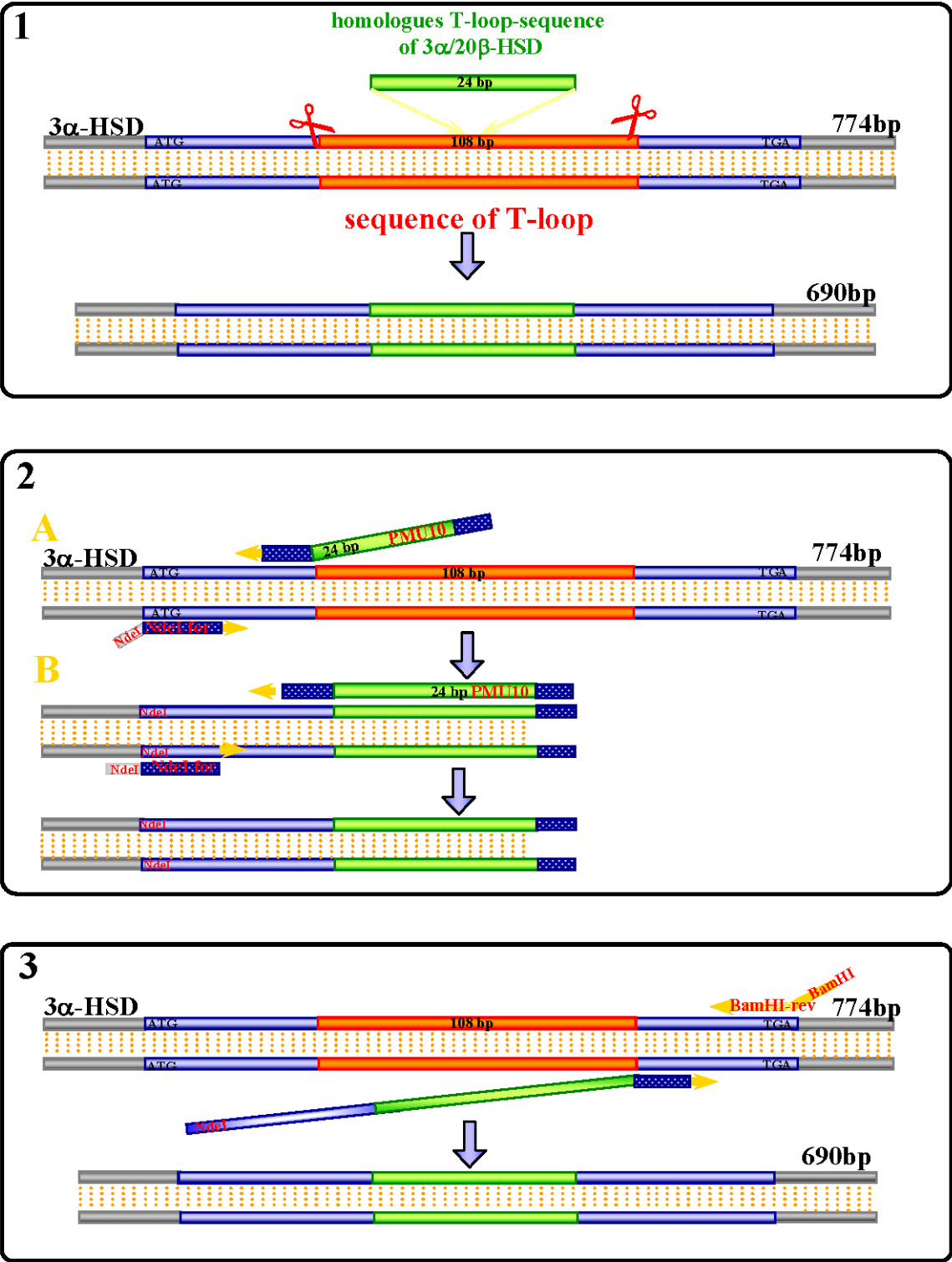
**Fig. IV-15: PCR-strategy for substitution of the extraloop-domain (Overlap-Extension-PCR)**

The 108 bp-fragment (red) represents the „extraloop" in the wt-sequence which was replaced by the homologous 24 bp fragment (green) of 3α/20βHSD.

## IV.5.2    Overexpression of the Recombinant and Truncated 3α-HSD/CR Protein

Cloning and overexpression of the 3α-HSD/CR as well as the 3α-HSD/CR-tr gene from *C. testosteroni* ATCC 11996 was performed as described in chapter III.2  (page 99). Following this approach overexpression resulted in fusion proteins with an N-terminal His tag sequence. 3α-HSD/CR wildtype protein could be easily detected in the supernatant after the cells were harvested and broken. In early experiments 3α-HSD/CR-tr could only be found in inclusion bodies (Fig. IV-17).

Inclusion bodies are aggregates of stainable substances, in this case proteins. Bacteria use inclusion bodies amongst others to protect themselves from substances which could be harmful for them. Another reason to pack protein into inclusion bodies is that the bacteria is not able to perform correct folding of the protein expressed with high expression rates within the cell. The internal microenvironment (pH, osmolarity) of a prokaryotic cell which is used for protein overexpression may differ from that of the original source of the gene. Additionally mechanisms for folding a protein may also be absent, and hydrophobic residues that normally would remain buried may be exposed and available for interaction with similar exposed sites on other ectopic proteins. Processing systems for the cleavage and removal of internal peptides would also be absent in bacteria. In addition to the obstructive interactions between the overexpressed protein and the the proteins in the cell , the fine controls that may keep the concentration of a protein low will also be missing in a prokaryotic cell, and overexpression can result in filling a cell with ectopic protein that, even if it were properly folded, would precipitate by saturating its environment.

Protein inclusion bodies are classically thought to contain missfolded protein. However, this has recently been contested, as green fluorescent protein will sometimes fluoresce in inclusions bodies, which indicates some semblance of the native structure and researchers have recover folded protein from inclusion bodies (Przybycien *et al.*, 1994; Tsumoto *et al.*, 2003; Umetsu *et al.*, 2005).

To understand if the expression in general was successful and where the overexpressed protein can be localized ELIZA was performed.

### IV.5.3    Enzyme Linked ImmunoSorbent Assay (ELISA) to Detect Soluble Protein

To perform a distinct localization of soluble protein and overexpressed protein in general ELIZA was performed with several samples taken from different steps after the overexpression. To detect the 3α-HSD/CR-tr an antibody against the entire protein was used. Soluble protein should be able to be detected in the supernatant after harvesting the cells. 3α-HSD/CR-WT could be clearly detected in the supernatant whereas the truncated protein could only be found in small amounts in the supernatant. During different cycles of cell wash the cells were 3x sonified for 10 sec and ultracentrifugated. In a last step the remaining debris was resolubilized in 6M Urea which breaks the inclusion bodies and makes the protein accessable for the antibody. In spite of the fact that 3α-HSD/CR can be found in increased amounts in the supernatant after first round of ultracentrifugation most of the protein seams to be located in inclusion body too (Fig. V-2). In contrast to the wildtype protein the truncated protein can only be detected in higher amounts in inclusion bodies. Therefore additional strategies to renaturate the protein from inclusion bodies as well as to improve protein expression in terms of solubility have to be developed.
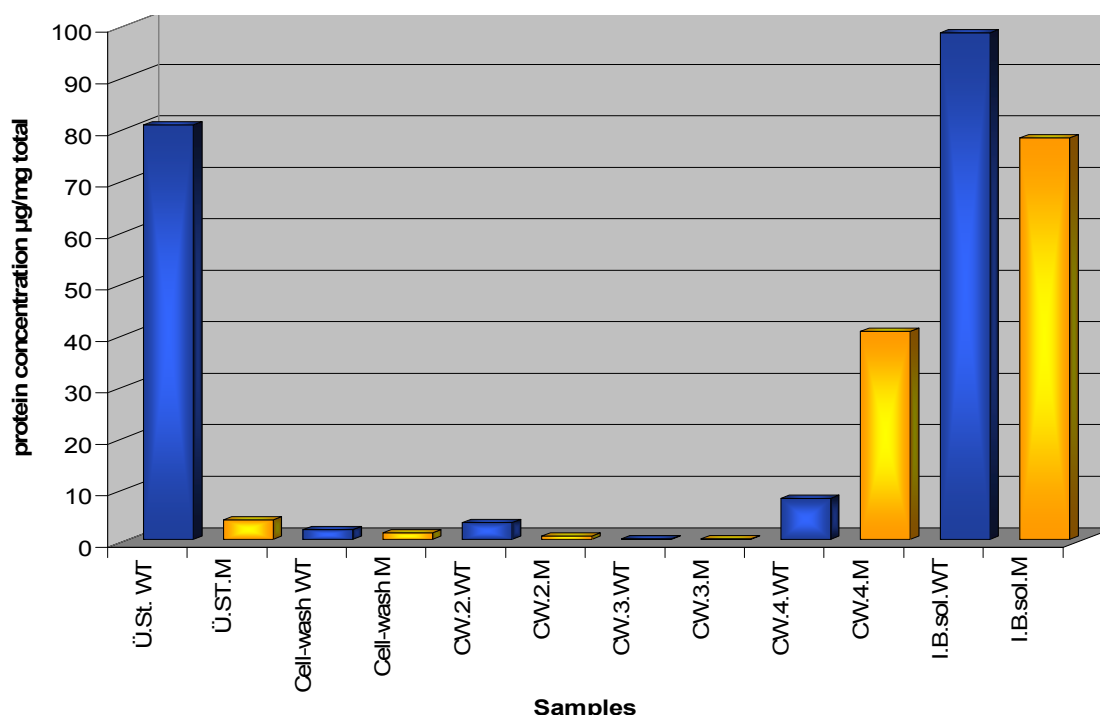


**Fig. IV-16: Distribution and protein concentration of truncated 3α-HSD/CR**

| sample | adsorbtion | protein concentration in ng/mg total protein diluted 1:100 | protein concentration in µg/mg total protein |
|---|---|---|---|
| Ü.St. WT | 1,985 | 804,42 | 80,44 |
| Ü.St. M | 0,606 | 37,52 | 3,75 |
| Cell Wash 1 WT | 0,345 | 18,44 | 1,84 |
| Cell Wash 1 M | 0,237 | 12,01 | 1,20 |
| Cell Wash 2 WT | 0,542 | 32,28 | 3,23 |
| Cell Wash 2 M | 0,124 | 5,96 | 0,60 |
| Cell Wash 3 WT | 0,008 | 0,38 | 0,04 |
| Cell Wash 3 M | 0,016 | 0,77 | 0,08 |
| Cell Wash 4 WT | 0,982 | 78,96 | 7,90 |
| Cell Wash 4 M | 1,788 | 403,88 | 40,39 |
| I.B.sol.WT | 1,978 | 779,59 | 77,96 |
| I.B.sol. M | 2,026 | 983,60 | 98,36 |

**Table IV-1: Protein concentration of 3α-HSd/CR-tr after different steps during protein overexpression**

## IV.5.4 Refolding of Denatured Protein

It has been shown that protein folding is an enhanceable process (Rudolph and Lilie, 1996; Xie and Wetlaufer, 1996; Gupta *et al.*, 1998) and that insoluble proteins can be refolded (Kurucz *et al.*, 1995; Rudolph and Lilie, 1996; Mukhopadhyay, 1997). Most protocols describe the isolation of insoluble inclusion bodies by centrifugation followed by solubilisation under denaturing conditions. The protein is then dialyzed or diluted into a non-denaturating buffer where refolding occurs. Because every protein possesses unique folding properties, the optimal refolding protocol for any given protein must be empirically determined. Optimal refolding conditions can be rapidly determined on a small scale by a matrix approach, in which variables such as protein concentration, reducing agent, redox treatment, divalent cations, etc., are tested. Once the optimal concentrations are found, they can be applied to a larger scale solubilisation with refolding of the target protein. Because of the fact that for identifying the critical parameters for refolding not too much parameter should be varied in parallel a large number of experiments is required.

After refolding of the protein all substances used in the approach have to be removed prior to activity testing which was ideally done by gentle dialysis against the buffer used for subsequent activity testing. To ensure that all approaches have been treated exactly in the same way all refolding experiments of a charge of overexpressed protein have been done simultaneously.
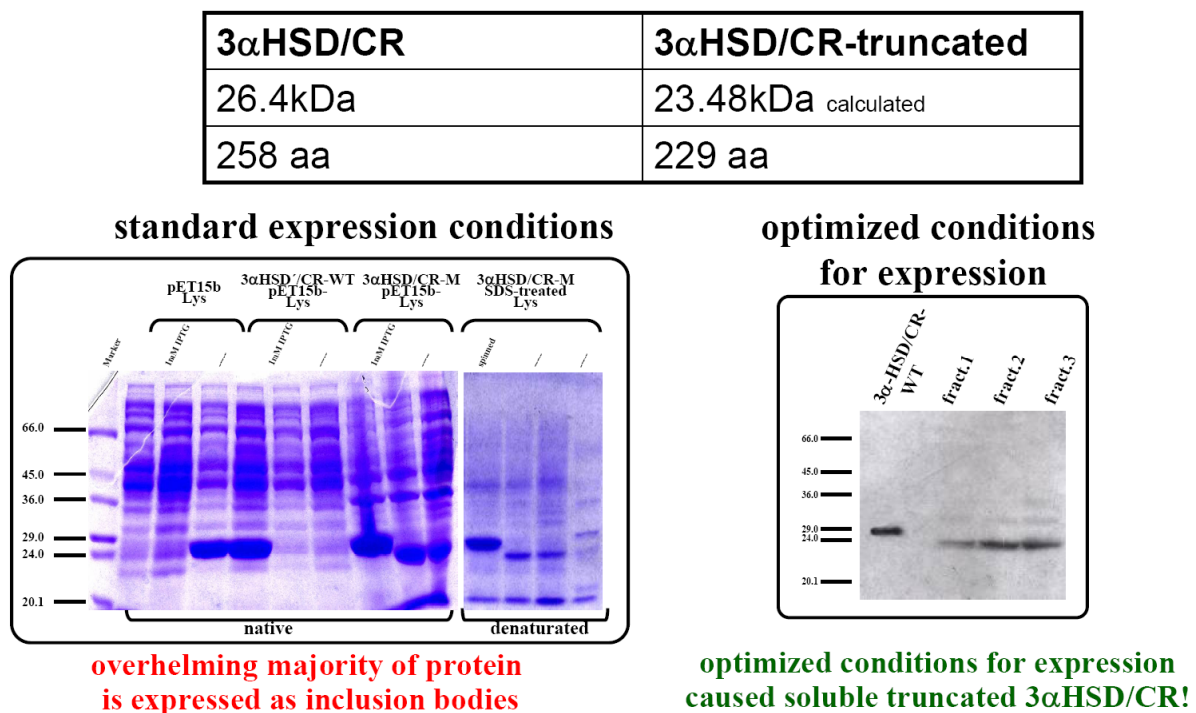
Resuspensation of the inclusion bodies was performed as described in "Materials and Methods". The method of dialysis was chosen for refolding the protein as this is a very gentle way of changing the conditions for the denatured protein. All refolding approaches were done in parallel to use exactly the same stock solutions of the reagents and to avoid degradation (e.g. Arginin).

After refolding all protein solutions solubility was tested by ultracentrifugation followed by western blot analysis. To be able to detect also very small amounts of soluble protein the refolded samples were tested by HPLC analysis as described in chapter III.11 , page 115.  All samples showed insoluble protein aggregates which is a hint that most of the protein is still denatured. To enhance refolding the protein concentration was decreased to 0.1mg/ml. After dialysis against 50mM Tris buffer and centrifugation the supernatant was again tested for activity by HPLC. In the p-Nitrobenzaldehyde as well as in the assay with metyrapone as substrate no protein activity could be detected. This led to the conclusion that the approach to refold the truncated 3α-HSD/CR should not be further followed.

### IV.5.5     Optimized Expression Leads to a Soluble Truncated 3α-HSd/CR Protein.

As refolding of the truncated protein was not successful optimizing the conditions for protein overexpression seemed to be the only approach to produce soluble protein which could be used for activity testing by HPLC.

Several different approaches were performed to optimize the conditions for expression. Based on the fact that proper folding of a protein is a time depending process and that to high concentrations of overexpressed protein could prevent correct folding the expression temperature was decreased to finally RT, the expression time was extended from 4 to up to 12 hours and induction of expression by IPTG was decreased by more that a factor of 10. Additionally several E.Coli strains were tested for protein expression (see Material and Methods). Among these the best results could be identified with the strain BL21(DE3)pLysS (Stratagene). After protein expression the supernatant was tested by SDS-PAGE and Western Blot analysis for successful protein expression in parallel to the supernatant of wildtype 3α-HSD/CR expression. Finally Optimizing the conditions for overexpression let to sufficient amounts of soluble protein which could be detected by Western Blot analysis (Fig. IV-17). The protein was then further purified by Affinity Chromatography.

| 3αHSD/CR | 3αHSD/CR-truncated |
|---|---|
| 26.4kDa | 23.48kDa calculated |
| 258 aa | 229 aa |

**standard expression conditions**          **optimized conditions for expression**



**overhelming majority of protein is expressed as inclusion bodies**

**optimized conditions for expression caused soluble truncated 3αHSD/CR!**

**Fig. IV-17: Overexpression of 3α-HSD/CR-tr**

**3α**-HSD/CR-tr was initially found only in inclusion bodies (left, lanes 5+6; lanes 8+9 after SDS-treatment). Optimized conditions for expression let to soluble 3α-HSD/CR-tr which was detected by western blot analysis (right).

## IV.5.6    Affinity Chromatography Yields Purified Protein.

Affinity Chromatography was performed as described in chapter III.9 , page 111. The recombinant 3α-HSD/CR and the 3α-HSD/CR-tr could be purified in one step using metal chelate chromatography, and the purity of the protein was greater than 98% as judged by Coomassie staining of SDS-polyacrylamide gels. The molecular mass of the recombinant 3α-HSD/CR-tr as seen in the SDS gel was identical to the 23.38 kDa predicted from the genomic sequence (in comparison to the wt-protein with 26.4 kDa (Maser et al., 2000)).  Previous tests for enzymatic activity with steroids and metyrapone as substrates for 3α-HSD/CR gave first hints for activity of the 3α-HSD/CR-tr.

### IV.5.7 HPLC-Activity Testing Detects Carbonyl Reduction Activity for Truncated Protein.

After purification of the recombinant 3α-HSD/CR WT and the 3α-HSD/CR-tr protein derived from the optimized expression approach HPLC testing was performed to test the overexpressed truncated protein in comparison to the also overexpressed wildtype protein. For this approach HPLC testing was performed as described in chapter III.11 , page 115.

Fig. IV-18 shows the results of the HPLC activity testing.

To define the correct elution time of the used substrate *p*-nitrobenzaldehyde as well as of the product of the reaction both substances were injected into the system together with the same purified protein used for the complete reaction samples (Fig. IV-18). As a positive standard for the reaction substrate *p*-nitrobenzaldehyde was injected into the system and an elution peak at ~ 10.5 min can be detected. As a positive standard for the reaction product *p*-nitrobenzalcohol was also injected into the system and can be detected at ~ 5.7 min. Different samples of 3α-HSD/CR wildtype protein as well as the overexpressed and purified 3α-HSD/CR truncated protein were tested in the HPLC activity test for different incubation times. An overview of the tested samples can be found in Table IV-2.

Fig. IV-18 clearly shows that for the overexpressed and purified truncated 3α-HSD/CR protein carbonyl reduction activity can be detected. In comparison to the activity of the also overexpressed and purified wildtype 3α-HSD/CR protein this enzymatic activity seems to be decreased. In further activity testing with the substrate metyrapone no enzymatic activity could be detected.

| Sample | Figure | Label | Retention Time |
|--------|--------|-------|----------------|
| **Positive Standard for reaction substrate** | | | |
| *p*-nitrobenzaldehyde | Fig. IV-18 A | Peak of pNB-aldeh. at ~ 10.5 min | 10.5 min |
| **Positive Standard for reaction product** | | | |
| *p*-nitrobenzalcohol | Fig. IV-18 C | pNB-alc. | 5.7 min |
| **Positive Standard for enzymatic reaction** | | | |
| + *p*-nitrobenzaldehyde<br>+ incl. WT-protein<br>+ incl. NADPH-regenerating system | Fig. IV-18 B | Peak of WT pNB-alc, 15 min incubation | 5.65 min |
| + p-nitrobenzaldehyde<br>+ incl. WT-protein<br>+ incl. NADPH-regenerating system | Fig. IV-18 C | WT, 5' inc. | 5.65 min |
| **Negative Standard for enzymatic reaction** | | | |
| + p-nitrobenzaldehyde<br>+ incl. WT-protein<br>- excl. NADPH-regenerating system | Fig. IV-18 C | WT - pNBA | n.a. |
| **Enzymatic Reaction with mutated 3α-HSD/CR** | | | |
| + *p*-nitrobenzaldehyde<br>+ incl. truncated-protein<br>+ incl. NADPH-regenerating system | Fig. IV-18 C | M, 5' inc. | 5.63 min |
| + *p*-nitrobenzaldehyde<br>+ incl. truncated-protein<br>+ incl. NADPH-regenerating system | Fig. IV-18 C | M, 15' inc. | 5.6 min |

**Table IV-2: Overview on tested samples for HPLC activity testing**
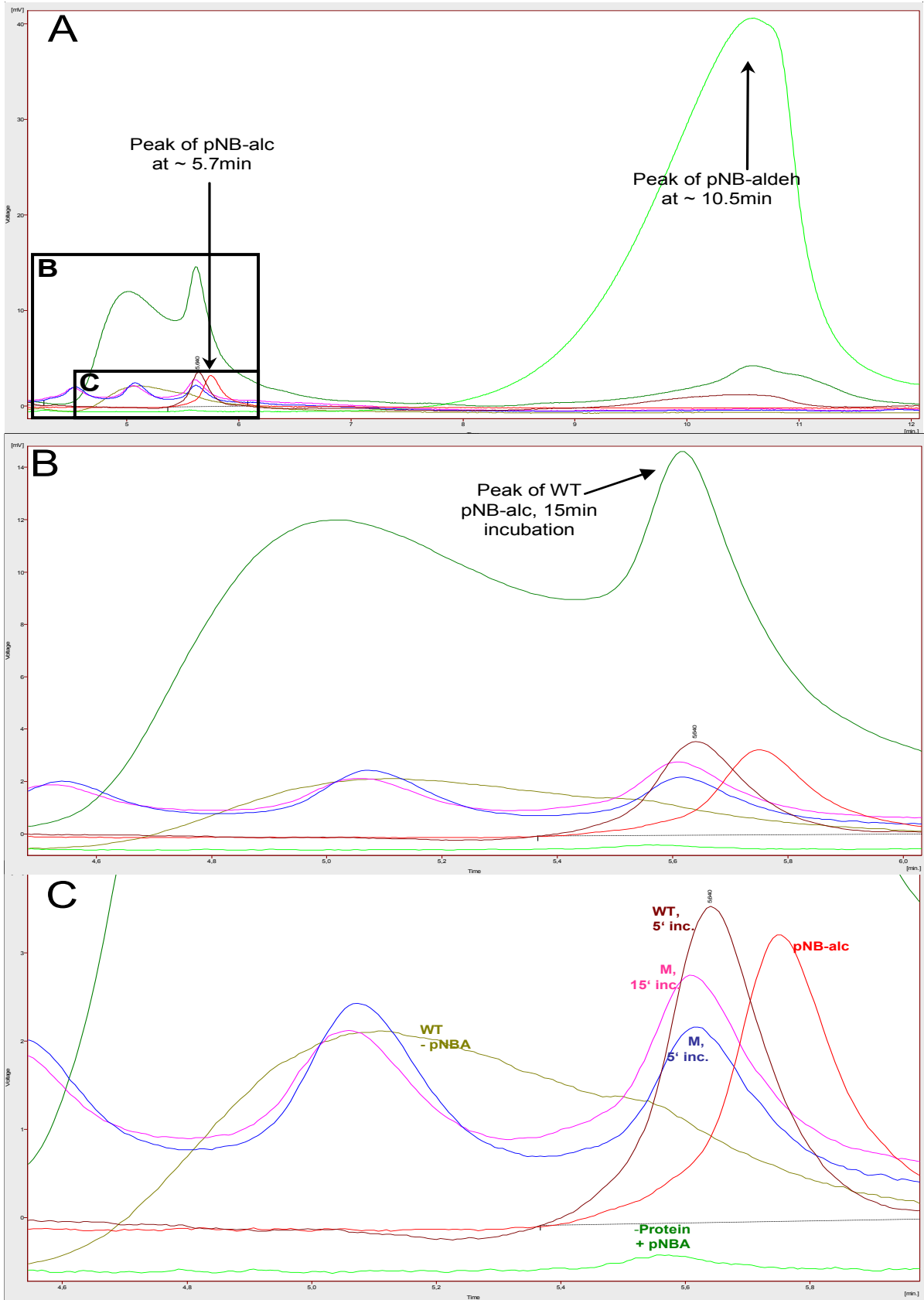
**Fig. IV-18: HPLC chromatograms of activity testing**

## IV.6 How do the Simulation Data Fit to the Experimental Data?

This study aimed for answering two different questions with respect to enzymatic characterization. **First**, what is the role of the crystallographic determined alpha-helical subdomain and its relevance for the catalytic activity of 3α-HSD/CR? And **second**, has the extraloop domain any relevance for the oligomerization behaviour of 3α-HSD/CR? Additionally, from the methodically aspect this study should show if deletions and insertions as comprehensive as in this study can be effectively modelled and simulated prior to a molecular biology approach to provide an understanding if the planned mutations appears reasonable and if the observed effects of the truncation refer to the mutation of the protein or only to a structurally destroyed protein.

The combined *in silico* and molecular biology approach revealed two different perspectives of the characteristics of 3α-HSD/CR.

### IV.6.1 First: Homology Modeling and MD Simulation of the Truncated Protein Showed, that the Protein is not Particular Instable or Seems to Adopt Untypical Conformations.

Simulation of 3α-HSD/CR wildtype as well as the truncated protein provides a first insight into the behaviour and the stability of the structural architecture of the truncated protein after deletion of the alpha-helical subdomain (extraloop) and the insertion of a shortened loop from 3α20β-HSD. Different single modeling and simulation steps were necessary to create comparable starting structures. This included the modeling of the substrate binding loop on the basis of the SBL from Alcohol dehydrogenase, the modeling of the shortened loop region from 3α20β-HSD from *Streptomyces hydrogenans* and the comparative simulation of the wildtype structure of 3α-HSD/CR with prior also modeling of the structurally unordered SBL in the Wildtype structure.

All simulation approaches are based on different parameters which have to be defined prior to simulation and which all can have critical influence on the outcome of the simulation.

The MD simulation of the truncated protein showed that the orientation of the three catalytic residues (Ser 114, Tyr 127, Lys 131) keeps relatively stable during the simulation and their mutual $C^{\alpha}$ distance in the starting model is perfectly maintained throughout the simulation (Fig. IV-12; Fig. IV-14).

The structural fluctuations within the entire protein as well as between the catalytic residues or the domains of the protein, which need distinct flexibility to be biological active, are not notably more instable or flexible than in the Wildtype protein. The all-atom rmsd on a per-residue basis shows that apart from some rather exposed side chains the largest deviations and motions occur in the C-terminal area (residues 218-229) and in the substrate binding loop. This substrate binding loop (SBL) was expected to show higher flexibility than the rest of the protein as this SBL had to be modelled into the structure of 3α-HSD/CR to yield a one-chain protein for simulation (cf. chapter IV.4 , page 132). In addition this SBL is responsible for substrate binding. Crystallographic studies done by Grimm and coworkers (Grimm *et al.*, 2000b) also showed that this substrate binding loop becomes only structurally ordered as soon as the substrate was bound to the protein and covered by this loop region.

Fig. IV-12 shows the close position of the alpha helical subdomain in 3α-HSD/CR to the residues of the catalytic triad. In Fig. IV-14 the close distance of these catalytic residues to the inserted loop region can be seen. Only small deviations can be found after the MD simulation for the inserted 3α/20β-HSD loop and the distance of between the terminal residues this loop region (Leu 118 and Ser 125) remains close to the starting value of of 13.8 Å. But the close position of the SBL, the inserted loop region and the catalytic residues Ser 114, Tyr 127, Lys 131 leads to the assumption that somewhat larger deviations in comparison to the wildtype structure can be found in the experimentally determined structure of the truncated 3α-HSD/CR.

The approach of simulating the wildtype protein whose structure has already been solved should serve as a standard for evaluating the observed structural fluctuations in the truncated protein. Comparative simulation of the WT-protein even showed that the standard deviations of the rmsd averages (and thus the structural fluctuations) are increased by more than a factor of two (0.12 Å for the $C^\alpha$ atoms in the mutant, 0.30 Å in the wildtype). This increased flexibility in the wildtype protein leads also to distortions in the active-site, where the catalytic residues occasionally adopt alternative conformations and show on average larger mutual distances than in the starting structure (Fig. IV-12; Fig. IV-14). Therefore the structural fluctuations observed during the MD simulation of the truncated protein seem to be rather small.

### IV.6.2 Second, the Molecular Biology Approach Served as a Control for the Tendencies Yielded by the in silico Approach.

Predictions on the structural level investigated by the modeling and simulation approaches should be able to be confirmed by molecular biology techniques. The most relevant tendency from the *in silico* approach is, that the truncated protein, which lacks the α-helical subdomain ("extraloop"), seems to be structurally stable with the respect to the overall architecture of the protein as well as the structural orientation of the catalytic residues.

With respect to the question on the catalytic activity of 3α-HSD/CR the obvious stability of the entire protein and of the catalytic triade could be demonstrated by overexpression, subsequent affinity chromatography and western blot analysis. These overexpression experiments yielded a soluble protein with a molecular mass which corresponds to a dimerized truncated protein. Enzymatic activity could be shown by HPLC analysis for carbonyl reduction activity. In comparison to the Wildtype protein, for which all steps were done in parallel, the yield of soluble protein was significantly reduced. Only extensive optimization experiments on protein expresion yielded amounts of soluble protein which could be further characterized. This decrease in solubility could be attributed to the fact, that the in the truncated protein a significant number of amino acids were exchanged or deleted in comparison to the wildtype protein.

In HPLC analysis carbonyl reduction activity could be showed for the truncated protein with the substrate p-nitrobenzaldehyde. Here again, carbonyl activity was decreased significantly in comparison to the wildtype.

Redesign of the extraloop-domain in the truncated 3α-HSD/CR protein seems not to destroy catalytic activity but leads to a significant decrease in carbonyl reduction activity.

However, as the correct orientiation of the catalytic residues is critical for enzyme activity the decrease in enzyme activity is possible to be caused by small structural deviations in comparison to the wildtype protein. This decrease in enzyme activity can be caused by the enzymatic truncation of the mutant.

### IV.6.3    Limitations of the Approach

First tendencies were obtained by the modeling and simulation approach that the redesign of the α-helical subdomain in 3α-HSD/CR on the basis of the corresponding region of 3α20β-HSD was feasible. Although this investigation is based on *in silico* data, a general tendency of the truncated protein to keep its entire architecture, especially in the biological active catalytic residues, can be identified. Particularly the parallel simulation of the three-dimensional structure of the Wildtype protein served as a suitable tool to assess the validity of the modeling and simulation.

Additionally, the MD simulation of the refined three dimensional structure of the Wildtype protein showed, that the structure of a protein, which is described by its pdb-file, is always some kind of snapshot with areas of more and areas of less flexibility, depending on its role for the biological function of the entire protein. A crystal structure is more than the stable conformation, described by the pdb file. Only a closer look in the parameters of this refined crystal structure shows which regions of the protein need to be flexible for proper enzymatic protein function. Even the refined crystal structure of 3αHSD/CR wildtype protein showed regions of higher flexibility in the simulation which appears reasonable as the protein has to adapt its 3D architecture to use, e.g., different substances as substrates.

Therefore the comparative simulation of the wildtype protein showed how difficult the evaluation of the structural flexibilities observed in the truncated protein is.

# V  Outlook

In the present study it was shown that it's feasible to combine an in silico and a molecular biology approach to optimize protein-redesign which aims for a better understanding of structural features of proteins and their teamwork to enable proper protein function. Especially changes to the extent performed in this study, which can be suspected to have significant impact on the structural architecture of a protein, cannot be simply performed by "cut and paste" of complete structural domains. Although the overall protein architecture remains stable after the deletion of the alpha-helical subdomain and the insertion of the shortened loop from 3α20β-HSD these data are based only on simulation strategies which cannot replace clear crystallographic data after redesign of 3α-HSD/CR. Simulation strategies which use the wild-type protein for assessment of fluctuations observed during simulation are a must to get a feeling of regions within the protein structure which show per se structural flexibility, e.g. to adapt on different substrates.

Therefore, based on the present *in silico data* and first *in vitro* characterizations of this study, thoroughly enzymatic characterization including complete kinetic data should yield insight into the catalytic effects of the redesigned protein. The question should be further investigated if the performed changes of the protein have an influence on the kinetic parameters or on the use of different substrates of the protein.

Further enzymatic characterization on the structural level by Dynamic Light Scattering techniques (DLS) together with Size Exclusion Chromatography (SEC) are planned to elucidate the oligomerization behaviour after redesign of the original oligomerization interface.

As a long term goal crystal structure analysis of the mutated protein is planned to investigate, if the fraction of dimers in comparison to other forms of oligomerization has eventually changed.

With respect to the role of 3αHSD/CR for the steroid metabolizing pathway as one of the initiating enzymes of the steroid degradation pathway enabling procaryotes to grow on the steroids, to be resistance towards steroid antibiotics and non-steroid insecticides, further understanding of the properties of this enzyme could lead to applications within toxicology or biotechnology.

# VI Summary

On the basis of 3α-HSD/CR from *Comamonas testosteroni* , which serves as a model system for bacterial steroid degradation, the relationship of structural elements, correct protein folding and proper protein function with respect to its biological function was investigated.

On the structural level the additional extraloop domain, which is unique in the class of dimeric SDR enzymes, was identified as a putative sterical inhibitor of oligomerization via the Q-axis interface as the typical oligomerization interface of dimeric SDR enzymes. Structural alignments with dimeric and tetrameric members of the SDR superfamily identified the α-helical subdomain, called extraloop, as a structural element responsible for deviating oligomerization behaviour. To investigate the question, which role the additional extraloop domain plays in 3α-HSD/CR from *C. testosteroni* and if this structural feature has a fundamental role for protein stability and/or functionality in 3α-HSD/CR a mutated 3α-HSD/CR-protein (3α-HSD/CR-tr) had to be established which lacks the extraloop domain. An approach combining "in silico" and "wet chemistry" was performed to redesign a complete loop region in 3α-HSD/CR by substitution of the extraloop domain by a shortened homologous loop of 3α/20β-HSD on the basis of two crystallographically determined structures.

To yield a one-chain protein as basis for Molecular Dynamic simulation the structurally unordered Substrate Binding Loop (SBL) of 3α-HSD/CR was first successfully modelled on the basis of the structurally determined SBL of Alcohol Dehydrogenase (ADH) of *Drosophila Lebadonensis*. A second modelling step lead to a pdb-structure of a mutated 3α-HSD/CR protein in which at the end 36 amino acids of the alpha-helical extraloop-domain were substituted by an 8-residue loop of the homologous region of 3α/20β-HSD of *S. hydrogenans*.

Molecular Dynamic (MD) Simulation were performed of both, the untruncated wildtype protein including the re-modelled SBL as well as the truncated protein including the re-modelled SBL together with the shortened 8-residue loop from 3α/20β-HSD.

Analysis of the root-mean-square deviation (rmsd) of the Cα atoms indicated that the overall fold of 3α-HSD/CR-tr is well maintained.

Analysis on a per-residue basis showed that the largest deviations and motions occur in the C-terminal area and in the substrate binding loop. Especially the latter is not unexpected given the experimentally known flexibility of this loop. The inserted 3α/20β-HSD loop shows somewhat smaller deviations and less pronounced mobility compared to the substrate binding loop. The distance between the terminal residues of the extraloop remains close to the starting

value. As a consequence, no significant changes are also observed with respect to the orientation of the three catalytic residues.

The comparative simulation of the 3α-HSD/CR wildtype with the modelled substrate binding loop reveals a higher overall flexibility for the wildtype than for the mutant. This increased flexibility leads also to distortions in the active-site, where the catalytic residues occasionally adopt alternative conformations and show on average larger mutual distances than in the starting structure. Simulation of 3α-HSD/CR wildtype as a monomer (in analogy to the mutant) and therefore the lack of the dimer interface can be seen as the main reason for their increased flexibility. In contrast, the mutant monomer shows less pronounced flexibility. Apparently, in the absence of the stabilizing dimer contact the short 3α/20β-HSD loop of the mutant confers higher stability to the protein than the much longer extraloop of the wildtype. Based on these analyses, the model appears reasonable and suggests that the 3α-HSD/CR-tr construct should also be catalytically active.

The amino acid sequence successfully modelled and simulated in the *in silico* approach was transferred in the molecular biology approach to an active and soluble protein. Overlap extension PCR yielded the correct DNA sequence coding for the truncated 3α-HSD/CR-tr protein. Standard overexpression conditions resulted in high amounts of recombinant protein which could be located in inclusion bodies by ELIZA techniques. A broad assay testing well-established conditions for refolding of denatured proteins didn't result in renatured recombinant protein. Optimization of conditions for overexpression enabled expression of soluble and native truncated 3α-HSD/CR-tr protein which could be detected and clearly identified in Western Blot analysis and purified by Affinity Chromatography. Further HPLC characterization showed clearly carbonyl reducing activity for truncated 3α-HSD/CR-tr protein which in comparison to wildtype protein was significantly reduced.

# VII  Zusammenfassung

Auf Basis von 3α-HSD/CR von *Comamonas testosteroni*, das als Modelsystem für den bakteriellen Steroidabbau dient, wurde der Zusammenhang von Strukturelementen, korrekter Proteinfaltung und Proteinfunktion bezüglich ihrer biologischen Funktion untersucht.

Auf struktureller Ebene wurde die zusätzliche Extraloop-Domäne, die einzigartig in der Klasse der dimeren SDR Enzyme ist, als als vermeintlicher sterischer Inhibitor einer Oligomerisierung entlang der sonst in dimeren SDRs üblichen Q-Achse identifiziert. Strukturbasierte alignments zwischen dimeren und tetrameren Enzymen der SDR Protein-Superfamilie identifizierten die alpha-helikale Untereinheit (extraloop) als das Strukturelement, das für das von anderen vergleichbaren SDR Enzymen abweichende Oligomerisierungsverhalten verantwortlich zu sein scheint. Um der Frage nachzugehen welche Rolle die zusätzliche extraloop-Domäne in 3α-HSD/CR spielt und ob dieses Strukturelement eine fundamentale Bedeutung für die Proteinstabilität und Funktionalität für das Protein besitzt, wurde ein mutiertes 3α-HSD/CR-tr Protein generiert, dem diese zusätzliche Untereinheit fehlt. Es wurde ein kombinierter Ansatz aus computerbasierter Modellierung und Simulation sowie molekularbiologischen Methoden verfolgt, der die vollständige extraloop-Region in 3α-HSD/CR durch den verkürzten homologen Strukturbereich aus 3α/20β-HSD auf Basis zweier kristallographischer Strukturen substituiert.

Der strukturell ungeordnete Bereich des Substrate Binding Loops (SBL) wurde zuerst erfolgreich auf der Basis des strukturell geordneten SBL aus Alkohol Dehydrogenase (ADH) von *Drosophila Lebadonensis* modelliert um eine einkettige Proteinstruktur als Basis für die Molecular Dynamic (MD) Simulationen zu erhalten. Für die Modellierung der Mutante wurden in einem zweiten Modellierungsschritt am Ende 36 Aminosäuren der alpha-helikalen Untereinheit (extraloop) durch eine 8 Aminosäuren lange homologe loop-Region der 3α/20β-HSD aus *S. hydrogenans* ersetzt.

Die Analyse der „root-mean-square deviation" (rmsd) (Wurzel der mittleren quadratischen Abweichung) der Cα-Atome zeigte, dass die Gesamtfaltung der Mutante 3α-HSD/CR-tr weitestgehend erhalten bleibt. Die Analyse der rmsd auf Basis der Aminosäure-Reste zeigte, dass die größten Abweichungen im Bereich des C-terminalen Endes der Aminosäurekette und im Bereich des SBL zu finden sind. Vor allem das Letztere ist zu erwarten, spiegelt dies doch die experimentell bekannte und für die biologische Funktion erforderliche Flexibilität dieser Region wider. Der eingesetzte Loop der 3α/20β-HSD zeigt geringere Abweichungen und eine weniger stark ausgeprägte Flexibilät im Vergleich zum SBL. Die Distanz zwischen den ter-

minalen Resten des eingesetzten Extraloops bleibt im Rahmen der Startwerte. Daher werden ebenfalls keine signifikanten Änderungen in Bezug auf die Orientierung der biologisch wichtigen katalytischen Aminosäuren beobachtet.

Vergleichssimulation des 3α-HSD/CR Wildtyp-Proteins, das den nachmodellierten SBL trägt, zeigte eine höhere Gesamtflexibilität als die Mutante. Diese Flexibilität führte in der Simulation u.a. zu Verzerrungen im Bereich der katalytischen Triarde, in dem die katalytischen Aminosäuren in der Simulation gelegentlich alternative Konformationen einnehmen und im Mittel größere gegenseitige Distanzen auftreten als in der Startstruktur vor der Simulation. Als Grund für die erhöhte Flexibilität kann die Simulation des 3α-HSD/CR-Wildtyp Proteins als Monomer (in Analogie zur Simulation der Mutante) sowie daraus folgernd das Fehlen der Dimer-Schnittstelle angesehen werden. Anscheinend ermöglicht der eingesetzte verkürzte Loop der 3α/20β-HSD bei einem Fehlen der stabilisierenden Dimer-Schnittstelle eine höhere Proteinstabilität als dies der viel längere Extraloop des Wildtyp Proteins tut. Basierend auf diesen Analysen erscheint das Modell schlüssig zu sein und lässt erwarten, dass das molekularbiologisch umgesetzte Modell katalytisch aktiv ist.

Die erfolgreich im computerbasierten Ansatz modellierte und simulierte Aminosäuresequenz wurde in den molekularbiologischen Ansatz transferiert und darin in ein lösliches und biologisch aktives Protein umgesetzt. „Overlap extension PCR" ermöglichte den Nachbau der DNA-Sequenz, die für das mutierte 3α-HSD/CR-tr Protein kodiert. Standardbedingungen für Protein-Überexpression ermöglichten zwar die Produktion großer Mengen rekombinanten Proteins, das allerdings unlöslich in „inclusion bodies" durch ELIZA-Techniken lokalisiert werden konnte. Ein breit angelegter Ansatz zur Renaturierung des unlöslichen Proteines durch etablierte Rückfaltungsbedingungen führte ebenfalls nicht zu löslichem Protein. Erst optimierte Bedingungen für die Proteinexpression selber resultierten in löslichem und nativem rekombinantem mutiertem 3α-HSD/CR-tr Protein. Dies konnte anschließend durch Western Blot Techniken nachgewiesen sowie durch Affinitätschromatographie aufgereinigt werden. HPLC Charakterisierung zeigten eindeutig, dass das mutierte 3α-HSD/CR-tr Protein eine, wenn auch im Vergleich zum Wildtyp-Protein reduzierte, Carbonylreduktion-Aktivität besitzt.

# VIII References

Abalain JH, Di Stefano S, Abalain-Colloc ML and Floch HH (1995)
Cloning, sequencing and expression of Pseudomonas testosteroni gene encoding 3 alpha-hydroxysteroid dehydrogenase.
*J Steroid Biochem Mol Biol* **55:**233-238.

Adams JD, LaVoie EJ and Hoffmann D (1985a)
On the pharmacokinetics of tobacco-specific N-nitrosamines in Fischer rats.
*Carcinogenesis* **6:**509-511.

Adams JD, Lavoie EJ, O'Mara-Adams KJ, Hoffmann D, Carey KD and Marshall MV (1985b)
Pharmacokinetics of N'-nitrosonornicotine and 4-(methylnitrosamino)-1-(3-pyridyl)-1-butanone in laboratory animals.
*Cancer Lett* **28:**195-201.

Adams MD Celniker SE Holt RA Evans CA Gocayne JD Amanatides PG Scherer SE Li PW Hoskins RA Galle RF George RA Lewis SE Richards S Ashburner M Henderson SN Sutton GG Wortman JR Yandell MD Zhang Q Chen LX Brandon RC Rogers YH Blazej RG Champe M Pfeiffer BD Wan KH Doyle C Baxter EG Helt G Nelson CR Gabor GL Abril JF Agbayani A An HJ Andrews-Pfannkoch C Baldwin D Ballew RM Basu A Baxendale J Bayraktaroglu L Beasley EM Beeson KY Benos PV Berman BP Bhandari D Bolshakov S Borkova D Botchan MR Bouck J Brokstein P Brottier P Burtis KC Busam DA Butler H Cadieu E Center A Chandra I Cherry JM Cawley S Dahlke C Davenport LB Davies P de Pablos B Delcher A Deng Z Mays AD Dew I Dietz SM Dodson K Doup LE Downes M Dugan-Rocha S Dunkov BC Dunn P Durbin KJ Evangelista CC Ferraz C Ferriera S Fleischmann W Fosler C Gabrielian AE Garg NS Gelbart WM Glasser K Glodek A Gong F Gorrell JH Gu Z Guan P Harris M Harris NL Harvey D Heiman TJ Hernandez JR Houck J Hostin D Houston KA Howland TJ Wei MH Ibegwam C Jalali M Kalush F Karpen GH Ke Z Kennison JA Ketchum KA Kimmel BE Kodira CD Kraft C Kravitz S Kulp D Lai Z Lasko P Lei Y Levitsky AA Li J Li Z Liang Y Lin X Liu X Mattei B McIntosh TC McLeod MP McPherson D Merkulov G Milshina NV Mobarry C Morris J Moshrefi A Mount SM Moy M Murphy B Murphy L Muzny DM Nelson DL Nelson DR Nelson KA Nixon K Nusskern DR Pacleb JM Palazzolo M Pittman GS Pan S Pollard J Puri V Reese MG Reinert K Remington K Saunders RD

Scheeler F Shen H Shue BC Siden-Kiamos I Simpson M Skupski MP Smith T Spier E Spradling AC Stapleton M Strong R Sun E Svirskas R Tector C Turner R Venter E Wang AH Wang X Wang ZY Wassarman DA Weinstock GM Weissenbach J Williams SM WoodageT Worley KC Wu D Yang S Yao QA Ye J Yeh RF Zaveri JS Zhan M Zhang G Zhao Q Zheng L Zheng XH Zhong FN Zhong W Zhou X Zhu S Zhu X Smith HO Gibbs RA Myers EW Rubin GM and Venter JC (2000)
The genome sequence of Drosophila melanogaster.
*Science* **287:**2185-2195.

Agarwal AK, Tusie-Luna MT, Monder C and White PC (1990)
Expression of 11 beta-hydroxysteroid dehydrogenase using recombinant vaccinia virus.
*Mol Endocrinol* **4:**1827-1832.

Ahmed NK, Felsted RL and Bachur NR (1978)
Heterogeneity of anthracycline antibiotic carbonyl reductases in mammalian livers.
*Biochem Pharmacol* **27:**2713-2719.

Ahmed NK, Felsted RL and Bachur NR (1979)
Comparison and characterization of mammalian xenobiotic ketone reductases.
*J Pharmacol Exp Ther* **209:**12-19.

Ahmed NK, Felsted RL and Bachur NR (1981)
Daunorubicin reduction mediated by aldehyde and ketone reductases.
*Xenobiotica* **11:**131-136.

Ahrendt SA, Chow JT, Yang SC, Wu L, Zhang MJ, Jen J and Sidransky D (2000)
Alcohol consumption and cigarette smoking increase the frequency of p53 mutations in non-small cell lung cancer.
*Cancer Res* **60:**3155-3159.

Alberts P, Engblom L, Edling N, Forsgren M, Klingstrom G, Larsson C, Ronquist-Nii Y, Ohman B and Abrahmsen L (2002)
Selective inhibition of 11beta-hydroxysteroid dehydrogenase type 1 decreases blood glucose concentrations in hyperglycaemic mice.

*Diabetologia* **45:**1528-1532.

Anfinsen CB (1973)
Principles that govern the folding of protein chains.
*Science* **181:**223-230.

Aoki H, Okada T, Mizutani T, Numata Y, Minegishi T and Miyamoto K (1997)
Identification of two closely related genes, inducible and noninducible carbonyl reductases in the rat ovary.
*Biochem Biophys Res Commun* **230:**518-523.

Apweiler R, Attwood TK, Bairoch A, Bateman A, Birney E, Biswas M, Bucher P, Cerutti L, Corpet F, Croning MD, Durbin R, Falquet L, Fleischmann W, Gouzy J, Hermjakob H, Hulo N, Jonassen I, Kahn D, Kanapin A, Karavidopoulou Y, Lopez R, Marx B, Mulder NJ, Oinn TM, Pagni M, Servant F, Sigrist CJ and Zdobnov EM (2000)
InterPro--an integrated documentation resource for protein families, domains and functional sites.
*Bioinformatics* **16:**1145-1150.

Arda B, Aydemir S, Yamazhan T, Hassan A, Tunger A and Serter D (2003)
Comamonas testosteroni meningitis in a patient with recurrent cholesteatoma.
*Apmis* **111:**474-476.

Atalla A, Breyer-Pfaff U and Maser E (2000)
Purification and characterization of oxidoreductases-catalyzing carbonyl reduction of the tobacco-specific nitrosamine 4-methylnitrosamino-1-(3-pyridyl)-1-butanone (NNK) in human liver cytosol.
*Xenobiotica* **30:**755-769.

Atalla A and Maser E (1999)
Carbonyl reduction of the tobacco-specific nitrosamine 4-(methylnitrosamino)-1-(3-pyridyl)-1-butanone (NNK) in cytosol of mouse liver and lung.
*Toxicology* **139:**155-166.

Auerbach G, Herrmann A, Gutlich M, Fischer M, Jacob U, Bacher A and Huber R (1997)

The 1.25 A crystal structure of sepiapterin reductase reveals its binding mode to pterins and brain neurotransmitters.
*Embo J* **16:**7219-7230.

Aukrust LE, Norum KR and Skalhegg BA (1976)
Affinity chromatography of 3 alpha-hydroxysteroid dehydrogenase from Pseudomonas testosteroni. Use of N,N-dimethylformamide to prevent hydrophobic interactions between the enzyme and the ligand.
*Biochim Biophys Acta* **438:**13-22.

Ausubel FM, Bren R, Kingston RE, Moore DD, Seidmann JG, Smith JA and Struhl K (1993)
*Current protocols in molecular biology.*
John Wiley & Sons, New York.

Ax W, Soldan M, Koch L and Maser E (2000)
Development of daunorubicin resistance in tumour cells by induction of carbonyl reduction.
*Biochem Pharmacol* **59:**293-300.

Bachur NR (1976)
Cytoplasmic aldo-keto reductases: a class of drug metabolizing enzymes.
*Science* **193:**595-597.

Backlund MG, Mann JR, Holla VR, Buchanan FG, Tai HH, Musiek ES, Milne GL, Katkuri S and DuBois RN (2005)
15-Hydroxyprostaglandin dehydrogenase is down-regulated in colorectal cancer.
*J Biol Chem* **280:**3217-3223.

Bairoch A and Apweiler R (2000)
The SWISS-PROT protein sequence database and its supplement TrEMBL in 2000.
*Nucleic Acids Res* **28:**45-48.

Baker D and Agard DA (1994)
Kinetics versus thermodynamics in protein folding.
*Biochemistry* **33:**7505-7509.

Bates PA, Kelley LA, MacCallum RM and Sternberg MJ (2001)
Enhancement of protein modeling by human intervention in applying the automatic programs 3D-JIGSAW and 3D-PSSM.
*Proteins* **Suppl 5:**39-46.

Belai I, Darvas B, Bauer K and Tag El-Din MH (1995)
Effects of anti-ecdysteroid azaloe analogues of metyrapone on the larval development of the fleshfly, *Neobellieria bullata*.
*Pestic. Sci.* **44:**225-232.

Benach J, Atrian S, Gonzalez-Duarte R and Ladenstein R (1998)
The refined crystal structure of Drosophila lebanonensis alcohol dehydrogenase at 1.9 A resolution.
*J Mol Biol* **282:**383-399.

Benach J, Atrian S, Gonzalez-Duarte R and Ladenstein R (1999)
The catalytic reaction and inhibition mechanism of Drosophila alcohol dehydrogenase: observation of an enzyme-bound NAD-ketone adduct at 1.4 A resolution by X-ray crystallography.
*J Mol Biol* **289:**335-355.

Beran M, Andersson B, Eksborg S and Ehrsson H (1979)
Comparative studies on the in vitro killing of human normal and leukemic clonogenic cells (CFUc) by daunorubicin, daunorubicinol, and daunorubicin-DNA complex.
*Cancer Chemother Pharmacol* **2:**19-24.

Berendsen HJC, Postma JPM, van Gunsteren WF, Di Nola A and Haak JR (1984)
Molecular dynamics with coupling to an external bath.
*J.Chem.Phys.* **81:**3684-3690.

Birnboim HC and Doly J (1979)
A rapid alkaline extraction procedure for screening recombinant plasmid DNA.
*Nucleic Acids Res* **7:**1513-1523.

Boeijinga PH, Galvan M, Baron BM, Dudley MW, Siegel BW and Slone AL (1992)

Characterization of the novel 5-HT3 antagonists MDL 73147EF (dolasetron mesilate) and MDL 74156 in NG108-15 neuroblastoma x glioma cells.
*Eur J Pharmacol* **219:**9-13.


Bohren KM, Bullock B, Wermuth B and Gabbay KH (1989)
The aldo-keto reductase superfamily. cDNAs and deduced amino acid sequences of human aldehyde and aldose reductases.
*J Biol Chem* **264:**9547-9551.


Bohren KM, von Wartburg JP and Wermuth B (1987)
Kinetics of carbonyl reductase from human brain.
*Biochem J* **244:**165-171.


Bohren KM, Wermuth B, Harrison D, Ringe D, Petsko GA and Gabbay KH (1994)
Expression, crystallization and preliminary crystallographic analysis of human carbonyl reductase.
*J Mol Biol* **244:**659-664.


Botella JA, Ulschmid JK, Gruenewald C, Moehle C, Kretzschmar D, Becker K and Schneuwly S (2004)
The Drosophila carbonyl reductase sniffer prevents oxidative stress-induced neurodegeneration.
*Curr Biol* **14:**782-786.


Bradford MM (1976)
A rapid and sensitive method for the quantitation of microgram quantities of protein utilizing the principle of protein-dye binding.
*Anal Biochem* **72:**248-254.


Breyer-Pfaff U, Martin HJ, Ernst M and Maser E (2004)
Enantioselectivity of carbonyl reduction of 4-methylnitrosamino-1-(3-pyridyl)-1-butanone by tissue fractions from human and rat and by enzymes isolated from human liver.
*Drug Metab Dispos* **32:**915-922.


Breyer-Pfaff U and Nill K (1999)

Stereoselective high-affinity reduction of ketonic nortriptyline metabolites and of ketotifen by aldo-keto reductases from human liver.
*Adv Exp Med Biol* **463:**473-480.


Breyer-Pfaff U and Nill K (2000)
High-affinity stereoselective reduction of the enantiomers of ketotifen and of ketonic nortriptyline metabolites by aldo-keto reductases from human liver.
*Biochem Pharmacol* **59:**249-260.


Breyer-Pfaff U and Nill K (2004)
Carbonyl reduction of naltrexone and dolasetron by oxidoreductases isolated from human liver cytosol.
*J Pharm Pharmacol* **56:**1601-1606.


Browne WJ, North AC, Phillips DC, Brew K, Vanaman TC and Hill RL (1969)
A possible three-dimensional structure of bovine alpha-lactalbumin based on that of hen's egg-white lysozyme.
*J Mol Biol* **42:**65-86.


Brunmark A, Cadenas E, Segura-Aguilar J, Lind C and Ernster L (1988)
DT-diaphorase-catalyzed two-electron reduction of various p-benzoquinone- and 1,4-naphthoquinone epoxides.
*Free Radic Biol Med* **5:**133-143.


Buffinton GD, Ollinger K, Brunmark A and Cadenas E (1989)
DT-diaphorase-catalysed reduction of 1,4-naphthoquinone derivatives and glutathionyl-quinone conjugates. Effect of substituents on autoxidation rates.
*Biochem J* **257:**561-571.


Cagen LM, Zusman RM and Pisano JJ (1979)
Formation of 1a, 1b dihomoprostaglandin E2 by rabbit renal intersititial cell cultures.
*Prostaglandins* **18:**617-621.


Caldwell J (1989)
The biochemical pharmacology of fenofibrate.

*Cardiology* **76 Suppl 1:**33-41; discussion 41-34.

Carmella SG, Akerkar SA, Richie JP, Jr. and Hecht SS (1995)

Intraindividual and interindividual differences in metabolites of the tobacco-specific lung carcinogen 4-(methylnitrosamino)-1-(3-pyridyl)-1-butanone (NNK) in smokers' urine.
*Cancer Epidemiol Biomarkers Prev* **4:**635-642.

Carmella SG, Borukhova A, Akerkar SA and Hecht SS (1997)

Analysis of human urine for pyridine-N-oxide metabolites of 4-(methylnitrosamino)-1-(3-pyridyl)-1-butanone, a tobacco-specific lung carcinogen.
*Cancer Epidemiol Biomarkers Prev* **6:**113-120.

Case DA, Pearlman DA, Caldwell JW, Cheatham III TE, Ross WS, Simmerling CL, Darden TA, Merz KM, Stanton RV and Cheng ALea (1999)

Amber 6. University of California, San Francisco.

Chang DG and Tai HH (1981)

Prostaglandin 9-ketoreductase/type II 15-hydroxyprostaglandin dehydrogenase is not a prostaglandin specific enzyme.
*Biochem Biophys Res Commun* **101:**898-904.

Claessens M, Van Cutsem E, Lasters I and Wodak S (1989)

Modeling the polypeptide backbone with 'spare parts' from known protein structures.
*Protein Eng* **2:**335-345.

Coenye T, Goris J, Spilker T, Vandamme P and LiPuma JJ (2002)

Characterization of unusual bacteria isolated from respiratory secretions of cystic fibrosis patients and description of Inquilinus limosus gen. nov., sp. nov.
*J Clin Microbiol* **40:**2062-2069.

Cornell WD, Cieplak P, Bayly CI, Gould IR, Merz Jr KM, Ferguson DM, Spellmayer DC, Fox T, Caldwell JW and Kollman PA (1995)

A second generation force field for the simulation of protein, nucleid acids, and organic molecules.
*J Am Chem Soc* **117:**5179 - 5197.

Cromlish JA, Yoshimoto CK and Flynn TG (1985)

Purification and characterization of four NADPH-dependent aldehyde reductases from pig brain.

*J Neurochem* **44:**1477-1484.


Crouse J and Amorese D (1987)

Ethanol precipitation: ammonium acetate as an alternative to sodium acetate.

*Focus* **9-2:**3-5.


Darden T, York D and Pedersen L (1993)

Particle mesh Ewald -An N.log(N) method for Ewald sums in large systems.

*J Chem Phys* **98:**10089 - 10092.


Darvas B, Belai I, Fonagy A, Kulcsar P and Tag El-Din MH (1991)

Lethal disturbances in larval development of *Neobellieria bullata* caused by metyrapone deri-vates.

*Pestic. Sci.* **32:**133-139.


Dawson TM and Dawson VL (2003)

Molecular pathways of neurodegeneration in Parkinson's disease.

*Science* **302:**819-822.


Dayton HE and Inturrisi CE (1976)

The urinary excretion profiles of naltrexone in man, monkey, rabbit, and rat.

*Drug Metab Dispos* **4:**474-478.


Dessypris EN, Brenner DE and Hande KR (1986)

Toxicity of doxorubicin metabolites to human marrow erythroid and myeloid progenitors in vitro.

*Cancer Treat Rep* **70:**487-490.


Dinner AR, Sali A and Karplus M (1996)

The folding mechanism of larger model proteins: role of native structure.

*Proc Natl Acad Sci U S A* **93:**8356-8361.

Doorn JA, Maser E, Blum A, Claffey DJ and Petersen DR (2004)
Human carbonyl reductase catalyzes reduction of 4-oxonon-2-enal.
*Biochemistry* **43:**13106-13114.

Duax WL, Ghosh D and Pletnev V (2000)
Steroid dehydrogenase structures, mechanism of action, and disease.
*Vitam Horm* **58:**121-148.

Duplomb L, Lee Y, Wang MY, Park BH, Takaishi K, Agarwal AK and Unger RH (2004)
Increased expression and activity of 11beta-HSD-1 in diabetic islets and prevention with tro-
glitazone.
*Biochem Biophys Res Commun* **313:**594-599.

Ellis EM (2002)
Microbial aldo-keto reductases.
*FEMS Microbiol Lett* **216:**123-131.

Ellis EM and Hayes JD (1995)
Substrate specificity of an aflatoxin-metabolizing aldehyde reductase.
*Biochem J* **312 ( Pt 2):**535-541.

Ensor CM and Tai HH (1991)
Site-directed mutagenesis of the conserved tyrosine 151 of human placental NAD(+)-
dependent 15-hydroxyprostaglandin dehydrogenase yields a catalytically inactive enzyme.
*Biochem Biophys Res Commun* **176:**840-845.

Espey LL, Yoshioka S, Russell D, Ujioka T, Vladu B, Skelsey M, Fujii S, Okamura H and
Richards JS (2000)
Characterization of ovarian carbonyl reductase gene expression during ovulation in the go-
nadotropin-primed immature Rat.
*Biol Reprod* **62:**390-397.

Esterbauer H, Cheeseman KH, Dianzani MU, Poli G and Slater TF (1982)
Separation and characterization of the aldehydic products of lipid peroxidation stimulated by
ADP-Fe2+ in rat liver microsomes.

*Biochem J* **208:**129-140.


Faber K (1998)

*Biotransformations in organic chemistry.*

in: *2nd Edition. Springer-verlag. Berlin.* (


Felsted RL and Bachur NR (1980)

Mammalian carbonyl reductases.

*Drug Metab Rev* **11:**1-60.


Felsted RL and Bachur NR (1982)

Human liver daunorubicin reductases.

*Prog Clin Biol Res* **114:**291-305.


Fischer SM, Klein-Szanto AJ, Adams LM and Slaga TJ (1985)

The first stage and complete promoting activity of retinoic acid but not the analog RO-10-9359.

*Carcinogenesis* **6:**575-578.


Floch HH, Abalain JH, Di Stefano S, Carre JL and Abalain-Colloc ML (1995)

[Cloning of genes coding for 3-alpha-hydroxysteroid dehydrogenase and for (3-17)-beta-hydroxysteroid dehydrogenase from Pseudomonas testosteroni].

*C R Seances Soc Biol Fil* **189:**705-712.


Flynn TG and Green NC (1993)

The aldo-keto reductases: an overview.

*Adv Exp Med Biol* **328:**251-257.


Ford G and Ellis EM (2001)

Three aldo-keto reductases of the yeast Saccharomyces cerevisiae.

*Chem Biol Interact* **130-132:**685-698.


Ford G and Ellis EM (2002)

Characterization of Ypr1p from Saccharomyces cerevisiae as a 2-methylbutyraldehyde reductase.

*Yeast* **19:**1087-1096.

Forrest GL, Akman S, Krutzik S, Paxton RJ, Sparkes RS, Doroshow J, Felsted RL, Glover
CJ, Mohandas T and Bachur NR (1990)
Induction of a human carbonyl reductase gene located on chromosome 21.
*Biochim Biophys Acta* **1048:**149-155.

Forrest GL and Gonzalez B (2000)
Carbonyl reductase.
*Chem Biol Interact* **129:**21-40.

Fujii J, Iuchi Y and Okada F (2005)
Fundamental roles of reactive oxygen species and protective mechanisms in the female repro-
ductive system.
*Reprod Biol Endocrinol* **3:**43.

Gersl V, Mazurova Y, Bajgar J, Melka M, Hrdina R and Palicka V (1996)
Lack of cardiotoxicity of a new antineoplastic agent, a synthetic derivative of indenoisochino-
line: comparison with daunorubicin in rabbits.
*Arch Toxicol* **70:**645-651.

Gessner T, Vaughan LA, Beehler BC, Bartels CJ and Baker RM (1990)
Elevated pentose cycle and glucuronyltransferase in daunorubicin-resistant P388 cells.
*Cancer Res* **50:**3921-3927.

Ghosh D, Erman M, Pangborn W, Duax WL and Baker ME (1992)
Inhibition of Streptomyces hydrogenans 3 alpha,20 beta-hydroxysteroid dehydrogenase by
licorice-derived compounds and crystallization of an enzyme-cofactor-inhibitor complex.
*J Steroid Biochem Mol Biol* **42:**849-853.

Ghosh D, Erman M, Pangborn W, Duax WL, Nakajin S, Ohno S and Shinoda M (1993)
Crystallization and preliminary X-ray diffraction studies of a mammalian steroid dehydro-
genase.
*J Steroid Biochem Mol Biol* **46:**103-104.

Ghosh D, Erman M, Wawrzak Z, Duax WL and Pangborn W (1994a)
Mechanism of inhibition of 3 alpha, 20 beta-hydroxysteroid dehydrogenase by a licorice-derived steroidal inhibitor.
*Structure* **2:**973-980.

Ghosh D, Pletnev VZ, Zhu DW, Wawrzak Z, Duax WL, Pangborn W, Labrie F and Lin SX (1995)
Structure of human estrogenic 17 beta-hydroxysteroid dehydrogenase at 2.20 A resolution.
*Structure* **3:**503-513.

Ghosh D, Sawicki M, Pletnev V, Erman M, Ohno S, Nakajin S and Duax WL (2001)
Porcine carbonyl reductase. structural basis for a functional monomer in short chain dehydrogenases/reductases.
*J Biol Chem* **276:**18457-18463.

Ghosh D, Wawrzak Z, Weeks CM, Duax WL and Erman M (1994b)
The refined three-dimensional structure of 3 alpha,20 beta-hydroxysteroid dehydrogenase and possible roles of the residues conserved in short-chain dehydrogenases.
*Structure* **2:**629-640.

Ghosh D, Weeks CM, Grochulski P, Duax WL, Erman M, Rimsay RL and Orr JC (1991)
Three-dimensional structure of holo 3 alpha,20 beta-hydroxysteroid dehydrogenase: a member of a short-chain dehydrogenase family.
*Proc Natl Acad Sci U S A* **88:**10064-10068.

Gonzalez B, Sapra A, Rivera H, Kaplan WD, Yam B and Forrest GL (1995)
Cloning and expression of the cDNA encoding rabbit liver carbonyl reductase.
*Gene* **154:**297-298.

Grimm C, Maser E, Mobus E, Klebe G, Reuter K and Ficner R (2000a)
The crystal structure of 3alpha -hydroxysteroid dehydrogenase/carbonyl reductase from Comamonas testosteroni shows a novel oligomerization pattern within the short chain dehydrogenase/reductase family.
*J Biol Chem* **275:**41333-41339.

Grimm C, Maser E, Möbus E, Klebe G, Reuter K and Ficner R (2000b)
The crystal structure of 3alpha -hydroxysteroid dehydrogenase/carbonyl reductase from Co-mamonas testosteroni shows a novel oligomerization pattern within the short chain dehydro-genase/reductase family.
*J Biol Chem* **275:**41333-41339.

Guan G, Tanaka M, Todo T, Young G, Yoshikuni M and Nagahama Y (1999)
Cloning and expression of two carbonyl reductase-like 20beta-hydroxysteroid dehydrogenase cDNAs in ovarian follicles of rainbow trout (Oncorhynchus mykiss).
*Biochem Biophys Res Commun* **255:**123-128.

Guda C, Lu S, Scheeff ED, Bourne PE and Shindyalov IN (2004)
CE-MC: a multiple protein structure alignment server.
*Nucleic Acids Res* **32:**W100-103.

Guda C, Pal LR and Shindyalov IN (2006)
DMAPS: a database of multiple alignments for protein structures.
*Nucleic Acids Res* **34:**D273-276.

Guda C, Scheeff ED, Bourne PE and Shindyalov IN (2001)
A new algorithm for the alignment of multiple protein structures using Monte Carlo optimiza-tion.
*Pac Symp Biocomput***:**275-286.

Gunsteren v, WF and Berendsen H (1990)
Computer simulation of molecular dynamics: methodology, applications, and perspectives in chemistry.
*Angew Chem Int. Ed. Engl* **29:**992-1023.

Gupta P, Hall CK and Voegler AC (1998)
Effect of denaturant and protein concentrations upon protein refolding and aggregation: a simple lattice model.
*Protein Sci* **7:**2642-2652.

Habrych M, Rodriguez S and Stewart JD (2002)

Purification and identification of an Escherichia coli beta-keto ester reductase as 2,5-diketo-D-gluconate reductase YqhE.
*Biotechnol Prog* **18:**257-261.

Hara A, Hasebe K, Hayashibara M, Matsuura K, Nakayama T and Sawada H (1986a)
Dihydrodiol dehydrogenases in guinea pig liver.
*Biochem Pharmacol* **35:**4005-4012.

Hara A, Nakayama T, Deyashiki Y, Kariya K and Sawada H (1986b)
Carbonyl reductase of dog liver: purification, properties, and kinetic mechanism.
*Arch Biochem Biophys* **244:**238-247.

Hara A, Oritani H, Deyashiki Y, Nakayama T and Sawada H (1992)
Activation of carbonyl reductase from pig lung by fatty acids.
*Arch Biochem Biophys* **292:**548-554.

Hara A, Usui S, Hayashibara M, Horiuchi T, Nakayama T and Sawada H (1987)
Microsomal carbonyl reductase in rat liver. Sex difference, hormonal regulation, and characterization.
*Prog Clin Biol Res* **232:**401-414.

Hara A, Yamamoto H, Deyashiki Y, Nakayama T, Oritani H and Sawada H (1991)
Aldehyde dismutation catalyzed by pulmonary carbonyl reductase: kinetic studies of chloral hydrate metabolism to trichloroacetic acid and trichloroethanol.
*Biochim Biophys Acta* **1075:**61-67.

Hartl FU, Pfanner N, Nicholson DW and Neupert W (1989)
Mitochondrial protein import.
*Biochim Biophys Acta* **988:**1-45.

Havel TF and Snow ME (1991)
A new method for building protein conformations from sequence alignments with homologues of known structure.
*J Mol Biol* **217:**1-7.

Hayashi H, Fujii Y, Watanabe K, Urade Y and Hayaishi O (1989)
Enzymatic conversion of prostaglandin H2 to prostaglandin F2 alpha by aldehyde reductase from human liver.
*Prog Clin Biol Res* **290:**365-379.

Hecht SS (1994)
Metabolic activation and detoxification of tobacco-specific nitrosamines--a model for cancer prevention strategies.
*Drug Metab Rev* **26:**373-390.

Hecht SS (1996)
Recent studies on mechanisms of bioactivation and detoxification of 4-(methylnitrosamino)-1-(3-pyridyl)-1-butanone (NNK), a tobacco-specific lung carcinogen.
*Crit Rev Toxicol* **26:**163-181.

Hecht SS (1998)
Biochemistry, biology, and carcinogenicity of tobacco-specific N-nitrosamines.
*Chem Res Toxicol* **11:**559-603.

Hecht SS, Carmella SG, Murphy SE, Akerkar S, Brunnemann KD and Hoffmann D (1993)
A tobacco-specific lung carcinogen in the urine of men exposed to cigarette smoke.
*N Engl J Med* **329:**1543-1546.

Heredia VV, Cooper WC, Kruger RG, Jin Y and Penning TM (2004)
Alanine scanning mutagenesis of the testosterone binding site of rat 3 alpha-hydroxysteroid dehydrogenase demonstrates contact residues influence the rate-determining step.
*Biochemistry* **43:**5832-5841.

Higuchi T, Imamura Y and Otagiri M (1993)
Kinetic studies on the reduction of acetohexamide catalyzed by carbonyl reductase from rabbit kidney.
*Biochim Biophys Acta* **1158:**23-28.

Hoffmann D, Lavoie EJ and Hecht SS (1985)
Nicotine: a precursor for carcinogens.

*Cancer Lett* **26:**67-75.


Hoffmann F, Sotriffer C, Evers A, Xiong G and Maser E (2006)

Understanding oligomerization in 3 -hydroxysteroid dehydro-genase /carbonyl reductase from Comamonas testosteroni: an in silico approach and evidence for an active protein.

*J. Biotechnol.* *129:*131-139.


Hoffmann F, Xiong G, Sotriffer C, Reuter K and Maser E (2003)

*Structural aspects of oligomerization in 3alpha-hydroxysteroid dehydrogenase from Comamonas testosteroni: Redesign of an "extraloop"-domain on the basis of 3alpha/20beta-HSD.*

Medimond, Bologna.


Hyndman D, Bauman DR, Heredia VV and Penning TM (2003)

The aldo-keto reductase superfamily homepage.

*Chem Biol Interact* **143-144:**621-631.


Iino T, Tabata M, Takikawa S, Sawada H, Shintaku H, Ishikura S and Hara A (2003)

Tetrahydrobiopterin is synthesized from 6-pyruvoyl-tetrahydropterin by the human aldo-keto reductase AKR1 family members.

*Arch Biochem Biophys* **416:**180-187.


Iino T, Takikawa SI, Yamamoto T and Sawada H (2000)

The enzyme that synthesizes tetrahydrobiopterin from 6-pyruvoyl-tetrahydropterin in the lemon mutant silkworm consists of two carbonyl reductases.

*Arch Biochem Biophys* **373:**442-446.


Ikeda M, Hattori H and Ohmori S (1984)

Properties of NADPH-dependent carbonyl reductases in rat liver cytosol.

*Biochem Pharmacol* **33:**3957-3961.


Imamura Y, Higuchi T, Nozaki Y, Sugino E, Hibino S and Otagiri M (1993)

Purification and properties of carbonyl reductase from rabbit kidney.

*Arch Biochem Biophys* **300:**570-576.


Imamura Y, Migita T, Anraku M and Otagiri M (1999a)

Inhibition of rabbit heart carbonyl reductase by fatty acids.
*Biol Pharm Bull* **22:**731-733.


Imamura Y, Migita T, Otagiri M, Choshi T and Hibino S (1999b)
Purification and catalytic properties of a tetrameric carbonyl reductase from rabbit heart.
*J Biochem (Tokyo)* **125:**41-47.


Inazu N and Fujii T (1997)
Pre- and post-ovulatory changes in carbonyl reductase in ovarian follicles and corpora lutea in rats.
*Res Commun Mol Pathol Pharmacol* **98:**325-334.


Inazu N, Inaba N, Satoh T and Fujii T (1992a)
Human chorionic gonadotropin causes an estrogen-mediated induction of rat ovarian carbonyl reductase.
*Life Sci* **51:**817-822.


Inazu N, Ruepp B, Wirth H and Wermuth B (1992b)
Carbonyl reductase from human testis: purification and comparison with carbonyl reductase from human brain and rat testis.
*Biochim Biophys Acta* **1116:**50-56.


Inazu N and Satoh T (1994)
Activation by human chorionic gonadotropin of ovarian carbonyl reductase in mature rats exposed in vivo to estrogens.
*Biochem Pharmacol* **47:**1489-1496.


Iwata N, Inazu N and Satoh T (1989)
The purification and properties of NADPH-dependent carbonyl reductases from rat ovary.
*J Biochem (Tokyo)* **105:**556-564.


Iwata N, Inazu N and Satoh T (1990a)
Immunological and enzymological localization of carbonyl reductase in ovary and liver of various species.
*J Biochem (Tokyo)* **107:**209-212.

Iwata N, Inazu N, Takeo S and Satoh T (1990b)
Carbonyl reductases from rat testis and vas deferens. Purification, properties and localization.
*Eur J Biochem* **193:**75-81.

Jarabak J, Luncsford A and Berkowitz D (1983)
Substrate specificity of three prostaglandin dehydrogenases.
*Prostaglandins* **26:**849-868.

Jez JM, Bennett MJ, Schlegel BP, Lewis M and Penning TM (1997a)
Comparative anatomy of the aldo-keto reductase superfamily.
*Biochem J* **326 ( Pt 3):**625-636.

Jez JM, Flynn TG and Penning TM (1997b)
A new nomenclature for the aldo-keto reductase superfamily.
*Biochem Pharmacol* **54:**639-647.

Jones TA and Thirup S (1986)
Using known substructures in protein model building and crystallography.
*Embo J* **5:**819-822.

Jorgensen WL, Chandrasekhar J, Madura JP, Impey RW and Klein ML (1983)
Comparison of simple poteintial functions for simulating liquid water.
*J.Chem.Phys.* **79:**926-935.

Jornvall H, Hoog JO and Persson B (1999)
SDR and MDR: completed genome sequences show these protein families to be large, of old origin, and of complex nature.
*FEBS Lett* **445:**261-264.

Jornvall H, Persson B, Krook M, Atrian S, Gonzalez-Duarte R, Jeffery J and Ghosh D (1995)
Short-chain dehydrogenases/reductases (SDR).
*Biochemistry* **34:**6003-6013.

Jörnvall H, Persson B, Krook M, Atrian S, Gonzalez-Duarte R, Jeffery J and Ghosh D (1995)
Short-chain dehydrogenases/reductases (SDR).

*Biochemistry* **34:**6003-6013.

Jornvall H, Persson M and Jeffery J (1981)
Alcohol and polyol dehydrogenases are both divided into two protein types, and structural properties cross-relate the different enzyme activities within each type.
*Proc Natl Acad Sci U S A* **78:**4226-4230.

Kallberg Y, Oppermann U, Jornvall H and Persson B (2002a)
Short-chain dehydrogenase/reductase (SDR) relationships: a large family with eight clusters common to human, animal, and plant genomes.
*Protein Sci* **11:**636-641.

Kallberg Y, Oppermann U, Jörnvall H and Persson B (2002b)
Short-chain dehydrogenase/reductase (SDR) relationships: a large family with eight clusters common to human, animal, and plant genomes.
*Protein Sci* **11:**636-641.

Kallberg Y and Persson B (1999)
KIND-a non-redundant protein database.
*Bioinformatics* **15:**260-261.

Karplus K, Barrett C and Hughey R (1998)
Hidden Markov models for detecting remote protein homologies.
*Bioinformatics* **14:**846-856.

Karplus K, Karchin R, Shackelford G and Hughey R (2005)
Calibrating E-values for hidden Markov models using reverse-sequence null models.
*Bioinformatics* **21:**4107-4115.

Karplus M and Petsko GA (1990)
Molecular dynamics simulations in biology.
*Nature* **347:**631-639.

Kita K, Fukura T, Nakase KI, Okamoto K, Yanase H, Kataoka M and Shimizu S (1999)

Cloning, overexpression, and mutagenesis of the Sporobolomyces salmonicolor AKU4429 gene encoding a new aldehyde reductase, which catalyzes the stereoselective reduction of ethyl 4-chloro-3-oxobutanoate to ethyl (S)-4-chloro-3-hydroxybutanoate.
*Appl Environ Microbiol* **65:**5207-5211.

Klapper MH (1971)
On the nature of the protein interior.
*Biochim Biophys Acta* **229:**557-566.

Koehl P and Levitt M (1999)
A brighter future for protein structure prediction.
*Nat Struct Biol* **6:**108-111.

Kotelevtsev Y, Holmes MC, Burchell A, Houston PM, Schmoll D, Jamieson P, Best R, Brown R, Edwards CR, Seckl JR and Mullins JJ (1997)
11beta-hydroxysteroid dehydrogenase type 1 knockout mice show attenuated glucocorticoid-inducible responses and resist hyperglycemia on obesity or stress.
*Proc Natl Acad Sci U S A* **94:**14924-14929.

Krook M, Ghosh D, Duax W and Jornvall H (1993a)
Three-dimensional model of NAD(+)-dependent 15-hydroxyprostaglandin dehydrogenase and relationships to the NADP(+)-dependent enzyme (carbonyl reductase).
*FEBS Lett* **322:**139-142.

Krook M, Ghosh D, Duax W and Jörnvall H (1993b)
Three-dimensional model of NAD(+)-dependent 15-hydroxyprostaglandin dehydrogenase and relationships to the NADP(+)-dependent enzyme (carbonyl reductase).
*FEBS Lett* **322:**139-142.

Krook M, Ghosh D, Stromberg R, Carlquist M and Jornvall H (1993c)
Carboxyethyllysine in a protein: native carbonyl reductase/NADP(+)-dependent prostaglandin dehydrogenase.
*Proc Natl Acad Sci U S A* **90:**502-506.

Krozowski Z (1992)

11 beta-hydroxysteroid dehydrogenase and the short-chain alcohol dehydrogenase (SCAD) superfamily.
*Mol Cell Endocrinol* **84:**C25-31.

Kurucz I, Titus JA, Jost CR and Segal DM (1995)
Correct disulfide pairing and efficient refolding of detergent-solubilized single-chain Fv proteins from bacterial inclusion bodies.
*Mol Immunol* **32:**1443-1452.

Kyhse-Andersen J (1984)
Electroblotting of multiple gels: a simple apparatus without buffer tank for rapid transfer of proteins from polyacrylamide to nitrocellulose.
*J Biochem Biophys Methods* **10:**203-209.

Labrie F, Luu-The V, Lin SX, Labrie C, Simard J, Breton R and Belanger A (1997)
The key role of 17 beta-hydroxysteroid dehydrogenases in sex steroid biology.
*Steroids* **62:**148-158.

Laemmli UK (1970)
Cleavage of structural proteins during the assembly of the head of bacteriophage T4.
*Nature* **227:**680-685.

Lakhman SS, Ghosh D and Blanco JG (2005)
Functional significance of a natural allelic variant of human carbonyl reductase 3 (CBR3).
*Drug Metab Dispos* **33:**254-257.

Lee SC and Levine L (1974a)
Prostaglandin metabolism. I. Cytoplasmic reduced nicotinamide adenine dinucleotide phosphate-dependent and microsomal reduced nicotinamide adenine dinucleotide-dependent prostaglandin E 9-ketoreductase activities in monkey and pigeon tissues.
*J Biol Chem* **249:**1369-1375.

Lee SC and Levine L (1974b)
Purification and properties of chicken heart prostaglandin delta13-reductase.
*Biochem Biophys Res Commun* **61:**14-21.

Levinthal C (1968)

Are there pathways for ptotein folding?

*C J Chim Phys* **65:**44-45.


Levitt M (1992)

Accurate modeling of protein conformation by automatic segment matching.

*J Mol Biol* **226:**507-533.


Li KX, Obeyesekere VR, Krozowski ZS and Ferrari P (1997)

Oxoreductase and dehydrogenase activities of the human and rat 11beta-hydroxysteroid de-hydrogenase type 2 enzyme.

*Endocrinology* **138:**2948-2952.


Lin D, Lee HG, Liu Q, Perry G, Smith MA and Sayre LM (2005)

4-Oxo-2-nonenal is both more neurotoxic and more protein reactive than 4-hydroxy-2-nonenal.

*Chem Res Toxicol* **18:**1219-1231.


Lind C, Cadenas E, Hochstein P and Ernster L (1990)

DT-diaphorase: purification, properties, and function.

*Methods Enzymol* **186:**287-301.


Lind C, Hochstein P and Ernster L (1982)

DT-diaphorase as a quinone reductase: a cellular control device against semiquinone and su-peroxide radical formation.

*Arch Biochem Biophys* **216:**178-185.


Luque I and Freire E (2000)

Structural stability of binding sites: consequences for binding affinity and allosteric effects.

*Proteins* **Suppl 4:**63-71.


Marcus PI and Talalay P (1956)

Induction and purification of alpha- and beta-hydroxysteroid dehydrogenases.

*J Biol Chem* **218:**661-674.

Marti-Renom MA, Stuart AC, Fiser A, Sanchez R, Melo F and Sali A (2000)
Comparative protein structure modeling of genes and genomes.
*Annu Rev Biophys Biomol Struct* **29:**291-325.

Martin HJ, Breyer-Pfaff U, Wsol V, Venz S, Block S and Maser E (2006)
Purification and characterization of akr1b10 from human liver: role in carbonyl reduction of xenobiotics.
*Drug Metab Dispos* **34:**464-470.

Maser E (1993)
The purification and properties of a novel carbonyl reducing enzyme from mouse liver microsomes.
*Adv Exp Med Biol* **328:**339-350.

Maser E (1995)
Xenobiotic carbonyl reduction and physiological steroid oxidoreduction. The pluripotency of several hydroxysteroid dehydrogenases.
*Biochem Pharmacol* **49:**421-440.

Maser E (1997)
Stress, hormonal changes, alcohol, food constituents and drugs: factors that advance the incidence of tobacco smoke-related cancer?
*Trends Pharmacol Sci* **18:**270-275.

Maser E (1998)
11Beta-hydroxysteroid dehydrogenase responsible for carbonyl reduction of the tobacco-specific nitrosamine 4-(methylnitrosamino)-1-(3-pyridyl)- 1-butanone in mouse lung microsomes.
*Cancer Res* **58:**2996-3003.

Maser E (2004)
Significance of reductases in the detoxification of the tobacco-specific carcinogen NNK.
*Trends Pharmacol Sci* **25:**235-237.

Maser E and Bannenberg G (1994a)

11 beta-hydroxysteroid dehydrogenase mediates reductive metabolism of xenobiotic carbonyl compounds.
*Biochem Pharmacol* **47:**1805-1812.

Maser E and Bannenberg G (1994b)
The purification of 11 beta-hydroxysteroid dehydrogenase from mouse liver microsomes.
*J Steroid Biochem Mol Biol* **48:**257-263.

Maser E, Friebertshauser J and Mangoura SA (1994)
Ontogenic pattern of carbonyl reductase activity of 11 beta-hydroxysteroid dehydrogenase in mouse liver and kidney.
*Xenobiotica* **24:**109-117.

Maser E, Friebertshauser J and Volker B (2003)
Purification, characterization and NNK carbonyl reductase activities of 11beta-hydroxysteroid dehydrogenase type 1 from human liver: enzyme cooperativity and significance in the detoxi-fication of a tobacco-derived carcinogen.
*Chem Biol Interact* **143-144:**435-448.

Maser E, Hoffmann JG, Friebertshauser J and Netter KJ (1992)
High carbonyl reductase activity in adrenal gland and ovary emphasizes its role in carbonyl compound detoxication.
*Toxicology* **74:**45-56.

Maser E, Möbus E and Xiong G (2000)
Functional expression, purification, and characterization of 3alpha- hydroxysteroid dehydro-genase/carbonyl reductase from Comamonas testosteroni.
*Biochem Biophys Res Commun* **272:**622-628.

Maser E and Oppermann UC (1995)
Molecular cloning and sequencing of mouse hepatic 11 beta-hydroxysteroid dehydro-genase/carbonyl reductase. A member of the short chain dehydrogenase superfamily.
*Adv Exp Med Biol* **372:**211-221.

Maser E and Oppermann UC (1997)

Role of type-1 11beta-hydroxysteroid dehydrogenase in detoxification processes.
*Eur J Biochem* **249:**365-369.

Maser E, Richter E and Friebertshauser J (1996)
The identification of 11 beta-hydroxysteroid dehydrogenase as carbonyl reductase of the to-
bacco-specific nitrosamine 4-(methylnitrosamino)-1-(3-pyridyl)-1-butanone.
*Eur J Biochem* **238:**484-489.

Maser E, Volker B and Friebertshauser J (2002)
11 Beta-hydroxysteroid dehydrogenase type 1 from human liver: dimerization and enzyme
cooperativity support its postulated role as glucocorticoid reductase.
*Biochemistry* **41:**2459-2465.

Maser E, Wsol V and Martin HJ (2006)
11Beta-hydroxysteroid dehydrogenase type 1: purification from human liver and characteriza-
tion as carbonyl reductase of xenobiotics.
*Mol Cell Endocrinol* **248:**34-37.

Masuzaki H, Paterson J, Shinyama H, Morton NM, Mullins JJ, Seckl JR and Flier JS (2001)
A transgenic model of visceral obesity and the metabolic syndrome.
*Science* **294:**2166-2170.

Matsuda T, Harada T, Nakajima N, Itoh T and Nakamura K (2000)
Two classes of enzymes of opposite stereochemistry in an organism: one for fluorinated and
another for nonfluorinated substrates.
*J Org Chem* **65:**157-163.

Matsunaga T, Shintani S and Hara A (2006)
Multiplicity of mammalian reductases for xenobiotic carbonyl compounds.
*Drug Metab Pharmacokinet* **21:**1-18.

Matsuura K, Bunai Y, Ohya I, Hara A, Nakanishi M and Sawada H (1994)
Ultrastructural localization of carbonyl reductase in mouse lung.
*Histochem J* **26:**311-316.

Matsuura K, Hara A, Sawada H, Bunai Y and Ohya I (1990)
Localization of pulmonary carbonyl reductase in guinea pig and mouse: enzyme histochemical and immunohistochemical studies.
*J Histochem Cytochem* **38:**217-223.

Matsuura K, Naganeo F, Hara A, Nakayama T, Nakagawa M and Sawada H (1989)
Pulmonary carbonyl reductase: metabolism of carbonyl products in lipid peroxidation.
*Prog Clin Biol Res* **290:**335-349.

Matsuura K, Nakayama T, Nakagawa M, Hara A and Sawada H (1988)
Kinetic mechanism of pulmonary carbonyl reductase.
*Biochem J* **252:**17-22.

McGrath T and Center MS (1987)
Adriamycin resistance in HL60 cells in the absence of detectable P-glycoprotein.
*Biochem Biophys Res Commun* **145:**1171-1176.

Meger M, Meger-Kossien I, Dietrich M, Tricker AR, Scherer G and Adlkofer F (1996)
Metabolites of 4-(N-methylnitrosamino)-1-(3-pyridyl)-1-butanone in urine of smokers.
*Eur J Cancer Prev* **5 Suppl 1:**121-124.

Melka M (1993)
Oracin-preclinical summary report of the research Institute for Pharmacy and Biochemistry.**:**Prague, Czech Republic.

Michel-Briand Y (1969)
[Relationship between the structure of a steroid and the inducing effect on 3 alpha-hydroxysteroid: NAD oxidoreductase of Pseudomonas testosteroni].
*Eur J Biochem* **10:**132-139.

Michel-Briand Y and Roux J (1969)
[Role of the composition of the culture medium in the delay of appearance of the 3 alpha-hydroxysteroid enzyme: NAD-oxidoreductase (EC I.I.I.50) of Pseudomonas testoteroni. (Catabolic repression phenomenon)].
*Ann Inst Pasteur (Paris)* **116:**448-473.

Miko M, Krepelka J and Melka M (1991)

Effects of benfluron and its two metabolites on respiratory processes in P388 murine leukemia and Ehrlich ascites cells.

*Biochem Pharmacol* **42 Suppl:**S214-216.


Miko M, Poturnajova M and Soucek R (2002)

Cytotoxicity and mode of action of the potential cytostatic drug oracin.

*Neoplasma* **49:**167-171.


Möbus E, Jahn M, Schmid R, Jahn D and Maser E (1997)

Testosterone-regulated expression of enzymes involved in steroid and aromatic hydrocarbon catabolism in Comamonas testosteroni.

*J Bacteriol* **179:**5951-5955.


Mobus E and Maser E (1998)

Molecular cloning, overexpression, and characterization of steroid-inducible 3alpha-hydroxysteroid dehydrogenase/carbonyl reductase from Comamonas testosteroni. A novel member of the short-chain dehydrogenase/reductase superfamily.

*J Biol Chem* **273:**30888-30896.


Möbus E and Maser E (1998)

Molecular cloning, overexpression, and characterization of steroid- inducible 3alpha-hydroxysteroid dehydrogenase/carbonyl reductase from Comamonas testosteroni. A novel member of the short-chain dehydrogenase/reductase superfamily.

*J Biol Chem* **273:**30888-30896.


Monder C and Shackleton CH (1984)

11 beta-Hydroxysteroid dehydrogenase: fact or fancy?

*Steroids* **44:**383-417.


Monder C, Stewart PM, Lakshmi V, Valentino R, Burt D and Edwards CR (1989)

Licorice inhibits corticosteroid 11 beta-dehydrogenase of rat kidney and liver: in vivo and in vitro studies.

*Endocrinology* **125:**1046-1053.

Monder C and White PC (1993)

11 beta-hydroxysteroid dehydrogenase.

*Vitam Horm* **47:**187-271.


Monks TJ, Hanzlik RP, Cohen GM, Ross D and Graham DG (1992)

Quinone chemistry and toxicity.

*Toxicol Appl Pharmacol* **112:**2-16.


Moore CC, Mellon SH, Murai J, Siiteri PK and Miller WL (1993)

Structure and function of the hepatic form of 11 beta-hydroxysteroid dehydrogenase in the squirrel monkey, an animal model of glucocorticoid resistance.

*Endocrinology* **133:**368-375.


Mukhopadhyay A (1997)

Inclusion bodies and purification of proteins in biologically active forms.

*Adv Biochem Eng Biotechnol* **56:**61-109.


Nadkarni DV and Sayre LM (1995)

Structural definition of early lysine and histidine adduction chemistry of 4-hydroxynonenal.

*Chem Res Toxicol* **8:**284-291.


Nakajin S, Tamura F, Takase N and Toyoshima S (1997)

Carbonyl reductase activity exhibited by pig testicular 20 beta-hydroxysteroid dehydrogenase.

*Biol Pharm Bull* **20:**1215-1218.


Nakanishi M, Deyashiki Y, Nakayama T, Sato K and Hara A (1993)

Cloning and sequence analysis of a cDNA encoding tetrameric carbonyl reductase of pig lung.

*Biochem Biophys Res Commun* **194:**1311-1316.


Nakanishi M, Deyashiki Y, Ohshima K and Hara A (1995)

Cloning, expression and tissue distribution of mouse tetrameric carbonyl reductase. Identity with an adipocyte 27-kDa protein.

*Eur J Biochem* **228:**381-387.

Nakayama T, Hara A and Sawada H (1982)

Purification and characterization of a novel pyrazole-sensitive carbonyl reductase in guinea pig lung.

*Arch Biochem Biophys* **217:**564-573.


Nakayama T, Hara A, Yashiro K and Sawada H (1985)

Reductases for carbonyl compounds in human liver.

*Biochem Pharmacol* **34:**107-117.


Nakayama T, Yashiro K, Inoue Y, Matsuura K, Ichikawa H, Hara A and Sawada H (1986)

Characterization of pulmonary carbonyl reductase of mouse and guinea pig.

*Biochim Biophys Acta* **882:**220-227.


Neupert W, Hartl FU, Craig EA and Pfanner N (1990)

How do polypeptides cross the mitochondrial membranes?

*Cell* **63:**447-450.


Norrander J, Kempe T and Messing J (1983)

Construction of improved M13 vectors using oligodeoxynucleotide-directed mutagenesis.

*Gene* **26:**101-106.


O'Brien PJ (1991)

Molecular mechanisms of quinone cytotoxicity.

*Chem Biol Interact* **80:**1-41.


Ogata K, Arakawa M, Kasahara T, Shioiri-Nakano K and Hiraoka K (1983)

Detection of toxoplasma membrane antigens transferred from SDS-polyacrylamide gel to nitrocellulose with monoclonal antibody and avidin-biotin, peroxidase anti-peroxidase and immunoperoxidase methods.

*J Immunol Methods* **65:**75-82.


Oh JW, Lee HB, Kim CR, Yum MK, Koh YJ, Moon SJ, Kang JO and Park IK (1999)

Analysis of induced sputum to examine the effects of inhaled corticosteroid on airway inflammation in children with asthma.

*Ann Allergy Asthma Immunol* **82:**491-496.

Ohara H, Miyabe Y, Deyashiki Y, Matsuura K and Hara A (1995)
Reduction of drug ketones by dihydrodiol dehydrogenases, carbonyl reductase and aldehyde reductase of human liver.
*Biochem Pharmacol* **50:**221-227.


Ohno S, Nakajin S and Shinoda M (1991)
20 beta-hydroxysteroid dehydrogenase of neonatal pig testis: 3 alpha/beta-hydroxysteroid dehydrogenase activities catalyzed by highly purified enzyme.
*J Steroid Biochem Mol Biol* **38:**787-794.


Olson LE, Bedja D, Alvey SJ, Cardounel AJ, Gabrielson KL and Reeves RH (2003)
Protection from doxorubicin-induced cardiac toxicity in mice with a null allele of carbonyl reductase 1.
*Cancer Res* **63:**6602-6606.


Oppermann CT, Netter KJ and Maser E (1993)
Carbonyl reduction by 3 alpha-HSD from Comamonas testosteroni--new properties and its relationship to the SCAD family.
*Adv Exp Med Biol* **328:**379-390.


Oppermann UC, Belai I and Maser E (1996)
Antibiotic resistance and enhanced insecticide catabolism as consequences of steroid induction in the gram-negative bacterium Comamonas testosteroni.
*J Steroid Biochem Mol Biol* **58:**217-223.


Oppermann UC and Maser E (1996)
Characterization of a 3 alpha-hydroxysteroid dehydrogenase/carbonyl reductase from the gram-negative bacterium Comamonas testosteroni.
*Eur J Biochem* **241:**744-749.


Oppermann UC and Maser E (2000)
Molecular and structural aspects of xenobiotic carbonyl metabolizing enzymes. Role of reductases and dehydrogenases in xenobiotic phase I reactions.
*Toxicology* **144:**71-81.

Oppermann UC, Maser E, Mangoura SA and Netter KJ (1991)
Heterogeneity of carbonyl reduction in subcellular fractions and different organs in rodents.
*Biochem Pharmacol* **42 Suppl:**S189-195.

Oppermann UC, Nagel G, Belai I, Bueld JE, Genti-Raimondi S, Koolman J, Netter KJ and Maser E (1998)
Carbonyl reduction of an anti-insect agent imidazole analogue of metyrapone in soil bacteria, invertebrate and vertebrate species.
*Chem Biol Interact* **114:**211-224.

Oppermann UC, Netter KJ and Maser E (1995)
Cloning and primary structure of murine 11 beta-hydroxysteroid dehydrogenase/microsomal carbonyl reductase.
*Eur J Biochem* **227:**202-208.

Oritani H, Deyashiki Y, Nakayama T, Hara A, Sawada H, Matsuura K, Bunai Y and Ohya I (1992)
Purification and characterization of pig lung carbonyl reductase.
*Arch Biochem Biophys* **292:**539-547.

Ota T Suzuki Y Nishikawa T Otsuki T Sugiyama T Irie R Wakamatsu A Hayashi K Sato H Nagai K Kimura K Makita H Sekine M Obayashi M Nishi T Shibahara T Tanaka T Ishii S Yamamoto J Saito K Kawai Y Isono Y Nakamura Y Nagahari K Murakami K Yasuda T Iwayanagi T Wagatsuma M Shiratori A Sudo H Hosoiri T Kaku Y Kodaira H Kondo H Su-gawara M Takahashi M Kanda K Yokoi T Furuya T Kikkawa E Omura Y Abe K Kamihara K Katsuta N Sato K Tanikawa M Yamazaki M Ninomiya K Ishibashi T Yamashita H Murakawa K Fujimori K Tanai H Kimata M Watanabe M Hiraoka S Chiba Y Ishida S Ono Y Takiguchi S Watanabe S Yosida M Hotuta T Kusano J Kanehori K Takahashi-Fujii A Hara H Tanase TO Nomura Y Togiya S Komai F Hara R Takeuchi K Arita M Imose N Musashino K Yuuki H Oshima A Sasaki N Aotsuka S Yoshikawa Y Matsunawa H Ichihara T Shiohata N Sano S Moriya S Momiyama H Satoh N Takami S Terashima Y Suzuki O Nakagawa S Senoh A Mizoguchi H Goto Y Shimizu F Wakebe H Hishigaki H Watanabe T Sugiyama A Takemoto M Kawakami B Watanabe K Kumagai A Itakura S Fukuzumi Y Fujimori Y Komiyama M Tashiro H Tanigami A Fujiwara T Ono T Yamada K Fujii Y Ozaki K Hirao M Ohmori Y

Kawabata A Hikiji T Kobatake N Inagaki H Ikema Y Okamoto S Okitani R Kawakami T Noguchi S Itoh T Shigeta K Senba T Matsumura K Nakajima Y Mizuno T Morinaga M Sasaki M Togashi T Oyama M Hata H Komatsu T Mizushima-Sugano J Satoh T Shirai Y Takahashi Y Nakagawa K Okumura K Nagase T Nomura N Kikuchi H Masuho Y Yamashita R Nakai K Yada T Ohara O Isogai T and Sugano S (2004)
Complete sequencing and characterization of 21,243 full-length human cDNAs.
*Nat Genet* **36:**40-45.


Ozols RF, Willson JK, Weltz MD, Grotzinger KR, Myers CE and Young RC (1980)
Inhibition of human ovarian cancer colony formation by adriamycin and its major metabolites.
*Cancer Res* **40:**4109-4112.


Pal L and Basu G (1999)
Novel protein structural motifs containing two-turn and longer 3(10)-helices.
*Protein Eng* **12:**811-814.


Paolini M, Barillari J, Broccoli M, Pozzetti L, Perocco P and Cantelli-Forti G (1999)
Effect of liquorice and glycyrrhizin on rat liver carcinogen metabolizing enzymes.
*Cancer Lett* **145:**35-42.


Park YS, Heizmann CW, Wermuth B, Levine RA, Steinerstauch P, Guzman J and Blau N (1991)
Human carbonyl and aldose reductases: new catalytic functions in tetrahydrobiopterin biosynthesis.
*Biochem Biophys Res Commun* **175:**738-744.


Penning TM (1997)
Molecular endocrinology of hydroxysteroid dehydrogenases.
*Endocr Rev* **18:**281-305.


Penning TM (2005)
AKR1B10: A New diagnostic marker of Non-Small Cell Lung Carcinoma in Smokers.
*Clinical Cancer Research* **11:**1687-1690.

Penning TM, Bennett MJ, Smith-Hoog S, Schlegel BP, Jez JM and Lewis M (1997)
Structure and function of 3 alpha-hydroxysteroid dehydrogenase.
*Steroids* **62:**101-111.

Penning TM, Mukharji I, Barrows S and Talalay P (1984)
Purification and properties of a 3 alpha-hydroxysteroid dehydrogenase of rat liver cytosol and its inhibition by anti-inflammatory drugs.
*Biochem J* **222:**601-611.

Penning TM, Pawlowski JE, Schlegel BP, Jez JM, Lin HK, Hoog SS, Bennett MJ and Lewis M (1996)
Mammalian 3 alpha-hydroxysteroid dehydrogenases.
*Steroids* **61:**508-523.

Persson B, Kallberg Y, Oppermann U and Jörnvall H (2003)
Coenzyme-based functional assignments of short-chain dehydrogenases/reductases (SDRs).
*Chem Biol Interact* **143-144:**271-278.

Persson B, Krook M and Jornvall H (1991)
Characteristics of short-chain alcohol dehydrogenases and related enzymes.
*Eur J Biochem* **200:**537-543.

Peters J, Minuth T and Kula MR (1993)
A novel NADH-dependent carbonyl reductase with an extremely broad substrate range from Candida parapsilosis: purification and characterization.
*Enzyme Microb Technol* **15:**950-958.

Pfanner N, Hartl FU and Neupert W (1988)
Import of proteins into mitochondria: a multi-step process.
*Eur J Biochem* **175:**205-212.

Pfanner N, Ostermann J, Rassow J, Hartl FU and Neupert W (1990a)
Stress proteins and mitochondrial protein import.
*Antonie Van Leeuwenhoek* **58:**191-193.

Pfanner N, Rassow J, Guiard B, Sollner T, Hartl FU and Neupert W (1990b)
Energy requirements for unfolding and membrane translocation of precursor proteins during import into mitochondria.
*J Biol Chem* **265:**16324-16329.

Pietruszko R and Chen FF (1976)
Aldehyde reductase from rat liver is a 3 alpha-hydroxysteroid dehydrogenase.
*Biochem Pharmacol* **25:**2721-2725.

Propper D and Maser E (1997)
Carbonyl reduction of daunorubicin in rabbit liver and heart.
*Pharmacol Toxicol* **80:**240-245.

Przybycien TM, Dunn JP, Valax P and Georgiou G (1994)
Secondary structure characterization of beta-lactamase inclusion bodies.
*Protein Eng* **7:**131-136.

Puranen T, Poutanen M, Ghosh D, Vihko P and Vihko R (1997)
Characterization of structural and functional properties of human 17 beta-hydroxysteroid dehydrogenase type 1 using recombinant enzymes and site-directed mutagenesis.
*Mol Endocrinol* **11:**77-86.

Quinkler M, Kosmale B, Bahr V, Oelkers W and Diederich S (1997)
Evidence for isoforms of 11 beta-hydroxysteroid dehydrogenase in the liver and kidney of the guinea pig.
*J Endocrinol* **153:**291-298.

Ramachandran C, Yuan ZK, Huang XL and Krishan A (1993)
Doxorubicin resistance in human melanoma cells: MDR-1 and glutathione S-transferase pi gene expression.
*Biochem Pharmacol* **45:**743-751.

Ratnam K, Ma H and Penning TM (1999)
The arginine 276 anchor for NADP(H) dictates fluorescence kinetic transients in 3 alpha-hydroxysteroid dehydrogenase, a representative aldo-keto reductase.

*Biochemistry* **38:**7856-7864.


Reidenberg MM (2000)

Environmental inhibition of 11beta-hydroxysteroid dehydrogenase.

*Toxicology* **144:**107-111.


Rekka EA, Soldan M, Belai I, Netter KJ and Maser E (1996)

Biotransformation and detoxification of insecticidal metyrapone analogues by carbonyl reduction in the human liver.

*Xenobiotica* **26:**1221-1229.


Revie D, Smith DW and Yee TW (1988)

Kinetic analysis for optimization of DNA ligation reactions.

*Nucleic Acids Res* **16:**10301-10321.


Ris MM and von Wartburg JP (1973)

Heterogenity of NADPH-dependent aldehyde reductase from human and rat brain.

*Eur J Biochem* **37(1):**69-77.


Roberts S (1997)

*Preparative Biotrransformations.*

Wiley & Sons, Chichester - New York.


Rosemond MJ and Walsh JS (2004)

Human carbonyl reduction pathways and a strategy for their study in vitro.

*Drug Metab Rev* **36:**335-361.


Ross D, Siegel D, Beall H, Prakash AS, Mulcahy RT and Gibson NW (1993)

DT-diaphorase in activation and detoxification of quinones. Bioreductive activation of mitomycin C.

*Cancer Metastasis Rev* **12:**83-101.


Rossmann MG, Liljas A, Bränden CI and Banaszal LJ (1975)

in: *in "The Enzymes".* (

Rudolph R and Lilie H (1996)

In vitro folding of inclusion body proteins.

*Faseb J* **10:**49-56.


Ryckaert JP, Ciccotti G and Berendsen HJC (1977)

NUmerical integration of the Cartesian equations of motion of a system with constrains: molecular dynamics of n-alkanes.

*J.Comp.Phys.* **23:**327-341.


Sali A (1995a)

Comparative protein modeling by satisfaction of spatial restraints.

*Mol Med Today* **1:**270-277.


Sali A (1995b)

Modeling mutations and homologous proteins.

*Curr Opin Biotechnol* **6:**437-451.


Sali A and Blundell TL (1993)

Comparative protein modeling by satisfaction of spatial restraints.

*J Mol Biol* **234:**779-815.


Sambrook J, Fritsch EF and Maniatis T (1989)

*Molecular Cloning. A laboratory manual.*

Cold Spring Harbor Laboratory Press, Cold Spring Harbor.


Sanchez R and Sali A (1998)

Large-scale protein structure modeling of the Saccharomyces cerevisiae genome.

*Proc Natl Acad Sci U S A* **95:**13597-13602.


Sawada H and Hara A (1979)

The presence of two NADPH-linked aromatic aldehyde-ketone reductases different from aldehyde reductase in rabbit liver.

*Biochem Pharmacol* **28:**1089-1094.


Sawada H, Hara A, Kato F and Nakayama T (1979)

Purification and properties of reductases for aromatic aldehydes and ketones from guinea pig liver.
*J Biochem (Tokyo)* **86:**871-881.

Sawada H, Hara A, Nakayama T and Kato F (1980)
Reductases for aromatic aldehydes and ketones from rabbit liver. Purification and characterization.
*J Biochem (Tokyo)* **87:**1153-1165.

Sawada H, Hara A, Nakayama T, Nakagawa M, Inoue Y, Hasebe K and Zhang YP (1988)
Mouse liver dihydrodiol dehydrogenases. Identity of the predominant and a minor form with 17 beta-hydroxysteroid dehydrogenase and aldehyde reductase.
*Biochem Pharmacol* **37:**453-458.

Sayre LM, Smith MA and Perry G (2001)
Chemistry and biochemistry of oxidative stress in neurodegenerative disease.
*Curr Med Chem* **8:**721-738.

Schieber A, Frank RW and Ghisla S (1992)
Purification and properties of prostaglandin 9-ketoreductase from pig and human kidney. Identity with human carbonyl reductase.
*Eur J Biochem* **206:**491-502.

Schieber A and Ghisla S (1992)
Prostaglandin 9-ketoreductase from pig and human kidney: purification, properties and identity with human carbonyl reductase.
*Eicosanoids* **5 Suppl:**S37-38.

Schott B and Robert J (1989)
Comparative activity of anthracycline 13-dihydrometabolites against rat glioblastoma cells in culture.
*Biochem Pharmacol* **38:**4069-4074.

Schwartz AG, Yang P and Swanson GM (1996)
Familial risk of lung cancer among nonsmokers and their relatives.

*Am J Epidemiol* **144:**554-562.

Sciotti M and Wermuth B (2001)
Coenzyme specificity of human monomeric carbonyl reductase: contribution of Lys-15, Ala-37 and Arg-38.
*Chem Biol Interact* **130-132:**871-878.

Sciotti MA, Nakajin S, Wermuth B and Baker ME (2000)
Mutation of threonine-241 to proline eliminates autocatalytic modification of human carbonyl reductase.
*Biochem J* **350 Pt 1:**89-92.

Seckl JR (1997)
11beta-Hydroxysteroid dehydrogenase in the brain: a novel regulator of glucocorticoid action?
*Front Neuroendocrinol* **18:**49-99.

Sgraja T, Ulschmid J, Becker K, Schneuwly S, Klebe G, Reuter K and Heine A (2004)
Structural insights into the neuroprotective-acting carbonyl reductase Sniffer of Drosophila melanogaster.
*J Mol Biol* **342:**1613-1624.

Shapiro HK (1998)
Carbonyl-trapping therapeutic strategies.
*Am J Ther* **5:**323-353.

Shikita M and Talalay P (1979)
Preparation of highly purified 3 alpha- and 3 beta-hydroxysteroid dehydrogenases from Pseudomonas sp.
*Anal Biochem* **95:**286-292.

Skalhegg BA (1975)
3Alpha-hydroxysteroid dehydrogenase from Pseudomonas testosteroni: kinetic properties with NAD and its thionicotinamide analogue.
*Eur J Biochem* **50:**603-609.

Skalova L, Nobilis M, Szotakova B, Kondrova E, Savlik M, Wsol V, Pichard-Garcia L and Maser E (2002)
Carbonyl reduction of the potential cytostatic drugs benfluron and 3,9-dimethoxybenfluron in human in vitro.
*Biochem Pharmacol* **64:**297-305.

Smolen A and Anderson AD (1976)
Partial purification and characterization of a reduced nicotinamide adenine dinucleotide phosphate-linked aldehyde reductase from heart.
*Biochem Pharmacol* **25:**317-323.

Soldan M, Nagel G, Losekam M, Ernst M and Maser E (1999)
Interindividual variability in the expression and NNK carbonyl reductase activity of 11beta-hydroxysteroid dehydrogenase 1 in human lung.
*Cancer Lett* **145:**49-56.

Soldan M, Netter K and Maser E (1996a)
Enzymatic detoxification of daunorubicin as supplementary mechanism to multidrug resistance. .
*Exp Toxic Path* **48 (Suppl.II):**370-376.

Soldan M, Netter KJ and Maser E (1996b)
Induction of daunorubicin carbonyl reducing enzymes by daunorubicin in sensitive and resistant pancreas carcinoma cells.
*Biochem Pharmacol* **51:**117-123.

Somers WS, Stahl ML and Sullivan FX (1998)
GDP-fucose synthetase from Escherichia coli: structure of a unique member of the short-chain dehydrogenase/reductase family that catalyzes two distinct reactions at the same active site.
*Structure* **6:**1601-1612.

Srinivasan S, March CJ and Sudarsanam S (1993)
An automated method for modeling proteins on known templates using distance geometry.

*Protein Sci* **2:**277-289.

Stewart PM, Krozowski ZS, Gupta A, Milford DV, Howie AJ, Sheppard MC and Whorwood CB (1996)
Hypertension in the syndrome of apparent mineralocorticoid excess due to mutation of the 11 beta-hydroxysteroid dehydrogenase type 2 gene.
*Lancet* **347:**88-91.

Stewart PM, Murry BA and Mason JI (1994)
Type 2 11 beta-hydroxysteroid dehydrogenase in human fetal tissues.
*J Clin Endocrinol Metab* **78:**1529-1532.

Strausberg RL, Feingold EA, Grouse LH, Derge JG, Klausner RD, Collins FS, Wagner L, Shenmen CM, Schuler GD, Altschul SF, Zeeberg B, Buetow KH, Schaefer CF, Bhat NK, Hopkins RF, Jordan H, Moore T, Max SI, Wang J, Hsieh F, Diatchenko L, Marusina K, Farmer AA, Rubin GM, Hong L, Stapleton M, Soares MB, Bonaldo MF, Casavant TL, Scheetz TE, Brownstein MJ, Usdin TB, Toshiyuki S, Carninci P, Prange C, Raha SS, Loquellano NA, Peters GJ, Abramson RD, Mullahy SJ, Bosak SA, McEwan PJ, McKernan KJ, Malek JA, Gunaratne PH, Richards S, Worley KC, Hale S, Garcia AM, Gay LJ, Hulyk SW, Villalon DK, Muzny DM, Sodergren EJ, Lu X, Gibbs RA, Fahey J, Helton E, Ketteman M, Madan A, Rodrigues S, Sanchez A, Whiting M, Madan A, Young AC, Shevchenko Y, Bouffard GG, Blakesley RW, Touchman JW, Green ED, Dickson MC, Rodriguez AC, Grimwood J, Schmutz J, Myers RM, Butterfield YS, Krzywinski MI, Skalska U, Smailus DE, Schnerch A, Schein JE, Jones SJ and Marra MA (2002)
Generation and initial analysis of more than 15,000 full-length human and mouse cDNA sequences.
*Proc Natl Acad Sci U S A* **99:**16899-16903.

Suzuki K, Ueda S, Sugiyama M and Imamura S (1993)
Cloning and expression of a Pseudomonas 3 alpha-hydroxysteroid dehydrogenase-encoding gene in Escherichia coli.
*Gene* **130:**137-140.

Sweet F and Samant BR (1980)

Bifunctional enzyme activity at the same active site: study of 3 alpha and 20 beta activity by affinity alkylation of 3 alpha, 20 beta-hydroxysteroid dehydrogenase with 17-(bromoacetoxy)steroids.
*Biochemistry* **19:**978-986.

Szotakova B, Wsol V, Treitjnar F, Skalova L and Kvasnickova E (1996)
Studies on the metabolism of the potential cytostatic drug oracin. Species differences. .
*Exp. Toxic. Pathol.* **48 Suppl. II:**377-388.

Szweda LI, Uchida K, Tsai L and Stadtman ER (1993)
Inactivation of glucose-6-phosphate dehydrogenase by 4-hydroxy-2-nonenal. Selective modification of an active-site lysine.
*J Biol Chem* **268:**3342-3347.

Tajima K, Hashizaki M, Yamamoto K, Narimatsu S and Mizutani T (1999)
Purification and some properties of two enzymes from rat liver cytosol that catalyze carbonyl reduction of 6-tert-butyl-2, 3-epoxy-5-cyclohexene-1,4-dione, a metabolite of 3-tert-butyl-4-hydroxyanisole.
*Arch Biochem Biophys* **361:**207-214.

Talalay P, Dobson MM and Tapley DF (1952)
Oxidative degradation of testosterone by adaptive enzymes.
*Nature* **170:**620-621.

Tamaoka J, Ha DM and Komagata K (1987)
Reclassification of pseudomonas acidovorans den Dooren de Jong 1926 and Pseudomonas testosteroni Marcus and Talaly 1956 as Comamonas acidovorans comb. nov. and Comamonas testosteroni comb. nov., with an amended decription of genus comamonas.
*Int.J.Syst. Bacteriol.* **37:**52-59.

Tanaka M, Bateman R, Rauh D, Vaisberg E, Ramachandani S, Zhang C, Hansen KC, Burlingame AL, Trautman JK, Shokat KM and Adams CL (2005)
An unbiased cell morphology-based screen for new, biologically active small molecules.
*PLoS Biol* **3:**e128.

Tanaka M, Ohno S, Adachi S, Nakajin S, Shinoda M and Nagahama Y (1992)
Pig testicular 20 beta-hydroxysteroid dehydrogenase exhibits carbonyl reductase-like structure and activity. cDNA cloning of pig testicular 20 beta-hydroxysteroid dehydrogenase.
*J Biol Chem* **267:**13451-13455.

Tanaka N, Nonaka T, Nakanishi M, Deyashiki Y and Hara A (1995)
Crystallization of mouse lung carbonyl reductase complexed with NADPH and analysis of symmetry of its tetrameric molecule.
*J Biochem (Tokyo)* **118:**871-873.

Tanaka N, Nonaka T, Nakanishi M, Deyashiki Y, Hara A and Mitsui Y (1996a)
Crystal structure of the ternary complex of mouse lung carbonyl reductase at 1.8 A resolution: the structural origin of coenzyme specificity in the short-chain dehydrogenase/reductase family.
*Structure* **4:**33-45.

Tanaka N, Nonaka T, Tanabe T, Yoshimoto T, Tsuru D and Mitsui Y (1996b)
Crystal structures of the binary and ternary complexes of 7 alpha-hydroxysteroid dehydrogenase from Escherichia coli.
*Biochemistry* **35:**7715-7730.

Terada T, Sugihara Y, Nakamura K, Mizobuchi H and Maeda M (2003)
Further characterization of Chinese hamster carbonyl reductases (CHCRs).
*Chem Biol Interact* **143-144:**373-381.

Terada T, Sugihara Y, Nakamura K, Sato R, Sakuma S, Fujimoto Y, Fujita T, Inazu N and Maeda M (2001)
Characterization of multiple Chinese hamster carbonyl reductases.
*Chem Biol Interact* **130-132:**847-861.

Thibault ST, Singer MA, Miyazaki WY, Milash B, Dompe NA, Singh CM, Buchholz R, Demsky M, Fawcett R, Francis-Lang HL, Ryner L, Cheung LM, Chong A, Erickson C, Fisher WW, Greer K, Hartouni SR, Howie E, Jakkula L, Joo D, Killpack K, Laufer A, Mazzotta J,

Smith RD, Stevens LM, Stuber C, Tan LR, Ventura R, Woo A, Zakrajsek I, Zhao L, Chen F, Swimmer C, Kopczynski C, Duyk G, Winberg ML and Margolis J (2004)
A complementary transposon tool kit for Drosophila melanogaster using P and piggyBac.
*Nat Genet* **36:**283-287.

Toffoli G, Simone F, Gigante M and Boiocchi M (1994)
Comparison of mechanisms responsible for resistance to idarubicin and daunorubicin in multidrug resistant LoVo cell lines.
*Biochem Pharmacol* **48:**1871-1881.

Towbin H, Staehelin T and Gordon J (1979)
Electrophoretic transfer of proteins from polyacrylamide gels to nitrocellulose sheets: procedure and some applications.
*Proc Natl Acad Sci U S A* **76:**4350-4354.

Tropschug M, Nicholson DW, Hartl FU, Kohler H, Pfanner N, Wachter E and Neupert W (1988)
Cyclosporin A-binding protein (cyclophilin) of Neurospora crassa. One gene codes for both the cytosolic and mitochondrial forms.
*J Biol Chem* **263:**14433-14440.

Tsigelny I and Baker ME (1995a)
Structures important in mammalian 11 beta- and 17 beta-hydroxysteroid dehydrogenases.
*J Steroid Biochem Mol Biol* **55:**589-600.

Tsigelny I and Baker ME (1995b)
Structures stabilizing the dimer interface on human 11 beta-hydroxysteroid dehydrogenase types 1 and 2 and human 15-hydroxyprostaglandin dehydrogenase and their homologs.
*Biochem Biophys Res Commun* **217:**859-868.

Tsumoto K, Umetsu M, Kumagai I, Ejima D and Arakawa T (2003)
Solubilization of active green fluorescent protein from insoluble particles by guanidine and arginine.
*Biochem Biophys Res Commun* **312:**1383-1386.

Umetsu M, Tsumoto K, Nitta S, Adschiri T, Ejima D, Arakawa T and Kumagai I (2005)
Nondenaturing solubilization of beta2 microglobulin from inclusion bodies by L-arginine.
*Biochem Biophys Res Commun* **328:**189-197.

Upadhyaya P, Kenney PM, Hochalter JB, Wang M and Hecht SS (1999)
Tumorigenicity and metabolism of 4-(methylnitrosamino)-1-(3-pyridyl)-1-butanol enanti-
omers and metabolites in the A/J mouse.
*Carcinogenesis* **20:**1577-1582.

Usami N, Ishikura S, Abe H, Nagano M, Uebuchi M, Kuniyasu A, Otagiri M, Nakayama H,
Imamura Y and Hara A (2003)
Cloning, expression and tissue distribution of a tetrameric form of pig carbonyl reductase.
*Chem Biol Interact* **143-144:**353-361.

Valentino R, Tommaselli AP, Savastano S, Stewart PM, Ghiggi MR, Galletti F, Mariniello P,
Lombardi G and Edwards CR (1995)
Alcohol inhibits 11-beta-hydroxysteroid dehydrogenase activity in rat kidney and liver.
*Horm Res* **43:**176-180.

Varughese KI, Skinner MM, Whiteley JM, Matthews DA and Xuong NH (1992)
Crystal structure of rat liver dihydropteridine reductase.
*Proc Natl Acad Sci U S A* **89:**6080-6084.

Wada M, Kataoka M, Kawabata H, Yasohara Y, Kizaki N, Hasegawa J and Shimizu S (1998)
Purification and characterization of NADPH-dependent carbonyl reductase, involved in
stereoselective reduction of ethyl 4-chloro-3-oxobutanoate, from Candida magnoliae.
*Biosci Biotechnol Biochem* **62:**280-285.

Waksman SA (1961)
*The Actinomycetes*.
Williams and Wilkins Co, Baltimore.

Watanabe K, Sugawara C, Ono A, Fukuzumi Y, Itakura S, Yamazaki M, Tashiro H, Osoe-
gawa K, Soeda E and Nomura T (1998)

Mapping of a novel human carbonyl reductase, CBR3, and ribosomal pseudogenes to human chromosome 21q22.2.
*Genomics* **52:**95-100.

Wermuth B (1981)
Purification and properties of an NADPH-dependent carbonyl reductase from human brain. Relationship to prostaglandin 9-ketoreductase and xenobiotic ketone reductase.
*J Biol Chem* **256:**1206-1213.

Wermuth B (1982)
Human carbonyl reductases.
*Prog Clin Biol Res* **114:**261-274.

Wermuth B (1985)
Aldo-keto reductases.
*Prog Clin Biol Res* **174:**209-230.

Wermuth B (1995)
Expression of human and rat carbonyl reductase in E. coli. Comparison of the recombinant enzymes.
*Adv Exp Med Biol* **372:**203-209.

Wermuth B, Bohren KM and Ernst E (1993)
Autocatalytic modification of human carbonyl reductase by 2-oxocarboxylic acids.
*FEBS Lett* **335:**151-154.

Wermuth B, Bohren KM, Heinemann G, von Wartburg JP and Gabbay KH (1988)
Human carbonyl reductase. Nucleotide sequence analysis of a cDNA and amino acid sequence of the encoded protein.
*J Biol Chem* **263:**16185-16188.

Wermuth B, Burgisser H, Bohren K and von Wartburg JP (1982)
Purification and characterization of human-brain aldose reductase.
*Eur J Biochem* **127:**279-284.

Wermuth B, Mader-Heinemann G and Ernst E (1995)

Cloning and expression of carbonyl reductase from rat testis.

*Eur J Biochem* **228:**473-479.


Wermuth B, Platts KL, Seidel A and Oesch F (1986)

Carbonyl reductase provides the enzymatic basis of quinone detoxication in man.

*Biochem Pharmacol* **35:**1277-1282.


Willems A, de Vos P and de Lay J (1992)

*The Prokaryotes, a Handbook on the Biology of Bacteria, Ecophysiology, Isolation, Identification an Applications*.

Balows A, Trueper, H.G., Dworkin, M. ed)Springer Verlag, Berlin.


Wilmot CM and Thornton JM (1988)

Analysis and prediction of the different types of beta-turn in proteins.

*J Mol Biol* **203:**221-232.


Winberg JO, Brendskag MK, Sylte I, Lindstad RI and McKinley-McKee JS (1999)

The catalytic triad in Drosophila alcohol dehydrogenase: pH, temperature and molecular modeling studies.

*J Mol Biol* **294:**601-616.


Wirth H and Wermuth B (1992)

Immunohistochemical localization of carbonyl reductase in human tissues.

*J Histochem Cytochem* **40:**1857-1863.


Wirth HP and Wermuth B (1985)

Immunochemical characterization of aldo-keto reductases from human tissues.

*FEBS Lett* **187:**280-282.


Wsol V, Kvasnickova E, Szotakova B and Hais IM (1996)

High-performance liquid chromatographic assay for the separation and characterization of metabolites of the potential cytostatic drug oracine.

*J Chromatogr B Biomed Appl* **681:**169-175.

Wsol V, Skalova L, Szotakova B, Trejtnar F and Kvasnickova E (1999)
Sex differences in stereospecificity of oracin reductases in rat in vitro and in vivo.
*Chirality* **11:**505-509.

Wsol V, Szotakova B, Kvasnickova E and Fell AF (1998)
High-performance liquid chromatography study of stereospecific microsomal enzymes cata-
lysing the reduction of a potential cytostatic drug, oracin. Interspecies comparison.
*J Chromatogr A* **797:**197-201.

Wsol V, Szotakova B, Skalova L, Cepkova H and Kvasnickova E (2000)
The main metabolic pathway of oracin, a new potential cytostatic drug, in human liver micro-
somes and cytosol: stereoselectivity of reoxidation of the principal metabolite 11-
dihydrooracin to oracin.
*Enantiomer* **5:**263-270.

Wsol V, Szotakova B, Skalova L and Maser E (2003)
Stereochemical aspects of carbonyl reduction of the original anticancer drug oracin by mouse
liver microsomes and purified 11beta-hydroxysteroid dehydrogenase type 1.
*Chem Biol Interact* **143-144:**459-468.

Wsol V, Szotakova B, Skalova L and Maser E (2004)
The novel anticancer drug oracin: different stereospecificity and cooperativity for carbonyl
reduction by purified human liver 11beta-hydroxysteroid dehydrogenase type 1.
*Toxicology* **197:**253-261.

Xie Y and Wetlaufer DB (1996)
Control of aggregation in protein refolding: the temperature-leap tactic.
*Protein Sci* **5:**517-523.

Yamano S, Nakamoto N and Toki S (1999)
Purification and characterization of rat liver naloxone reductase that is identical to 3alpha-
hydroxysteroid dehydrogenase.
*Xenobiotica* **29:**917-930.

Yesair DW, Thayer PS, McNitt S and Teague K (1980)

Comparative uptake, metabolism and retention of anthracyclines by tumors growing in vitro and in vivo.
*Eur J Cancer* **16:**901-907.


Yokota H, Yuasa A and Sato R (1992)
Topological disposition of UDP-glucuronyltransferase in rat liver microsomes.
*J Biochem (Tokyo)* **112:**192-196.


Yum DY, Lee BY and Pan JG (1999a)
Identification of the yqhE and yafB genes encoding two 2, 5-diketo-D-gluconate reductases in Escherichia coli.
*Appl Environ Microbiol* **65:**3341-3346.


Yum MK, Kim NS, Oh JW, Kim CR, Lee JW, Kim SK, Noh CI, Choi JY and Yun YS (1999b)
Non-linear cardiac dynamics and morning dip: an unsound circadian rhythm.
*Clin Physiol* **19:**56-67.


Zelinski T, Peters J and Kula MR (1994)
Purification and characterization of a novel carbonyl reductase isolated from Rhodococcus erythropolis.
*J Biotechnol* **33:**283-292.

# IX Figure/Table List:

## Part I:

## Part II:

# Erklärung

Ich versichere, dass ich meine Dissertation

*„Carbonyl Reductases and Pluripotent Hydroxysteroid Dehydrogenases of the Short-Chain Dehydrogenase/Reductase Superfamily:*
*Structural aspects of oligomerization in 3$\alpha$-Hydroxysteroid dehydrogenase /carbonyl reductase from Comamonas testosteroni: New approaches for efficient protein design"*

selbständig ohne unerlaubte Hilfe angefertigt und mich dabei keiner anderen als der von mir ausdrücklich bezeichneten Quellen bedient habe.

Die Dissertation wurde in der jetzigen oder einer ähnlichen Form noch bei keiner anderen Hochschule eingereicht und hat noch keinen sonstigen Prüfungszwecken gedient.

Aachen, im April 2009
Frank Hoffmann

# Lebenslauf

| | |
|---|---|
| Geburtstag: | 20. August 1973 |
| Geburtsort: | Siegen |
| August 1984 – Juni 1993 | Fürst Johann Moritz Gymnasium Siegen<br>Abschluss: Allgemeine Hochschulreife |
| Oktober 1994 – April 1999 | Studium der Biologie an der Philipps-Universität Marburg<br>*Schwerpunkte*: Molekulargenetik molekulare Entwicklungsbiologie, Immunologie<br>Abschluss: „sehr gut" |
| Mai 1999 – Mai 2000 | Diplomarbeit bei Prof. Dr. R. Renkawitz-Pohl in molekularer Entwicklungsbiologie, Abschluss: „sehr gut" |
| Juni 2000 – März 2001 | Forschungspraktikum Prof. Dr. Gerhard Klebe, Institut für Pharmazeutische Chemie, Philipps-Universität Marburg<br>*Schwerpunkt*: „Wirkstoffdesign" und „Molecular Modeling" |
| 04/2001 – Juli 2006 | Promotion bei Prof. Dr. E. Maser, Pharmakologie und Toxikologie, Marburg<br>*„Carbonyl Reductases and Pluripotent Hydroxysteroid Dehydrogenases of the Short-Chain Dehydrogenase/Reductase Superfamily: Structural Aspects of Oligomerization in 3$\alpha$-Hydroxysteroid Dehydrogenase /Carbonyl Reductase from Comamonas testosteroni: New Approaches for efficient Protein Design"* |
| August 2006 – heute | Tätigkeit als „Regulatory Affairs Manager", Grünenthal GmbH, Aachen |